ADAPTIVE DISTANCE RELAYING SCHEME FOR

THE PROTECTION OF TEED CIRCUITS

A thesis submitted to

CITY UNIVERSITY

for the Degree of

DOCTOR OF PHILOSOPHY

by

MOHAMAD TELIANI

Power Systems Protection Laboratory
Department of Electrical, Electronic
and Information Engineering

City University
Northampton Square
London EC1V 0HB
U.K.

JANUARY 1991

I dedicate this thesis to my family

ABSTRACT

This thesis describes an adaptive digital distance protection scheme suitable for Teed transmission line applications. The scheme utilises the line and source impedances in order to measure the exact line impedance at the reach point and gives correct discrimination between in-zone and out-of-zone faults.

The relay requires some information about the system operating conditions at the remote terminals. This data is not required in real-time but has to be available at the measuring point. Thus, the speed and accuracy during a fault is not affected.

The implementation of the scheme requires a central computer system where information about the system operating conditions can be provided. The update at the relay is initiated by the control centre and is transmitted by a low-speed channel to modify the setting each time the system operating conditions change.

Tests to show the likely scheme performance for different loading conditions and for different short circuit levels are presented. Some of the more interesting results are compared with conventional distance relays for solid and resistive faults. These illustrate the advantage offered by implementing such scheme.

The relay which is simulated in software, calculates the line impedance by solving the first order differential line equation. In order to remove the travelling wave distortion and exponentials, analogue and digital filtering techniques are employed.

Results are presented, on a typical 400kV system, for single phase to earth faults and phase to phase faults, where particular emphasis is placed on the effect of short circuit level and fault inception angle. The relay is also tested for closeup faults in the forward and reverse direction. Finally, another method to implement the scheme is introduced and results are presented showing its likely performance.

ACKNOWLEDGEMENTS

COPYRIGHT DECLARATION

LIST OF CONTENTS

vi

LIST OF PRINCIPAL SYMBOLS

Z_{mP} = Measured impedance at end P

Z_{mPQ} = Modified measured impedance at end P for faults on leg Q

Z_{mPR} = Modified measured impedance at end P for faults on leg R

K_Q = Infeed factor for faults on leg Q

K_R = Infeed factor for faults on leg R

Z_P = PS impedance of leg P

Z_Q = PS impedance of leg Q

Z_R = PS impedance of leg R

I_{QS} = Steady state pre-fault current of leg Q

I_{RS} = Steady state pre-fault current of leg R

α_{RS} = Fault position for a fault at the relay zone-1 reach point along line T-R

α_{QS} = Fault position for a fault at the relay zone-1 reach point along line T-Q

α_R = Fractional per-unit length of leg R

α_Q = Fractional per-unit length of leg Q

Z_{PS} = Effective source impedance at end P

Z_{QS} = Effective source impedance at end Q

Z_{RS} = Effective source impedance at end R

V_{PT} = Superimposed voltage at end P

I_{PT} = Superimposed current at end P

I_{QT} = Superimposed current at end Q

I_{RT} = Superimposed current at end R

V_P = Total voltage at end P

I_P = Total current at end P

I_{PS} = Steady state pre-fault current at end P

S_Q = Setting along line PQ

S_R = Setting along line PR

S_{MR} = Adaptive setting along line PR

K = Residual compensation factor

V_{Pa} = Voltage of phase 'a' at end P

I_{PSa} = Steady state current of phase 'a' at end P

I_{RSa} = Steady state current of phase 'a' at end R

I_{QSa} = Steady state current of phase 'a' at end Q

I_{resP} = Residual current at end P

I_{resR} = Residual current at end R

I_{resQ} = Residual current at end Q

I_{resPS} = Steady state residual current at end P

I_{resRS} = Steady state residual current at end R

I_{resQS} = Steady state residual current at end Q

V_{resPS} = Steady state residual voltage at end P

V_{resRS} = Steady state residual voltage at end R

V_{resQS} = Steady state residual voltage at end Q

V_{resP} = Residual voltage at end P

$I_{PTa}, I_{QTa}, I_{RTa}$ = Superimposed current of phase 'a' at terminals P, Q and R

$V_{PTa}, V_{QTa}, V_{RTa}$ = Superimposed voltage of phase 'a' at terminals P, Q and R

I_{Pa}, I_{Qa}, I_{Ra} = Phase 'a' current at terminals P, Q and R

V_{TTa} = Superimposed voltage of phase 'a' at the Tee point

K_{Rs}, K_{Qs} = Residual compensation factor for source impedance measurement

x

I_{RTa}, I_{RTb}, I_{RTc} = Superimposed current of phases a, b, and c at end R

Z_{P1}, Z_{R1}, Z_{Q1} = Positive sequence impedance of legs P, R and Q

Z_{PO}, Z_{RO}, Z_{QO} = Zero sequence impedance of legs P, R and Q

K_{Qa}, K_{Qb}, K_{Qc} = Infeed factor for phases a, b and c for faults on leg Q

K_{Ra}, K_{Rb}, K_{Rc} = Infeed factor for phases a, b and c for faults on leg R

Z_{mPa}, Z_{mPb}, Z_{mPc} = Measured impedance of phases a, b and c

Z_{mPQa}, Z_{mPQb}, Z_{mPQc} = Modified measured impedance of phases a, b and c along line PQ

Z_{mPRa}, Z_{mPRb}, Z_{mPRc} = Modified measured impedance of phases a, b and c along line PR

I_{resPT}, I_{resQT}, I_{resRT} = Superimposed residual currents at terminals P, Q and R

$v_{(t)}$, $i_{(t)}$ = Time domain voltage and current

$v_{(k)}$, $i_{(k)}$ = Discrete time voltage and current

f_s = Sampling frequency

T_s = Sampling interval $1/f_s$

$h_{(t)}$ = Impulse response

$v'_{(t)}$, $i'_{(t)}$ = Voltage and current derivatives

w_o = Fundamental frequency

w_n = Cut-off frequency of analogue filter

X_M = Directional reactance

X_{MA} = Directional reactance setting

X_t = Measured reactance

R_t = Measured resistance

CVT = Capacitor voltage transformer

CT = Current transformer

VT = Voltage transformer

T = Sampling time step

τ = Dummy time variable

d = Damping coefficient

SCL = Short circuit level

A/D = Analogue to digital converter

CHAPTER 1

INTRODUCTION AND LITERATURE SURVEY

The interconnection of load and supply points by means of a multi-ended transmission line, rather than by a number of separately switched feeders, has certain advantages which may outweigh any resulting loss of flexibility in system operation. Reduced to their simplest form, a case of three points being interconnected by a Teed circuit is shown in Figure 1.1. In Figure 1.2 the three points are directly interconnected by three plain feeders.
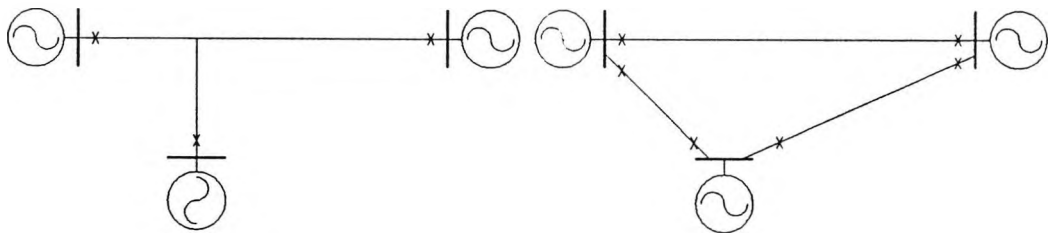
Fig. 1.1   Fig 1.2

The benefits of Teed circuits can be identified on the basis of [1]:

a- Economic saving

The cost difference between one 3-terminal and two 2-terminal lines of EHV and UHV transmission networks may be substantial. The former requires fewer circuit breakers, and can give a higher conductor utilisation. On the other hand the Teed system requires switching at the three ends in operation compared with two in the loop circuit case.

1

b- Ecological benefits

Obtaining a site near a metropolitan area, scarcity of
right of way and other environmental restrictions make
the building of individual two-terminal lines more
difficult to justify. One solution is to minimise the
building of individual two-terminal lines and instead
to install three-terminal lines.

1.1 Conventional Protection Schemes Applied for Multi-Terminal Lines and Their Limitations

The protection of Teed circuits introduces additional
difficulties to those encountered on two ended circuits
and it may not be possible to apply feeder protection
systems designed for simple feeder protection without loss
of discrimination [2,4]. The almost infinite combinations
of line arrangements, source strengths, line lengths,
system loading requirements and system operating
conditions is an important factor which must be considered
when selecting a protective system for multi-terminal
feeders.

An illustration of some technical problems involved
in the protection of multi-ended feeders is summarised in
the following:

1.1.1 AC Pilot Wire Differential Protection

Unit protection schemes compare quantities derived from
the input and output currents of a protected circuit. For
all healthy-system or through-fault conditions, the
quantities are balanced within the relay, which remains

2

inoperative, whilst for internal fault conditions this balance is disturbed and relay operation occurs. The pilot-wire circuit provides the necessary interchange of information between ends of the protected circuit which may utilise either the circulating-current or opposed-voltage principles [4].

In a Teed scheme, three unequal quantities are balanced and this can be done satisfactorily only if the characteristic of the current transformers at all ends are linear [4], therefore the CT must be designed to be substantially linear up to maximum through-fault current. Voltage unbalance in a healthy Teed system may occur when through fault current from two ends of a Teed system is fed to a fault through a third end. Then the CT of the third end may saturate while the corresponding CT's at the other ends are still within their linear range. The usual method of overcoming this difficulty is to circulate the bias current and the operating current independently using three or four pilot wires. The restraint current will be proportional to the scalar sum of the secondary voltage of the CT [4]. The use of three or four pilot conductors also creates inherent difficulties in devising satisfactory compensation for pilot-circuit constants. The length of the feeder that can be protected by pilot-wire is limited by the characteristics of these wires. The pilot wire resistance increases with the length of the feeder and, as seen by the protection, appears increasingly like an open circuit. Similarly, the shunt capacitance also increases and tends to become, in effect

3

an ac short circuit across the pilots. If certain limiting values of pilot resistance and capacitance are exceeded, loss of sensitivity for internal faults and maloperation for external faults may occur. Moreover, the protection can be unreliable if the current at one terminal reverses direction for an internal fault.

1.1.2 Distance Protection of Teed Feeders

Distance protection is widely used in the protection of Teed feeders. However, its application requires careful consideration. The measurement of impedance in distance protection is made from relaying signals derived from the primary voltage and current at the relay location only and takes no account of the fault current infeed or outfeed at the remote circuit termination. In order to avoid incorrect tripping for all system operating conditions, the common practice is to set the relay for the remote short section assuming that there is no infeed from the remote end [2,3]. Consequently, with infeed, the relay sees an apparent impedance which is greater than the actual line value, i.e., it underreaches. In the case of an outfeed, the relay sees an impedance which is smaller than the actual line impedance, thereby resulting in an overreach. Outfeed is a condition that could be encountered on Teed systems if there are ties (other than the Tee) between the terminating points and the current flows out of the circuit for an internal fault.

1.2 Feeder Protection Based on Travelling Wave Theory

Power system networks are subjected to many forms of transients as a result of switching operation, or under fault conditions. With increasing operating voltage levels, these transients play a large part in determining the system insulation level and the circuit breaker duty. So many precautions have to be taken to avoid these transients completely or at least to minimise their effects; at the same time, there are strong economic reasons for keeping them as low as possible. On the other hand some protection research engineers have attempted to use the transients generated by a fault by detecting and processing them in order to clear the faults with minimal time. Also, the availability of fast communication channels (particularly fiber optics) opens new dimensions in the field of ultra high speed relaying by bringing the information at remote terminals together, as a means to improve system transient stability and increase the transfer power capability over existing high voltage transmission lines.

The occurrence of a fault on a transmission line can be considered as equivalent to superimposing a voltage at the point of a fault which is equal and opposite to the prefault steady state voltage. The postfault voltage and current can be considered as made up of the prefault steady state components and the fault injected components [5]. The superimposed voltage and current component contain both the transient components, such as exponentials and travelling waves, and the difference

5

between the pre- and postfault power frequency components.

A scheme for protection of two terminal line based on travelling wave theory filter out the pre-fault steady state component [5]. So any signal appearing in the filter output in an indication of a possible fault. A comparison between the change of the voltage and current signals, directly after fault inception, will give the direction of motion of the first travelling wave. The relay operates on the principle that the superimposed values of the voltage and current signals are of opposite polarity for a forward fault and of like polarity for a reverse fault. The protection at the two ends of the line are linked via a communication channel and operates in a blocking mode. The fundamental requirement of blocking schemes is that the line relay sensitivities are set so that an external fault is always detected by the blocking relay, regardless of whether the tripping or forward looking relay detects a fault or not. This could introduce problems for inception angles close to the voltage zero crossing. In such cases, the initial polarities of the voltage and current changes are correctly indicative of the direction to fault for only 2-3 msec, followed by a similar period in which they are characteristic of a fault in the other direction [6]. Should the forward to reverse sensitivity ratio be too high, then it is feasible for the relay to render an incorrect decision. In addition a simple comparison of the relative polarities of the voltage and current changes is not a totally reliable method of determining the

6

direction to the fault. In the case of the protective scheme connected to a source of very high capacity, the superimposed component of voltage will not be significant and incorrect operation may result.

One scheme [1] has succeeded, at least in theory, in extending the relative polarity of voltage and current changes approach to Teed circuits. By observing the sign of the voltage wave with respect to the current wave immediately after fault inception, a directional discrimination to the fault can be based on the principle that for internal faults the current and voltage waves created by the fault will be opposite in sign at all terminals, while for external faults they will be of equal sign at the relay closest to the fault. The relays have independent settings in the forward and reverse direction. This may cause maloperation in the case of an external fault, since it is possible that the terminal seeing the fault in the forward direction may start to operate, while the remaining terminals would not detect the fault at all (the current change being insufficient for each of these terminals). The tripping signal is initiated when both voltage and current waves exceed a certain threshold. At an infinitely strong source, when a fault occurs at the far end of a long line, the superimposed components of voltage will not be significant and consequently the relay could fail to operate.

The performance of the relay has been examined for a limited number of system and fault conditions. No mention has been made of the outfeed current where, due to the

7

presence of circuits external to the Tee ends, certain internal faults may cause the current and voltage sensed at one end to be similar to those experienced under external fault conditions.

Aggarwal and Johns [7] described a new differential scheme using the modal signals for the protection of Teed circuits. This approach avoids the blind spot problems sometimes encountered when using a single summated quantity. Also, the use of modal quantities eliminates the effect of the mutual coupling between the phases of a transmission line. The basic relay operating principle relies upon deriving a differential quantity and a bias quantity using the instantaneous values of the modal current at the three ends. The scheme can be implemented using the total or the superimposed time variation of the relaying signals. Although the scheme can perform well if there is infeed from the three ends of the line, under two terminal operation the magnitude of the bias and differential signal is the same. This can lead to incorrect operation for external faults in particular when there is a high degree of CT saturation if the decision process as reported by the authors is not employed. Limited field experience is available on this topic at present. Also the scheme relies totally, as any other differential or directional comparison scheme, on the communication link between the ends of the line.

From the foregoing, it is evident that the use of either unit or non-unit protection may not be satisfactory for the protection of Teed lines, and new concepts have to

8

be introduced for improving their performance.

However, with present day state of the art digital technology, it will be possible to design an impedance measuring device which can communicate with a control centre where information about the system operating conditions can be provided, to adapt its parameters according to the new state of the system.

Recent years shows the emergence of new concepts that can be applied in the protection of a power system. Horowitz, Phadke and Thorp [9] described the results of an investigation into the possibilities of using digital techniques to adapt transmission system protection and control to real-time power system changes. They defined adaptive protection as:

"A protection philosophy which permits and seeks to make adjustments to various protection functions in order to make them more attuned to prevailing power system conditions".

At the same time Rockefeller and his associates [8] presented the concepts for adaptive protective relaying of transmission lines. They defined adaptive protection as:

"An on-line activity that modifies the preferred protective response to a change in system conditions or requirements".

Distance relays which have been successfully employed in plain feeder applications for many years, do not provide a generally satisfactory response when applied to Teed feeders. The problem stems from the current contribution from the active taps, and the difference in

9

relay response when the contribution is, or is not, present. Thus, the objective of this thesis is to investigate the possibility of applying an adaptive distance protection to achieve a reliable protection for Teed lines which is comparable to that obtained with a two-terminal line. Included also is the simulation of the relaying system to determine the likely relay performance under different system and fault condition in some 400kV applications.

The proposed protection, based on distance measuring principles, relies on transmitting the source impedances and the load currents from the remote terminals to the measuring point. This data is then used to modify the impedance seen by a conventional distance relay so that it can measure the exact line impedance for faults at the reach point and gives the proper discrimination between internal and external faults. The adaptivity described here refers to the ability of the protection system to automatically alter its operating parameters in response to changing network conditions to maintain optimal performance.

The data from the remote ends are not required in real-time during a fault. It only has to be available at the relay in time for the next disturbance making use of the fact that the system operating conditions vary slowly and are cyclical in nature. Thus the speed and accuracy of the relay during faults will not be affected. The data can be provided to the relay periodically as suggested be Rockefeller [8] i.e, by using an up-to-date central

10

impedance model.

Since impedance measurement is based on power frequency components of voltage and current signals, special filtering needs to be employed to attenuate all frequencies other than power frequency.

Distance protection algorithms have evolved over the years. Algorithms based on conventional Fourier Transform techniques [10,11,12] are effective in extracting the fundamental components from highly distorted fault waveforms, but their response to a fault is slow. The response of the Fourier Transform can be improved by using a smaller data window, but small data windows produce problems in current offset conditions and are influenced by travelling wave components. However, the Finite Fourier Transform can be satisfactorily implemented if used with appropriate filtering [13].

The main disadvantage of the latter method is that the magnitude response of orthogonal filters is not the same. Hence, they must be equalised at the power frequency which means that any drift by the system frequency from nominal frequency causes errors in the impedance measurement. Furthermore, low order harmonics in the relaying signals have a detrimental effect on the performance [14].

A modified method uses two direct samples on the relaying signals to solve for the resistive and reactive components of the line impedance. This method has the advantage of being immune to power frequency changes and system harmonics [14].

1.3 Summary of the Thesis

The fundamental principles of the new adaptive relay are described in Chapter 2, which includes the requirements and the way the system parameters are employed within the relay to restore the zone-1 reach. In order to protect the line against all types of faults, the performance equations for phase-earth and phase to phase faults are derived.

Chapter 3 is concerned with the simulation of a Teed transmission line. The symmetrical component technique is employed to represent the transmission lines; included also is an introduction to the representation of the circuit elements and the solution method used in the Electromagnetic Transient Programme (EMTP). The EMTP is fast becoming the preferred software in industry and research institutes for the simulation of complex power systems.

A complete breakdown of the individual states within the adaptive relay, as implemented in software, is given in Chapter 4. The various analogue and digital functions including prefiltering, analogue to digital conversion, digital filtering, impedance calculation, relay directionality, digital smoothing of the calculated impedance and counting strategy are all explained.

In Chapter 5 the fault area in the impedance plane, for different system operating conditions, is defined together with the possible improvement the adaptive scheme can afford over conventional distance relays. The effect of fault resistance on the relay coverage and the relay

12

sensitivity for different signals and parameters used within the relay is also investigated.

A full relay performance evaluation, on a typical faulted Teed system, is included in Chapter 6. The operating time of the relay as a function of: fault position, fault inception angle, fault type, source capacity etc is investigated. Attention is also focused upon the relay directional stability and the relay behaviour under forward and reverse close-up fault conditions. The rest of the Chapter is devoted to an investigation of the relay performance on sustained faults.

Chapter 7 introduces an alternative method for the implementation of the adaptive scheme. The signals and parameters are used to adjust the relay setting instead of measured impedance. This method requires two separate algorithms to convert the voltage and current signals into a measured resistance and reactance. The rest of the Chapter is devoted to presenting some results to show the difference between the two methods.

A complete concluding summary of the thesis is given in Chapter 8 together with some proposals for future work.

CHAPTER 2

THEORY OF THE ADAPTIVE DISTANCE SCHEME

Conventional distance relays when applied to transmission
lines of Teed type can measure the correct distance up to
the Tee point, but from thereon, their reach on one remote end
is affected by the magnitude and direction of the current
from the other far end. Since the zone-1 must never
overreach the remote shortest leg, under all system
operating conditions, the relay is set without in-feed
[2,3,15], i.e., assuming a two terminal configuration.
Thus, with in-feed, the relay reach is reduced. This
Chapter describes a new adaptive digital distance relaying
scheme which is fundamentally a distance relay which is
compensated for the fault current from the remote end.
The relay could give an accurate measurement at the reach
point and a proper discrimination between internal and
external faults. The in-feed current can be determined in
terms of circuit parameters where some of these are
constant and the others could be considered periodically
constant. The scheme relies on transmitting and updating
the system operating conditions at the remote ends by
means of slow speed non-continuous communication links.
To aid comprehension of the fundamental operating and
compensation principle the following analyses refer at the
beginning to single conductor system and are then extended
to cover the practical three phase configuration.

14

2.1 Single Phase Circuit

The underlying principle of the new technique is best illustrated by reference to Figure 2.1, which represents a single phase Teed circuit subject to a solid fault at leg Q. The measured impedance, using the local current and voltage signals, for a relay at end P, is given by:

$$Z_{mP} = \frac{V_P}{I_P} = \frac{I_P Z_P + \alpha_Q Z_Q (I_P + I_R)}{I_P} \qquad 2.1$$

$$Z_{mP} = Z_P + \alpha_Q Z_Q + \alpha_Q Z_Q (\frac{I_R}{I_P}) \qquad 2.2$$

where

Z_P = total impedance of leg P-T

Z_Q = total impedance of leg Q-T

$\alpha_Q Z_Q$ = proportional impedance to fault for T-F

I_R is the contribution of fault current from end R and can be written as:

$$I_R = I_{RS} + I_{RT} \qquad 2.3$$

I_{RS} is the load current

I_{RT} is the superimposed current

By relating the superimposed currents at end R to those at end P as shown in Appendix 2A gives:

$$Z_{mP} = Z_P + \alpha_Q Z_Q + \alpha_Q Z_Q [\frac{I_{RS}}{I_P} + \frac{Z_P I_{PT} - V_{PT}}{(Z_R + Z_{RS}) I_P}] \qquad 2.4$$

where Z_{RS} is the source impedance at end R and is determined from

$$Z_{RS} = - \frac{V_{RT}}{I_{RT}} \qquad 2.5$$

Assuming zero prefault loading

$$I_P = I_{PT}$$

15

$$I_{RS} = 0$$

Then

$$Z_{mP} = Z_P + \alpha_Q Z_Q + \alpha_Q Z_Q(\frac{Z_P + Z_{PS}}{Z_R + Z_{RS}}) \qquad 2.6$$

Similarly the measured impedance at end P for a fault on leg R is given generally by Equation 2.7, and for the special case of zero prefault load in Equation 2.8.

$$Z_{mP} = Z_P + \alpha_R Z_R + \alpha_R Z_R[\frac{I_{QS}}{I_P} + \frac{Z_P I_{PT} - V_{PT}}{(Z_Q + Z_{QS})\ I_P}] \qquad 2.7$$

$$Z_{mP} = Z_P + \alpha_R Z_R + \alpha_R Z_R(\frac{Z_P + Z_{PS}}{Z_Q + Z_{QS}}) \qquad 2.8$$

Similar measurands could be obtained for the relays at the other ends.

The basic principle employed would involve transmitting the values I_{RS}, I_{QS}, Z_{RS}, Z_{QS} to end P.

Z_{RS}, Z_{QS} are the effective source impedances looking into the busbar remote from the point of measurement for the critical fault position i.e., at zone-1 reach. In other words for a fault at zone-1 reach on leg R, Z_{QS} should be determined and for faults at zone-1 reach on leg Q, Z_{RS} should be determined. It should be noted that the effective source impedance of the system considered in Figure 2.1 is constant for all fault locations, but if there are ties between the three generating stations, other than the Teed, the effective fault impedance varies with fault position. These impedances could be obtained, as suggested by Rockefeller et al [8] i.e. by using a central computer system to update an impedance model each

16

time the system changes. These could be updated periodically so as to correspond to the system configuration.

Similarly I_{RS}, I_{QS} are steady-state prefault values; their values changes only slowly and periodically. Updating via a slow speed channel is what is required. It should be noted that, only one of the remote ends steady state currents need to be transmitted to the relaying point as the other can be calculated simply from the local load current and one of the remote ends current.

How often are the remote source impedances and currents required to be updated to the relay ?. If their values, for example, are assumed to follow the same pattern as the load curve then updating on an hourly basis could be a reasonable justification.

In essence, the relay would adapt its setting so as to be set optimally irrespective of any prospective fault condition. The advantages of this adaptive approach are:

1- A slow speed non-continuous single value communication channel is all that is required, as the data from the far ends has to be made available at the relay in time for the next disturbance. This contrasts sharply with the differential scheme where integrity is determined largely by the security and dependability of the channel itself.

2- Speed of tripping can be retained without having to employ wideband (expensive) signalling equipment.

The scheme would thus retain the desirable features of non-unit measurement (distance protection) principles

17

and, in the event of no periodic update, the setting could revert to values producing a performance that is no worse than that of conventional distance protection commonly applied to Teed feeders.

2.2 Compensation Method Consideration

Consider for example Equation 2.4 which is the measured impedance at end P, for a fault on leg Q, written in the form of Equation 2.9.

$$Z_{mP} = \frac{V_P}{I_P} = Z_P + \alpha_Q Z_Q + \alpha_Q Z_Q K_Q \qquad 2.9$$

where

$$K_Q = \frac{I_{RS}}{I_P} + \frac{Z_P I_{PT} - V_{PT}}{(Z_R + Z_{RS}) I_P} \qquad 2.10$$

If the measured impedance Z_{mP} is as in a conventional distance relay, compared with a fixed zone-one boundary for example on the basis of $0.8(Z_P + Z_Q)$ i.e., corresponding to $\alpha_Q = \alpha_{QS} = 0.8 - 0.2(Z_P/Z_Q)$ that extends into leg Q then the relay will in general underreach by the nature of the measured impedance being greater than the actual impedance to the fault $(Z_P + \alpha_Q Z_Q)$ by an amount $\alpha_Q Z_Q K_Q$ see Equation 2.9. This is the classical underreaching phenomena caused by the component of current fed from end R that is fed through leg Q over an impedance $\alpha_Q Z_Q$ which in turn causes an additional voltage drop and therefore increases the apparent impedance measured at end P. It is important to mention that, the scheme is applicable only for line configuration where the relay can be set to cover a certain distance beyond the Tee point.

18

By using an alternative measurand to Equations 2.4 and 2.7 written in the form of Equations 2.11 and 2.12, it is possible to compensate for the infeed from the remote ends R and Q. In this way, the modified measurand corresponds exactly to the actual line impedance at the critical fault position.

$$Z_{mPQ} = Z_{mP} - \alpha_{QS}Z_QK_Q = Z_P + \alpha_{QS}Z_Q \qquad 2.11$$

$$Z_{mPR} = Z_{mP} - \alpha_{RS}Z_RK_R = Z_P + \alpha_{RS}Z_R \qquad 2.12$$

The scheme in effect comprises two distance relays each set for one remote leg. The two relays will measure simultaneously and the following questions then arise.

1- In what way would the measurand Z_{mPQ} behave for a fault on leg R and vice versa, how would Z_{mPR} behave for a fault on leg Q.?

2- In what way would they behave for a fault on leg P.?

Some idea of the answer to this can be gained from the analytical examples in the next section.

It should be noted that, although the in-feed from end R is in general such as to cause underreach, i.e the argument of K_Q tends to zero, there are a few possible operating conditions where the current fed from end R is in anti-phase to the current fed from measuring end P. This in turn can cause overreaching. A configuration where this could be so is sketched in Figure 2.2.

Figure 2.2 illustrates physically instantaneous relative directions for the current in the circuit, and it is apparent that, in this case, the effective source impedance at end R is negative. In the method proposed, the source impedances are those that would be measured

19

with the circuit in the superimposed state i.e. with all source voltages de-energised and the fault excited from a superimposed generator as shown in Figure 2.3.

The flow of superimposed current is into the line at end R and consequently Z_{RS} is negative. It should be noted that the effective source impedances for a circuit with feed-rounds varies with the fault position so that it is necessary when dealing with such circuits to evaluate the source impedances for the extreme fault position i.e. with the superimposed circuit energised at the zone-1 reach point.

2.3 Examples of Teed Circuits

Sketches of some three terminal line configurations will be utilised to illustrate the variation of the apparent impedance with fault position for a conventional relay together with the measurands of the adaptive scheme. For simplicity, scalar values of the line and source impedances are assumed.

2.3.1 Teed Circuit with Equal Leg Lengths and Equal Source Impedances

A single phase Teed circuit is shown in Figure 2.4, which is taken to be symmetrical, in that the distance from each bus bar to the Tee point is the same ($Z_P = Z_Q = Z_R = Z$) and the fault level at the busbars are equal, from which we can find the corresponding source impedances ($Z_{PS} = Z_{QS} = Z_{RS} = Z_S$). Taking the case for a zero prefault condition and for scalar values of the system

20

impedance. The relays at each end are set to cover 80% of the circuit length between each pair of busbars; with conventional distance schemes, the fault location that corresponds to the limit of operation for any two remote infeeding ends is given by:

$$0.8(Z + Z) = Z + \alpha Z + \alpha Z \left[\frac{Z + Z_s}{Z + Z_s}\right] \qquad 2.13$$

where α is a p.u distance measured from the T point. solving for α gives:

$\alpha = 0.3$ p.u

The actual fault is at $\alpha = 0.6$ p.u

Therefore, the effect of fault infeed is to increase the apparent impedance at the terminals and thereby to cause the fault to appear more distant than is actually the case, i.e. underreach.

By using the adaptive scheme the impedance presented to the relay at end P, for a fault along line PQ in Figure 2.4 is:

$$Z_{mPQ} = Z_P + \alpha_Q Z_Q + \alpha_Q Z_Q K_Q - \alpha_{Qs} Z_Q K_Q \qquad 2.14$$

since the circuit is symmetrical we can write

$$Z_{mPQ} = Z + \alpha_Q Z + \alpha_Q Z K_Q - \alpha_{Qs} Z K_Q \qquad 2.15$$

where

α_Q is a per unit distance along line TQ

α_{Qs} is a fractional portion of line TQ, which is determined from the following equation assuming 80% of the line PQ is the desired reach.

$$\alpha_{Qs} = 0.8 - 0.2\left(\frac{Z_P}{Z_Q}\right) \qquad 2.16$$

21

$$\alpha_{Qs} = 0.6 \text{ p.u}$$

$$K_O = \frac{Z_P + Z_{PS}}{Z_R + Z_{RS}}$$

$$K_Q = 1.0$$

If a fault occurs at the relay reach i.e. $\alpha_Q = \alpha_{Qs}$ the last two factors of Equation 2.15 will cancel each other and we are left with $Z + \alpha_{Qs}Z$ which is equal to the actual line impedance, if $\alpha_Q > \alpha_{Qs}$ the measured impedance will be greater than the setting and if $\alpha_Q < \alpha_{Qs}$ the measurand will be smaller.

Considering a fault along line PTR then

$$Z_{mPR} = Z + \alpha_R Z + \alpha_R Z K_R - \alpha_{RS} Z K_R \qquad\qquad 2.17$$

The Z_{mPR} measurand is equal to the relay setting for faults at the reach point ($\alpha_R = \alpha_{RS}$), higher for $\alpha_R > \alpha_{RS}$ and smaller for $\alpha_R < \alpha_{RS}$.

From Equations 2.15 and 2.17 we conclude that the two measurands give the correct discrimination for faults each on its own leg.

Now in what way Z_{mPQ} behaves for faults on leg R, and how does Z_{mPR} behave for faults on leg Q ?

Consider a fault on leg Q

$$Z_{mPQ} = Z + \alpha_Q Z + \alpha_Q Z K_Q - \alpha_{Qs} Z K_Q$$

$$Z_{mPR} = Z + \alpha_Q Z + \alpha_Q Z K_Q - \alpha_{RS} Z K_R \qquad\qquad 2.18$$

For faults on leg R

$$Z_{mPR} = Z + \alpha_R Z + \alpha_R Z K_R - \alpha_{RS} Z K_R$$

$$Z_{mPQ} = Z + \alpha_R Z + \alpha_R Z K_R - \alpha_{Qs} Z K_Q \qquad\qquad 2.19$$

The apparent impedance measured with a conventional distance relay and the measurands of Equation 2.18 are depicted in Figure 2.5 along with the two settings, which

22

are identical for this system, $S_Q = Z + \alpha_{QS}Z$ and $S_R = Z + \alpha_{RS}Z$. Based on the logic that, the two measurands each should be below its own setting for a fault to be cleared, it is obvious that the relay gives the correct discrimination for all fault location. Clearly it can be noted from these graphs that a constant impedance is subtracted from the impedance measured by the conventional distance relay for all fault locations. Similar graphs, which are identical in this case, could be drawn for the measurands of Equation 2.19.

In this case, the same graphs could be obtained for the relays at ends R and Q.

In Figure 2.4, if the source impedance at the relaying point varies, end P in this case, while keeping it equal at the other two ends, the relay still gives the correct discrimination between internal and external faults for all fault location along lines P-T-Q and P-T-R.

2.3.2 Teed Circuit with Equal Leg Lengths and One Remote End is Open Circuit

Considering an extreme case, in which the short circuit level at one end is reduced to zero, end R, in Figure 2.4. Assuming a fault on leg Q the infeed factor K_Q, for the relay at P, in this case is zero.

Rewriting the measurands given by Equations 2.18 and 2.19 for $K_Q = 0.0$ gives:

$$Z_{mPQ} = Z + \alpha_Q Z$$

$$Z_{mPR} = Z + \alpha_Q Z - \alpha_{RS} Z K_R$$

and for a fault on leg R

23

$$Z_{mPR} = Z + \alpha_R Z + \alpha_R Z K_R - \alpha_{RS} Z K_R$$

$$Z_{mPQ} = Z + \alpha_R Z + \alpha_R Z K_R$$

The above equations are drawn in Figure 2.6 and Figure 2.7. It can be seen from these graphs that for a fault on leg Q the correct discrimination is obtained, while for faults on leg R the relay underreaches. The measurand Z_{mPQ} for the above system coincides with the impedance measured with conventional distance relay. This is true since for faults on leg Q there is no infeed from leg R.

Therefore, it can be concluded that, for this system the adaptive scheme will behave equally as a conventional relay, but if an on-off signal can be transmitted, in real time, from the relay at end R giving an indication that the fault is on leg R then the desired reach could be achieved. This option will not be considered as it reduces the merits of the adaptive scheme in that no real time data is needed from the remote ends.

2.3.3 Teed Circuit with Unequal Leg Lengths and Source Impedances

Transmission lines of the same length to the Tee point were discussed in the previous sections for different source impedances. The general case is that of system having arms of unequal length, at the end of which the source impedances are different. Such a system is shown in Figure 2.8.

If the relay at end P is set to reach 80% of the distance from the relay location to the far ends, the

24

variation of the measurands with different fault locations along lines PQ and PR are shown in Figure 2.9 and Figure 2.10. The relay in this case gives a full coverage for faults on leg R (which is shorter than Q) and it underreaches for faults on leg Q. The maximum distance that can be protected on line TQ could be calculated by equating the setting of the line PR with the measurand allocated for faults on R when the fault is on Q i.e.:

$$Z_P + \alpha_{RS}Z_R = Z_P + \alpha_Q Z_Q + \alpha_Q Z_Q K_Q - \alpha_{RS}Z_R K_R$$

solving for α_Q gives:

$$\alpha_Q = \frac{\alpha_{RS}Z_R(1 + K_R)}{Z_Q(1 + K_Q)} \qquad\qquad 2.20$$

It may be concluded here that, in general the adaptive scheme can give an improved coverage over conventional distance scheme. The impedance measured with conventional schemes is correct for faults along line P-T, Z_{mPQ} is correct for faults along line T-Q and Z_{mPR} is correct for faults along line T-R. The adaptive scheme reach is determined by one of the measurands i.e. Z_{mPQ} or Z_{mPR} if no real time signalling is assumed between the three terminals.

2-4 Practical Implementation Consideration

In order to put the scheme into practice it is necessary to manipulate the various signals for its implementation in a microprocessor based distance relay. Considering for example Equation 2.11, where the measurand is of the form:

$$Z_{mPQ} = Z_{mP} - \alpha_{QS}Z_QK_Q \qquad 2.21$$

This can be written as

$$Z_{mPQ} = \frac{V_P}{I_P} - \alpha_{QS}Z_QK_Q \qquad 2.22$$

where

$$K_Q = \frac{I_{RS}}{I_P} + \frac{Z_PI_{PT} - V_{PT}}{(Z_R + Z_{RS})I_P} \qquad 2.23$$

we can write

$$V_{PT} = V_P - V_{PS} \qquad 2.24$$

$$I_{PT} = I_P - I_{PS} \qquad 2.25$$

where

V_{PT} and I_{PT} are the superimposed voltage and current at end P.

V_P and I_P are the postfault voltage and current at end P, and V_{PS} and I_{PS} are the prefault values.

$$Z_{mPQ} = \frac{V_P - \alpha_{QS}Z_QI_{RS} - \alpha_{QS}Z_Q\{\, [Z_P(I_P - I_{PS}) - (V_P - V_{PS})]/(Z_R + Z_{RS})]\}}{I_P}$$
$$2.26$$

$$Z_{mPQ} = \left\{ \frac{V_P\left(1 + \dfrac{\alpha_{QS}Z_Q}{Z_R + Z_{RS}}\right) - \alpha_{QS}Z_Q\left[I_{RS} - \dfrac{I_{PS}\,Z_P}{Z_R + Z_{RS}} + \dfrac{V_{PS}}{Z_R + Z_{RS}}\right]}{I_P} \right.$$
$$\left. - \frac{\alpha_{QS}\,Z_Q\,Z_P}{Z_R + Z_{RS}} \right\}$$

$$Z_{mPQ} = \frac{V_P + k_1V_P - k_1V_{PS} + k_2I_{PS} - k_3I_{RS}}{I_P} - k_2 \qquad 2.27$$

where

$$|k_1| = \left| \frac{\alpha_{QS}\,Z_Q}{Z_R + Z_{RS}} \right| \qquad\qquad \underline{/k_1} = \underline{/\_\dfrac{Z_Q}{Z_R + Z_{RS}}} \qquad 2.28$$

$$|k_2| = \left| \frac{\alpha_{QS}\,Z_Q\,Z_P}{Z_R + Z_{RS}} \right| \qquad\qquad \underline{/k_2} = \underline{/\_\dfrac{Z_Q\,Z_P}{Z_R + Z_{RS}}} \qquad 2.29$$

$$|k_3| = |\,\alpha_{QS}\,Z_Q\,| \qquad\qquad\qquad \underline{/k_3} = \underline{/\_Z_Q} \qquad 2.30$$

The following comments can be made on the above factors.

a) The angle of k_1 is in general negative but is small and tends to zero, because $/\underline{Z}_O$ tends to $/\underline{Z}_R + Z_{RS}$.

b) The component $|k_2|/\underline{k}_2 I_{PS}$ can be derived by passing I_P through a delay circuit adjusted to a value $nT - /\underline{k}_2/W_O$ where nT is an integer number of multiples of the nominal power frequency period T; $/\underline{k}_2$ is positive and hence the negative sign places I_P in the correct position. A value of $n=5$ would ensure that, following a fault, the steady state component of I_P is maintained long enough until the tripping is initiated.

c) The component $|k_1|/\underline{k}_1 V_{PS}$ is similarly derived by delaying V_P by an amount $nT - /\underline{k}_1/W_O$.

d) The component $|k_3|/\underline{k}_3 I_{RS}$ would need to be derived from a circuit generating a sine wave of magnitude $k_3|I_{RS}|$ and adjusted to be in phase with $/\underline{I}_{RS}$. This could be done by periodically transmitting a signal from end R to identify, say, the negative to positive zero crossing of I_{RS} together with a signal describing its peak value or magnitude. This could be achieved by means of a suitable array within a digital processor, which provides updating of the magnitude and phase of the generated sine wave in accordance with variations in $|I_{RS}|$ and $/\underline{I}_{RS}$ observed at the remote end. Since $/\underline{k}_3$ is positive it would be necessary to delay the output of the sine wave generator as described above by an amount $nT - /\underline{k}_3/W_O$.

e) If a voltage signal comprising the 4 components derived as indicated in (a) through (d) above is fed to an

impedance measurement processor together with the locally
derived signal I_P then each value of the sampled impedance
thereby derived can be used in conjunction with the real
and imaginary components of the constant values
α_{QS} Z_Q Z_P/Z_R + Z_{RS} as indicated in Figure 2.11.

Similar arrangement can be made for the measurand
Z_{mPR} by using the related parameters (see Appendix 2B).
The performance equation is reproduced below.

$$Z_{mPR} = \frac{V_P + k'_1 V_P - k'_1 V_{PS} + k'_2 I_{PS} - k'_3 I_{QS}}{I_P} - k'_2 \qquad 2.31$$

2.5 Three Phase System

The foregoing analysis and discussions were based on a
single phase system where the basic principle of the new
method is outlined. As it is usual in distance
protection, various measurands corresponding to each
element will be employed. If the phases of a three-phase
system are labelled as a, b, c then there are a total of
ten possible faults that can be seen by the relay [16,38].
They are:

    a-ground
    b-ground
    c-ground
    a-b
    a-c
    b-c
    a-b-ground
    a-c-ground
    b-c-ground
    a-b-c-ground

28

Any fault can be cleared by employing only six relays these correspond to three phase-ground faults and three phase-phase faults. For example, for an a-b-ground fault the a-b, a-ground and b-ground relays will produce the correct operation. In the following sections, the fault have been divided into two general types; phase-ground fault, and phase-phase faults.

2.5.1 Single Phase to Ground Faults

i- For a single phase to ground fault the basic voltage and current measurands would be V_a and $I_a + KI_{res}$ for the a-phase to ground faults.

The impedance measured using the normal residually compensated signals would be given by:

$$Z_{mPa} = \frac{V_{Pa}}{I_{Pa} + KI_{resP}} \qquad 2.32$$

As shown in Appendix 2C, the measurand for faults on leg Q after the compensation from end R will take the form below.

$$Z_{mPQa} = \frac{V_{Pa}}{I_{Pa} + KI_{resP}} - \alpha_{QS} Z_{Q1} K_{Qa} \qquad 2.33$$

where

$$K_{Qa} = \frac{I_{RSa} + KI_{resRS}}{I_{Pa} + KI_{resP}} + \frac{1}{(Z_{R1} + Z_{RS1})(I_{Pa} + KI_{resP})} *$$

$$[\frac{(K - K_{RS})Z_{RS1} ((1 + 3K)Z_{P1}I_{resPT} - V_{resPT})}{((1 + 3K)Z_{R1} + (1 + 3K_{RS})Z_{RS1})} -$$

$$V_{PTa} + (I_{PTa} + KI_{resPT})Z_{P1}] \qquad 2.34$$

the parameters of the above equation are also defined in

29

Appendix 2C.

In Equation 2.33, after substitution for the superimposed V_{resPT}, I_{resPTV}, V_{PTa}, I_{PTa} values by,

$$V_{resPT} = V_{resP} - V_{resPS} \qquad\qquad 2.35$$

$$I_{resPT} = I_{resP} - I_{resPS} \qquad\qquad 2.36$$

$$V_{PTa} = V_{Pa} - V_{PSa} \qquad\qquad 2.37$$

$$I_{PTa} = I_{Pa} - I_{PSa} \qquad\qquad 2.38$$

then, the practical equation could take the following form:

$$
\begin{aligned}
Z_{mPQa} = {} & \frac{1}{I_{Pa}+KI_{resP}} \left[\left(1 + \frac{\alpha_{QS}\ Z_{Q1}}{Z_{R1} + Z_{RS1}} \right) V_{Pa} - \right. \\[2ex]
& \left(\frac{\alpha_{QS}\ Z_{Q1}}{Z_{R1} + Z_{RS1}} \right) V_{PSa} - \left(\alpha_{QS}\ Z_{Q1} \right) I_{RSa} - \\[2ex]
& \left(\alpha_{QS}\ Z_{Q1}K \right) I_{resRS} + \left(\frac{\alpha_{QS}\ Z_{Q1}\ Z_{P1}}{Z_{R1} + Z_{RS1}} \right) I_{PSa} + \\[2ex]
& \left(\frac{\alpha_{QS}\ Z_{Q1}\ Z_{P1}\ K}{Z_{R1} + Z_{RS1}} \right) I_{resPS} + \\[2ex]
& \left(\frac{\alpha_{QS}\ Z_{P1}\ Z_{RS1}(K-K_{RS})}{(Z_{R1}+Z_{RS1})\ \{(1+3K)Z_{R1}+(1+3K_{RS})Z_{RS1}\}} \right) V_{resP} - \\[2ex]
& \left(\frac{\alpha_{QS}\ Z_{P1}\ Z_{RS1}(K-K_{RS})}{(Z_{R1}+Z_{RS1})\ \{(1+3K)Z_{R1}+(1+3K_{RS})Z_{RS1}\}} \right) V_{resPS} - \\[2ex]
& \left(\frac{\alpha_{QS}\ Z_{P1}\ Z_{Q1}\ Z_{RS1}(K-K_{RS})(1+3K)}{(Z_{R1}+Z_{RS1})\{\ (1+3K)Z_{R1}+(1+3K_{RS})Z_{RS1}\ \}} \right) I_{resP} + \\[2ex]
& \left(\frac{\alpha_{QS}\ Z_{P1}\ Z_{Q1}\ Z_{RS1}(K-K_{RS})(1+3K)}{(Z_{R1}+Z_{RS1})\{\ (1+3K)Z_{R1}+(1+3K_{RS})Z_{RS1}\ \}} \right) I_{resPS}] - \\[2ex]
& \left(\frac{\alpha_{QS}\ Z_{Q1}\ Z_{P1}}{Z_{R1} + Z_{RS1}} \right) \qquad\qquad 2.39
\end{aligned}
$$

In short Equation 2.39 can be written as:

$$Z_{mPQa} = \frac{1}{I_{Pa}+KI_{resP}}\{ V_{Pa}+ K_1V_{Pa} - K_1V_{PSa} -$$

$$K_2I_{RSa} - K_3I_{resRS} + K_4V_{resP} -$$

$$K_4V_{resPS} - K_5I_{resP} + K_5I_{resPS} +$$

$$K_6I_{PSa} + K_7I_{resPS} \} - K_6 \qquad\qquad 2.40$$

where

$$K_1 = \frac{\alpha_{QS} \, Z_{Q1}}{Z_{R1} + Z_{RS1}}$$

$$K_2 = \alpha_{QS} \, Z_{Q1}$$

$$K_3 = \alpha_{QS} \, Z_{Q1} \, K$$

$$K_4 = \frac{\alpha_{QS} \, Z_{P1} \, Z_{RS1}(K-K_{RS})}{(Z_{R1}+Z_{RS1}) \, \{(1+3K)Z_{R1}+(1+3K_{RS})Z_{RS1})\}}$$

$$K_5 = \frac{\alpha_{QS} \, Z_{P1} \, Z_{Q1} \, Z_{RS1}(K-K_{RS})(1+3K)}{(Z_{R1}+Z_{RS1}) \, \{(1+3K)Z_{R1}+(1+3K_{RS})Z_{RS1})\}}$$

$$K_6 = \frac{\alpha_{QS} \, Z_{Q1} \, Z_{P1}}{Z_{R1} + Z_{RS1}}$$

$$K_7 = \frac{\alpha_{QS} \, Z_{Q1} \, Z_{P1}K}{Z_{R1} + Z_{RS1}}$$

The following points should be noticed:

1) For a balanced system the steady state residual currents and voltages are zero.

2) The steady state voltages and currents may be derived as suggested for the case of a single phase representation. These will be explained further in Chapter 4.

For a symmetrical system the residual steady state voltages and currents are zero, therefore Equation 2.40 is reduced to the form:

31

$$Z_{mPQa} = \frac{1}{I_{Pa}+KI_{resP}} \{ \ V_{Pa}+ K_1V_{Pa} - K_1V_{PSa} -$$

$$K_2I_{RSa} + K_4V_{resP} - K_5I_{resP} +$$

$$K_6I_{PSa} \ \} - K_6 \qquad\qquad 2.41$$

ii- Similarly, for the a-ground fault on leg R, the measurand Z_{mPRa} will take the form:

$$Z_{mPRa} = \frac{V_{Pa}}{I_{Pa} + KI_{resP}} - \alpha_{RS} \ Z_{R1} \ K_{Ra} \qquad 2.42$$

where

$$K_{Ra} = \frac{I_{QSa}+KI_{resQS}}{I_{Pa}+KI_{resP}} + \frac{1}{(Z_{Q1}+ Z_{QS1})(I_{Pa}+KI_{resP})} \ *$$

$$[\ \frac{(K-K_{QS})Z_{QS1} \ ((1+3K)Z_{P1}I_{resPT}- V_{resPT})}{((1+3K)Z_{Q1}+(1+3K_{QS})Z_{QS1})} -$$

$$V_{PTa}+(I_{PTa}+KI_{resPT})Z_{P1} \ ] \qquad 2.43$$

The practical equation is given by:

$$Z_{mPRa} = \frac{1}{I_{Pa}+KI_{resP}} \ [\ (\ 1 + \frac{\alpha_{RS} \ Z_{R1}}{Z_{Q1} + Z_{QS1}} \ ) \ V_{Pa} -$$

$$(\ \frac{\alpha_{RS} \ Z_{R1}}{Z_{Q1} + Z_{QS1}} \ ) \ V_{PSa} - (\ \alpha_{RS} \ Z_{R1} \ ) \ I_{QSa} -$$

$$(\ \alpha_{RS} \ Z_{R1}K \ ) \ I_{resQS}+ (\ \frac{\alpha_{RS} \ Z_{R1} \ Z_{P1}}{Z_{Q1} + Z_{QS1}}) \ I_{PSa} +$$

$$(\ \frac{\alpha_{RS} \ Z_{R1} \ Z_{P1} \ K}{Z_{Q1} + Z_{QS1}} \ ) \ I_{resPS} \ +$$

$$(\ \frac{\alpha_{RS} \ Z_{P1} \ Z_{QS1}(K-K_{QS})}{(Z_{Q1}+Z_{QS1}) \ \{(1+3K)Z_{Q1}+(1+3K_{QS})Z_{QS1})\}} \ ) \ V_{resP} -$$

$$(\ \frac{\alpha_{RS} \ Z_{P1} \ Z_{QS1}(K-K_{QS})}{(Z_{Q1}+Z_{QS1}) \ \{(1+3K)Z_{Q1}+(1+3K_{QS})Z_{QS1})\}} \ ) \ V_{resPS} -$$

$$(\ \frac{\alpha_{RS} \ Z_{P1} \ Z_{R1} \ Z_{QS1}(K-K_{QS})(1+3K)}{(Z_{Q1}+Z_{QS1})\{ \ (1+3K)Z_{Q1}+(1+3K_{QS})Z_{QS1}) \ \}} \ ) \ I_{resP} +$$

$$(\ \frac{\alpha_{RS} \ Z_{P1} \ Z_{R1} \ Z_{QS1}(K-K_{QS})(1+3K)}{(Z_{Q1}+Z_{QS1})\{ \ (1+3K)Z_{Q1}+(1+3K_{QS})Z_{QS1}) \ \}} \ ) \ I_{resPS}]-$$

$$(\ \frac{\alpha_{RS} \ Z_{R1} \ Z_{P1}}{Z_{Q1} + Z_{QS1}}) \qquad\qquad 2.44$$

In short Equation 2.44 can be written as:

$$Z_{mPRa} = \frac{1}{I_{Pa}+KI_{resP}} \{ V_{Pa} + K'_1 V_{Pa} - K'_1 V_{PSa} -$$

$$K'_2 I_{QSa} - K'_3 I_{resQS} + K'_4 V_{resP} -$$

$$K'_4 V_{resPS} - K'_5 I_{resP} + K'_5 I_{resPS} +$$

$$K'_6 I_{PSa} + K'_7 I_{resPS} \} - K'_6 \qquad\qquad 2.45$$

where

$$K'_1 = \frac{\alpha_{RS} Z_{R1}}{Z_{Q1} + Z_{QS1}}$$

$$K'_2 = \alpha_{RS} Z_{R1}$$

$$K'_3 = \alpha_{RS} Z_{R1} K$$

$$K'_4 = \frac{\alpha_{RS} Z_{P1} Z_{QS1}(K-K_{QS})}{(Z_{Q1}+Z_{QS1}) \{(1+3K)Z_{Q1}+(1+3K_{QS})Z_{QS1}\}}$$

$$K'_5 = \frac{\alpha_{RS} Z_{P1} Z_{R1} Z_{QS1}(K-K_{QS})(1+3K)}{(Z_{Q1}+Z_{QS1}) \{(1+3K)Z_{Q1}+(1+3K_{QS})Z_{QS1}\}}$$

$$K'_6 = \frac{\alpha_{RS} Z_{R1} Z_{P1}}{Z_{Q1} + Z_{QS1}}$$

$$K'_7 = \frac{\alpha_{RS} Z_{R1} Z_{P1}K}{Z_{Q1} + Z_{QS1}}$$

Equations 2.40 and 2.45 are the general expressions for the a-phase to ground faults. Similar expressions apply for the b and c phases

2.5.2 Phase to Phase Faults

For the b-c element the following modified measurands could be employed (see Appendix 2D).

$$Z_{mPQbc} = Z_{mPbc} - \alpha_{QS} Z_{Q1} K_{Qbc} \qquad\qquad 2.46$$

This should be compared with $Z_{P1} + \alpha_{QS} Z_{Q1}$ for the faults on Q.

and

$$Z_{mPRbc} = Z_{mPbc} - \alpha_{RS} Z_{R1} K_{Rbc} \qquad\qquad 2.47$$

33

is compared with $Z_{P1} + \alpha_{RS} Z_{R1}$ for faults on leg R.

where

$$Z_{mPbc} = \frac{V_{bc}}{I_{Pb} - I_{Pc}} \qquad\qquad 2.48$$

$$= \frac{V_{bc}}{I_{Pbc}} \qquad\qquad 2.49$$

$$K_{Qbc} = \frac{I_{RSbc}}{I_{Pbc}} + \frac{Z_{P1} I_{PTbc} - V_{PTbc}}{(Z_{R1} + Z_{RS1}) I_{Pbc}} \qquad\qquad 2.50$$

$$K_{Rbc} = \frac{I_{QSbc}}{I_{Pbc}} + \frac{Z_{P1} I_{PTbc} - V_{PTbc}}{(Z_{Q1} + Z_{QS1}) I_{Pbc}} \qquad\qquad 2.51$$

2.6 Summary

In this Chapter an adaptive distance scheme for the protection of Teed circuits is introduced. The basic requirements, the performance equations and suggestions for its implementation in a microprocessor based distance relay have been discussed. In general, the scheme gives an improved coverage over conventional distance relays. The optimum performance can be achieved if the remote faulted leg can be identified locally; i.e. without real time signalling from the far ends, but this has not been accomplished.

34
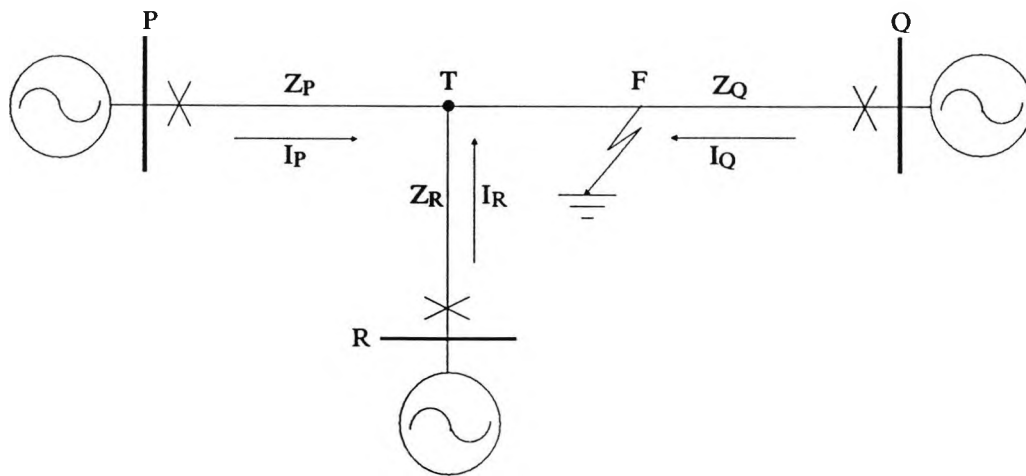
Fig. 2.1 Typical three teminal line with current contribution for a fault on leg Q
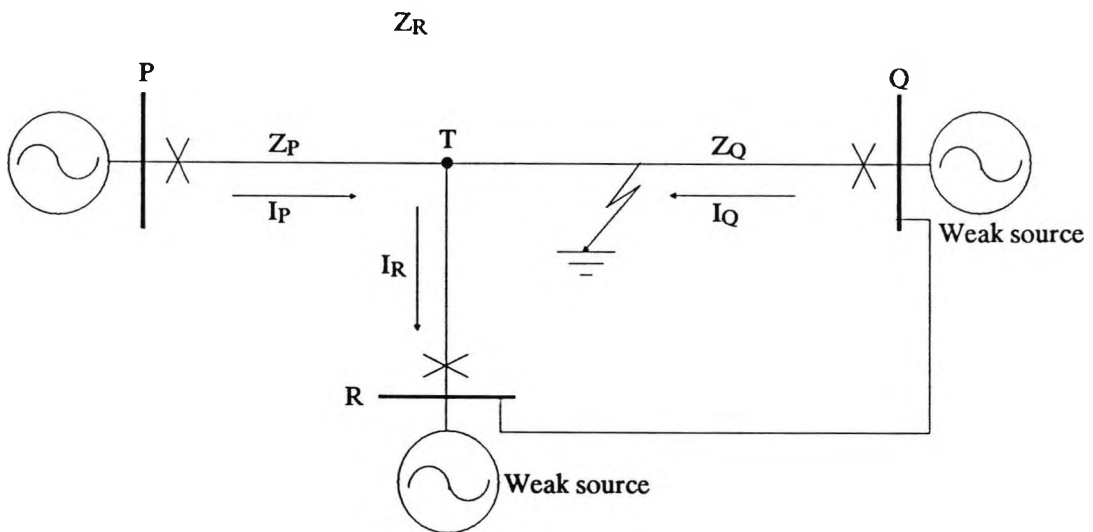
Fig. 2.2 Faulted Teed system with out-feed
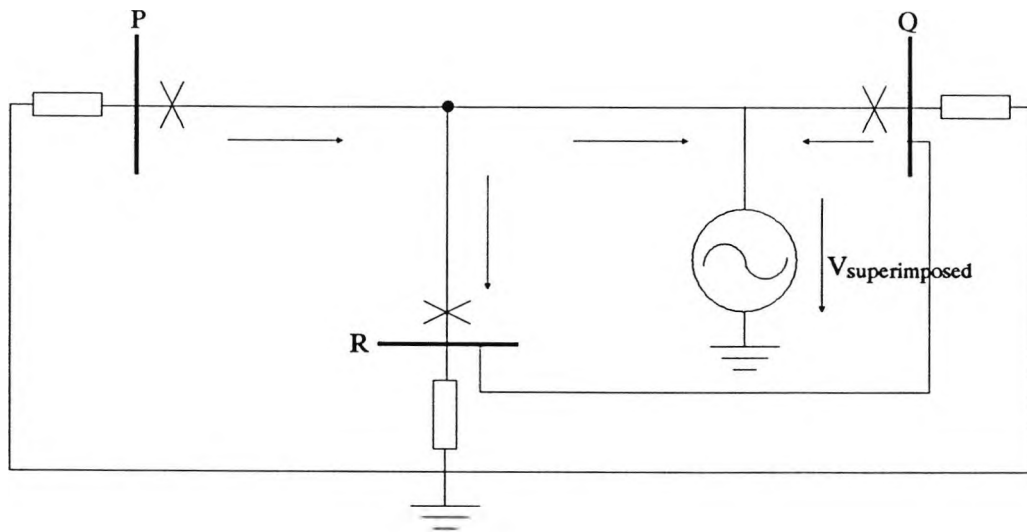
Fig 2.3 Teed system in the superimposed state with current distribution
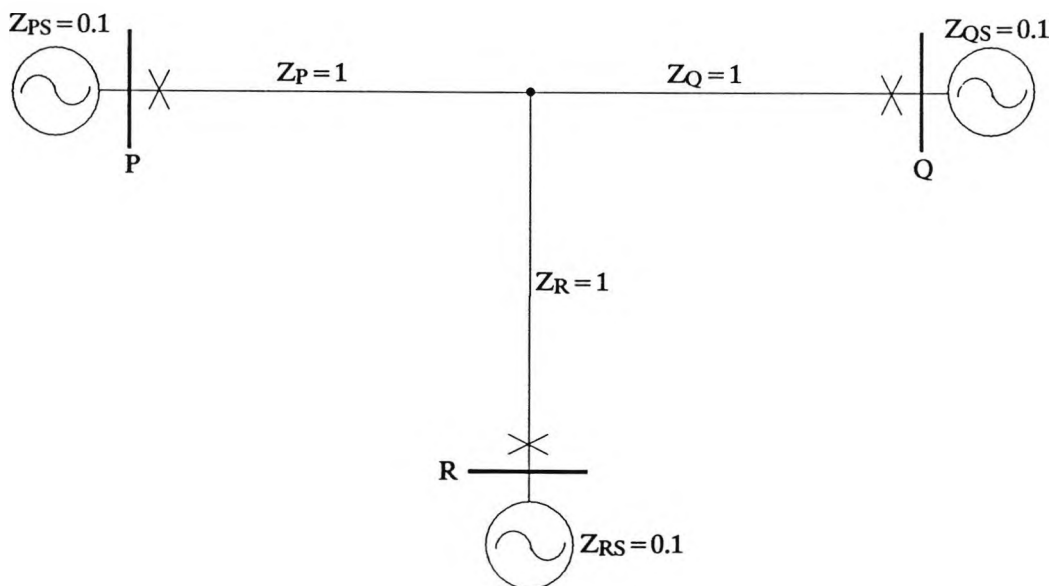
Fig. 2.4 Symmetrical Teed system
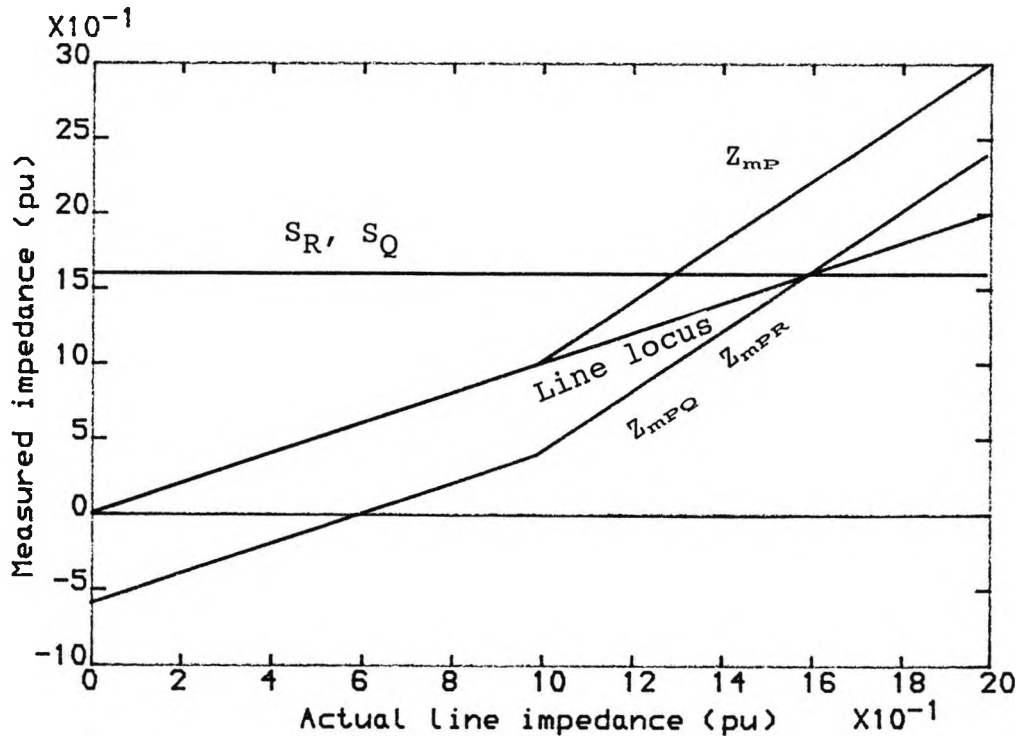
Fig.2.5 Relay measurement at end P for
faults along line P-T-Q
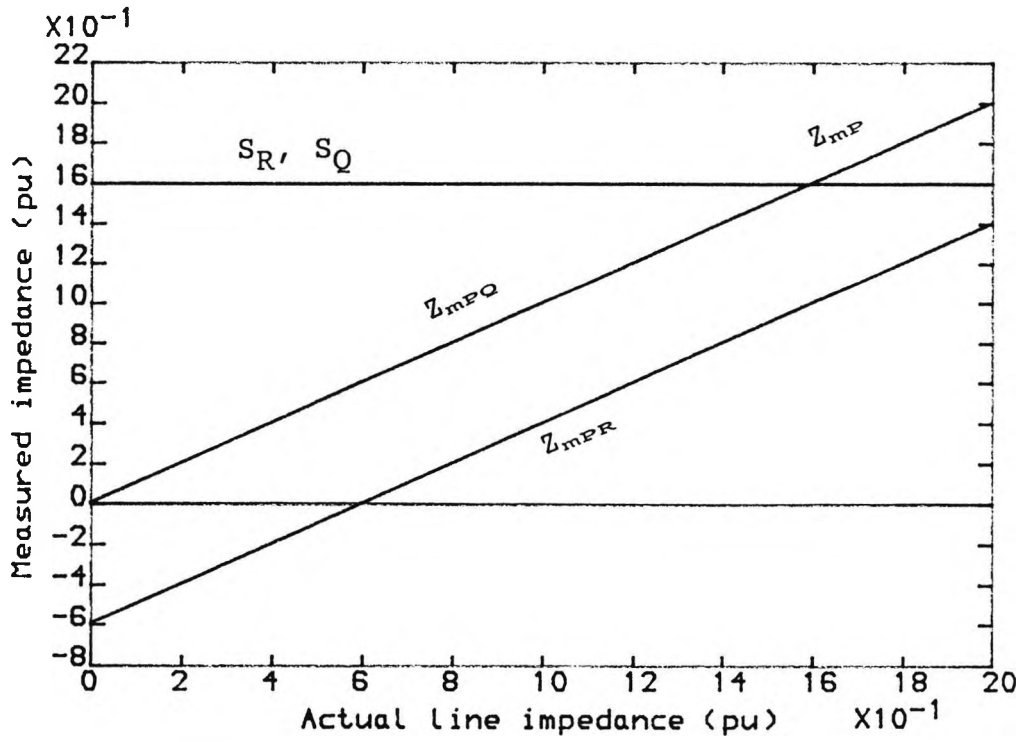
Fig.2.6 Relay measurement at end P for
faults along line P-T-Q
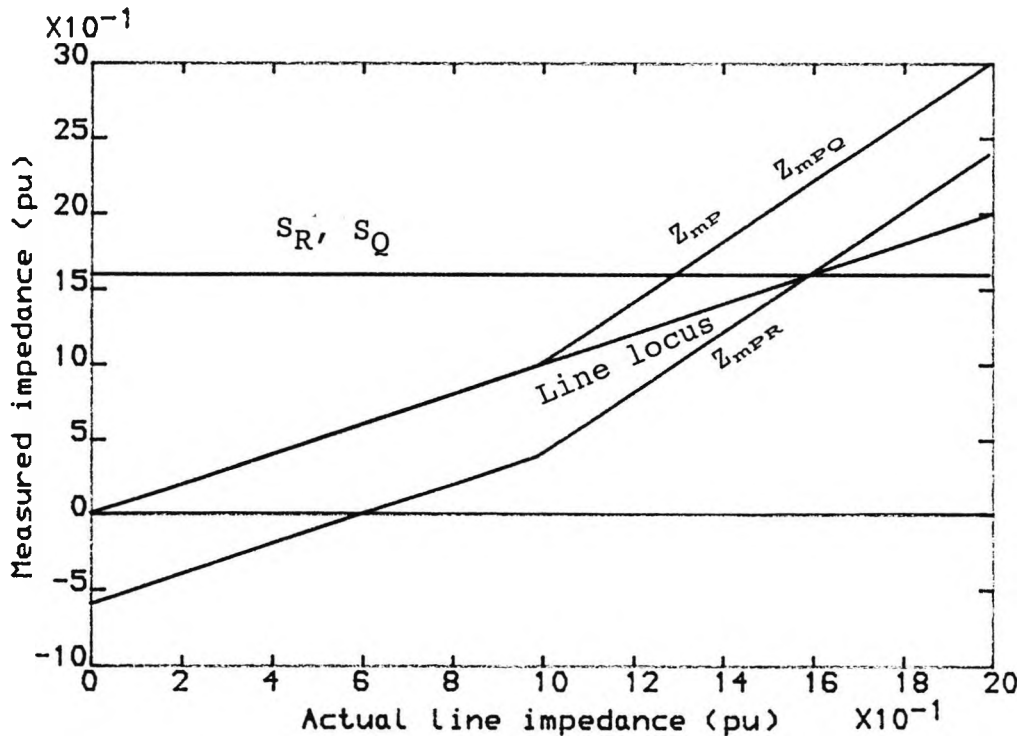
Fig.2.7 Relay measurement at end P for
faults along line P-T-R
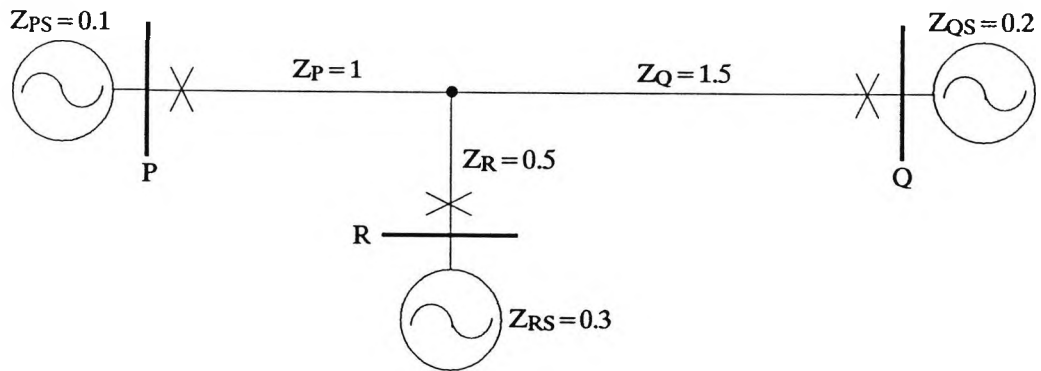
Fig 2.8 Teed system with different leg lengths & source impedances
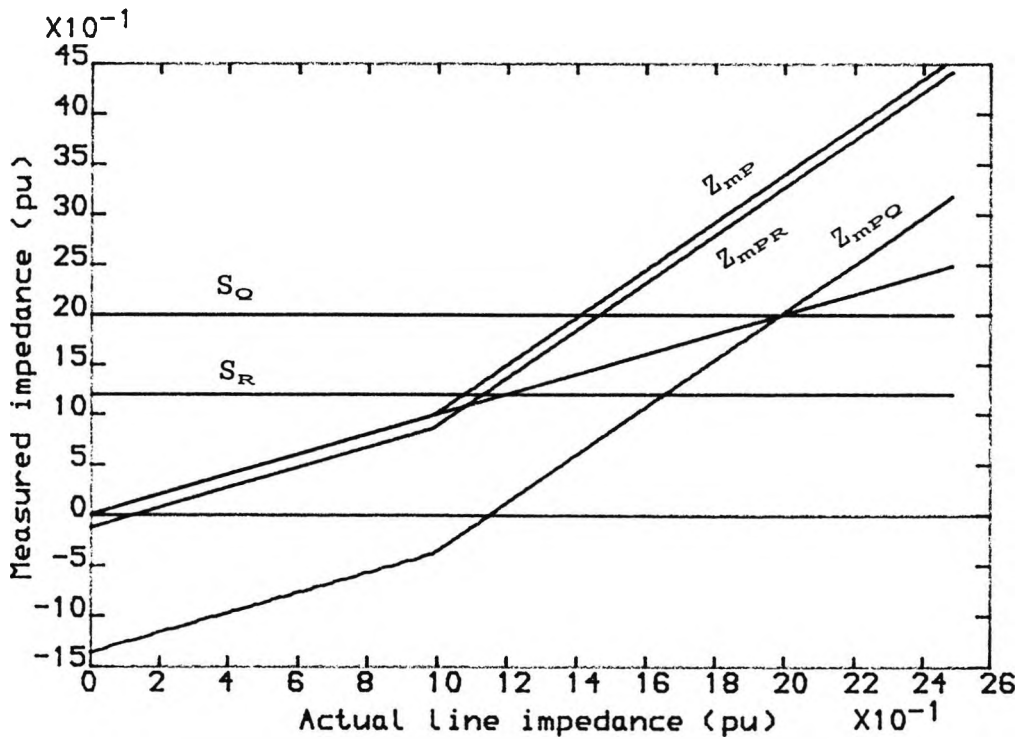
Fig.2.9 Relay measurement at end P for
faults along line P-T-Q
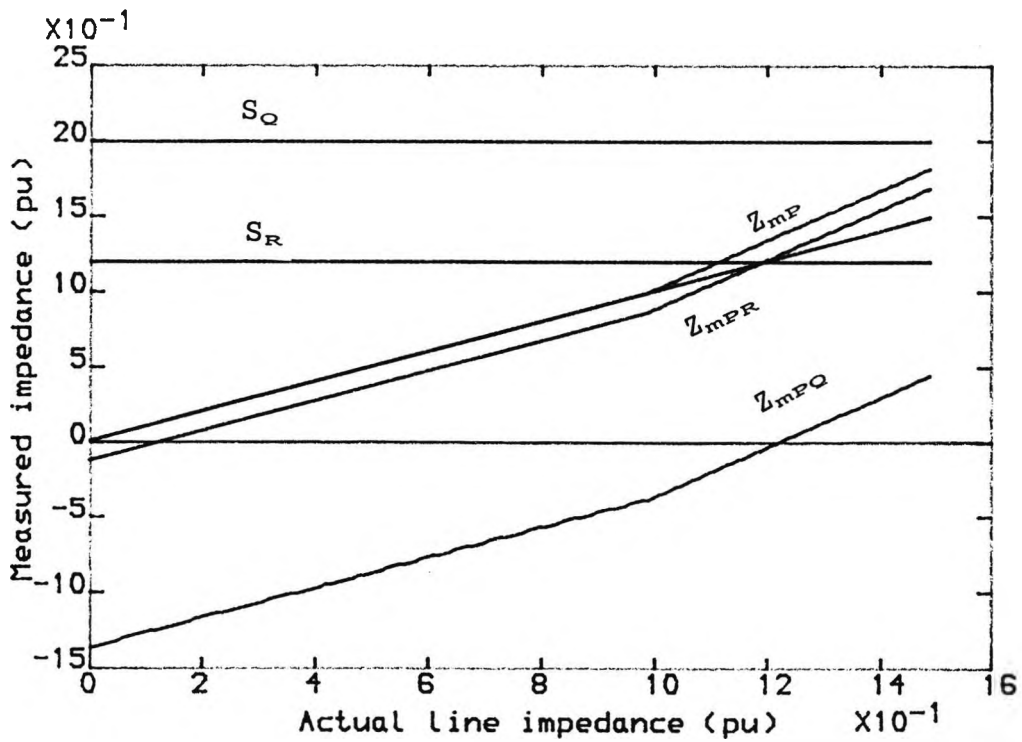
Fig.2.10 Relay measurement at end P for
faults along line P-T-R
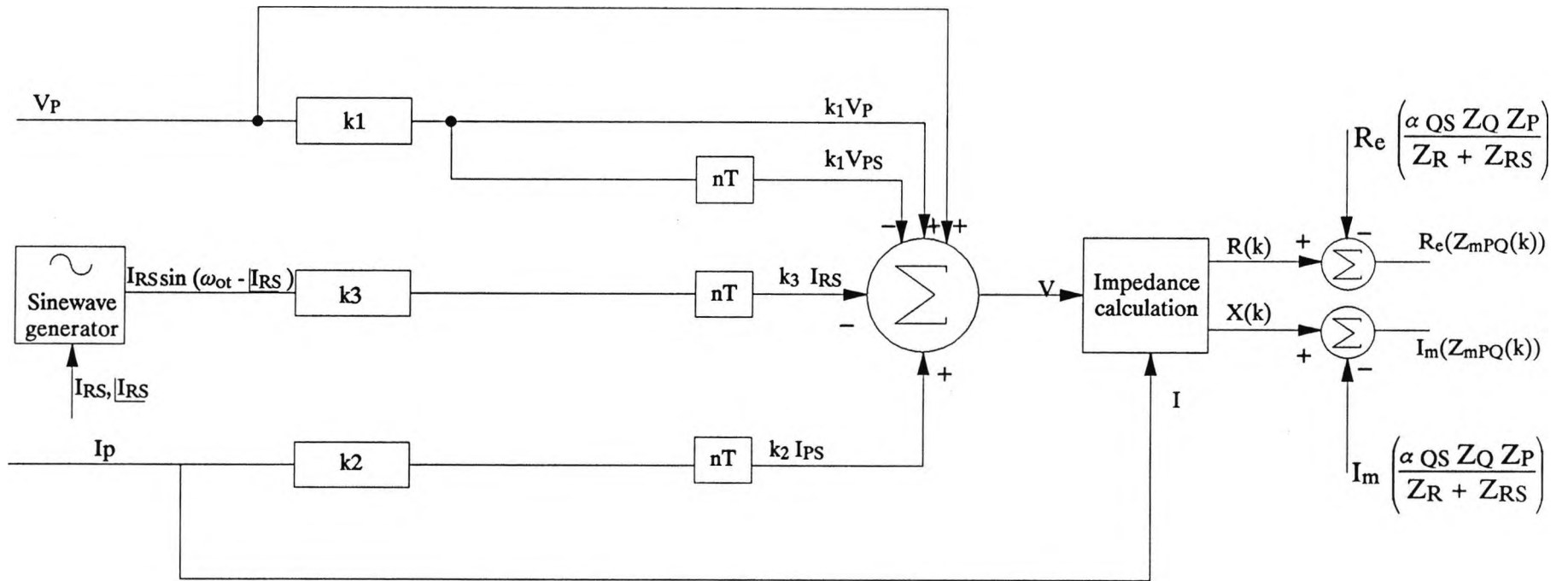
Fig 2.11 Basic arrangement of the adaptive distance relay

CHAPTER 3

PRIMARY SYSTEM SIMULATIONS

Digital computers nowadays are very powerful tools in engineering fields. They can be used to accurately simulate and test a system or component before they are actually built or manufactured.

The importance of digital computers in design and test stages of the components of power systems is well known. Advanced methods are now available for modelling and testing complex power systems on a digital computer [17,18,19]. These simulation programmes provide not only the steady state, but also the transient response. They are of great values to protective relays designers, new designs can be tested in laboratories before they are actually installed on the system. In particular, for Very and/or Ultra-High-Speed protection schemes, where the measurement is carried out in a very short time after fault inception, the waveforms from which measurement is made must contain all transient phenomena which occur in a real system after a short circuit fault. These simulation programmes provide, in numerical forms, the voltage and current waveforms at the relaying points.

In the early stages of the project a Fortran program, based on phasor values, was developed for the fault analysis of a Teed system, in which the changes in fault resistance, fault position, line length and source impedances are easily made. A connection matrix method of analysis has been used to represent faults of any type by

the choice of the matrix elements as described in reference [20]. The loop-current and nodal-voltage methods of analysis have been used in separate programmes for the prefault and fault calculations. A brief description of these methods is given in this Chapter.

At a later stage the Electromagnetic Transient Program [EMTP] became available and is used for the primary system simulation. This package can be used to solve any network which consists of interconnection of resistances, inductances, capacitances, single and multi-π-circuits, distributed-parameter lines, frequency dependent parameters, and certain other elements.

3.1 Prefault Calculation

Balanced operation i.e. each of the three phases of any part of the system has currents and voltages which are equal and 120° displaced with respect to each other, is the basis of the simplicity for three phase calculations. To maintain balanced operation each item of system plant must be symmetrical i.e. have identical impedances in each line, equal mutual impedances between phases and ground, and equal shunt admittance to ground/neutral. This is the case with machines and transformers, it is valid for transmission lines if these are fully transposed. For balanced conditions, a single phase representation gives the necessary solutions, and this is considered in the present simulation.

Figure 3.1 shows a system that contains a general configuration of a Teed system in which a double Teed

36

circuit is assumed and a remote ties exist between the three terminals. In what follows, it is assumed that the voltages and currents are sinusoidal, which means that they can be represented in phasor terms. Furthermore the system impedances are calculated at the power frequency i.e. 50 Hz, and the line shunt capacitance is neglected. Hence, the effective line impedance is equal to the positive sequence impedance component. The lines series impedance is calculated from the line length and the impedance per unit length. The source impedances are calculated from the short circuit levels(SCL) at the terminals using the following equation:

$$Z_s = (Voltage)^2 / SCL \qquad\qquad 3.1$$

In order to model a multi-node system it is convenient to represent it by a general admittance relationship in the frequency domain:

$$I = Y.V \qquad\qquad 3.2$$

For the evaluation of voltages and currents at various points of the system a systematic method based on the loop currents is used [20,21]. In a network if all the branches are replaced by lines, we obtain what is called a linear graph, or simply graph of the network. For example, for the system shown in Figure 3.2 the graph is drawn in Figure 3.3 on which also the basic loop currents are depicted. For this specific example the loop incidence matrix [C], whose elements are 0,1,-1, is:

$$[C] = \begin{array}{c} \text{Element} \\ \\ \begin{array}{c} 1 \\ 2 \\ 3 \\ 4 \\ 5 \\ 6 \end{array} \end{array} \begin{array}{cc} \text{Loop1} & \text{Loop2} \\ \left[\begin{array}{cc} 1 & 0 \\ 0 & 1 \\ -1 & -1 \\ 1 & 0 \\ 0 & 1 \\ -1 & -1 \end{array}\right] \end{array} \qquad 3.3$$

By using the same routine for the circuit of Figure 3.1 the [C] matrix is:

$$[C] = \begin{bmatrix} -1 & -1 & -1 & -1 & 1 & 1 & 0 \\ 1 & 1 & 0 & 0 & 0 & -1 & -1 \\ 0 & 0 & 1 & 1 & -1 & 0 & 1 \\ -1 & 0 & 0 & -1 & 0 & 0 & 0 \\ 0 & -1 & -1 & 0 & 0 & 0 & 0 \\ 1 & 0 & 0 & 0 & 0 & 0 & 0 \\ 0 & 1 & 0 & 0 & 0 & 0 & 0 \\ 0 & 0 & 1 & 0 & 0 & 0 & 0 \\ 0 & 0 & 0 & 1 & 0 & 0 & 0 \\ 0 & 0 & 0 & 0 & 1 & 0 & 0 \\ 0 & 0 & 0 & 0 & 0 & 1 & 0 \\ 0 & 0 & 0 & 0 & 0 & 0 & 1 \end{bmatrix} \qquad 3.4$$

In order to calculate the loop impedance matrix $[Z_{Loop}]$; first the branch and source impedances are calculated and stored in the square primitive impedance matrix $[Z]$ and then $[Z_{Loop}]$ is computed from:

$$[Z_{Loop}] = [C]^t[Z][C] \qquad 3.5$$

where $[C]^t$ is the transposed matrix of $[C]$.

The general equation for relating the loop currents and loop voltages is:

$$[E_{Loop}] = [Z_{Loop}][I_{Loop}] \qquad 3.6$$

where

$$[E_{Loop}] = [C]^t[E] \qquad 3.7$$

$[E]$ is the vector of source voltages

The loop currents are calculated by writing Equation 3.6 in the inverted form i.e.:

$$[I_{Loop}] = [Y_{Loop}][E_{Loop}] \qquad\qquad 3.8$$

where

$$[Y_{Loop}] = [Z_{Loop}]^{-1} \qquad\qquad 3.9$$

The following relation holds for branch currents, I_b, and the loop currents:

$$[I_b] = [C][I_{Loop}] \qquad\qquad 3.10$$

The voltage at the source busbars is:

$$[V] = [E] - [Z_s][I_s] \qquad\qquad 3.11$$

with

$[Z_s]$ = 3 x 3 source impedance matrix

$[I_s]$ = vector of the source currents

The Tee point voltage is determined from:

$$V_t = V_s - Z_t I_t \qquad\qquad 3.12$$

where

V_s is any element of the vector $[V]$

Z_t is the impedance of the branch connected to the Tee point and I_t is the current in the same branch.

The voltage at any point on the line connected to the Tee point is given by:

$$V_\alpha = V_t + \alpha Z_t I_t \qquad\qquad 3.13$$

where α is a p.u. line length measured from the Tee point

The above equations give the voltages and currents for a single phase system. As it is a balanced system the other phase values can be derived simply by shifting the above calculated quantities by 240 and 120 degrees.

Figure 3.4 shows the flow chart for the prefault calculation.

39

3.2 Short Circuit Studies

The symmetrical component technique is employed in the
short circuit analysis. This permits the complex
behaviour of the system to be analysed in terms of three
independent phase-sequence circuits i.e.; positive,
negative and zero sequence circuits. For example, the
three phase impedance matrix [z] given by Equation 3.14,
in which the diagonal elements represent the self
impedances and the off-diagonal elements are the mutual
impedances, the symmetrical component transformed
impedance matrix is given by Equation 3.15:

$$[z] = \begin{bmatrix} z_s & z_m & z_m \\ z_m & z_s & z_m \\ z_m & z_m & z_s \end{bmatrix} \qquad\qquad 3.14$$

$$[z_{sc}] = [T]^{-1} [z] [T] \qquad\qquad 3.15$$

where [T] is referred to as the symmetrical component
transformation matrix

$$[T] = \begin{bmatrix} 1 & 1 & 1 \\ 1 & a^2 & a \\ 1 & a & a^2 \end{bmatrix} \qquad\qquad 3.16$$

$$[z_{sc}] = \begin{bmatrix} z_0 & 0 & 0 \\ 0 & z_+ & 0 \\ 0 & 0 & z_- \end{bmatrix} \qquad\qquad 3.17$$

where z_0, z_+, z_- are the zero, positive, and negative
sequence impedances respectively.

$$z_0 = z_s + 2z_m \qquad\qquad 3.18$$

$$z_+ = z_- = z_s - z_m \qquad\qquad 3.19$$

The matrix $[z_{sc}]$ is diagonal, indicating decoupling

40

between the three sequence components.

The following simplifications are assumed in the short circuit analysis:

- Lines are perfectly transposed
- No positive and negative mutual coupling exist between the double circuits.
- Line capacitance is neglected.
- The sources are general and their associated impedances are calculated from the short circuit levels(SCL) at the terminals according to the following equation:

$$Z_s = (\text{Voltage})^2 / \text{SCL} \hspace{4cm} 3.20$$

In order to involve the digital computer in short circuit calculation the nodal-voltage method of network analysis is used to assemble the bus impedance matrix $[Z_{bus}]$ [20,21]. Since there is no coupling between the sequence impedances, the bus impedance matrix in terms of sequence quantities can be obtained by forming the positive, negative, and zero sequence bus impedance matrices independently. In order to facilitate faults on the lines connected to the Tee point, nodes are assumed to exist between the Tee point and the terminating busbars as shown in Figure 3.5. In this general system, from the knowledge of the positive-sequence impedances of the sources and transmission lines the primitive positive sequence impedance matrix $[Z_+]$ is formed. Figure 3.6 shows the graph of the system of Figure 3.5. From this graph the bus incidence matrix A whose elements are 0, 1, -1 is constructed [20]. The A matrix has the value:

41

$$[A] = \begin{bmatrix} -1 & 0 & 0 & 0 & 0 & 0 & 0 & 0 \\ 0 & 0 & 0 & -1 & 0 & 0 & 0 & 0 \\ 0 & 0 & 0 & 0 & -1 & 0 & 0 & 0 \\ 1 & 0 & 0 & 0 & 0 & 0 & 0 & -1 \\ 0 & -1 & 0 & 0 & 0 & 1 & 0 & 0 \\ 0 & 0 & 0 & 1 & 0 & -1 & 0 & 0 \\ 0 & 0 & -1 & 1 & 0 & 0 & 0 & 0 \\ 1 & 0 & -1 & 0 & 0 & 0 & 0 & 0 \\ 0 & -1 & 0 & 0 & 0 & 0 & 1 & 0 \\ 0 & 0 & 0 & 0 & 1 & 0 & -1 & 0 \\ 0 & 0 & -1 & 0 & 1 & 0 & 0 & 0 \\ 1 & 0 & 0 & 0 & -1 & 0 & 0 & 0 \\ 1 & 0 & 0 & -1 & 0 & 0 & 0 & 0 \\ 0 & 0 & 0 & -1 & 1 & 0 & 0 & 0 \\ 0 & -1 & 0 & 0 & 0 & 0 & 0 & 1 \end{bmatrix} \qquad 3.21$$

The positive sequence bus impedance matrix Z_{+bus} is obtained from:

$$[Z_{+bus}] = [A]^t [Z_+][A] \qquad\qquad 3.22$$

Since all elements considered are of static type and the sources are of general type, it is assumed that the negative-sequence bus matrix $[Z_{-bus}]$ is equal to the positive bus matrix $[Z_{+bus}]$.

The zero-sequence impedance bus impedance matrix $[Z_{obus}]$ is similarly computed from the A matrix and the zero sequence primitive impedance matrix $[Z_o]$. It should be noted that the bus incidence matrix A is identical for the three sequence components.

$$[Z_{obus}] = [A]^t [Z_o][A] \qquad\qquad 3.23$$

An important tool for investigating the present approach of fault voltage and current calculation by using the separate programmes, is the principle of superposition. When a fault occurs in a power system the postfault voltage and current are given by:

$$V_{post-fault} = V_{pre-fault} + V_{superimposed} \qquad 3.24$$

$$I_{post-fault} = I_{pre-fault} + I_{superimposed} \qquad 3.25$$

The superimposed components are obtained by replacing the fault by its equivalent impedance $[Z_f]$ in series with the prefault voltage at the fault point, and by short circuiting all the active sources. The superposition of the resulting signals and the prefault values produced by the load flow program then yield the postfault values. Figure 3.7 shows the system of Figure 3.5 in the superimposed state.

Having constructed the positive, negative, and zero sequence bus impedance matrices and stored in the computer, the symmetrical component postfault voltages and currents, for a system with n nodes, are computed from the following general formulas [21]:

$$[V^f_{s,bus}] = [V^o_{s,bus}] + [Z_{s,bus}] \, [I^f_{s,bus}] \qquad 3.26$$

where

s stands for symmetrical component transform.

$[V^f_{s,bus}]$ = 3n unknown postfault voltage vector

$[V^o_{s,bus}]$ = 3n prefault bus voltages vector and is known from the load flow calculation.

$[Z_{s,bus}]$ = 3n x 3n symmetrical component bus impedance matrix.

$[I^f_{s,bus}]$ = 3n unknown bus current vector

Equation 3.26 can be written for each node as:

$$[V^f_{s1}] = [V^o_{s1}] - [Z_{s1q}] \, [I^f_{sq}]$$
$$\cdots\cdots\cdots\cdots\cdots\cdots\cdots\cdots\cdots\cdots\cdots\cdots\cdots\cdots$$
$$[V^f_{sq}] = [V^o_{sq}] - [Z_{sqq}] \, [I^f_{sq}] \qquad 3.27$$
$$\cdots\cdots\cdots\cdots\cdots\cdots\cdots\cdots\cdots\cdots\cdots\cdots\cdots\cdots$$
$$[V^f_{sn}] = [V^o_{sn}] - [Z_{snq}] \, [I^f_{sq}]$$

The voltage vector at the fault point q is:

$$[V^f_{sq}] = [Z^f_s] [I^f_{sq}] \qquad\qquad 3.28$$

or

$$[I^f_{sq}] = [Y^f_s] [V^f_{sq}] \qquad\qquad 3.29$$

where $[Y^f_s]$ is the fault admittance matrix whose elements are defined in reference [20] for all types of faults.

Substituting from Eqn. 3.29 for $[I^f_{sq}]$ the qth Eqn. of 3.27 and solving for the postfault voltage $[V^f_{sq}]$ yields:

$$[V^f_{sq}] = \{ [U] + [Z_{sqq}][Y^f_s] \}^{-1}[V^o_{sq}] \qquad\qquad 3.30$$

where U is a 3x3 identity matrix.

The postfault current at the faulted bus q is obtained by substitution of Eqn. 3.30 into Eqn. 3.29 then:

$$[I^f_{sq}] = [Y^f_s]\{[U] + [Z_{sqq}][Y^f_s]\}^{-1}[V^o_{sq}] \qquad 3.31$$

The voltages at buses other than q can be obtained by substituting for $[I^f_{sq}]$ from Eqn. 3.30. Then

$$[V^f_{si}]=[V^o_{si}]-[Z_{siq}][Y^f_s]\{[U]+[Z_{sqq}][Y^f_s]\}^{-1}[V^o_{sq}] \qquad 3.32$$

Fault current $[I^f_{sij}]$ flowing through the element ij of the network is given by:

$$[I^f_{sij}] = [Y_{sij}][[V^f_{si}] - [V^f_{sj}]] \qquad\qquad 3.33$$

All formulas give the voltages and currents in terms of the symmetrical components. The actual phase values are obtained by multiplying the sequence components values by the symmetrical transformation matrix [T]. For example, for the phase currents we have:

$$[I_{ph,ij}] = [T] [I^f_{sij}] \qquad\qquad 3.34$$

$$\begin{bmatrix} I_a \\ I_b \\ I_c \end{bmatrix} = \begin{bmatrix} 1 & 1 & 1 \\ 1 & a^2 & a \\ 1 & a & a^2 \end{bmatrix} \begin{bmatrix} I_o \\ I_+ \\ I_- \end{bmatrix} \qquad\qquad 3.35$$

44

where I_a, I_b, I_c are the phase currents of phase a, b, c respectively.

Figure 3.8 shows the flow chart for the fault calculation.

3.3 System Simulation Using the EMTP

The Electromagnetic Transient Program [EMTP] is a general program which can be used for the studying of power systems problems as well as some electronic circuits [19]. In this section the basic numerical equations for individual power system components used in the EMTP shall be explained for illustration.

Implicit in this explanation is the use of time-domain representation [19,22,23]. Considering, for example, the circuit in Figure 3.9 which shows the details of a single-phase network elements just for a region around node 1. The node voltages are used as state variables in the EMTP. It is therefore necessary to express the branch currents, i_{12}, i_{13}, etc., as functions of the node voltages.

For an inductance, the relationship between voltage and current is given by the differential equation:

$$v = L \frac{di}{dt} \qquad\qquad 3.36$$

Applying the trapezoidal rule of integration, using the central difference, with time step T to the differential equation yields:

45

$$\frac{v(t)+v(t-T)}{2} = L \frac{i(t)-i(t-T)}{T} \qquad 3.37$$

solving for i(t) gives

$$i(t) = i(t-T) + \frac{T}{2L} \{v(t)+v(t-T)\} \qquad 3.38$$

It is assumed that the variables are known for time t-T, representing initial conditions of the computation. That is, we want to advance the solution one time step, from t-T to time t. Regrouping Equation 3.38 gives:

$$i(t) = \frac{v(t)}{R} + I \qquad 3.39$$

where

$$R = \frac{2L}{T} \qquad 3.40$$

$$I = i(t-T) + \frac{1}{R} v(t-T) \qquad 3.41$$

Here the resistor R is constant, independent of time, while I represents a known current source which varies with time. Figure 3.10a shows the equivalent resistive circuit for the inductive element L.

Equation 3.41 can be written for the inductive element between nodes 1 and 3 of Figure 3.9 as

$$i_{13}(t) = I_{13}(t-T) + \frac{1}{R} \{ v_1(t) - v_3(t)\} \qquad 3.42$$

with $I_{13}(t-T)$ known from the values of the preceding time step.

$$I_{13}(t-T) = i_{13}(t-T) + \frac{1}{R} \{ v_1(t-T) - v_3(t-T)\} \qquad 3.43$$

46

For a capacitive element the differential equation relating the voltage and current is:

$$i = C \frac{dv}{dt} \qquad\qquad 3.44$$

The difference equation is:

$$\frac{i(t)+i(t-T)}{2} = C \frac{v(t)-v(t-T)}{T} \qquad\qquad 3.45$$

solving for i(t) gives

$$i(t) = - i(t-T) + \frac{2C}{T} \{v(t)-v(t-T)\} \qquad\qquad 3.46$$

$$i(t) = \frac{v(t)}{R} + I \qquad\qquad 3.47$$

where

$$R = \frac{T}{2C} \qquad\qquad 3.48$$

$$I = - i(t-T) - \frac{1}{R} v(t-T) \qquad\qquad 3.49$$

An equivalent resistance network is shown in Figure 3.10b. Its form is identical with that for the inductance.

Equation 3.47 can be written for the capacitive element between nodes 1 and 4 of Figure 3.9 as

$$i_{14}(t) = I_{14}(t-T) + \frac{1}{R} \{v_1(t) - v_4(t)\} \qquad\qquad 3.50$$

$$I_{14}(t-T) = - i_{14}(t-T) - \frac{1}{R} \{v_1(t-T) - v_4(t-T)\} \quad 3.51$$

The branch equation for the resistive component between nodes 1 and 2 in Figure 3.9 is:

$$i_{12} = \frac{1}{R} \{v_1(t) - v_2(t)\} \qquad\qquad 3.52$$

For completeness the equivalent circuit for the resistance is shown in Figure 3.10c.

For the transmission line between nodes 1 and 5, the well-known partial differential equation (the wave equation) which apply at each instant of time t and each position x on the line, assuming lossless line, is:

$$\frac{\delta v(x,t)}{\delta x} = - L \frac{\delta i(x,t)}{\delta t} \qquad 3.53$$

$$\frac{\delta i(x,t)}{\delta x} = - C \frac{\delta v(x,t)}{\delta t} \qquad 3.54$$

The general solution, given by D'Alembert, is

$$i(x,t) = f_1(x-st) + f_2(x+st) \qquad 3.55$$

$$v(x,t) = Z\, f_1(x-st) - Z\, f_2(x+st) \qquad 3.56$$

where

$Z=\sqrt{L/C}$ (characteristic impedance) $\qquad$ 3.57

$s=1/\sqrt{LC}$ (speed of wave propagation) $\qquad$ 3.58

Multiplying Eqn.3.55 by Z and add to Eqn.3.56, then

$$v(x,t) + Z\, i(x,t) = 2\, Z\, f_1(x-st) \qquad 3.59$$

The expression (v + Zi) will be constant at the other end of the line after a time to get from one end to the other. Therefore, for the branch between nodes 1 and 5 in Figure 3.9 we can write:

$$v_5(t-\tau) + Z\, i_{51}(t-\tau) = v_1(t) - Zi_{15}(t) \qquad 3.60$$

where

$$\tau = \frac{\text{line length}}{s} \quad \text{(travel time of the line)} \qquad 3.61$$

$$i_{15}(t) = \frac{1}{Z}\, v_1(t) - \frac{1}{Z}\, v_5(t-\tau) - i_{51}(t-\tau) \qquad 3.62$$

48

$$i_{15}(t) = \frac{1}{Z} \, v_1(t) + I_{15}(t-\tau) \qquad\qquad 3.63$$

where

$$I_{15}(t-\tau) = - \frac{1}{Z} \, v_5(t-\tau) - i_{51}(t-\tau) \qquad\qquad 3.64$$

and analogous

$$i_{51}(t) = \frac{1}{Z} \, v_5(t) + I_{51}(t-\tau) \qquad\qquad 3.65$$

where

$$I_{51}(t-\tau) = - \frac{1}{Z} \, v_1(t-\tau) - i_{15}(t-\tau) \qquad\qquad 3.66$$

Figure 3.10d shows the corresponding equivalent impedance network, which fully describes the lossless line at its terminals. Topologically the terminals are not connected; the conditions at the other end are only seen indirectly and with a time delay τ through the equivalent current source I.

References [19,22,23] gave a detailed treatment for mutual coupling and multiphase networks, the scalar quantities of a single branch are simply replaced by matrix quantities, and these will not be discussed here.

To summarise, the ordinary differential equations of uncoupled linear R, L, C elements are transformed by the trapezoidal rule of integration into equivalent constant resistors and known time-varying current sources. Simultaneous solution then requires the interconnection of such resistors and current sources, resulting in a linear resistive network that must be solved at each time step.

3.4 Network Solution in the EMTP

At any instant of time, the sum of currents at node 1 in Figure 3.9 must be equal to zero i.e.:

$$i_{12}(t) + i_{13}(t) + i_{14}(t) + i_{15}(t)=0 \qquad\qquad 3.67$$

If Equations 3.42, 3.50, 3.52, 3.63 are inserted into Equation 3.67, then the node equation for node 1 becomes:

$$\left\{ \frac{1}{R} + \frac{T}{2L} + \frac{2C}{T} + \frac{1}{Z} \right\}v_1(t) - \frac{1}{R} v_2(t) -$$

$$\frac{T}{2L} v_3(t) - \frac{2C}{T} v_4(t) =$$

$$- I_{13}(t-T) - I_{14}(t-T) - I_{15}(t-T) \qquad\qquad 3.68$$

which is simply a linear algebraic equation in unknown voltages, with the right hand side, which is so-called the past history term [19], known from values of preceding time steps.

For a network with n nodes, a system of n such equations can be formed,

$$[G][v(t)] = [I] \qquad\qquad 3.69$$

with   [G] = n x n nodal conductance matrix,

[v(t)] = vector of n node voltages,

[I] = vector of n known past history terms.

The actual computation in the EMTP proceeds as follows: Matrix [G] is built and triangularised with ordered elimination and exploitation of sparsity [22]. In each time step, the vector on the right hand side of Equation 3.69 is assembled from the historic terms, then the system of linear equation is solved for [v(t)], using the information contained in the triangularised

conductance matrix.

3.5 Example Teed System Faulted Response Using the EMTP

The system shown in Figure 3.11 was simulated with the fault at F being an a-earth fault occurring at the pre-fault maximum of the a-phase voltage. The line data is given in Appendix 3A. The lines are assumed continuously transposed and represented by a distributed parameter model. The primary system voltage and current variations for relay positions P, Q, R are shown in Figures 3.12, 3.13, 3.14 respectively.

Figures 3.15, 3.16, 3.17 show the primary measurands at P, Q, R when the lines are represented by lumped parameters model and the line shunt capacitance is neglected.
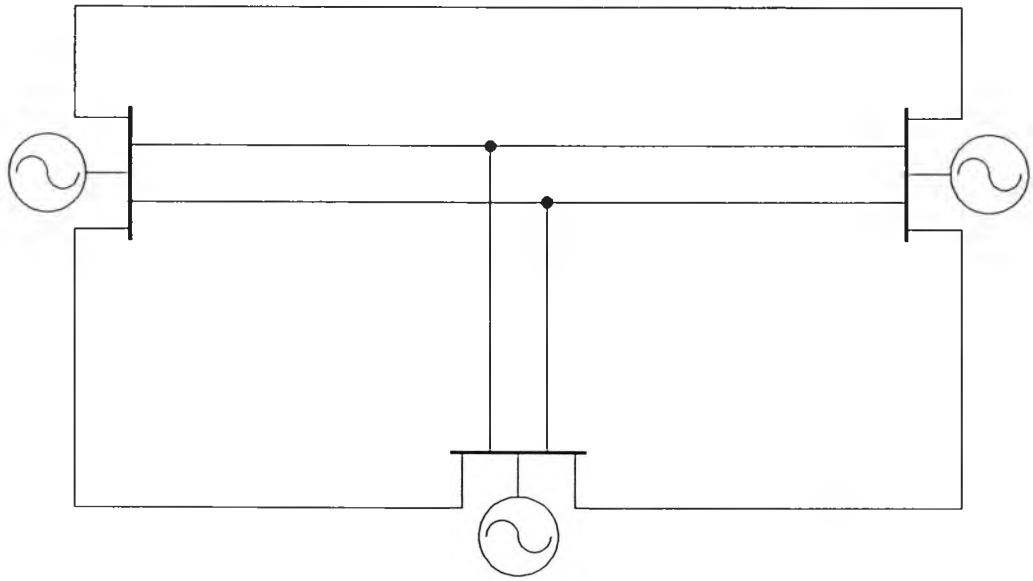
Fig. 3.1 General Teed system
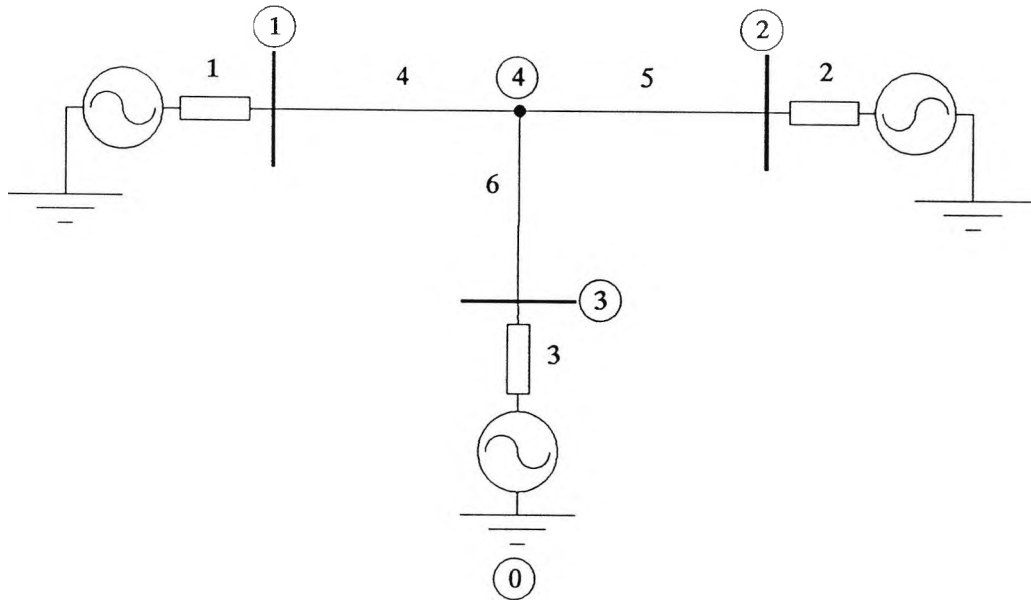
Fig. 3.2 Single circuit Teed system
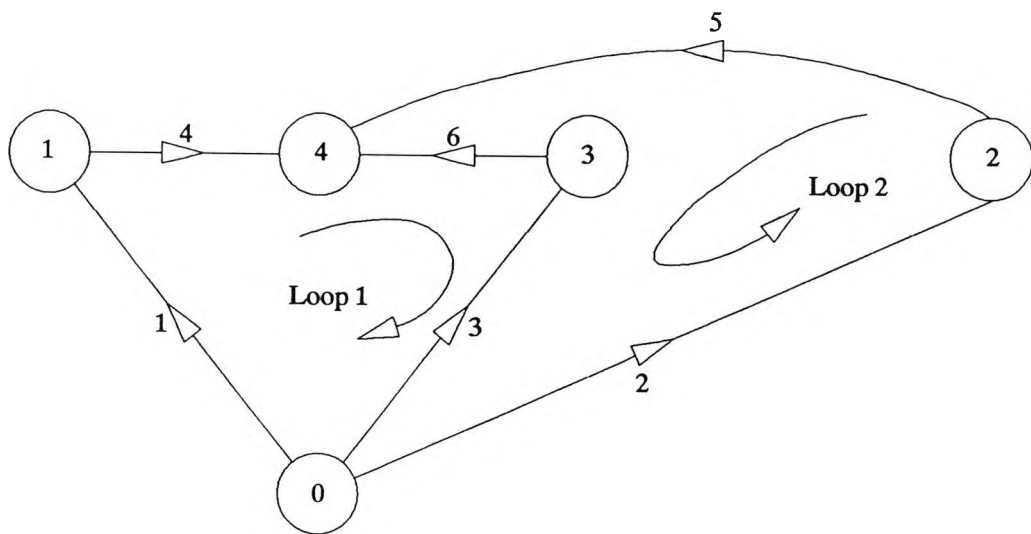
Fig. 3.3 System oriented connected graph

```
┌─────────────────────────────────────────────────────┐
│ Read:      1)  Loop incidence matrix C                │
│            2)  Line length                            │
│            3)  Source short circuit level             │
│            4)  Line impedance p. u. length            │
└─────────────────────────────────────────────────────┘
                          │
                          ▽
        ┌─────────────────────────────────────────┐
        │ Form:       Primitive impedance matrix Z  │
        └─────────────────────────────────────────┘
                          │
                          ▽
        ┌─────────────────────────────────────────┐
        │ Compute:   1)  Z loop                     │
        │            2)  Y loop                      │
        └─────────────────────────────────────────┘
                          │
                          ▽
┌─────────────────────────────────────────────────────┐
│ Compute:   1)  Branch currents        Eqn. 3.10      │
│            2)  Fault point voltage     Eqn. 3.13      │
└─────────────────────────────────────────────────────┘
```
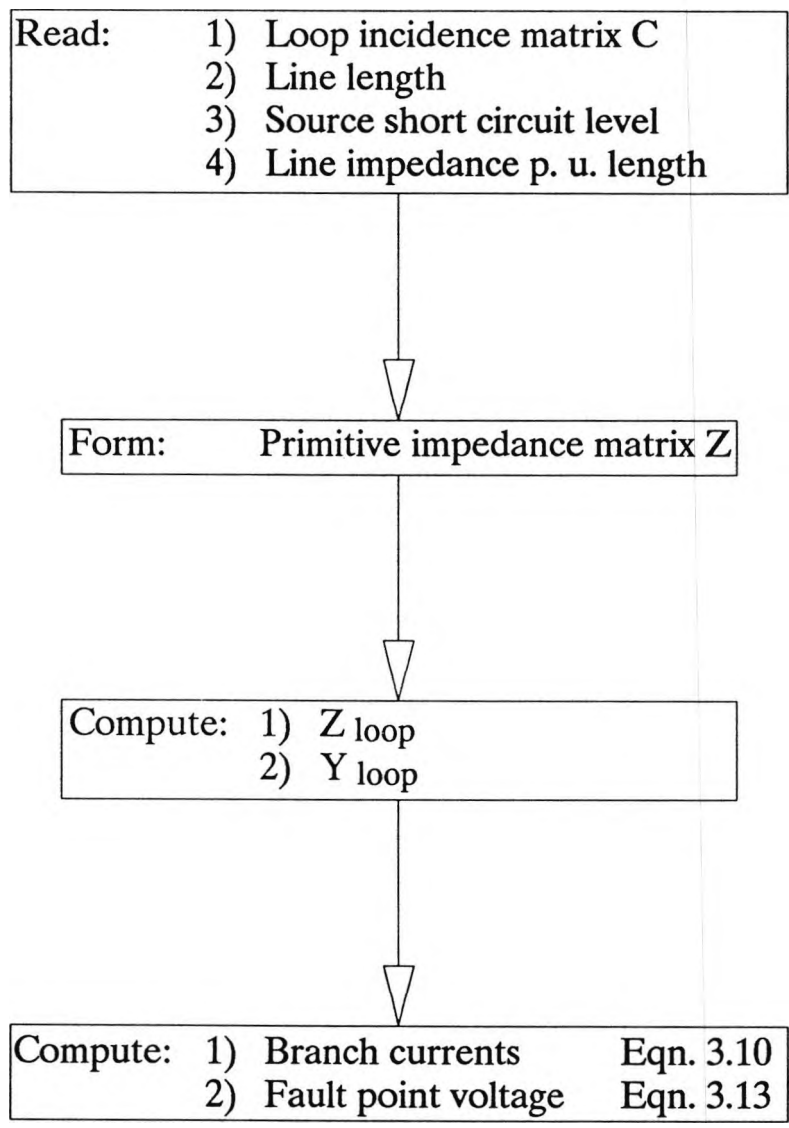
Fig. 3.4 computational flow diagram for pre-fault calculation
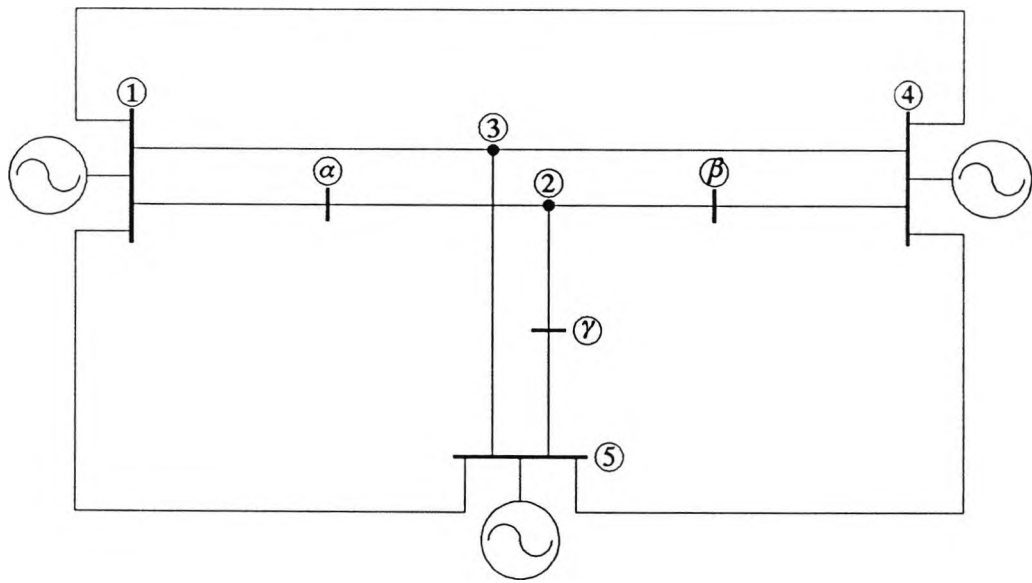
Fig. 3.5 General Teed system with extra nodes inserted on the
line connected to the Tee point
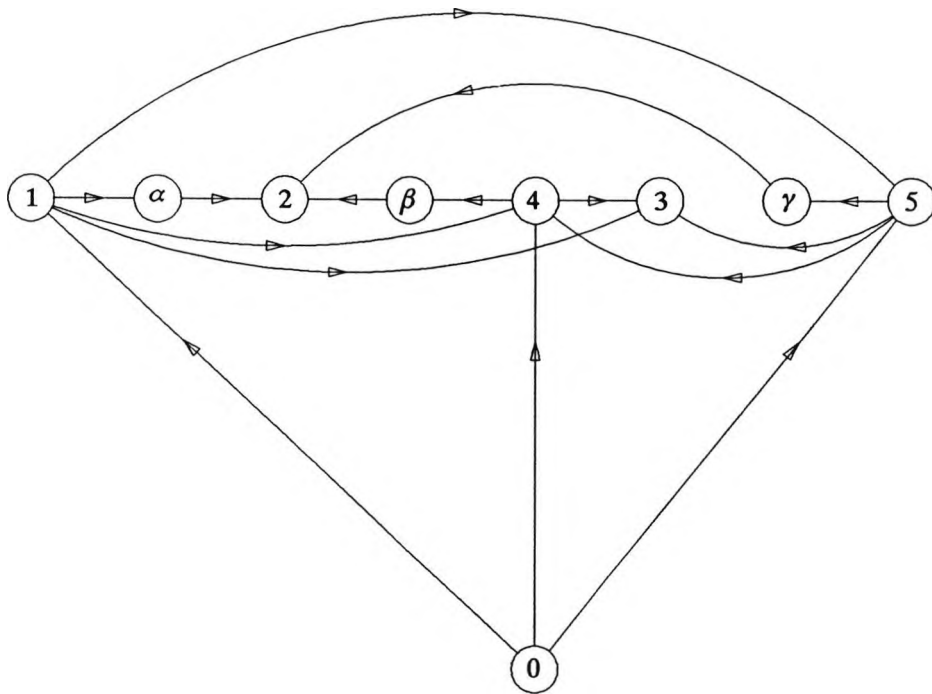

Fig 3.6 Graph of the system of Fig 3.5
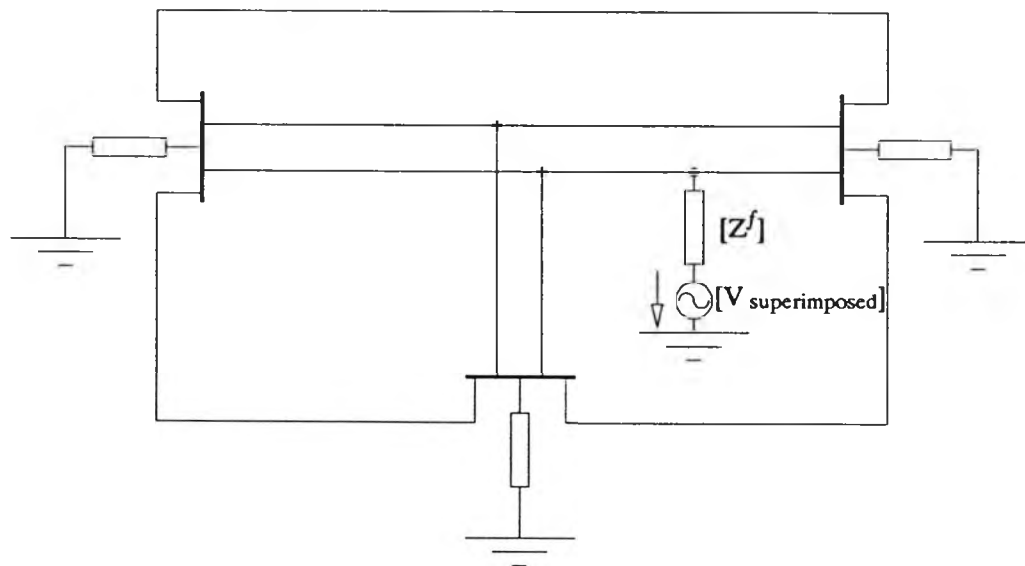
Fig. 3.7 Circuit representing the superimposed state

```
┌──────────────────────────────────────────────────────────┐
│ Read:        1)  Bus incidence matrix A                    │
│              2)  Line length                               │
│              3)  Source short circuit level                │
│              4)  Line impedance p.u. length               │
│              5)  Prefault data (bus voltage and           │
│                  line current)                            │
└──────────────────────────────────────────────────────────┘
                            │
                            ▽
┌──────────────────────────────────────────────────────────┐
│ Form:        1)  Primitive positive sequence              │
│                  impedance matrix $[Z_+]$                  │
│              2)  Primitive zero sequence                   │
│                  impedance matrix $[Z_0]$                  │
└──────────────────────────────────────────────────────────┘
                            │
                            ▽
┌──────────────────────────────────────────────────────────┐
│ Compute:  1)  $Z_{+bus}$                   Eqn.3.22       │
│           2)  $Z_{0\,bus}$                 Eqn.3.23       │
└──────────────────────────────────────────────────────────┘
                            │
                            ▽
┌──────────────────────────────────────────────────────────┐
│ Compute:  1)  Post fault voltage          Eqn. 3.32      │
│           2)  Post fault currents         Eqn. 3.33      │
└──────────────────────────────────────────────────────────┘
```
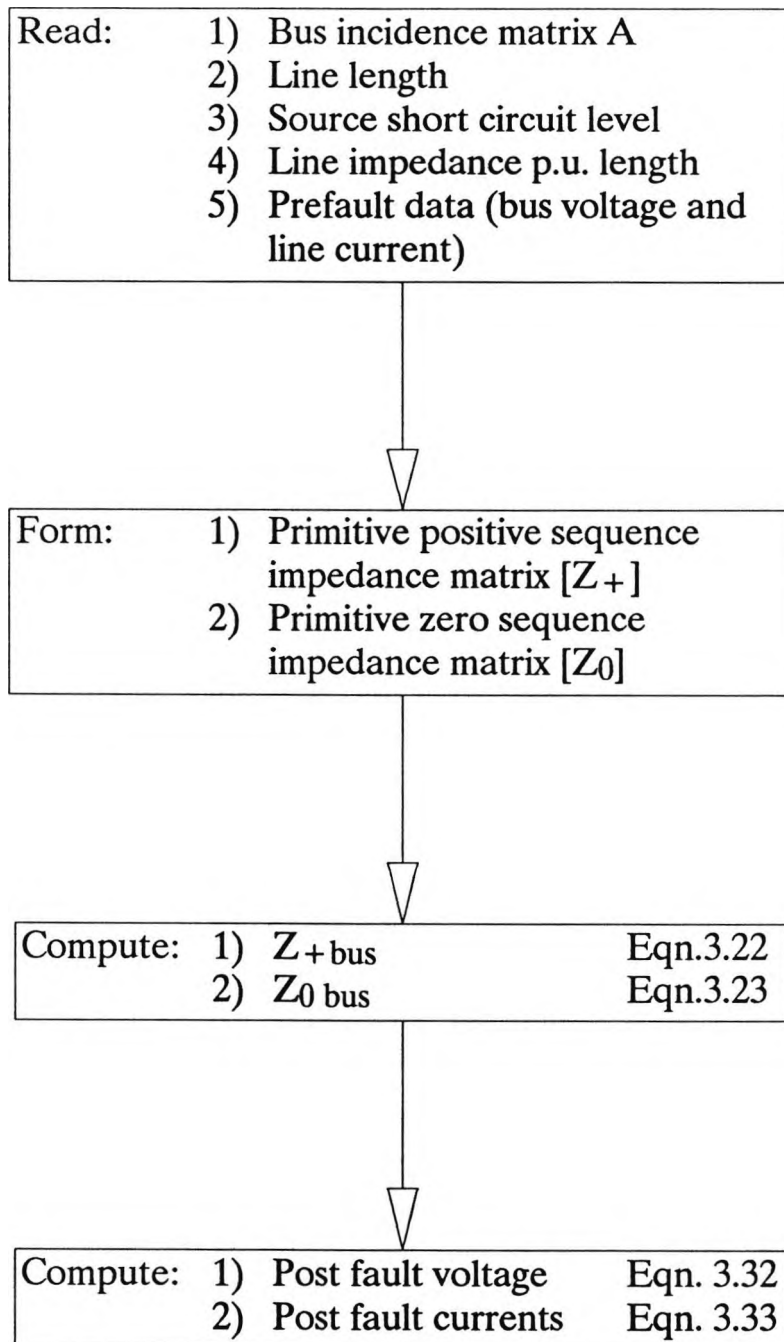
Fig. 3.8 computational flow diagram for fault calculation
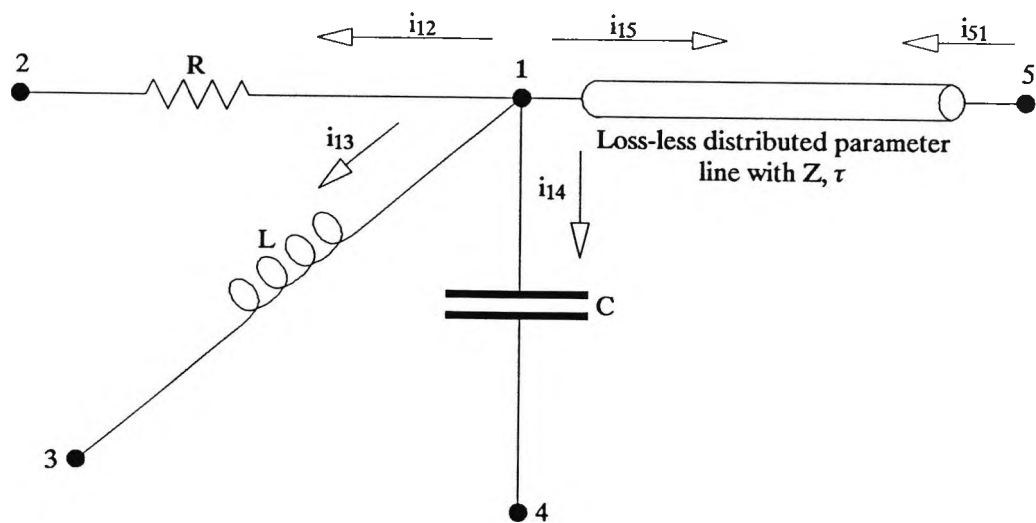
Fig. 3.9 Details of a network around node no.1
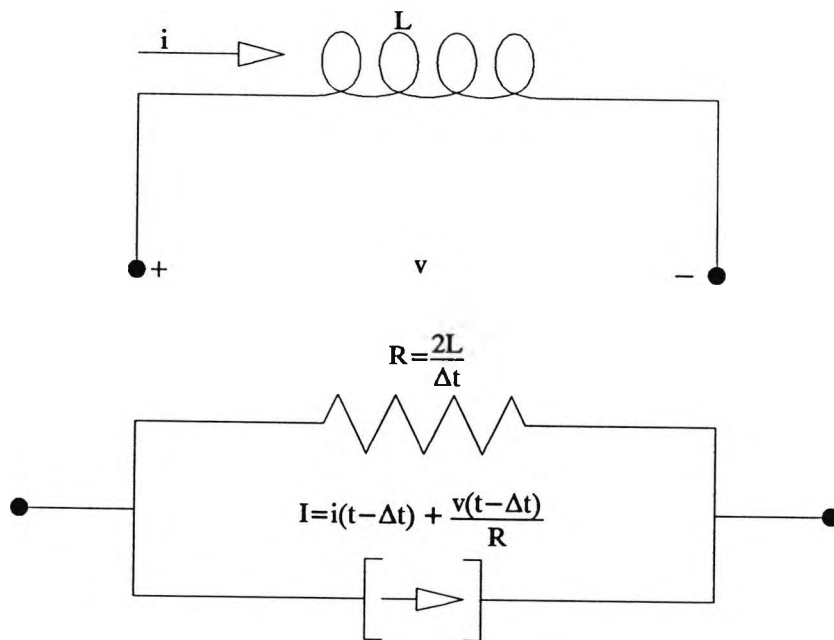
Fig. 3.10a Equivalent resistive circuit (bottom) for uncoupled, linear inductive element (top)
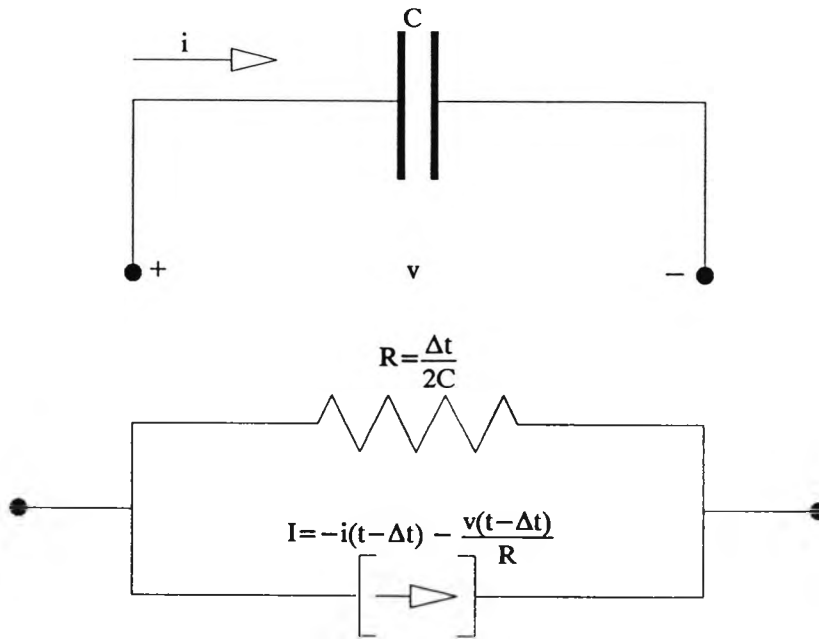
Fig. 3.10b Equivalent resistive circuit for uncoupled, linear capacitive element
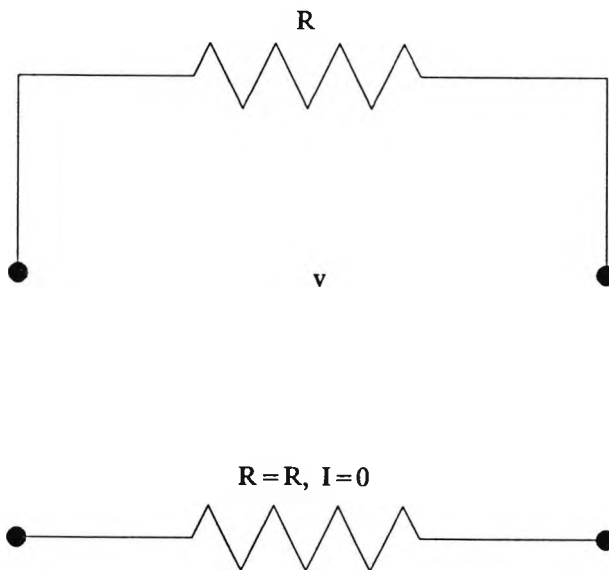
Fig.3.10c Equivalent resistive circuit for uncoupled, linear resistive element
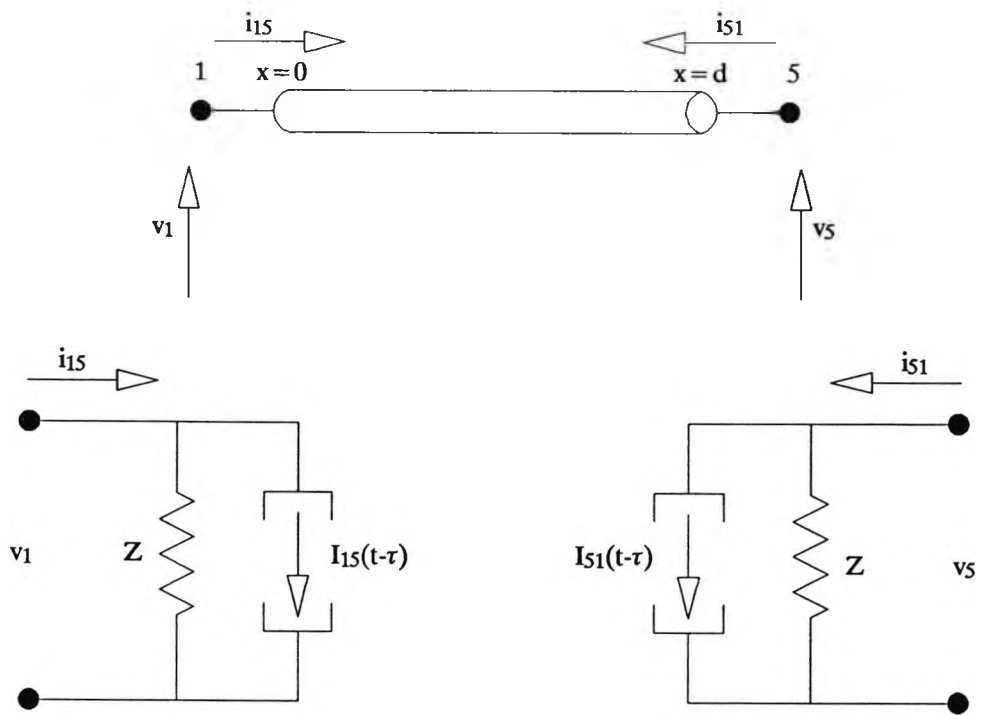
Fig. 3.10d Equivalent resistive circuit for a loss-less distributed parameter line
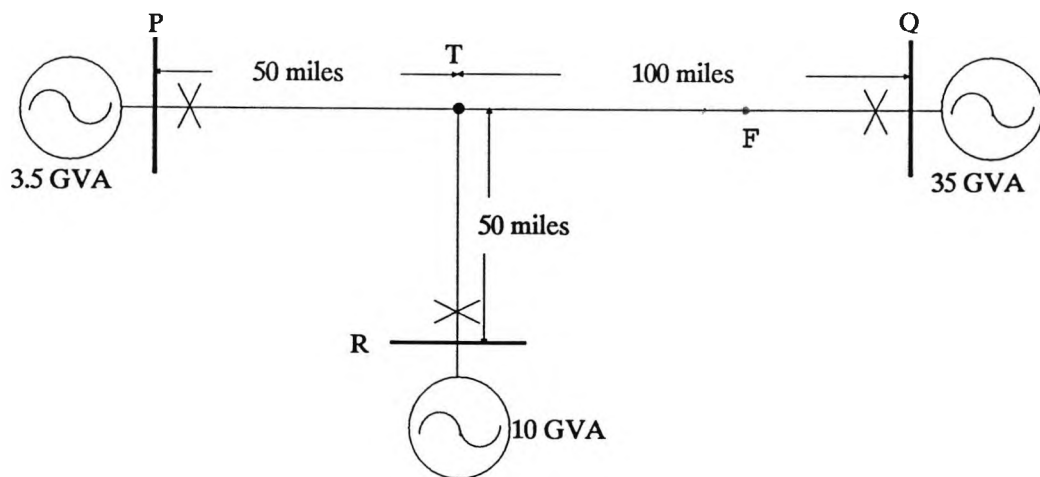
Fig. 3.11 Example of 400kV system
$Z_1 = 0.0288 + j0.4708$ ohms/mile
$Z_0 = 0.165 + j1.25$ ohms/mile
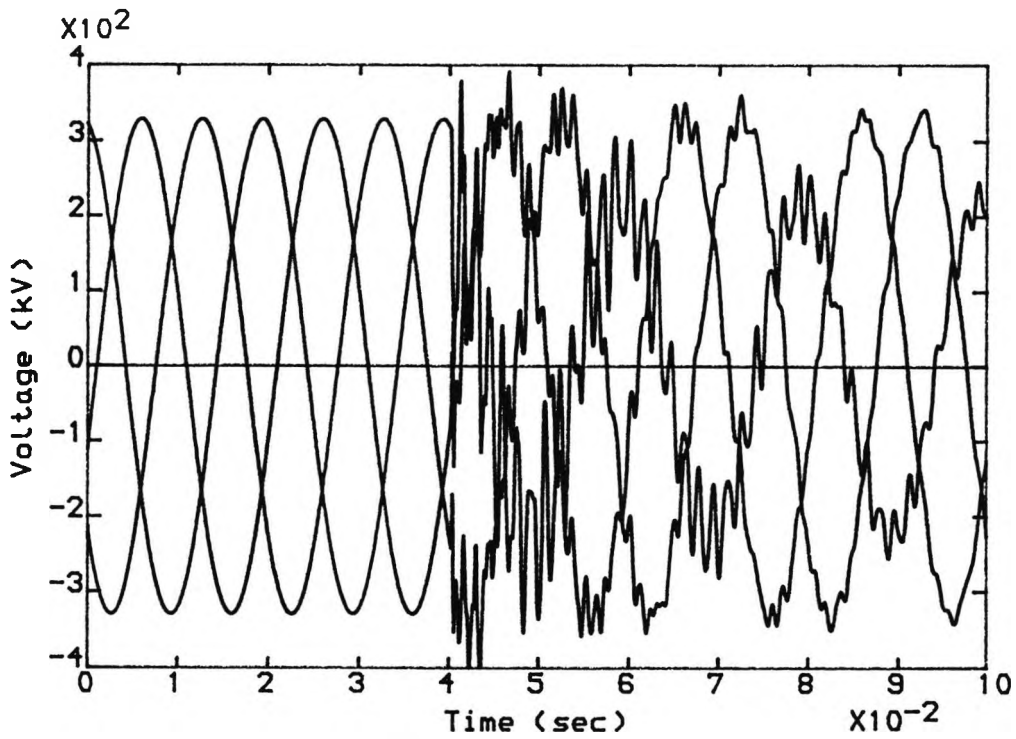
Fig.3.12a Primary voltage at P
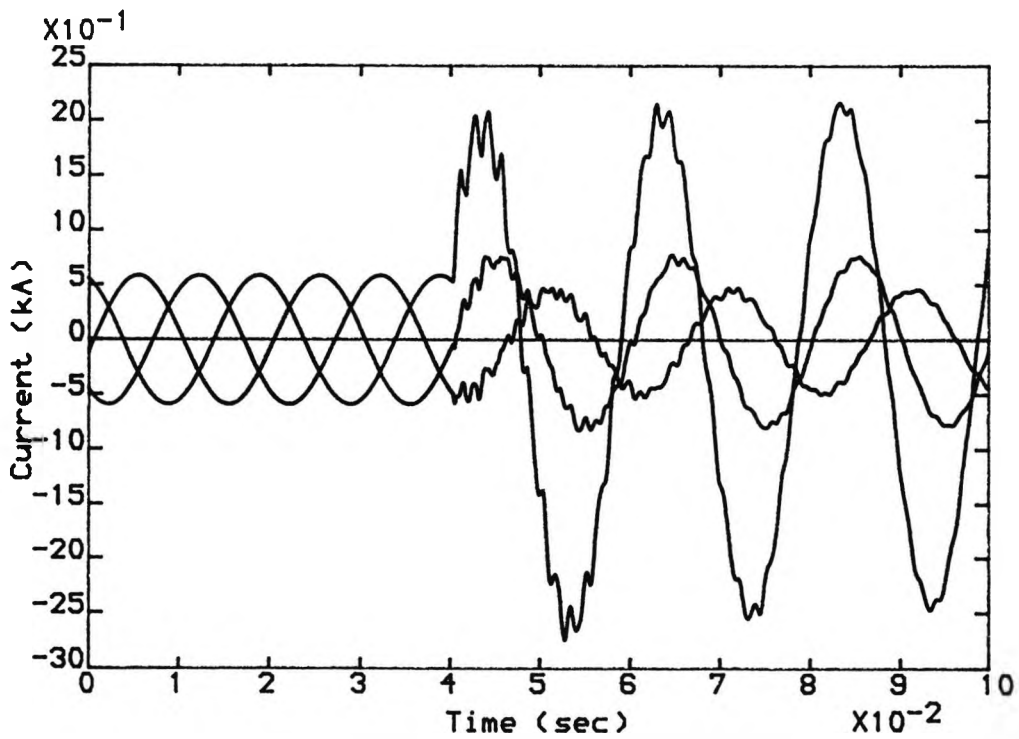

Fig.3.12b Primary current at P
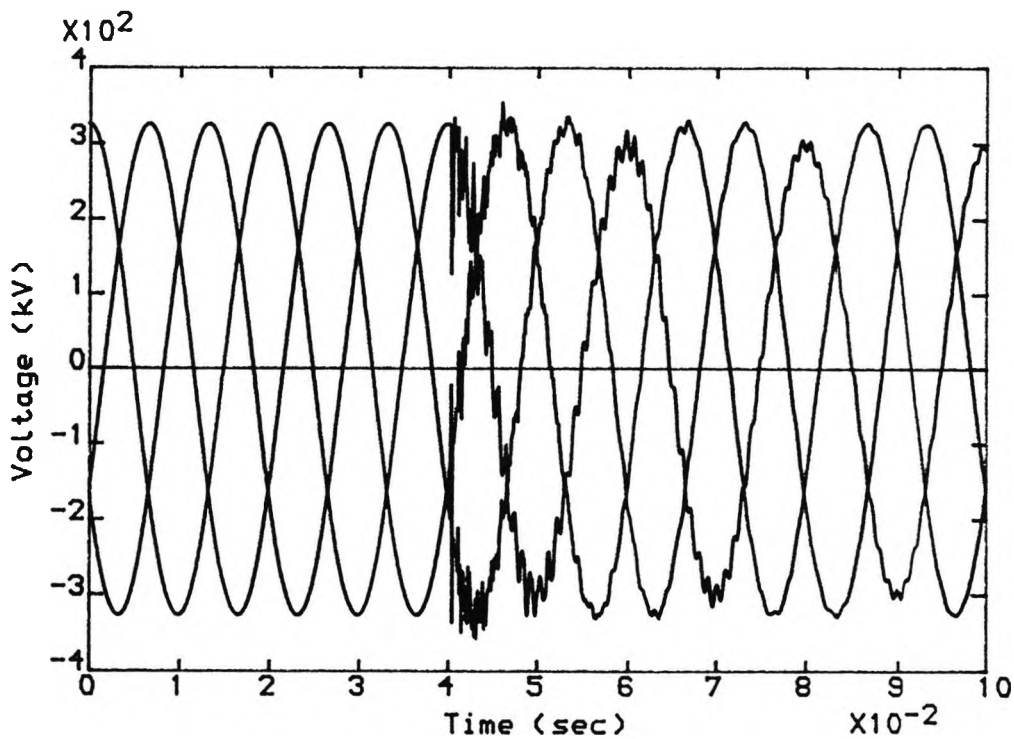
Fig.3.13a   Primary voltage at Q
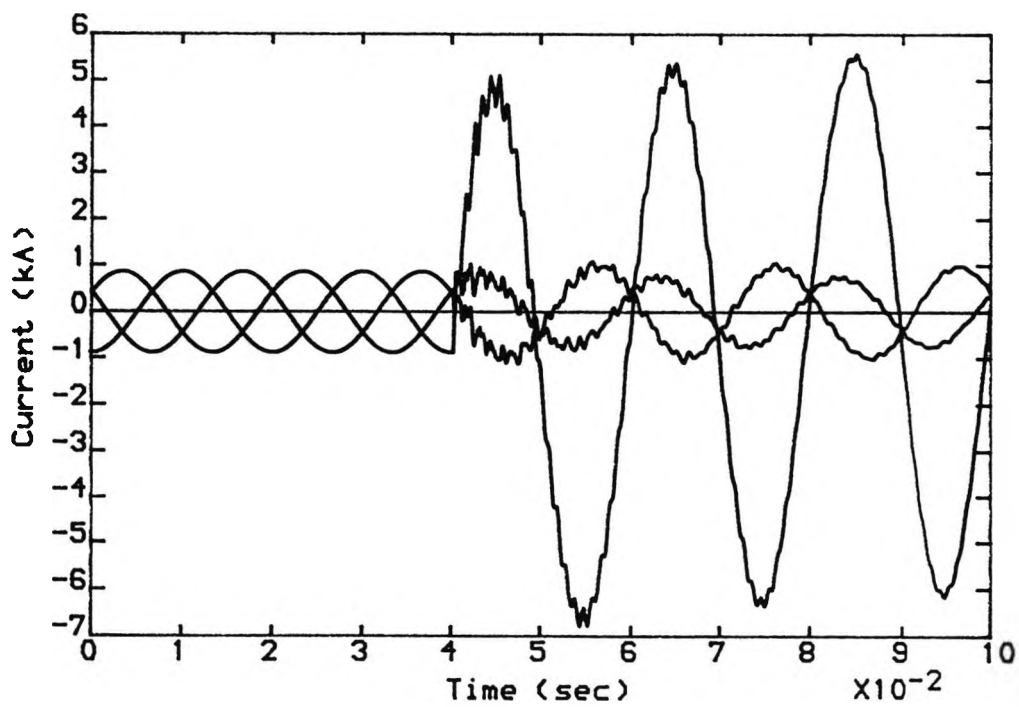

Fig.3.13b   Primary current at Q
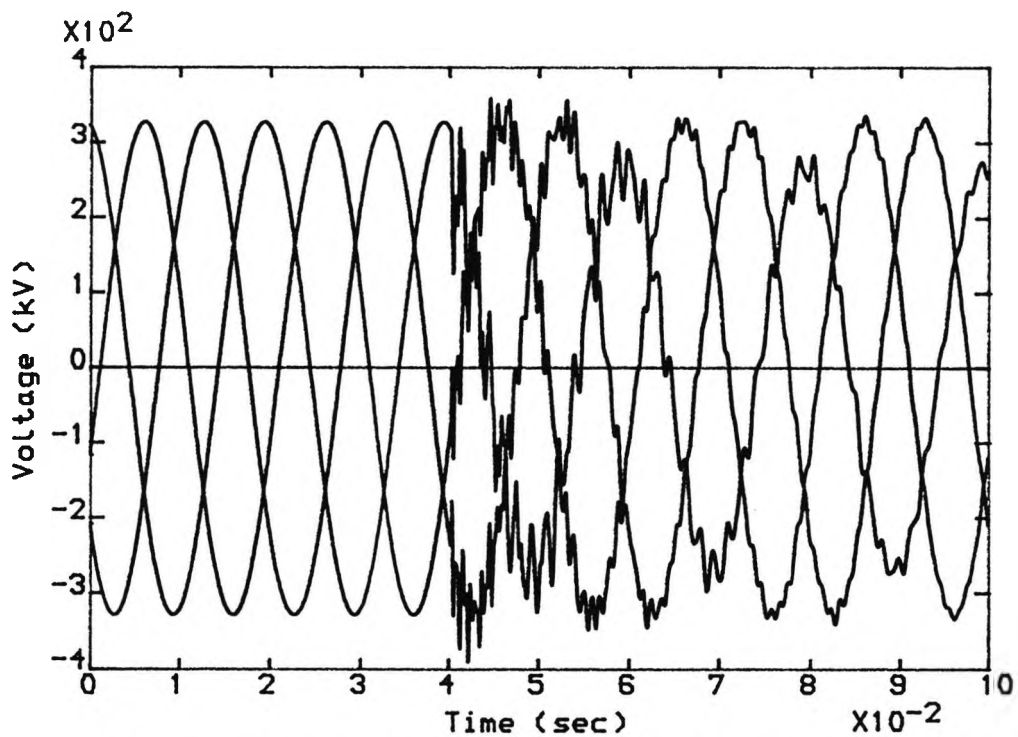
Fig.3.14a   Primary voltage at R
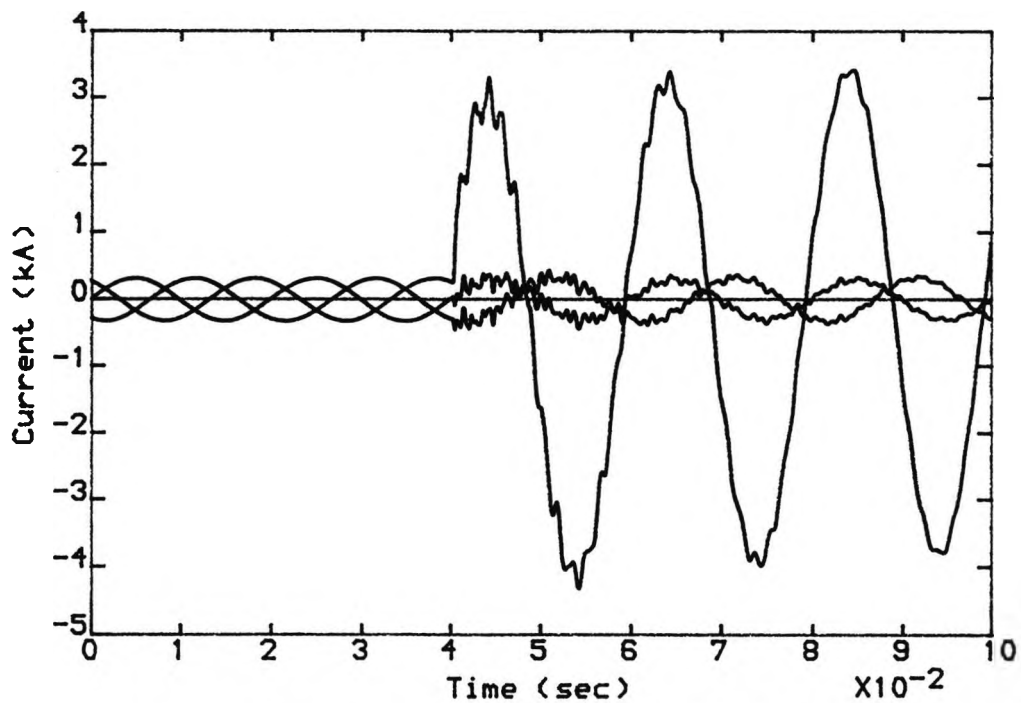
Fig.3.14b   Primary current at R
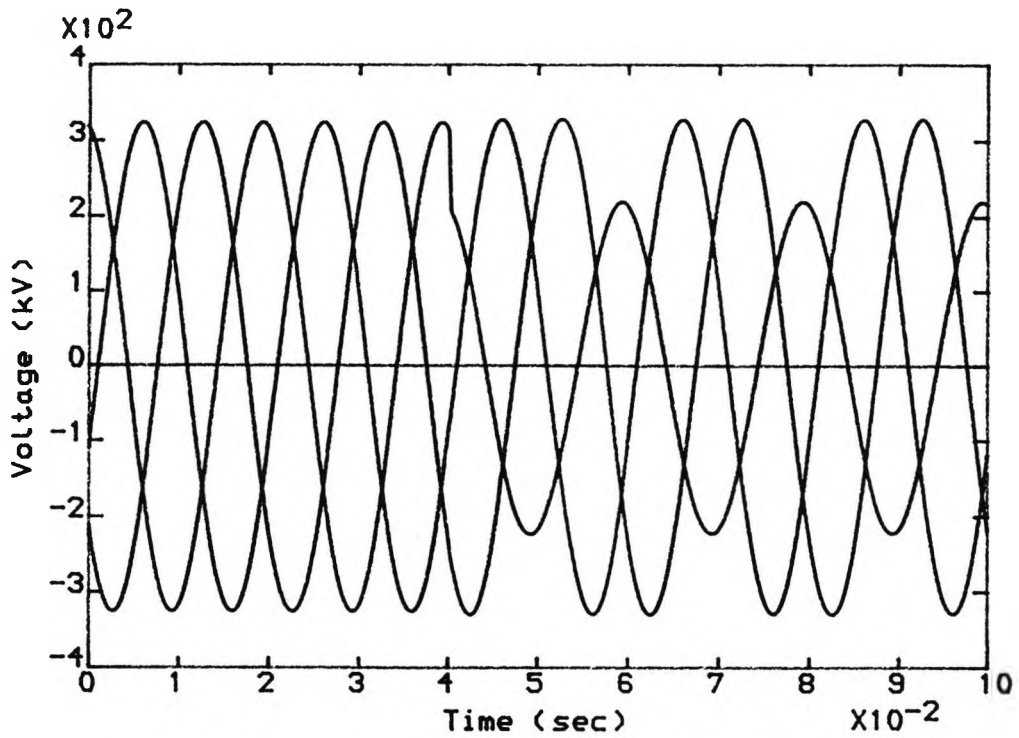
Fig.3.15a   Primary voltage at P
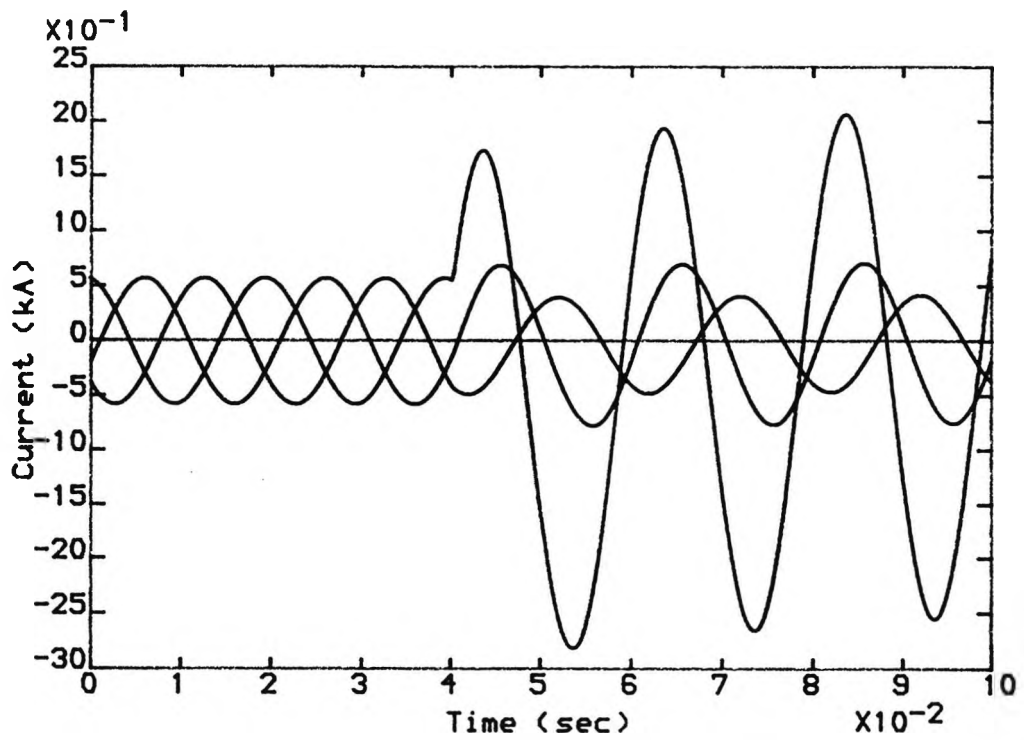

Fig.3.15b   Primary current at P
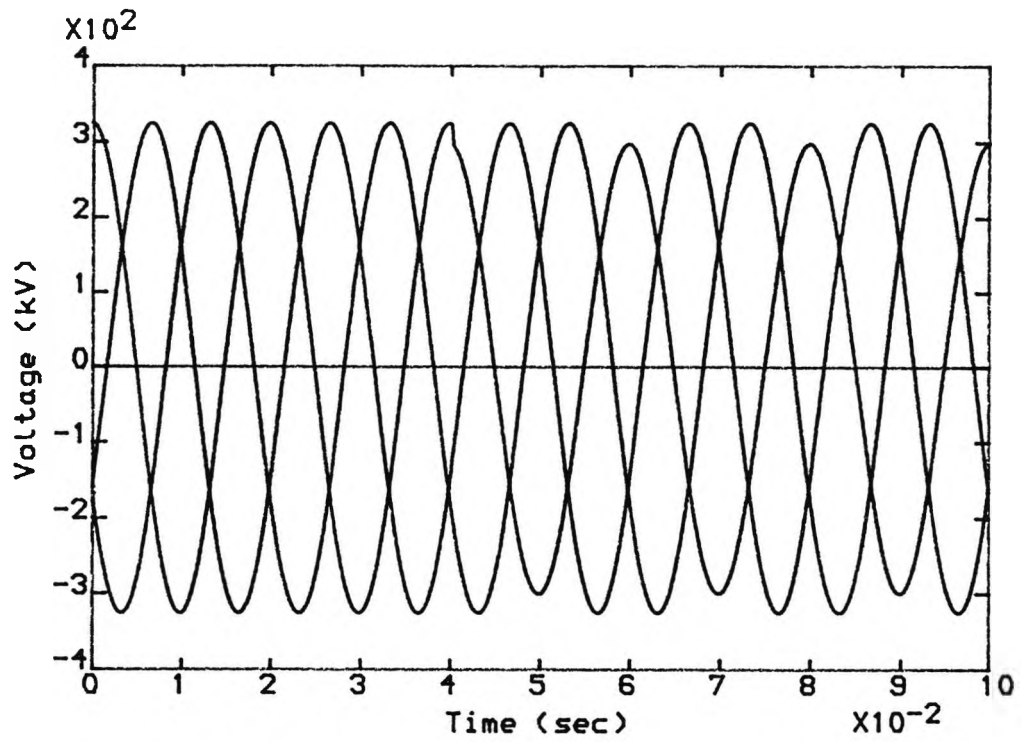
Fig.3.16a   Primary voltage at Q
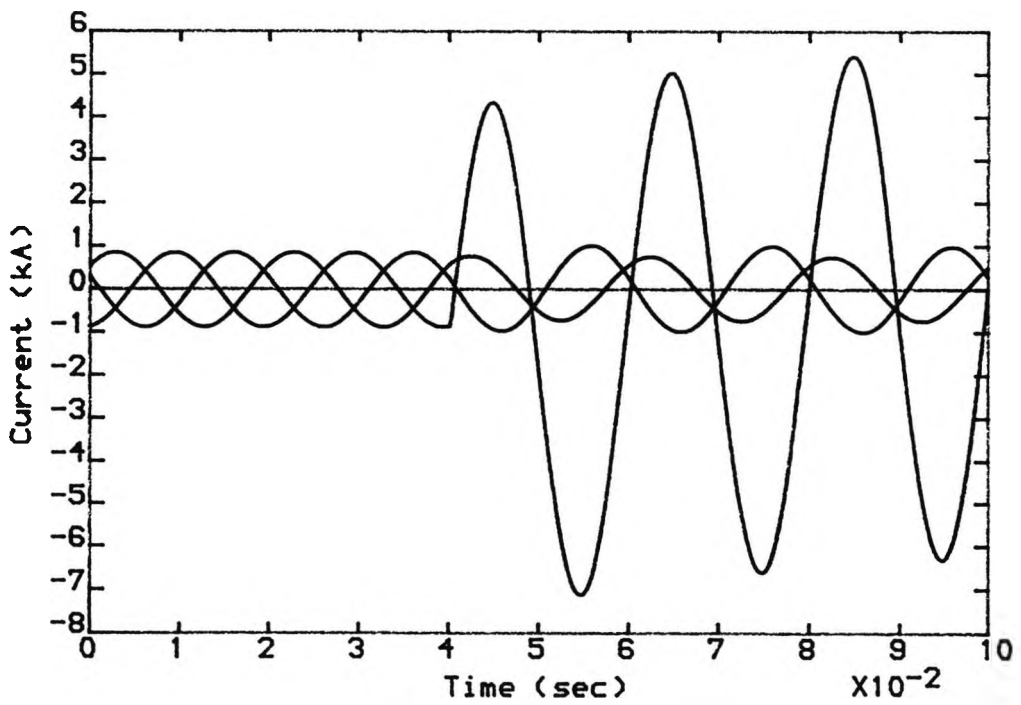

Fig.3.16b   Primary current at Q
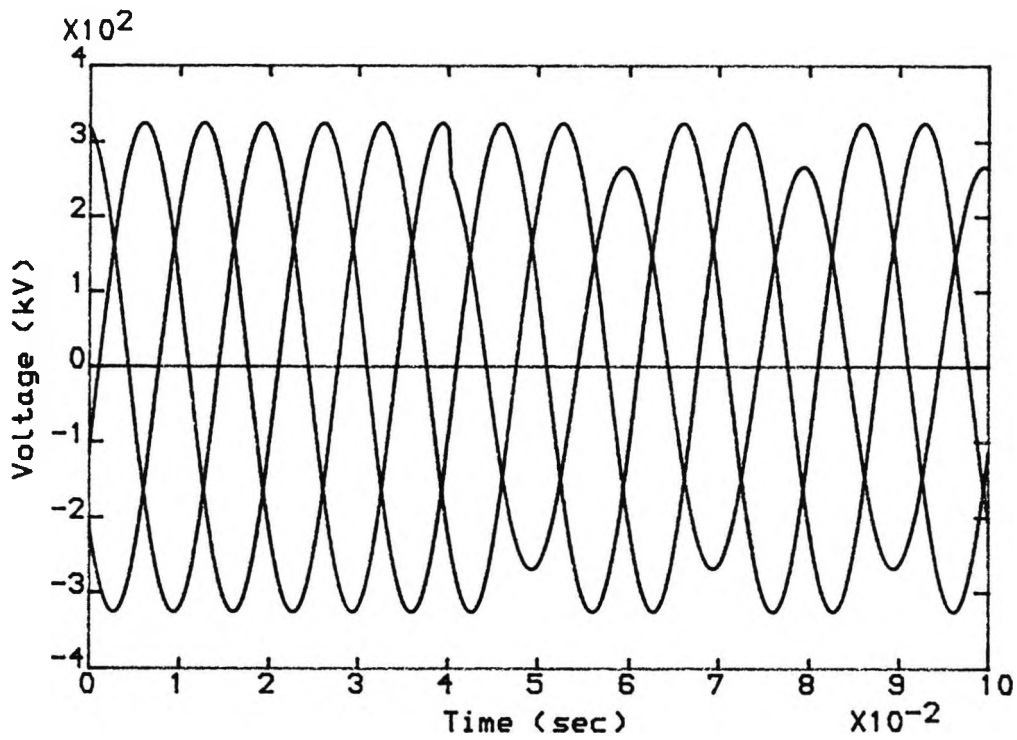
Fig.3.17a   Primary voltage at R
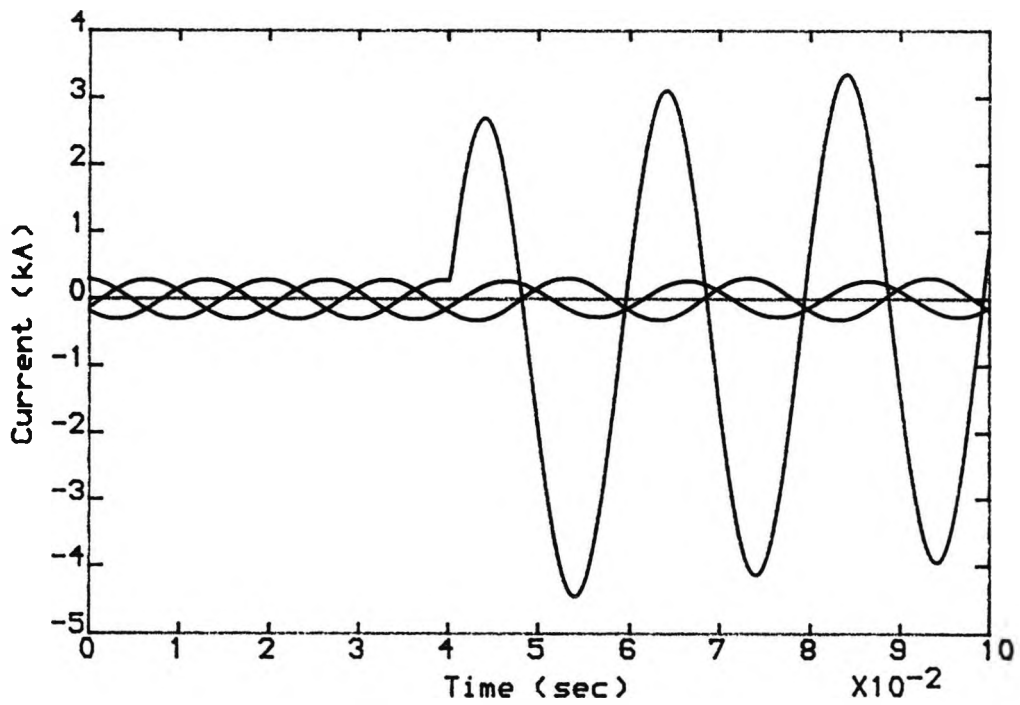
Fig.3.17b   Primary current at R

CHAPTER 4

DIGITAL DISTANCE RELAY

Power systems are obviously analogue in nature. The fault currents and voltages at the measuring point must be conditioned and eventually digitised for the computer relay to properly analyse the signals.

The first step in relaying is to secure information from the lines, a process typically accomplished through the use of current and voltage transformers. It is necessary for the received data from the current and potential transformers to be filtered by analogue methods according to the data requirements of the particular digital relaying technique being implemented. The purpose of this analogue filtering is to permit the transfer of certain frequencies and to attenuate other frequencies. The conversion of the instantaneous value of an analogue signal, a current or voltage, to a digital form is performed by an analogue to digital converter (ADC) and made available to the processor. The principal feature of the ADC is its word length, expressed in bits, which affects the ability of the ADC to represent the analogue signal with a sufficiently detailed digital representation. A digital filter is essential to all relaying applications. The analogue data samples are corrupted by noise from many sources. A power system transient is a very complicated function of time , and a substantial portion of its spectrum is noise as far as the relaying application is concerned. In addition, there may

52

be noise contributed by the A/D converters. In order to obtain accurate results, the digital filter must separate the desired components of the analogue signals from the noise components. This function is handled by the digital filter program. The filtered data of the voltage and current signals is used to calculate the fault impedance using the appropriate algorithm which can be implemented in the processor to produce numerical quantities from sequences of data samples. The derived quantities are compared against various preset relay characteristics and the result of the comparison determines whether a trip or no-trip decision is made.

4.1. Primary System Interface

The primary system interface comprise the C.V.T and C.T transducers.

4.1.1 Capacitive Voltage Transformer (C.V.T)

Although electromagnetic voltage transformers (V.T.s) meet modern protection requirements, at the higher transmission line voltages, the C.V.T provide the most economical means of obtaining the supply voltage for protective relaying. The device utilises the inherent voltage divider effect by connecting the primary of the auxiliary voltage transformer across a portion of the capacitor divider at the grounded end. Unfortunately, transient errors generated by C.V.T.s during rapidly changing conditions can have detrimental effects on the operation of protective relays [24,25,26]. These transients are

53

functions of C.V.T parameters, angle of incidence of primary fault, burden impedance and power factor. From the modelling point of view, the C.V.T.s have a well defined transfer function derived from their circuit elements and structures, from which the corresponding time domain responses are obtained via inverse Fourier methods.

The effect of any modifying function f(t), upon a time domain variation x(t), may be determined by a convolution thus:

$$y(t) = f(t) * x(t) = \int_{-\infty}^{+\infty} f(\tau) \cdot x(t-\tau) \cdot d\tau \qquad 4.1$$

where y(t) is the modified version of x(t), and τ is a dummy variable of integration.

If the time scale is divided by 'n+1' discrete samples into 'n' sections of width T, Equation 4.1 can be evaluated via simple numerical integration, which gives:

$$y(n) = \sum_{k=0}^{n} f(k) \cdot x(n-k) \cdot T \qquad 4.2$$

Hence, the primary voltages at any sample 'n', are found using the relevant impulse response f(k), together with the profile of the input signal. Figures 4.1.a and 4.1.b illustrate the impulse and frequency responses of the C.V.T. which was used in the present study.

The phase voltages are applied to the C.V.T. at their pre-fault peak, to ensure that, at the fault instance no transients are present except those generated by the faults.

54

The C.V.T. ratio in the simulation is taken as $400 \times 10^3/110$ for the 400 kV system.

4.1.2 Current Transformer (C.T)

It is assumed that the C.T. can reproduce in the secondary the proper current waveform found in the primary over the range of frequencies expected, and therefore the C.T. is simulated as a step down factor. The saturation of the C.T. core is neglected. The ratio considered is 2000/1.

It was suggested in Chapter 2 that a periodic signal which corresponds to the magnitude and phase of the remote load current is transmitted from the remote ends of a Teed line to the relay location. It should be noted that in the present simulation the actual remote currents are available and are processed continuously in the same way as the current at the measuring point.

4.2 Digital Relay Structure

The digital relay was simulated using a program written in standard FORTRAN. The relay can be divided into an analogue part which is mainly instrumentation and signal filtering and a digital part which include signal conditioning, impedance calculation and decision logic. Figure 4.2 shows the structure of the simulated relay. A description is given below.

4.2.1 Secondary Voltage Transformer

This is an instrument voltage transformer used for the purpose of signal level adjustment according to the

Analogue to Digital A/D converter requirements. The frequency response of such a transformer is taken to be ideal over the operating range of interest.

4.2.2 Current Interface

This is to convert the current into a proportional voltage. There are different devices, such as shunt resistance, the Hall effect device or a transformer with an air gap followed by an integrator, which can be employed [16]. This device is not simulated in the relay simulation. Instead a simple scaling factor was considered for signal level adjustment. The scaling factor is introduced to limit the voltage equivalents of the phase current inputs to ±10 V. The choice of the factor depends entirely upon the setting philosophy adopted for the relay. The range of current levels encountered in integrated networks is extremely large and it is necessary to limit or clip the input current if the latter is very high. This permits a larger gain for low current level faults, but introduces some degree of non-linearity into the process. Also the analogue filter used in the relay (discussed later) can suffer from saturation if the signal exceeds the power supply level available. Therefore, it is essential, at this stage, to adjust the signal level so that during external faults saturation or clipping is avoided even under the worst possible conditions.

4.2.3 Current Clip Detector

Any current clipping is detected at this analogue stage. If the fault current is very high (i.e. close-up faults) and causes saturation of the analogue electronic component of the relay, the clip detector will indicate the fact. This may be used by the relay to initiate the trip directly, irrespective of impedance measurement.

The residual currents, one derived from the currents at the local end and the other from the currents of the remote end, are formed at this stage by adding the three phase currents. The residual voltage is also formed at this stage by adding the three phase voltages.

4.2.4 Analogue Filter

It is necessary that considerable attention be given to the analogue prefiltering of the voltage and current waves before presentation to the digital relay. For a sampling frequency of f_s the Nyquist frequency is $f_s/2$. All components above $f_s/2$, if unfiltered, will be mapped down into the dc - $f_s/2$ Hz spectrum by the digital process. This is known as aliasing. The anti-aliasing analogue filter is used to filter out the frequencies above the Nyquist frequency. A second order low-pass Butterworth filter is suggested, the transfer function of which takes the standard form of:

$$G(s) = \frac{w_n^2}{s^2 + 2 \cdot d \cdot w_n \cdot s + w_n^2} \qquad 4.3$$

The choice of the cut-off frequency and required attenuation largely depends upon the digital stages of the relay. From the modelling point of view the filter is

implemented using the recursive equation which is derived from the transfer function of Equation 4.3 as shown in Appendix 4A. Figure 4.3 shows the frequency and impulse response of the analogue filter used where the desired cut-off frequency is 800 Hz.

4.2.5 Change in Data Sampling Rate

Although the relay operates at 4 kHz sampling frequency, the primary system simulation is derived at 8 kHz, allowing for an accurate simulation of the anti-aliasing filter. The sampling frequency of the relaying signals is reduced in time to 4 kHz at this stage by taking every other sample.

4.2.6 Analogue to Digital Converter

This is taken to be of 14 bit (13+sign) structure. The twelve available signals, three phase voltages, three local phase currents, the local residual current, the local residual voltage, the three phase currents and the residual current from the remote end, are sampled simultaneously by twelve sample and holds and then scanned by a multiplexer to a single A/D converter. This stage represents the link between the analogue and digital parts of the process.

The 14 bit converter (13 bit + sign) has 16384 quantisation levels (-8192 to 8191). The minimum input value of -10V is converted to the number -8192. The conversion gain of the A/D converter is then simply 8192/10=819.2 and the quantisation error is 2^{-14} pu.

4.2.7 Formation of Relaying Voltage and Current Signals

It was shown in Chapter 2 that a particular arrangement of voltage and current signals is required for real time impedance calculation. Consider Equation 2.40, reproduced below, which represents the case of a single phase to ground fault:

$$Z_{mPQa} = \frac{1}{I_{Pa} + KI_{resP}} \{ V_{Pa} + K_1 V_{Pa} - K_1 V_{PSa} -$$

$$K_2 I_{RSa} - K_3 I_{resRS} + K_4 V_{resP} -$$

$$K_4 V_{resPS} - K_5 I_{resP} + K_5 I_{resPS} +$$

$$K_6 I_{PSa} + K_7 I_{resPS} \} - K_6 \qquad\qquad 4.4$$

This equation is represented by the block diagram of Figure 4.4.

The phase voltage at P, (V_{Pa}) is available as sampled data. The product $K_1 V_{Pa}$ is made available by using a recursive equation derived from the definition of K_1 (see Appendix 4B). The equation can be regarded as a digital filter with the voltage samples as inputs. The output from the filter can be stored to provide, after a fault has occurred, the product $K_1 V_{PSa}$, where V_{PSa} is the steady state phase voltage at P.

Similarly, the phase current at P (I_{Pa}), the residual voltage at P (V_{resP}), the residual current at P (I_{resP}), the remote end phase current (I_{Ra}) and the remote end residual current (I_{resR}) are available as sampled data.

They are used as inputs to filters derived from the definitions of $K_2 - K_7$ and K (see Appendices 4C-4I) in order to provide the products $K_2 I_{Ra}$, $K_3 I_{resR}$, $K_4 V_{resP}$, $K_5 I_{resP}$, $K_6 I_{Pa}$ and $K_7 I_{resP}$.

These products are stored to provide, after a fault has occurred, values for $K_2 I_{RSa}$, $K_3 I_{resRS}$, $K_4 V_{resPS}$, $K_5 I_{resPS}$, $K_6 I_{PSa}$ and $K_7 I_{resPS}$.

In the simulation, the buffers used to store the pre-fault (steady state) values were each 240 samples (i.e. 3 cycles) long . It should be pointed out that if a fault occurs and the relay does not make a decision within 3 cycles, then the buffers will run out of prefault samples. It will be shown in the next Chapters that this does not have serious consequences.

4.2.8 Digital Filter

The main pre-filtering process is performed by the FIR (Finite Impulse Response) filters which have well defined transient responses and steady state frequency rejection characteristics.

Ideally, the duty of the filtering process is to filter out the dc component and all the frequencies other than the system frequency. However with Ultra-High-Speed operation in mind, the filtering of all unwanted frequencies is very difficult to achieve, since a long filtering process delays the transition of signals from prefault to postfault [27,28].

It is decided to design a filter with the following characteristics:
i) The filter length must be as short as possible in order to make the post-fault information available for processing in as short a time after the fault as possible. The time allowed for filtering depends upon the required

60

minimum operating time by the relay.

ii) To have a zero at dc. This rejects any dc off-set. Although the differential equation algorithm used to calculate the line impedance recognises the dc exponential component as a valid component, owing to the fact that voltage and current interfaces introduce some transients which are not related to the line equation, the final impedance measurement may be corrupted. It can be shown that if the dc components in the signals are not true reflections of the dc transients in the line model, the final impedance estimates oscillate at a frequency equal to the power frequency. Moreover the exponential component in the current affects the determinant (D) of matrix 4.15 (derived later) which may, in turn, cause ill conditioning of the solution [13]. Therefore it is essential to reject any dc components from voltage and current.

iii) To filter any travelling wave frequency. The main pass-band must be as narrow as possible with the second zero as close as possible to the system frequency. The side lobes must also be small.

The required filter is constructed by combining two filters [29]. The first has 9 points in impulse response and gives dc rejection and also has zeros at 0.5, 1, 1.5 and 2 kHz and has equal peaks at 0.25, 0.75, 1.25 and 1.75 kHz. Equation 4.5 gives the filter transfer function in digital form. The second filter is a low-pass filter with 6 points in impulse response. Its transfer function is given in Equation 4.6.

61

$$\frac{Y_{(z)}}{X_{(z)}} = a_0 Z^0 + a_8 Z^{-8} \qquad\qquad 4.5$$

$$\frac{Y_{(z)}}{X_{(z)}} = b_0 Z^0 + b_1 Z^{-1} + b_2 Z^{-2}$$
$$+ b_3 Z^{-3} + b_4 Z^{-4} + b_5 Z^{-5} \qquad\qquad 4.6$$

where:

$a_0 = 1.0$ and $a_8 = -1.0$

and

$b_0 = 0.2439$, $b_1 = 0.2148$, $b_2 = 0.3022$

$b_3 = b_2$, $b_4 = b_1$, $b_5 = b_0$

Using the convolution theorem the overall impulse response of the filters can be obtained by convolving the two impulse responses as given below:

$$h(t) = h1(t) * h2(t) = \int_{-\infty}^{+\infty} h1(\tau) \cdot h2(t-\tau) \; d\tau \qquad\qquad 4.7$$

in discrete form Equation 4.7 can be written as:

$$h(k) = \sum_{k=0}^{n} h1(k) \cdot h2(n-k) \qquad\qquad 4.8$$

It must be noted that, as one of the convolution properties, since h1(k) and h2(k) are finite the resulting h(k) will be of finite duration. Equation 4.9 gives the transfer function of the overall filter in digital form. It can be deduced that the filter has 14 points on its impulse response which corresponds to 3.5 msec when using a sampling frequency of 4 kHz.

$$\frac{Y_{(z)}}{X_{(z)}} = a_0 Z^0 + a_1 Z^{-1} + a_2 Z^{-2} + a_3 Z^{-3} + a_4 Z^{-4} + a_5 Z^{-5} + a_6 + a_7$$
$$+ a_8 Z^{-8} + a_9 Z^{-9} + a_{10} Z^{-10} + a_{11} Z^{-11} + a_{12} Z^{-12} + a_{13} Z^{-13} \qquad 4.9$$

where:

$a_0=0.4576$, $a_1=0.4051$, $a_2=0.5671$, $a_3=a_2$, $a_4=a_1$, $a_5=a_0$

$a_6=0.0$, $a_7=0.0$

$a_8=-a_0$, $a_9=-a_1$, $a_{10}=-a_2$, $a_{11}=a_{10}$, $a_{12}=a_9$, $a_{13}=a_8$

Figure 4.5 illustrates the impulse and frequency responses of the overall filter.

It can be seen, from the frequency response, that the side-lobes at high frequencies are not low enough compared to the gain at the power frequency. Also, the frequency components higher than the system frequency and lower than approximately 0.4 kHz are amplified by the filter. These components are usually associated with fault positions which are far from the relay points [10,27,30].

Since these components are not filtered from the system signals, the resulting measured reactance and resistance are affected. The attenuation of these frequencies is left to an averaging filter which will be described in Section 4.4.

4.2.9 Impedance Calculation Algorithm

During the past two decades, several algorithms for distance protection have been proposed based on real time impedance measurement. These algorithms can be categorised into two main types.

a) The first type is mainly based on the model of the waveform it self, i.e. the voltage and current [12,13,31,32].

b) The second type involves a model of the system rather than the waveforms. In particular a series R-L model of the faulted line implies that the instantaneous terminal

63

voltage and current must satisfy a first order differential equation [10,31,32]. This equation forms the basis for the digital algorithm used here.

Consider the transmission line model shown in Figure 4.6. The relationship between the relaying voltage, $v_{(t)}$, and current, $i_{(t)}$, is given by the expression,

$$v_{(t)} = Ri_{(t)} + L \frac{d}{dt} i_{(t)} \qquad\qquad 4.10$$

If the relay produces two linearly independent equations from the relaying signals ($v_{(t)}$ and $i_{(t)}$), then it is possible to calculate the line parameters, R and L [12,32]. This can be achieved by considering two points on the relaying measurands which are apart in time by Td sec. The two simultaneous equations can then be written as:

$$V_{1(t)} = R\, i_{1(t)} + L\, i'_{1(t)} \qquad\qquad 4.11$$
$$V_{2(t)} = R\, i_{2(t)} + L\, i'_{2(t)} \qquad\qquad 4.12$$

where:

$$i_{1(t)} = i_{(t)}$$
$$i_{2(t)} = i_{(t-\, Td)}$$

$$i'_{1(t)} = \frac{d}{dt}i_{1(t)} \qquad \text{and} \qquad i'_{2(t)} = \frac{d}{dt}i_{2(t)}$$

which may be written in the matrix form of Equation 4.13:

$$\begin{bmatrix} V_{1(t)} \\ V_{2(t)} \end{bmatrix} = \begin{bmatrix} i_{1(t)} & i'_{1(t)} \\ i_{2(t)} & i'_{2(t)} \end{bmatrix} \begin{bmatrix} R \\ L \end{bmatrix} \qquad\qquad 4.13$$

Inverting the 2x2 matrix in 4.13 to solve for R and L

64

gives:

$$\begin{bmatrix} R \\ L \end{bmatrix} = \frac{1}{D_{(t)}} \begin{bmatrix} i'_{2(t)} & -i'_{1(t)} \\ -i_{2(t)} & i_{1(t)} \end{bmatrix} \begin{bmatrix} v_{1(t)} \\ v_{2(t)} \end{bmatrix} \qquad 4.14$$

where the determinant is given by:

$$D_{(t)} = i_{1(t)} \, i'_{2(t)} - i'_{1(t)} \, i_{2(t)} \qquad\qquad 4.15$$

In discrete processing techniques, samples are fed to the process for individual impedance estimates. The filtered voltage and current can be made available as samples (using the discrete index k), at intervals T_s in time given by the relay sampling frequency f_s ($T_s = 1/f_s$).

In order to produce two simultaneous equations, the relay uses direct sample values from each input measurand which are time spaced by n samples as shown in Figure 4.7. Also since a given sample value contains no information about the derivative at the sampling instant, the current derivative can be approximated by computing the difference between two consecutive samples. Differentiation will amplify high frequency components on the signals and this could produce high oscillations in the measured impedance [31]. Therefore it is preferred that the derivative is computed from points further apart: one m samples to the left of, and one m samples to the right of the point at which the derivative is required. Figure 4.8 shows the frequency response of the difference equation for m=1 and Figure 4.9 the response for m=3. From these figures it is clear that the response improves as m increases. Since the relay has no information about the future samples, the

65

point of solution is delayed by m samples. Hence the two simultaneous equations from the line model can be expressed as;

$$v_{k-m} = R \cdot i_{k-m} + L \cdot i'_{k-m} \qquad\qquad 4.16$$

$$v_{k-n-m} = R \cdot i_{k-n-m} + L \cdot i'_{k-n-m} \qquad\qquad 4.17$$

where:

$$i'_{k-m} = \frac{i_k - i_{k-2m}}{2 \cdot m \cdot T_s}$$

$$i'_{k-n-m} = \frac{i_{k-n} - i_{k-n-2m}}{2 \cdot m \cdot T_s}$$

The main factors which determine the value of n are as follows:

1- 'n' must not correspond to an angular displacement of $k\pi$ (k=0, 1, 2, ...) of the fundamental component of the relaying signals [29].

2- In order to reduce the window width of the algorithm, which in turn avoids long operating times by the relay, 'n' must be close to unity.

3- To avoid ill conditioning of the algorithm under all operating conditions (to preserve independence of the solutions), when executed on a fixed word length processor, 'n' must be greater than unity [35].

A value of 6 has been suggested for n [14] which proved to be adequate for practical purposes and is used in the digital distance relay. The current differentiation is considered between 7 samples which corresponds to m=3. Therefore Equation 4.16 and 4.17 can be expressed in matrix form:

66

$$\begin{bmatrix} v_{k-3} \\ v_{k-9} \end{bmatrix} = \begin{bmatrix} i_{k-3} & i'_{k-3} \\ i_{k-9} & i'_{k-9} \end{bmatrix} \begin{bmatrix} R \\ L \end{bmatrix} \qquad 4.18$$

where:

$$i'_{k-3} = \frac{i_k - i_{k-6}}{6 \cdot T_e}$$

$$i'_{k-9} = \frac{i_{k-6} - i_{k-12}}{6 \cdot T_e}$$

Inverting the 2x2 matrix in 4.18 to solve for R and L yields:

$$\begin{bmatrix} R \\ L \end{bmatrix} = \frac{1}{D_{k-3}} \begin{bmatrix} i'_{k-9} & -i'_{k-3} \\ -i_{k-9} & i_{k-3} \end{bmatrix} \begin{bmatrix} v_{k-3} \\ v_{k-9} \end{bmatrix} \qquad 4.19$$

where:

$$D = i_{k-3} \cdot i'_{k-9} - i'_{k-3} \cdot i_{k-9}$$

R and L can therefore be expressed as:

$$R = \frac{1}{D_{k-3}} [v_{k-3} \cdot i'_{k-9} - v_{k-9} \cdot i'_{k-3}] \qquad 4.20$$

$$L = \frac{1}{D_{k-3}} [v_{k-9} \cdot i_{k-3} - v_{k-3} \cdot i_{k-9}] \qquad 4.21$$

Note that the algorithm has a window of 13 samples, which corresponds to 3.25 msec when using a sampling rate of 4 kHz.

The reactance is calculated by multiplying the measured L by the fundamental frequency of the power system. Hence:

$$X = w_o \cdot L$$

4.2.10 Impedance Conditioning

Once the discrete values of the resistance and inductance are calculated from the voltage and current signals, a further conditioning according to Equation 2.40 is required. The real, Rc, and the imaginary parts, Xc, of the complex division are shown in Appendix 4J. The real part is subtracted at each discrete value of the resistance and the imaginary part is subtracted at each discrete value of the reactance.

$$R_t = R - R_c \qquad\qquad\qquad 4.22$$

$$X_t = X - X_c \qquad\qquad\qquad 4.23$$

4.3-Relay Characteristic and Decision Logic

4.3.1-Production of Quadrilateral Characteristic

Conventional distance relay characteristic defines the region where the fault loop impedance converges after fault inception on a transmission line. It is usually plotted on an impedance diagram with R and jX axis. In general, the shape of quadrilateral characteristics required for the adaptive scheme are similar to those used in plain feeders with the exception that their negative boundary should be extended to cover the close-up faults, this will be discussed in future Chapters. Figure 4.10 shows a typical quadrilateral characteristic. The resistive reach is expanded to cover high fault resistance.

A trip is initiated if:

$$X_o < w_o L - X_c < X_r \qquad\qquad\qquad 4.24$$

$$R_o < R - R_c < R_r + (w_o L - X_c) \cdot \cot\phi_{L1} \qquad\qquad\qquad 4.25$$

where ϕ_{L1} is the angle of the line's positive phase sequence impedance.

Because division operations in a microprocessor are considered undesirable, the relay algorithm carries out none of the divisions involved in the calculations of the line resistance and reactance. Thus the quantities available to the relay are actually

$$D_m = i_{k-3} \cdot i'_{k-9} - i'_{k-3} \cdot i_{k-9} \qquad 4.26$$

$$R_m = v_{k-3} \cdot i'_{k-9} - v_{k-9} \cdot i_{k-3} \qquad 4.27$$

$$L_m = v_{k-9} \cdot i_{k-3} - v_{k-3} \cdot i_{k-9} \qquad 4.28$$

where:

$$i'_{k-3} = i_k - i_{k-6} \qquad 4.29$$

$$i'_{k-9} = i_{k-6} - i_{k-12} \qquad 4.30$$

so

$$D_m = 2 \cdot m \cdot T_s \cdot D \qquad 4.31$$

$$R_m = 2 \cdot m \cdot T_s \cdot D \cdot R = D_m R \qquad 4.32$$

$$L_m = D \cdot L = \frac{D_m L}{2.m.T_s} \qquad 4.33$$

To allow D_m, R_m and L_m to be used instead of D, R and L, Equations 4.24 and 4.25 can be rearranged as follows. Multiplying Equation 4.24 by D_m and dividing by $2mT_s w_o$ gives (for m=3):

$$\frac{X_o}{6T_s w_o} \cdot D_m \;<\; \frac{D_m L}{6T_s} - \frac{X_c}{6T_s w_o} \cdot D_m \;<\; \frac{X_r}{6T_s w_o} \cdot D_m \qquad 4.34$$

multiplying Equation 4.25 by D_m gives:

$$R_o D_m \;<\; R D_m - R_c D_m \;<\; R_r D_m + \left(6T_s w_o \frac{D_m L}{6T_s} - \frac{X_c}{6T_s w_o} \cdot D_m \right) \cdot \cot\phi_{L1}$$
$$4.35$$

Relationships 4.34 and 4.35 can be simplified in the form of Equations 4.36 and 4.37.

$$K_{Xo} \cdot D_m < L_m - K_{Xc} \cdot D_m < K_{Xr} \cdot D_m \qquad 4.36$$

$$R_o \cdot D_m < R_m - R_c \cdot D_m < R_r \cdot D_m + K_{Rr} \cdot L_m - K_c \cdot D_m \qquad 4.37$$

where the constants K_{Xo}, K_{Xc}, K_{Xr} and K_{Ro} are given by:

$$K_{Xo} = \frac{X_o}{6 \cdot T_s \cdot w_o} \qquad 4.38$$

$$K_{Xr} = \frac{X_r}{6 \cdot T_s \cdot w_o} \qquad 4.39$$

$$K_{Xc} = \frac{X_c}{6 \cdot T_s \cdot w_o} \qquad 4.40$$

$$K_{Rr} = 6 \cdot T_s \cdot w_o \cdot \cot\phi_{L1} \qquad 4.41$$

$$K_c = X_c \cdot \cot\phi_{L1} \qquad 4.42$$

Thus digital division is avoided by the relay logic.

4.3.2–Directional Reactance (X_M)

A distance protection relay must maintain consistency of performance for faults within the protected zone. However, the constraints of Equations 4.36 and 4.37 allow unwanted operation for reverse faults (faults behind the relay). This is very important in the proposed adaptive relay because, as Figure 4.11 clearly shows, a measured reactance for a fault behind the relaying point can behave similarly to that of a forward fault. In order to make the relay truly directional, a polarising signal is required for the calculation of the directional reactance X_M. The optimum polarising signal is one that maintains its vectorial position regardless of what system parameters, type of fault, fault location or fault

resistance occurs [33]. The use of memory to store pre-fault voltage signal or by using sound phase voltage is normally adequate in maintaining the directional stability of the relay.

The directional reactance measurement uses the delayed samples of the voltage in conjunction with the undelayed samples of the current component. This can be implemented by using a voltage memory bank, to hold the pre-fault samples of the voltage signals. It should be mentioned that the polarising signal used is derived from the actual phase voltage and not from the total voltage signal used for line impedance calculation. Within the simulation a memory of 3 power frequency cycles is used in the directional reactance calculation.

The measured directional reactance, X_M, is compared with the directional reactance setting, X_{MA}, and hence an additional constraint is added to that of Equations 4.36 and 4.37 as follows:

$$X_{MA} < w_o L_M \qquad\qquad 4.43$$

or

$$\frac{X_M}{6 \cdot T_s \cdot w_o} \cdot D_m < \frac{L_M D_m}{6 T_s} \qquad\qquad 4.44$$

Equation 4.44 can be written as:

$$K_M \cdot D_m < \frac{L_M D_m}{6 T_s} \qquad\qquad 4.45$$

where:

$$K_M = \frac{X_{MA}}{6 \cdot T_s \cdot w_o} \qquad\qquad 4.46$$

$L_M D_m / 6 T_s$ is directly obtained from the expression:

71

$$\frac{L_M D_m}{6T_e} = v_{k-6-N} \cdot i_{k-3} - v_{k-N} \cdot i_{k-9} \qquad\qquad 4.47$$

N is the number of delayed samples which in this case is equal to 240 at 80 samples per cycle (50 Hz system frequency). Figures 4.12 and 4.13 illustrate the measured X_M and X_t for reverse (just behind the relaying point) and forward (at the reach point) faults respectively.

4.3.3-Decision Logic

The measured impedance is compared with the predetermined characteristic of impedance which specifies a zone in the impedance plane. The tripping criterion, which is based on a single impedance estimate can lead to the degradation in protection integrity because, in practice, a significant fluctuation in impedance estimates occurs after fault inception. The algorithm simulation shows that a fault just beyond the relay reach can cause impedance estimates falling within the relay characteristic boundary [34]. The impedance transients can be illustrated for voltage maximum faults, where the relaying voltage signals are severely contaminated by travelling wave harmonics, and voltage minimum faults where the impedance estimates show a downward transient droop.

The relay trip mechanism comprises a trip counter which increments when any calculated impedance sample falls within the characteristic and decrements if a sample is outside the relay boundary. If the trip counter

reaches a preset trip level, then tripping is initiated [27,34].

The relay characteristic is divided into fast and slow counting regions which allow more time for the relay to reach a trip decision for faults near the boundary and also produce fast operation for close up faults. A typical characteristic with divided counting zones is shown in Figure 4.14.

The trip decision making process starts by detecting the disturbance. The disturbance detection is performed by monitoring the superimposed value of the line current. The process can be generally summarised as follows:

The trip level is set at 45. This means that when the trip-counter reaches this value a trip is initiated. The increment, INC, is 9 over the first 80% of the characteristic, 4 between 80% and 95%, and 1 from 95% to the reach point. The increments beyond the reach point are negative. Their size are the same as those of the increments at corresponding distances before the reach point. With this change in counting strategy, faults occurring close to the reach point will take longer to trip. For close-up faults the relay is required to be fast because the damage caused by high fault current is severe, and also the stability of the integrated power system may be jeopardised. On the other hand, for boundary faults near the forward reach of the relay the relay must be accurate in deciding whether the fault is inside or outside the protected zone. The speed of operation for such faults is the second priority.

4.4-Impedance Transient Suppression

When the window of the algorithm includes both prefault and postfault samples the results could traverse the entire relay characteristic and as the window moves into the fault values the results change more smoothly. Also, transients which cannot be eliminated completely by prefilter will, in general, give rise to the corruption of the calculated impedance. Two separate measures are taken to overcome these situations:

i)   In order to prevent a tripping during the transition from prefault to postfault it is advisable to monitor the rate of change of the measured reactance $D \cdot X_t$ and compare it with the reach point boundary $D \cdot X_r$ and then to alter the counting increment, INC, accordingly. Figure 4.15 shows how the $D \cdot X_t/dt$ value is calculated; $d(D \cdot X_t)/dt$ is the difference between two $D \cdot X_t$ values spaced by Ns samples apart and Nd samples from the most recent value of $D \cdot X_t$. Values of 6 and 3 are recommended for Ns and Nd respectively [35].

The value of the counter increment, INC, is modified in the following way:

If $\qquad\qquad |d(D \cdot X_t)/dt| \; > \; |D \cdot X_r/2|$ $\qquad$ then INC=0

If $\quad |D \cdot X_r/2| \; > \; |d(D \cdot X_t)/dt| \; > \; |D \cdot X_r/4|$ $\qquad$ then INC=INC/4

If $\quad |D \cdot X_r/4| \; > \; |d(D \cdot X_t)/dt| \; > \; |D \cdot X_r/8|$ $\qquad$ then INC=INC/2

If $\quad |D \cdot X_r/8| \; > \; |d(D \cdot X_t)/dt|$ $\qquad\qquad$ then INC unchanged

Figure 4.16 shows the behaviour of the measured reactance with and without counter inhibition using this method for a fault just beyond the relay reach with a fault angle of 60 degrees. It can be seen that the use of

74

this method prevents the relay maloperating.

ii)   Although the purpose of controlling the increment
value was to prevent maloperation during the transition
period from prefault to postfault, there are other
transients caused by the travelling waves and capacitive
voltage   transformer   (CVT) which cannot be removed
completely by pre-filter, due to restriction on window
length.   These transients will, in general, give rise to
the corruption of the calculated resistance and reactance
values.   However, it is possible to remove the R and X
distortion by the use of a selective signal averager which
is only invoked after a potential fault inception [35].

Equation 4.48 describes the operation of the signal
averager having been invoked to average a signal Y at time
sample 'n'.

$$Y_{A(n+k)} = \sum_{i=0}^{m} \frac{Y_{(n+k-i)}}{m+1} \qquad\qquad 4.48$$

m = k   if k ≤ 10

m = 10 if k > 10

It can be seen that the averaging window length
increases by one point from its initial value of one, at
each sampling interval, following invocation. The maximum
window length is 10 points. Figure 4.17 shows the
frequency and impulse response of the averager when the
averaging window is fully extended to 10 points. The
averaging process starts 3.25 msec (window of the
algorithm) after the first increment, this ensures that
all the calculated values of the resistance and reactance
are entirely post fault values. Figure 4.18 shows the

measured R and X with and without the averager, for a
single phase to earth fault at the relay reach point.

4.5 Scheme Tripping Logic

The foregoing discussions and simulations are for one
relay, but as outlined in Chapter 2, the scheme comprises
two relays which will operate simultaneously.   Therefore
an identical processing is made for the other relay; i.e.,
for Equation 2.45.

A tripping scheme can be defined as one which
requires the operation of both relays.   The overall
protection scheme operating time will, in general, depends
on the setting of the relay allocated for the remote
shortest leg because the other relay will see the
impedance well within its boundary; i.e. in the fast
counting region.
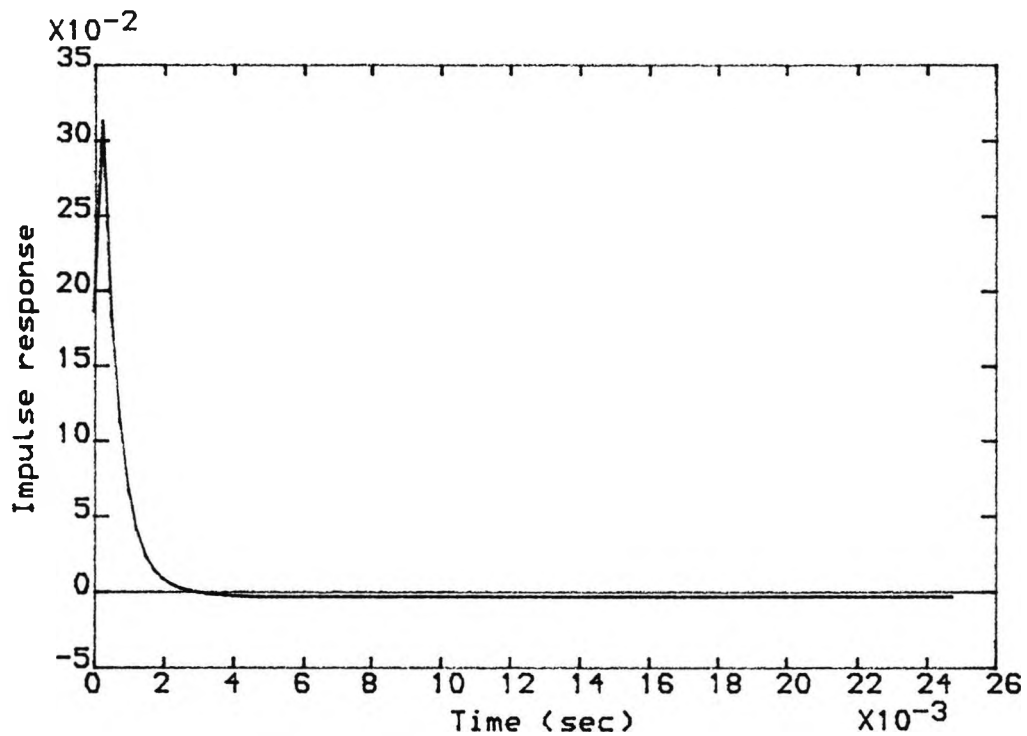
Fig. 4.1a   Impulse respnose of the C.V.T
used in the simulation

Fig. 4.1b   Frequency respnose of the C.V.T
used in the simulation

```
 V
———|  ANALOGUE  |    |   ANTI-   |    | ANALOGUE  |    | FORMATION |    |           |    | IMPEDANCE   |
      |    CLIP    |——|  ALIASING |——|     TO    |——|    OF     |——| PRE-FILTER|——| CALCULATION |———
 I    | DETECTION |    |  FILTER   |    |  DIGITAL  |    |   TOTAL   |    |           |    |    AND     |
———|           |    |           |    | CONVERTER |    |  VOLTAGE  |    |           |    | PROTECTION |
                                                        |    AND    |                    | ALOGORITHM |
                                                        |  CURRENT  |
                                                        |  SIGNALS  |
```
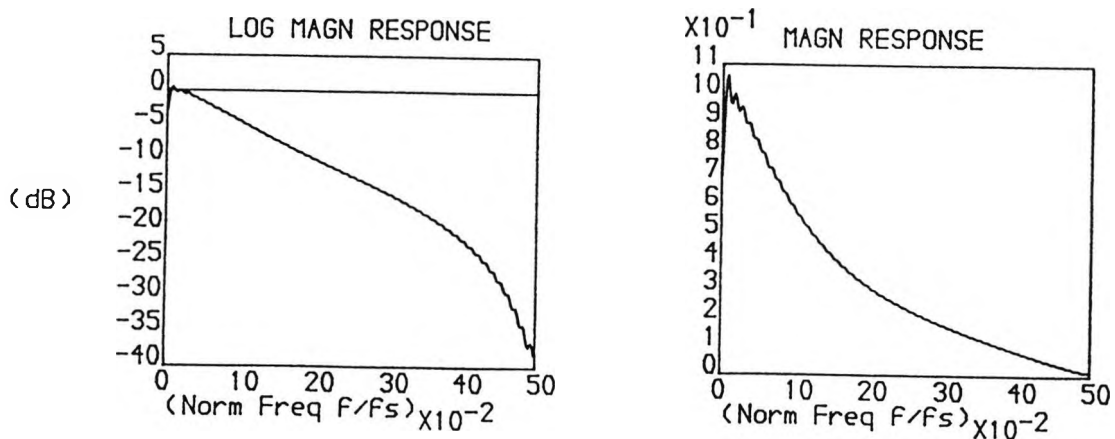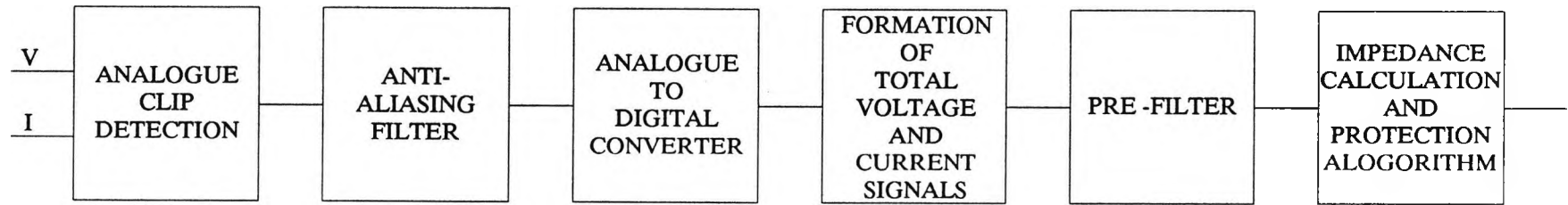
Fig. 4.2 Block diagram of relay simulation

LOG MAGN RESPONSE

MAGN RESPONSE

PHASE RESPONSE

IMPULSE RESPONSE
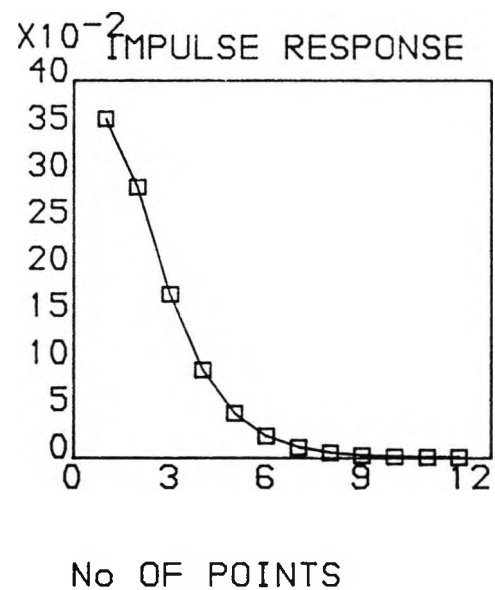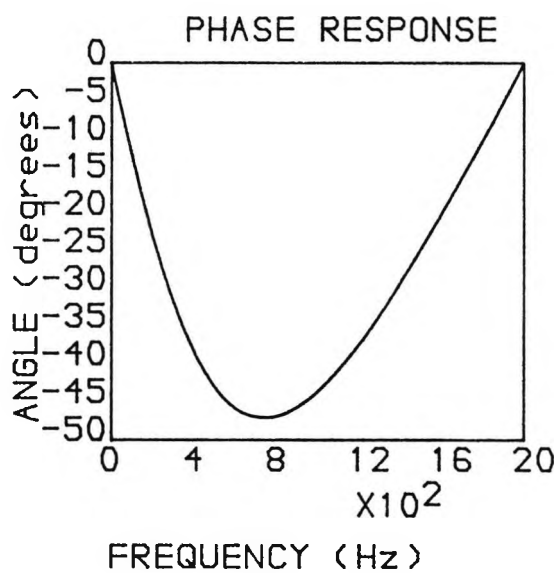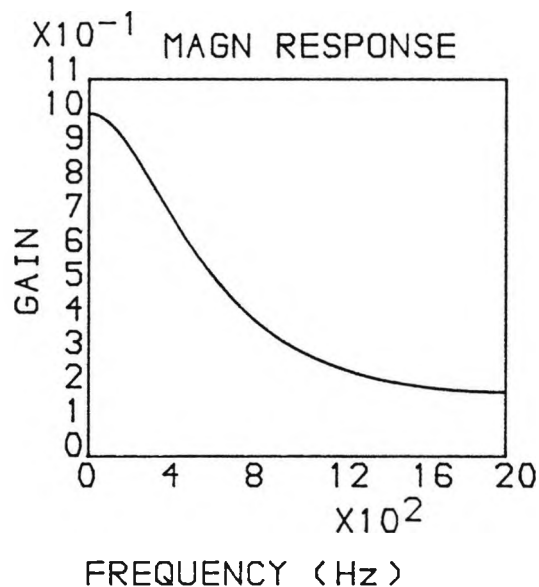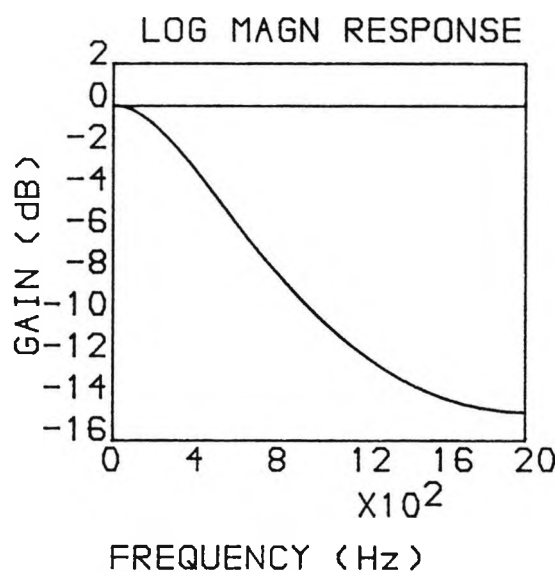
Fig. 4.3 Response of the analogue filter
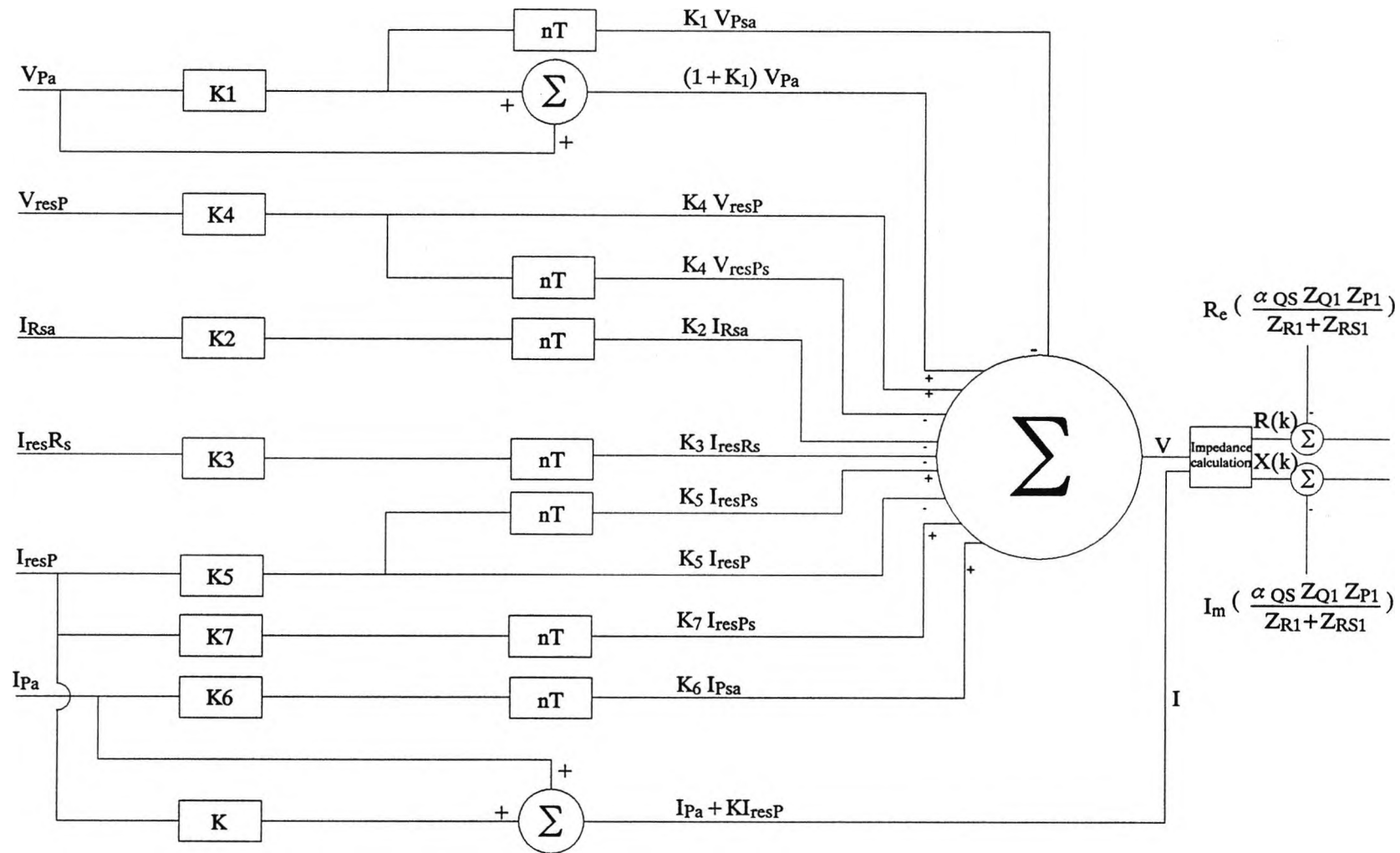
Fig 4.4 Basic signal arrangement for single phase to ground fault
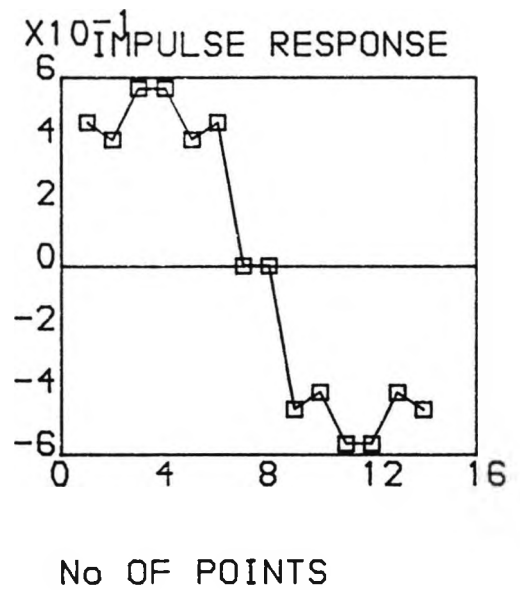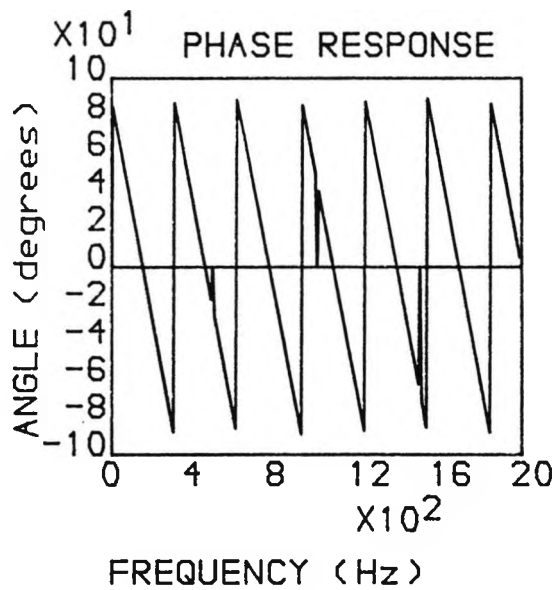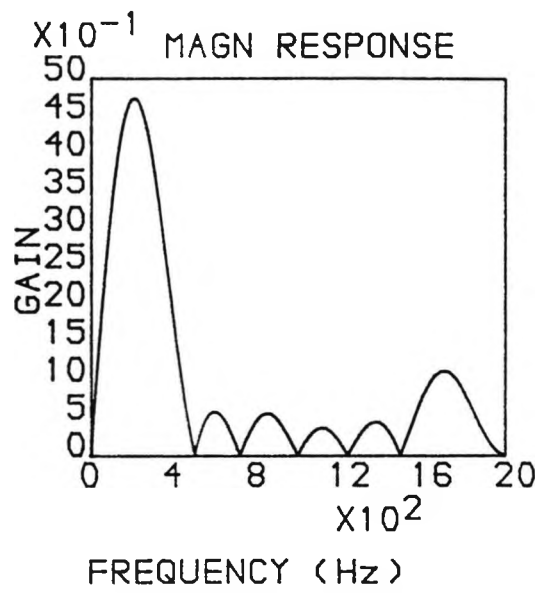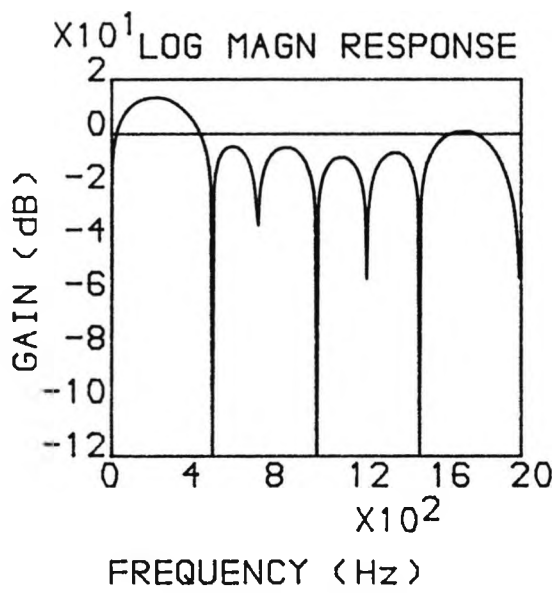
Fig. 4.5 Response of the digital filter
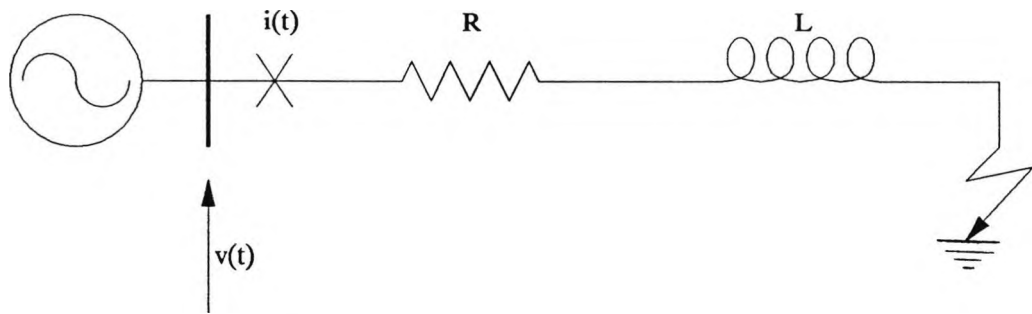
Fig. 4.6 Transmission line model
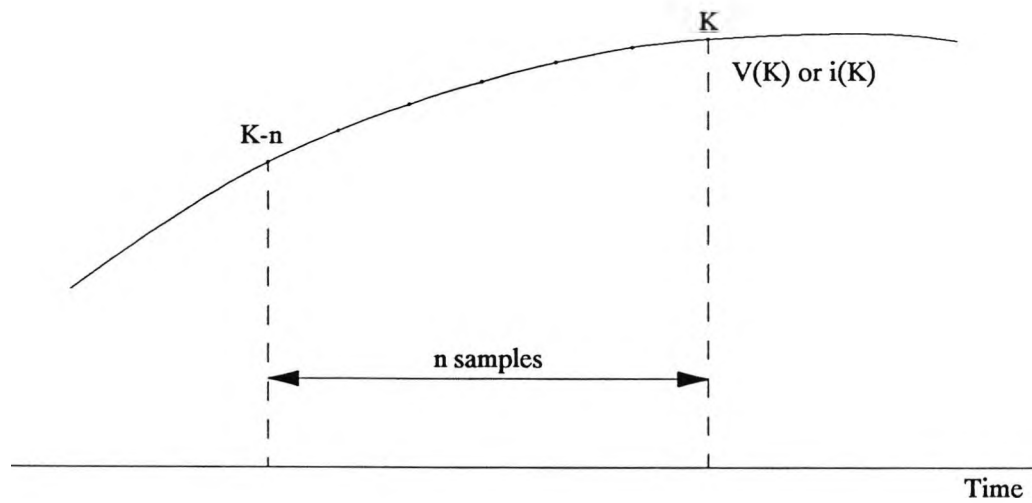
Fig. 4.7 Solution formation using time spacing
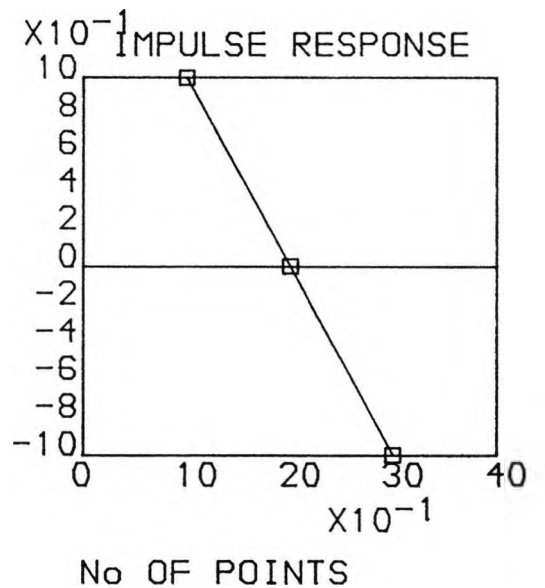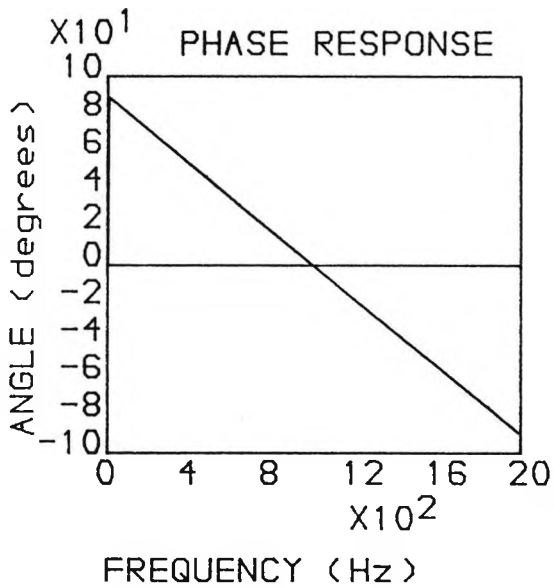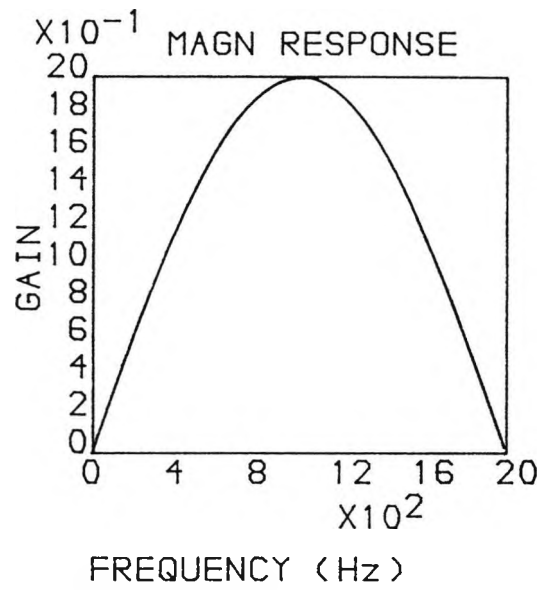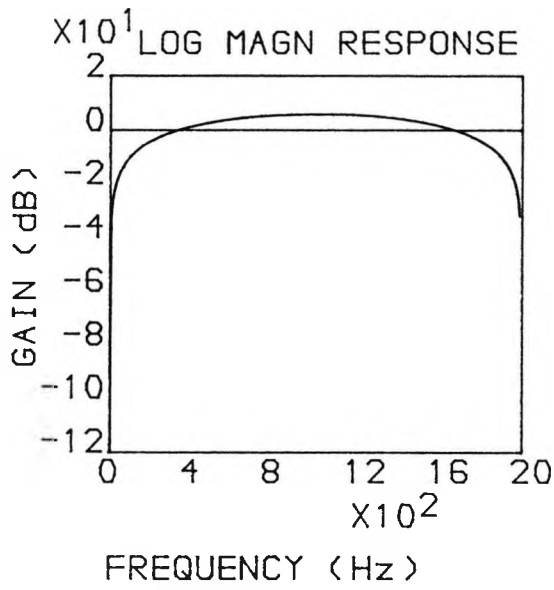
Fig. 4.8 Response of 3 point filter
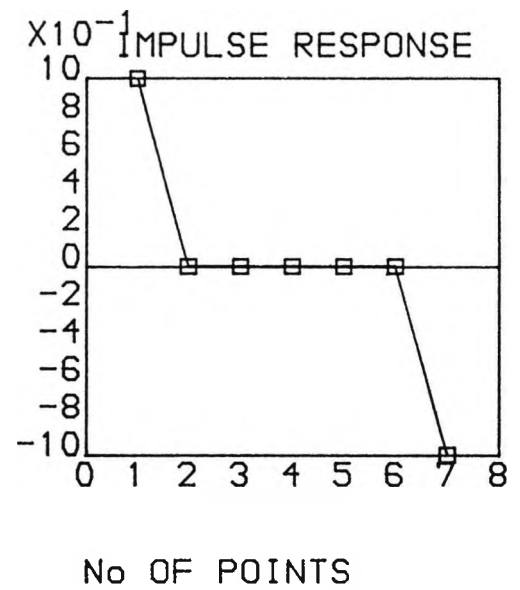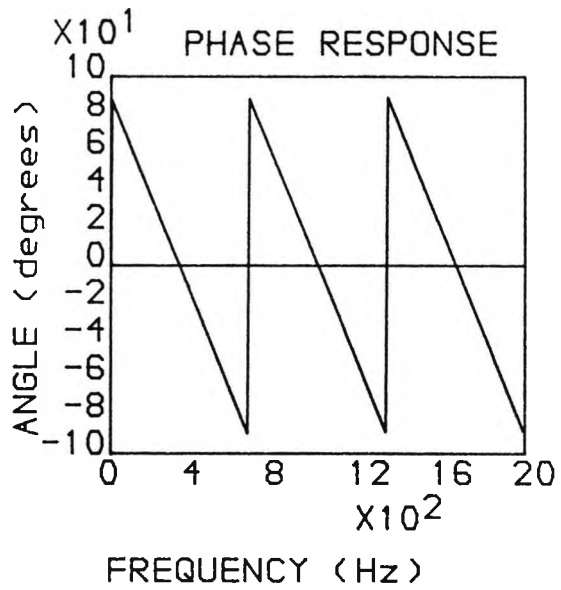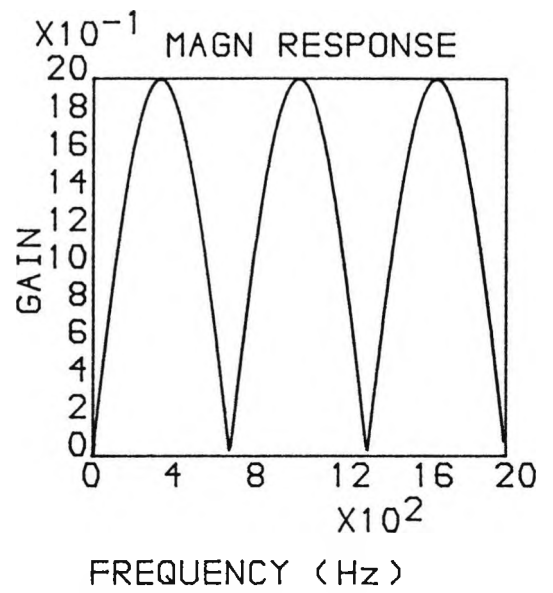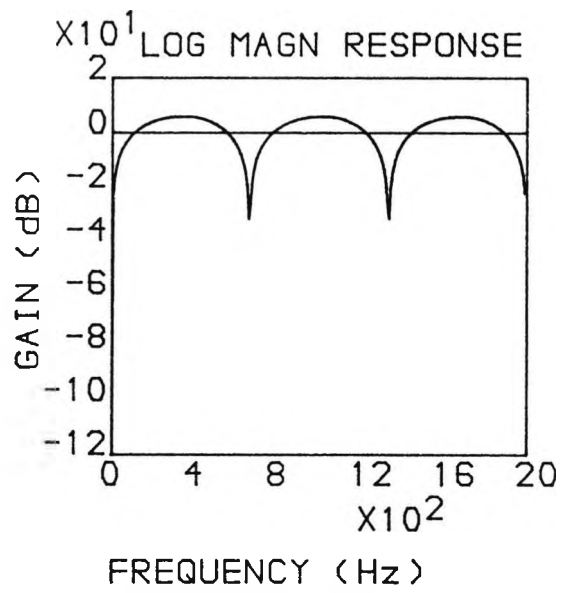
Fig. 4.9 Response of 7 point filter
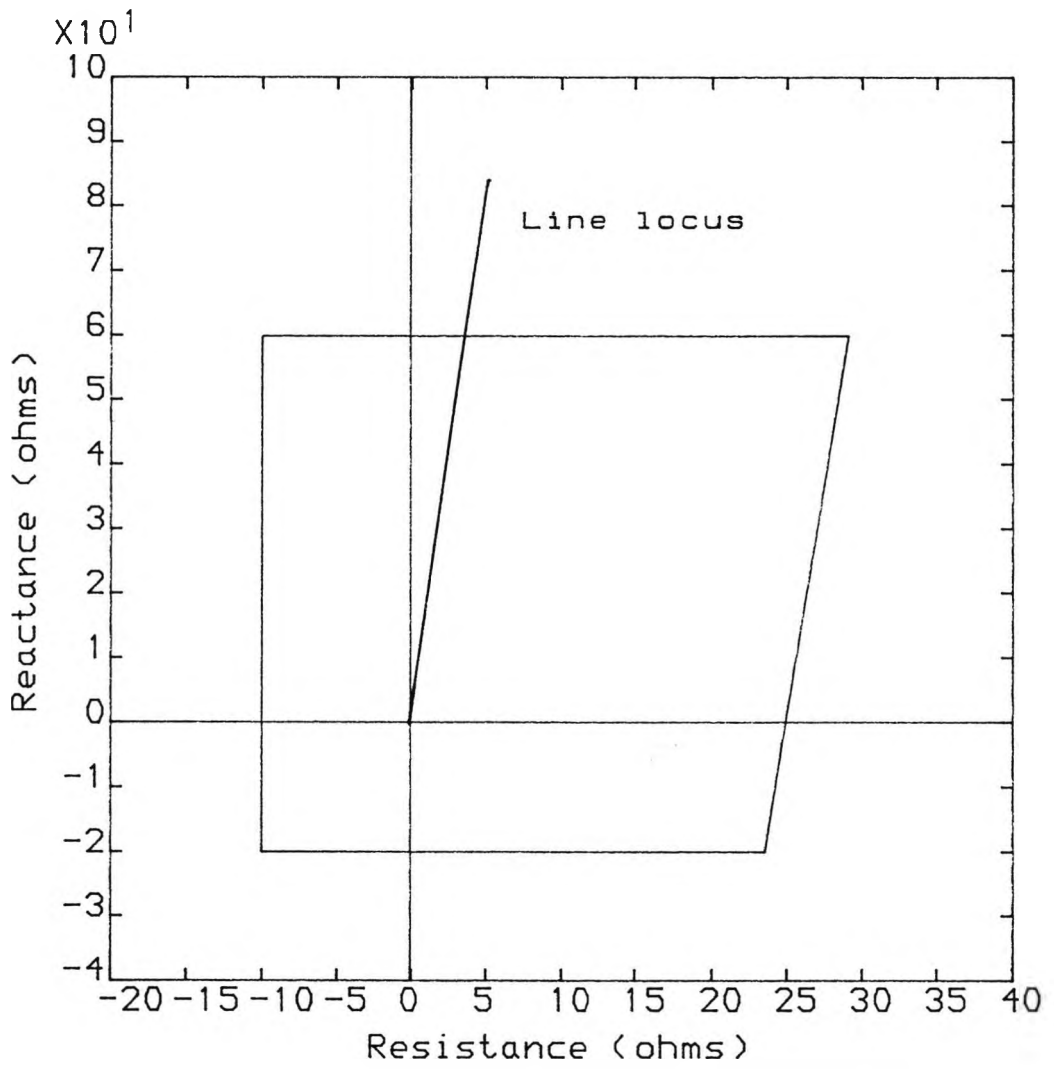
Fig.4.10 Relay quadrilateral characteristic.
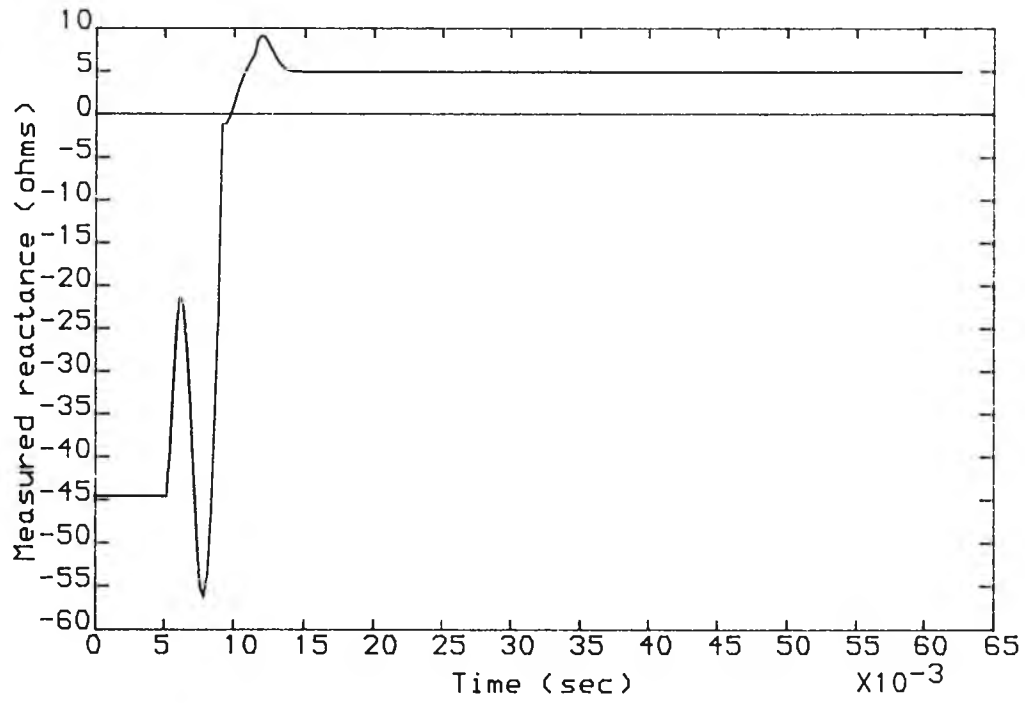
Fig.4.11   Measured reactance for a fault just
behind the relay
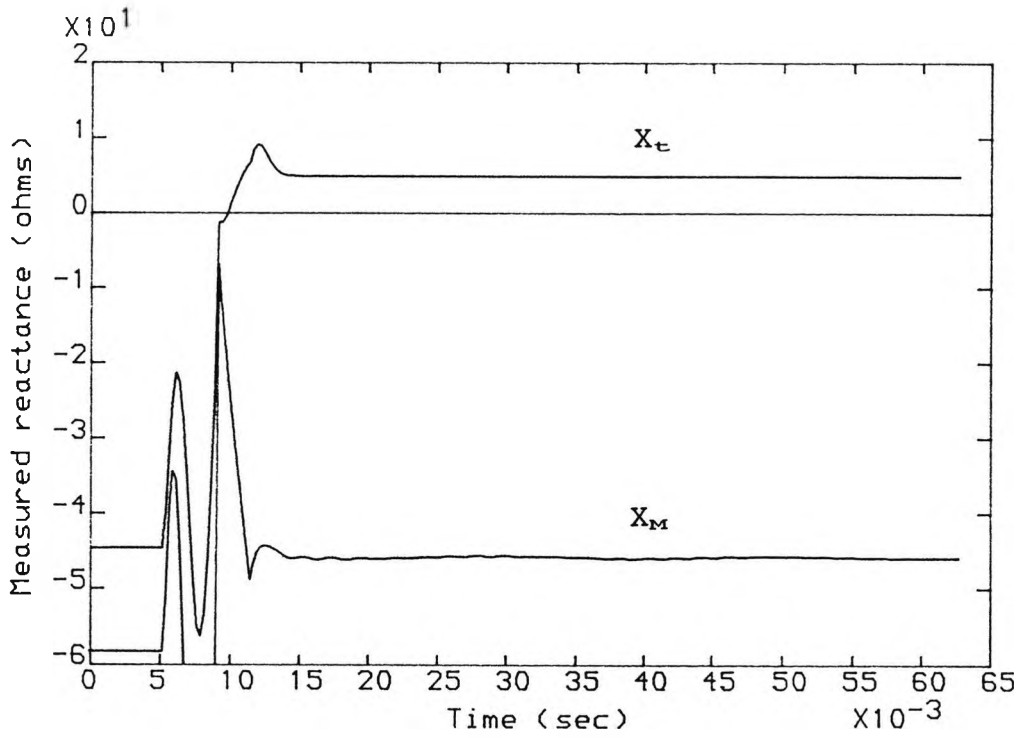
Fig.4.12   Measured XM and Xt for a fault
just behind the relay
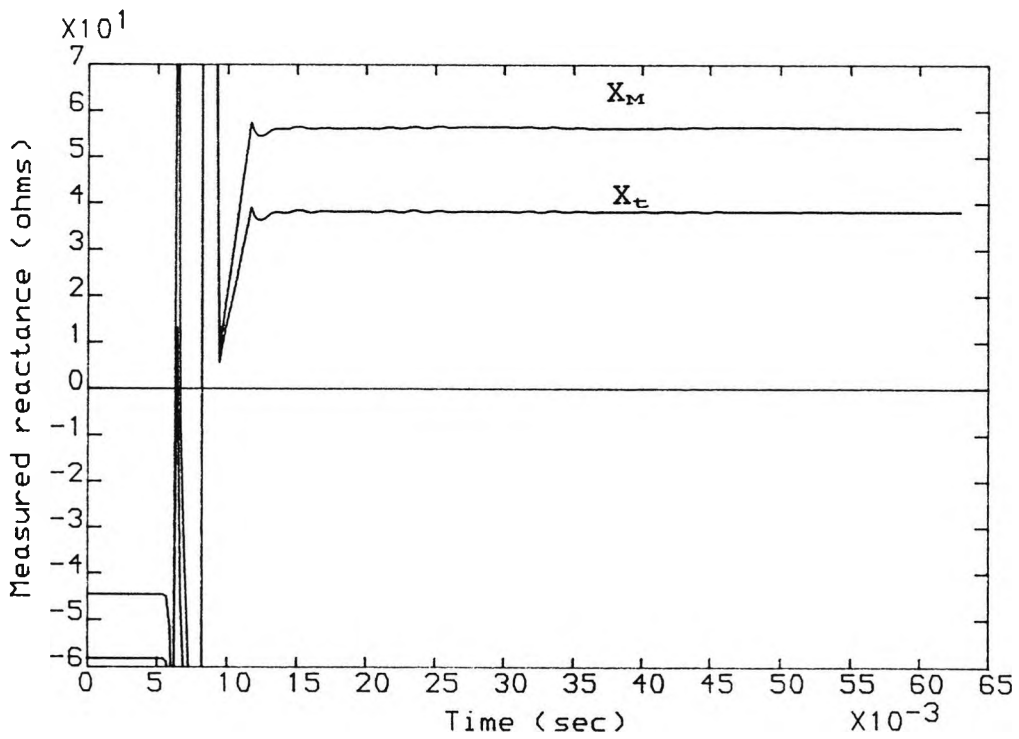
Fig.4.13 Measured XM and Xt for a fault
at the reach point
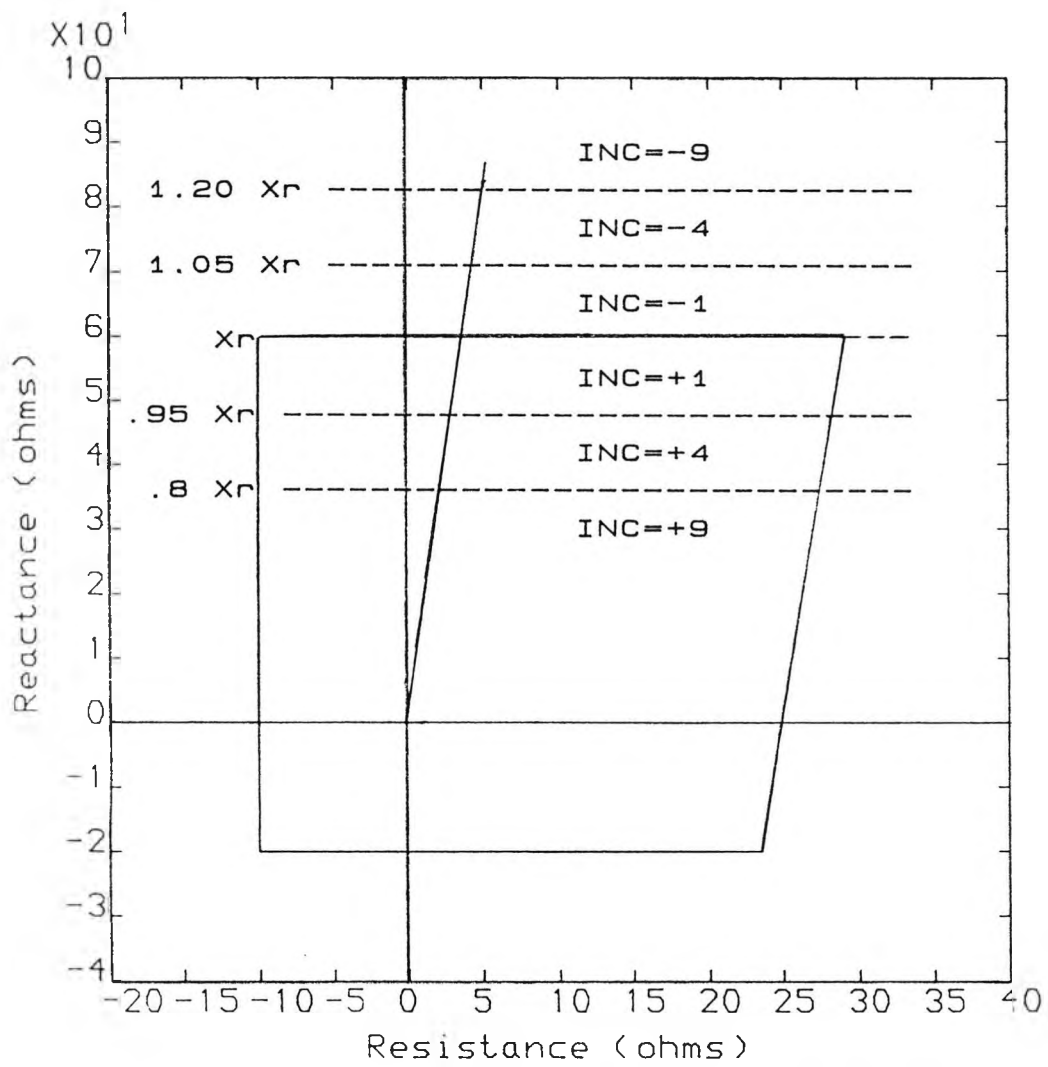
Fig.4.14 Relay quadrilateral characteristic
and counting strategy
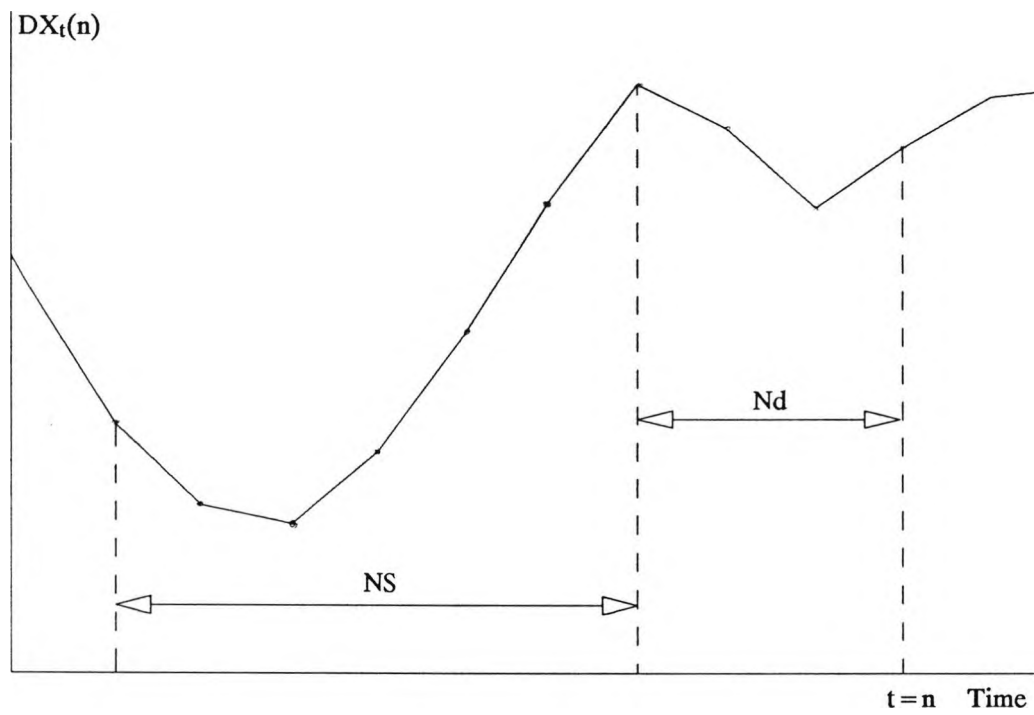
$$d(DXt)/dt = DX_t(n-Nd) - DX_t(n-Nd-Ns)$$

Fig. 4.15 Calculation of d(DXt)/dt used for counter inhibition
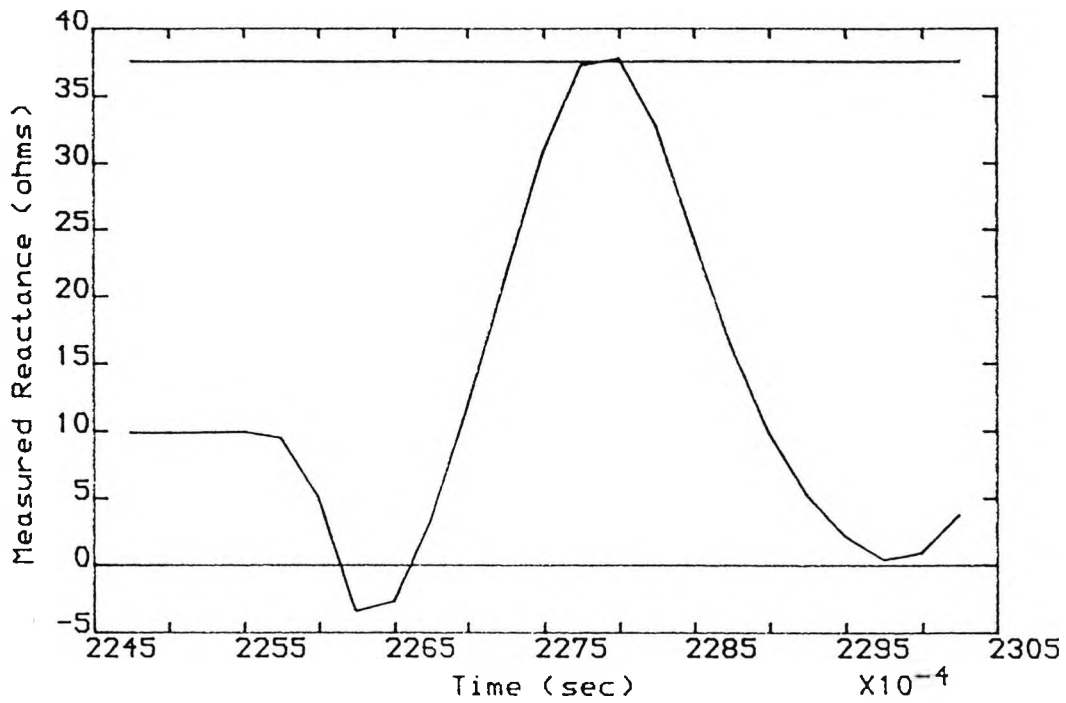
Fig.4.16a Measured reactance without counter
inhibition (maloperation)
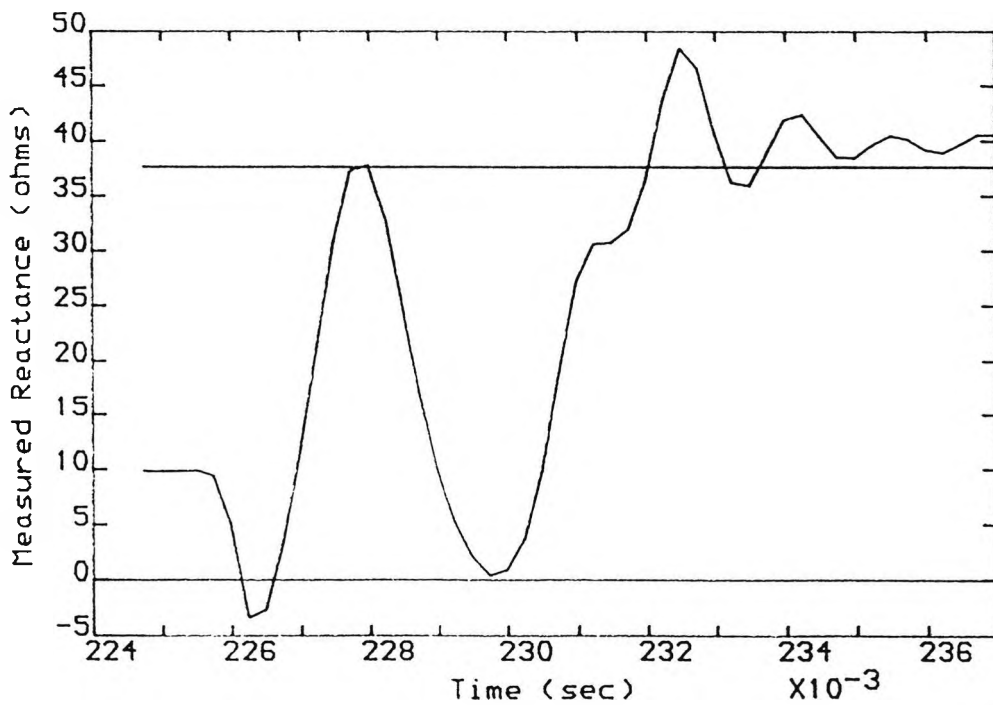
Fig.4.16b Measured reactance with counter
inhibition (correct operation)
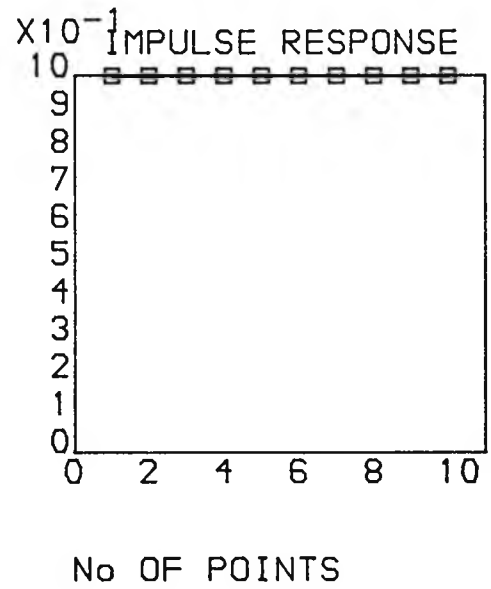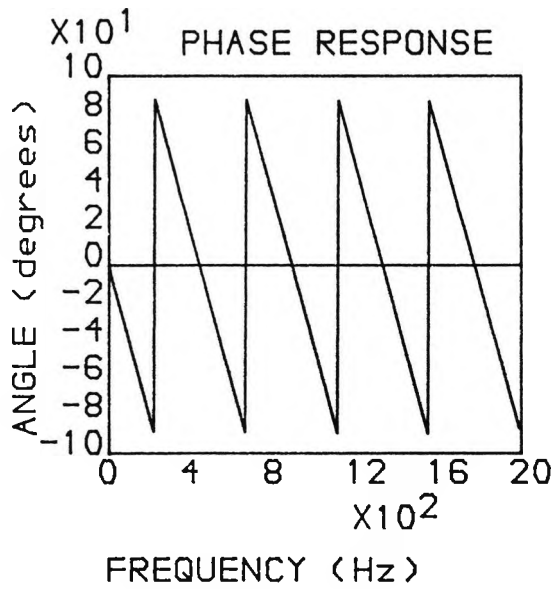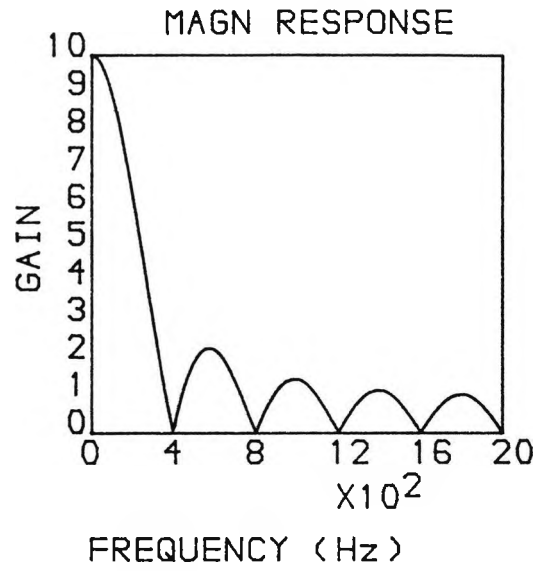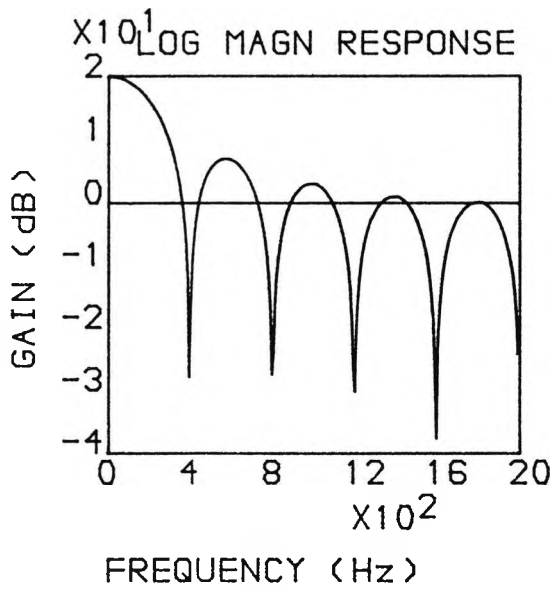
Fig. 4.17 The response of the averager with the
window length of maximum value of 10 points
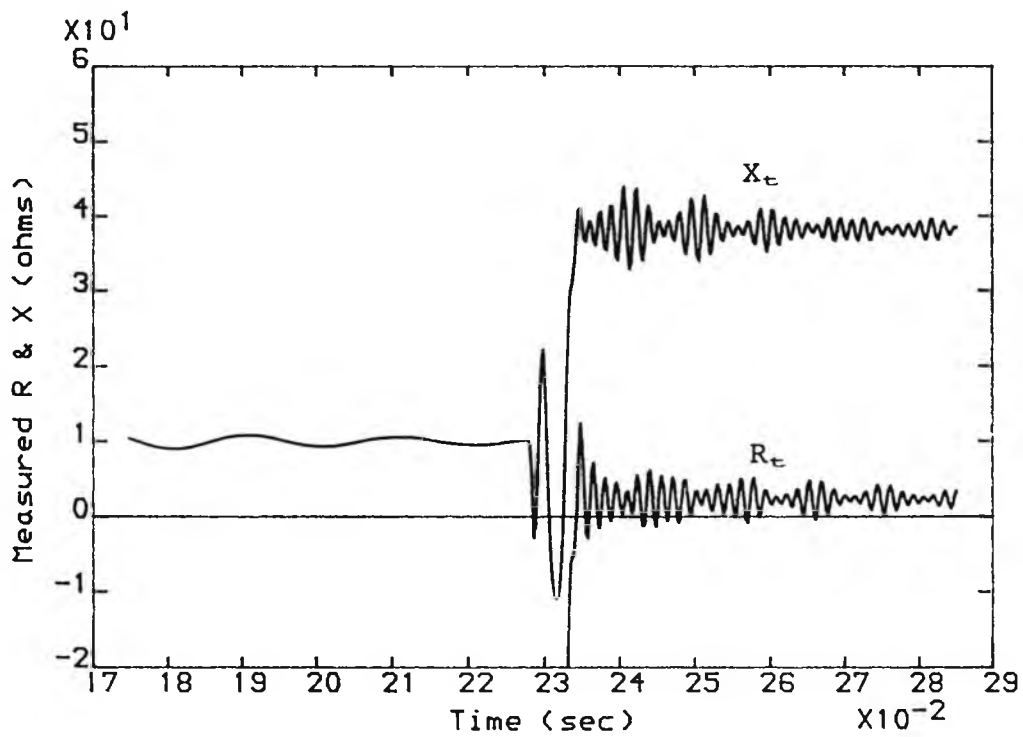
Fig.4.18a Measured Rt and Xt without averager
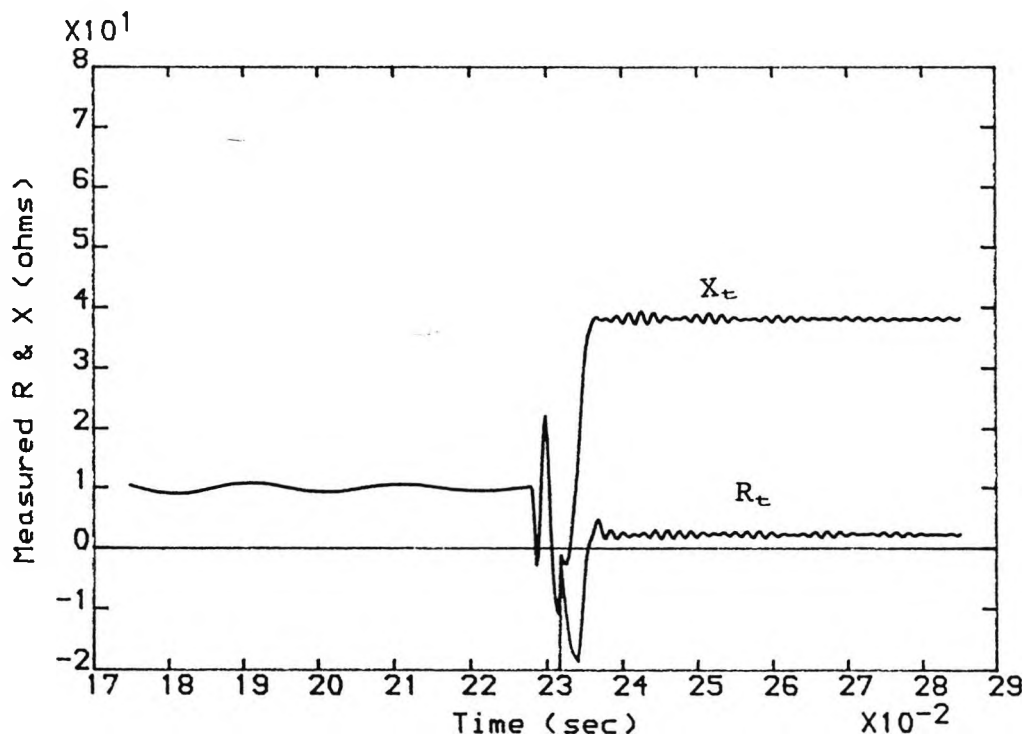
Fig.4.18b Measured Rt and Xt with averager

CHAPTER 5

ADAPTIVE SCHEME PERFORMANCE EVALUATION

In this Chapter a detailed evaluation of the performance of the adaptive scheme is presented. The assessments are based on the primary system phasor values and in this way the errors which could be introduced by the transducers and the hardware are avoided. The line is assumed perfectly transposed which is a normal practice when using distance protection. Non-transposition errors are small and are usually neglected in distance relaying schemes [36,37].

As part of the performance evaluation of the adaptive scheme, a number of tests were carried out to demonstrate the improvements achieved in reach point accuracy in comparison with conventional relays. The area covered by the impedance, for all fault conditions, and the factors influencing the size and shape of these areas is also discussed. The effect of fault resistance is studied to assist in the selection of the protection setting. The sound phase measurements are investigated. The relaying equation may be over demanding from the hardware point of view, and the investigations are therefore extended to quantify the contribution of various signals involved in order to simplify the relay. An example is given to study the relay sensitivity to possible errors introduced when the remote source impedance is different from the set value used in the relay.

5.1 Improvement in Relay Reach Over Conventional Relays

Before pursuing the analysis in detail, it is important to point out the improvements in the zone-1 reach that the adaptive scheme can offer over conventional distance relays; this is demonstrated in the following examples. The 400kV Teed system shown in Figure 5.1 is assumed to be purely inductive, the fault is a three phase fault and the prefault loading condition is zero. In this case Equations 2.27 and 2.31 derived for a single phase system are applicable. The relays considered are located at P, the conventional distance relay is set to cover 80% of the physical line from the relaying point to the remote nearest terminal. The adaptive scheme, as discussed in Chapter 2, comprises two relays; one is set for 80% of the line P-T-R, which in ohms is equal to $S_R=j37.66$, and the other for 80% of the line P-T-Q which corresponds to $S_Q=j56.4$ ohms.

The apparent impedance measured at end P for a fault on Section TR at the critical fault location is:

$$Z_{mP} = j61.6 \text{ ohms}$$

The maximum distance that could be protected along line TR measured from the Tee junction can be found by equating the measured impedance with the selected setting i.e.:

$$Z_P + \alpha_R Z_R + \alpha_R Z_R K_R = Z_P + \alpha_{RS} Z_R \qquad 5.1$$

$$\alpha_R = \frac{\alpha_{RS} Z_R}{Z_R + Z_R K_R} \qquad 5.2$$

$$= \frac{0.6 \times j23.54}{j23.54 + j23.54 \times 1.69}$$

$$= 0.222 \text{ p.u}$$

78

Therefore the total underreach along line PR is:

%UR = 23.6

The maximum distance that may be protected along Section TQ can be calculated from:

$$\alpha_Q = \frac{\alpha_{RS} \ Z_R}{Z_Q + Z_Q \ K_Q}$$ 5.3

= 0.093 p.u

giving a total underreach along line PQ of:

%UR = 25.8

It should be noticed that the underreach, on Section TQ, implies that the relay can cover a shorter physical distance than that on the Section TR.

By employing the adaptive scheme, Section TR can be protected completely to the reach point, while for faults on Section TQ the relay underreaches. The amount of underreach could be calculated from the following equation:

$$\alpha_Q = \frac{\alpha_{RS} \ Z_R(1 + K_R)}{Z_Q(\ 1 + K_Q)}$$ 5.4

%UR = 6.0

The foregoing values for %UR are for an arrangement where tripping requires the operation of both adaptive relays. From the above results it is clear that the adaptive scheme has great advantage over conventional distance protection regarding the zone-1 reach. For the above configuration the amount of underreach has changed from 23.6% for faults on Section TR to a full coverage, and that for faults on Q has reduced from 25.8% to 6%.

By considering the system of Figure 5.1, but with a

79

different fault level at the relaying point i.e., 2.5 GVA, the apparent impedance for a fault at the critical fault location on Section TR is found to be j45.85 ohms, compared with the j37.66 ohms setting. It is clear that the relay will underreach. The amount of underreach is 13.75% where the calculations for faults along Section TQ give the percentage underreach of 16.25. By applying the adaptive scheme the relay can give a full coverage for faults on line PR and it underreaches by 3.77% for faults on Section TQ. Again the adaptive scheme gives a better coverage over conventional distance schemes.

For certain operating conditions a full coverage of a whole Teed circuit could be achieved; this can be so if the fault level at the three terminals, in Figure 5.1, is assigned the following values: P = 2 GVA, R =0.48 GVA and Q = 35 GVA. The apparent impedances for faults at the critical fault point on Section TR and on Section TQ are equal to j66 ohms. With traditional distance relaying the relay would underreach by 25% for faults on Section TR and by 8% for faults on Section TQ. With the adaptive scheme the measurand which is allocated for faults on Section TR gives the correct discrimination between internal and external faults. The measurand which is allocated for faults on Section TQ also gives the correct discrimination for Section TR.

Similarly, for faults on Section TQ both measurands give the correct discrimination.

It cannot be taken for granted that the remote short section can be protected completely for all system operating conditions. The measurand allocated for faults on the remote longer section could underreach for faults on the shorter one. In Figure 5.1, if the fault levels at P, R and Q are 1, 0.2 and 35 GVA respectively, then the apparent impedance measured at end P for a fault at the critical fault location on Section TQ will be:

$Z_{mP} = j63.8$ ohms

where the measurands and the settings value are:

$Z_{mPQ} = j56.66$ ohms

$S_Q = j56.66$ ohms

$Z_{mPR} = j13.6$ ohms

$S_R = j37.66$ ohms

These figures ensure that, when Z_{mPQ} and S_Q, Z_{mPR} and S_R are compared with each other simultanously, the longer section can be protected completely.

The apparent impedance measured at end P for a fault on Section TR at the critical fault location is:

$Z_{mP} = j87.8$ ohms

where the measurands value are

$Z_{mPQ} = j80.5$ ohms

$Z_{mPR} = j37.66$ ohms

The maximum distance that could be protected along Section TR measured from the Tee point can be found from the following equation

$$\alpha_R = \frac{\alpha_{QS} \; Z_Q(1 + K_Q)}{Z_R(1 + K_R)} \qquad\qquad 5.5$$

$\alpha_R = .376$

81

$\%UR = 14.$

On the other hand, with conventional distance schemes the
relay would underreach by 29% for faults on R and by 6.8%
on Section TQ, when it is compared with the setting of the
shorter section i.e. with S_R.

Therefore, with reference to the zone-1 reach, it is
clear from the above examples that, the adaptive scheme
would again give substantial improvement.

5.2 Fault Area in the Impedance Plane

As mentioned in Chapter 2 the adaptive scheme comprises
two distance relays, each of which gives the exact line
impedance at the reach point on its allocated remote
section. For in-zone faults the impedance will be smaller
than the actual line impedance, and for out of zone faults
the impedance will be greater than the actual value. The
behaviour of the scheme, for different fault location and
loading conditions, applied to a typical 400kV system,
(Figure 5.1), was studied. The two adaptive relays
considered are located at end P (one is set for 80% of the
line P-T-R and the other for 80% of the line P-T-Q). The
task is to identify the extremes of the measured impedance
for different fault locations in order to assist in the
selection of the protection settings. The familiar R/X
impedance plane provides a convenient tool to visualise
the behaviour of the measured impedance for various
operating conditions. Typical impedance loci, for a
three-phase fault along line P-T-R, are shown in
Figures 5.2 and 5.3, where the system source strength are

82

as indicated on the diagrams. For each fault location the load angle was varied at each source point from 0 to 15°. Figure 5.2 shows the impedance presented to the conventional relay. The part of the locus on the right of the line locus corresponds to power being exported from P prior to fault inception, and the part on the left to power being imported at P. Point A marks the actual line impedance at the 80% of the line P-T-R which corresponds to 0.6 p.u of the line TR calculated from the Tee point. For faults at this location the relay would see the impedance marked α_R=0.6 on the graph. Thus, the effect of this difference between the actual and the measured impedance will make the relay underreach. Figure 5.3 illustrates the impedance presented to the adaptive relay allocated for this path of the Tee. Clearly, it can be seen that the impedance corresponds to the actual line impedance at the reach point for all loading conditions. For in-zone faults the reactive component would always fall short of the relay reactive reach. Also for close-up faults the relay would see a negative reactance. The incursion into the negative region is determined from the relative strength of the sources and the reach beyond the Tee point. The weaker the fault level at the point of measurement compared with that at the far ends and the longer the line section beyond the Tee junction, the higher the incursion into the negative region. Therefore, it is necessary to shape the protection characteristic so as to make sure that the impedance measured for close-up faults will fall within the relay boundary. This can be

easily achieved in a digital computer based distance relay.

The measured resistance is correct at the reach point; for internal faults the resistance could take a larger or smaller value than the actual line values and this depends mainly on the direction of the prefault current. The maximum negative resistance will be encountered when the power flow, prior to the fault, is exported from P and R. The maximum positive resistance is encountered when the power is exported from Q and imported at P and R, which in effect is the opposite trend compared with that of the conventional relay (Figure 5.2). These resistances could be contained within the relay characteristics as these are usually extended to cover certain fault resistance values. The measurand behaviour when a fault resistance is encountered will be discussed in a later section.

In conventional distance schemes applied to Teed feeders, the maximum underreach will be encountered when the source strength at the point of measurement is minimum and those at the far ends are maximum [3]. Figures 5.4 and 5.5 illustrate the variation of the measured impedance for various fault locations, along line P-T-R, when the fault level at the relaying point is 3.5 GVA and that at the remote ends is 35 GVA. As shown in Figures 5.3 and 5.5, the measurand gives the correct line impedance at the reach point. It is clear that the combination of low source capacity at P together with a high source capacity at the far ends causes a higher incursion into the

84

negative region, also the area covered by the resistive
component is increased which is mainly due to the load
current being comparable with the fault current at the
relaying point.

Another point which is worth noting is that the
maximum incursion into the negative region is roughly
equal to the difference between the conventional and the
adaptive measurand at the reach point. In theory this
could take very high value when the source strength at the
point of measurement is extremely low compared with that
at the far end, but if we restrict these values within the
recommended practical limits (for example, for a 400kV
system the maximum value is 35 GVA and the minimum is
3.5 GVA [38]) the relay boundary can be specified without
jeopardising the system operating conditions.

The relay performance for faults on the line P-T-R in
Figure 5.1 has now been discussed fully. Now the relay
allocated for the line P-T-Q will be discussed. Figures
5.6 and 5.7 show the impedance measured by the
conventional and the adaptive relay for faults along the
line P-T-Q, for a fault level of 35 GVA at the terminals.
It is clear that the adaptive relay gives the exact line
impedance at the reach point. For internal faults, the
region where the impedances fall are similar to those of
Figure 5.3, but are generally spread over a wider area.
This is because line Section TQ beyond the Tee point · is
longer than the line Section TR . Figures 5.8 and 5.9
show the measured impedances when the fault level at the
relaying point is reduced to 3.5 GVA. The point to be

noticed in Figure 5.9 is that, the incursion into the negative region is increased compared with that of Figure 5.5 which is due to the longer line section beyond the Tee point.

The response of the relay allocated for faults along line P-T-Q, when the fault is on the P-T-R, is shown in Figures 5.10 and 5.11. It can be seen that the reactive component can fall well inside the reactive reach, but the measured resistance could take larger values compared with when the fault is on Section TQ, (Figures 5.7 and 5.10). This is because the relay does not respond correctly to the direction of the load current in this path; nevertheless these values can be contained within the relay characteristics. Figures 5.12 and 5.13 illustrate the impedance measured by the adaptive relay allocated for faults along line P-T-R when the fault is on the line P-T-Q. Since the two adaptive relays cannot identify locally the remote faulted section, the relay allocated for the remote short section determines the zone-1 reach on the remote long section. It may not be possible for the Z_{mPR} measurand to identify, on Section TQ, a unique distance where simultaneously the resistive and reactive components can correspond to the exact line impedance unless the system is symmetrical and unloaded. Therefore, when calculating the reach on the remote longer section the reactive component is considered, the resistive component is normally of little consequence as the relay resistive reach is usually extended to contain certain fault resistance.

86

5.3 Scheme Behaviour on an Interconnected Teed System

The system shown in Figure 5.14 represents a Teed system with external ties between the generating stations; these ties are considered so remote that they do not have any mutual coupling with the Teed line. For this configuration, the effective source impedance would vary with the fault position. If the adaptive relay is to operate correctly, the remote source impedance which is utilised by the adaptive relay, needs to be calculated for a fault at the critical fault position, i.e. at zone-1 reach.

Figure 5.15 shows the variation of the source impedance at busbar Q for a three phase fault along line P-T-R. This impedance is calculated, as mentioned in Section 2.2, from the superimposed voltage and current at end Q. It is clear that the effective source impedance can vary considerably with the fault position. Thus the measured impedance will be affected if the remote source impedance is not calculated at the reach point. The effect, which errors in estimation of the remote end source impedance has on the impedance measurement, will be evaluated in a later section.

For the system under consideration the variation of the conventional and the Z_{mPR} measurands for different fault locations along line P-T-R are shown in Figures 5.16 and 5.17. It can be clearly seen that the adaptive relay is accurate at the reach point and performs correctly to discriminate between internal and external faults.

5.4 Effect of Fault Resistance

Fault resistance modifies the apparent impedance presented to the relaying system. This resistance is usually represented as an R component on the R-X plane, although in practice an apparent reactance component also exists, resulting from source impedance angle differences, load current flow, etc [39]. For Teed configurations the current at the fault point is a combination of the currents fed from the three ends and the local end relay cannot correctly take this into account. This in turn could substantially increase the value of the resistance, especially when the source capacity at the relaying point is weak compared to that at the remote ends. The adaptive relay effectively compensates for the infeed current at the reach point and therefore it is expected to behave, at the reach point, as a conventional relay applied to a plain feeder. Figures 5.18-5.20 show the measured impedances for single phase to earth faults along line P-T-R. For each fault location fault resistances of 0, 2, 5 ohms were assumed. In order to provide the basis for selecting the relay reach characteristics, the source capacity at the relaying point is taken as 3.5 GVA and those at the far ends are 35 GVA.

Figure 5.18 shows the apparent impedance for a zero prefault loading. For the fault at the reach point a small change in the apparent reactance can be seen, resulting from the impedance angle difference of the infeeds. The fault resistance is greatly magnified due to the infeed from the R terminal; thus a 5 ohms fault

88

resistance is seen by the relay as 30 ohms. On the same graph, for comparison purposes, the impedance presented to the conventional relay is included and it can be seen that the adaptive scheme effectively shifts down the fault area as seen by the conventional relay. For instance, considering the line at the reach point (α_R=0.6 on the graph), the two relays see approximately the same resistance, but the reactive reach, which is usually the main consideration in distance protection, is true only for the adaptive measurand.

An underreach or overreach could occur due to the effect of the load current which flows in the line but not in the fault. Figure 5.19 shows a case of underreach, the line loading is indicated on the graph by the phase shift of the voltages at the terminals. The measured reactance has its greatest value when power is exported from Q and imported at P and R.

Figure 5.20 shows a condition for overreach. Faults at the relay boundary cause a considerable reduction in the reactance due to the direction of flow of the load current. As the fault moves towards the point of measurement, the higher fault current tends to swamp out the influence of load current. The zone-1 limit almost excludes the α_R=0.8 locus in Figure 5.20 which ensures that selectivity is maintained over the fault resistances considered; these values can be sufficiently broad to include the most common fault resistances encountered in practice.

89

5.5 Investigation into Sound Phase Measurements

A complete distance protection terminal requires the relays to measure correctly for all types of phase and earth fault, and, because the fundamental basis of correct measurement differs for single phase to earth faults and faults involving more than one phase with or without earth, different relay connections are required in each case. This is arranged by employing separate relays for phase and earth fault measurements, on the basis that the faulted phase or phases will measure a lower impedance than those associated with the healthy phases.

Figure 5.21 illustrates the impedances presented to a 6-element distance scheme for phase to earth faults. The loci refer to close-up solid faults on the protected circuit. It is seen that, for high source capacity behind the point of measurement, the healthy phase relays will approach the reactive axis of the complex-impedance plane, and that operation of healthy relays is likely to occur. The difference between the adaptive and conventional relay is that the latter approaches the origin of the impedance plane as shown in Figure 5.21.

The operation of healthy phase relays for faults within the protected feeder, in addition to the faulted phase relay, is not usually important, except in cases where distance relay operation is required to provide a discriminative control of auto-reclosing sequences by indicating which phase is faulted [40]. It should be noted that this phenomena is not new but it occurs in conventional distance relays applied to plain and multi-

terminal lines.

5.6 Suitability of the Adaptive Scheme for Use on a System with Outfeed Conditions

In this section the applicability of the adaptive relay will be investigated for a system with outfeed conditions, i.e., the fault current could flow outwards for an internal fault. The outfeed and its effect on the impedance measurement can take different forms. This will be illustrated in the following examples.

Figure 5.22 shows a system for which there is no source on the remote terminals; this may not be a practical case, in particular, for a 400kV system, but it nevertheless helps to illustrate the point. The effects of current distribution on the impedance measurement is illustrated in Figure 5.23, which shows the variation of the measured reactance for different fault positions on line P-T-R. It can be seen that the apparent reactance, for faults beyond the Tee point, is smaller than the actual line value i.e., an overreach condition. The adaptive relay can perform correctly on such a system provided that it is supplied with the correct value of the remote source impedance which has, in this case, an effective negative value. The variation of the adaptive measurand is displayed on the same graph. It is clear that it gives the exact line value at the reach point and correct discrimination is achieved.

Figure 5.24 shows a system for which fault current flows outward at the point of measurement for an internal

fault. The fault current at the relaying point, for
faults on the remote section(TR) flows inwards for a
section of the line and then reverses, to become an
outfeed rather than infeed for the other section. The
effect of this current distribution on conventional and
adaptive relays is illustrated in Figure 5.25 which
displays the variation of the measured reactance for
different fault locations. It can be seen that the
adaptive relay can perform correctly for faults up to the
reach point, the reactance being smaller than the line
value, but for external faults an overreach results.
Also, for a certain fault location the relay will see an
infinite impedance because the current will cease to flow
in the relay, if this point happens to coincide with the
zone-1 reach then an incorrect performance will occur.
Therefore, careful consideration should be given before
applying the adaptive scheme for systems with outfeed
conditions as the relay will not perform correctly for
certain operating conditions. But, at the same time, it
must be realised that the conventional relay also will not
operate correctly on such systems either.

5.7 Contribution of Various Signal Components within the Adaptive Relay Measurands

The most common type of fault that could occur on a
transmission line is a single phase to earth fault
[40,41]. As mentioned in Chapter 2, for the relay to
measure accurately for such fault, various signal
combinations must be used. In order to show the likely

magnitude and behaviour of each signal involved, the
system of Figure 5.1 is considered again. The source
capacity, at the relaying point is assumed to change from
a minimum of 3.5 to a maximum of 35 GVA for specific
system loading and source conditions at the remote ends.
In this analysis the reach of the relay is governed by the
measurand allocated to faults on line P-T-R. The relay
considered is at end P and the fault is a solid single
phase to ground fault at the reach point on Section TR.
The value of the impedances measured using various signals
(namely V_{Pa}, K'_1*V_{Pa}, K'_1*V_{PSa}, K'_2*I_{QSa}, K'_4*V_{resP},
K'_5*I_{resP}, K'_6*I_{PSa}, K'_6) were evaluated as a percentage
of the actual line impedance at the reach point in the R
and X direction as shown in Figures 5.26 - 5.29; the
following conclusions can be made:

1- K'_4*V_{resP}, K'_5*I_{resP} have a negligible effect on the
measurand this being mainly due to two factors; firstly
the residual voltage and current, at the relaying point,
are small for faults at the reach point, secondly the
constants K'_4 and K'_5 which are functions of the system
impedance tend to be very small especially when the relay
can be set to cover a certain distance beyond the Tee
point. Their collective contribution to the measured
reactance varies from 0.1% to 4% and no more than 10% to
the resistance for extreme system operating conditions.
Practically speaking their effect can be ignored for two
reasons; first their contribution is very small and
secondly they may be subjected to uncertainties in
determining some of their parameters such as the sequence

93

impedances of the sources.

2- The steady state currents at the relaying point I_{Psa} and at the remote end I_{Qsa} are the main factors in adjusting the resistive component of the impedance; this resistance can have negative or positive values depending on the direction of power flow prior to a fault. Their effect on the measurand reactance is extremely small and does not exceed 1.0%. For the condition when the power is exported from Q and imported at P and R the steady state currents, for internal faults, cause the relay to measure a resistance which is greater than the actual line resistance and this would reduce the resistive coverage. Nevertheless, this could be no problem as the resistive setting is extended to contain a finite fault resistance.

3- The measurand is considerably influenced by $K'_1 * V_{Pa}$ and $K'_1 * V_{Psa}$; which are thus the main factors in adjusting the reactive and resistive components of the impedance. The contribution of these factors to the measured impedance depends on the system operating conditions at the relaying and remote end. In effect, the weaker the source at the relaying point (compared with the source at the remote end) the greater is their contribution.

The prefault voltage V_{Psa} is higher than the postfault voltage, V_{Pa}, neglecting fast transients. V_{Pa} gets smaller as the fault becomes closer to the relaying point. This makes the relay measure an impedance which is smaller than the actual line impedance and may be considered advantageous in that a better coverage can be achieved when an arc resistance is encountered.

94

4- The constant factor K'_6 is one of the major determining factors in adjusting the measurands and its possible magnitude for the different system conditions considered is illustrated in Figures 5.26 to 5.29.

Therefore, while the optimum accuracy of the relay is achieved by inclusion of all signal components, there are some which can be ignored with negligible error on the measurand and other signals have insignificant effect on the reactive component. The relay can be simplified dramatically if small errors in estimating the measured impedance can be tolerated.

Figure 5.30 shows the relay measurement when the signals $K'_2 * I_{QSa}$, $K'_4 * V_{resP}$, $K'_5 * I_{resP}$, $K'_6 * I_{PSa}$ are not considered; effectively, this reduces the signals to the case of the three phase fault with the steady state currents ignored (Equation 2.31). The normal residual current is added to the phase current. Comparing it with Figure 5.20, where all signals were used, it is obvious that there is no dramatic difference between the two cases. The reactive component has barely changed (the variation from the exact value accounts for about 1%) and the resistive part has increased by a small margin, in particular around the boundary. This may justify the application of the adaptive scheme in a simplified state. It can be noticed that the system operating condition considered is one of the worst since the source capacity at the point of measurement is relatively weak compared with that at the far ends.

5.8 Relay Sensitivity for Errors in the Remote Source Impedance

The remote source impedance, which is required to be updated periodically in the relay, is the key factor for applying the adaptive scheme. If this impedance is not estimated correctly then an error in the relay measurement can be expected. In general, the relay will overreach if the true source impedance is greater than the value fixed in the relay, and underreach when the actual source impedance is smaller than the value used in the relay.

The measured and the actual line impedance do not have a simple linear relationship. The relay measures the exact line impedance at the reach point only; for in-zone faults the measured reactance, in particular, will be smaller than the actual line reactance; and, for out-of-zone faults the measured reactance will be greater than the actual value. This can be regarded as an advantage to discriminate between internal and external faults near the boundary. To illustrate this point a three phase fault is applied around the reach point on line TR. For the selected operating condition the measured and the actual line values are depicted in Table 5.1. It can be seen that a bigger margin between the measured and actual reactance is encountered when the source strength is small compared with that at the remote end.

In order to show the likely magnitude of errors on the relay accuracy, when the remote source impedance utilised by the relay, does not represent the actual system value, the power sources, in Figure 5.1, are

assumed to be capable of creating a fault of 10 GVA. The fault considered is a single phase to earth fault along line P-T-R which means that the effects of the source impedance at end Q on the measurement accuracy need to be evaluated.

After extensive investigations , two cases (apart from the one where the source impedance utilised by the relay is the true value of the system) were considered:

a- when the actual source impedance is half the value used in the relay; in terms of fault level this represents 20 GVA.

b- when the actual source impedance is twice the value used in the relay; in terms of fault level this represents 5 GVA.

It should be noted that the value of the source impedance fixed in the relay represents the 10 GVA source strength. For the above cases, the variation of the measured reactance for different fault locations is shown in Figure 5.31. From this graph, it can be seen that the relay is not very sensitive for the variation in the remote source impedance, for instance, the 100% increase in the remote source impedance accounts for a 2.9% overreach, and for the 100% decrease the underreach is 2.6%. These results may suggest a simpler approach for the practical implementation of the scheme, for example, the remote source impedance may not be required to be updated periodically as suggested in Chapter 2. The history of the limits of the operating conditions could also be used to fix an average value for the remote source

impedance in the relay and only the operating status of the remote circuit breaker (whether open or closed) need to be transmitted.

5.9 Summary

From the foregoing results and discussions, it is clear that the adaptive scheme gives an improved coverage over conventional distance schemes. The relay can be used on systems with outfeed conditions provided that this does not occur at the point of measurement. The relay requires many signals to be manipulated in order to measure the exact line impedance at the reach point. It has been shown that ignoring some of these signals had an insignificant effect on the measurand.

Also, it has been shown that the measurand is not sensitive to large variations in the remote source impedance. In this respect, the scheme could be implemented with minimum information from the remote terminal which is not required in real time.

Table 5.1
Variation of measured impedance with fault position
Ra =actual line resistance
Xa =actual line reactance
Rm =measured resistance
Xm =measured reactance
— No-load condition

SCL P=3.5 (GVA)
SCL Q=35 (GVA)
SCL R=35 (GVA)

resist & react (ohms)	Fault position (% of reach)					
	80	90	95	100	105	110
Ra	1.8	2.0	2.2	2.3	2.4	2.5
Xa	30.1	33.9	35.7	37.7	39.5	41.4
Rm	1.8	2.0	2.2	2.3	2.4	2.5
Xm	22.6	30.0	34.0	37.7	41.3	45.2

SCL P=3.5 (GVA)
SCL Q=3.5 (GVA)
SCL R=3.5 (GVA)

Rm	1.6	1.95	2.1	2.3	2.5	2.6
Xm	25.1	31.3	34.5	37.7	41.2	44.3

SCL P=35 (GVA)
SCL Q=3.5 (GVA)
SCL R=3.5 (GVA)

Rm	1.6	1.95	2.1	2.3	2.5	2.6
Xm	28.6	32.5	35.0	37.7	40.2	42.8

99
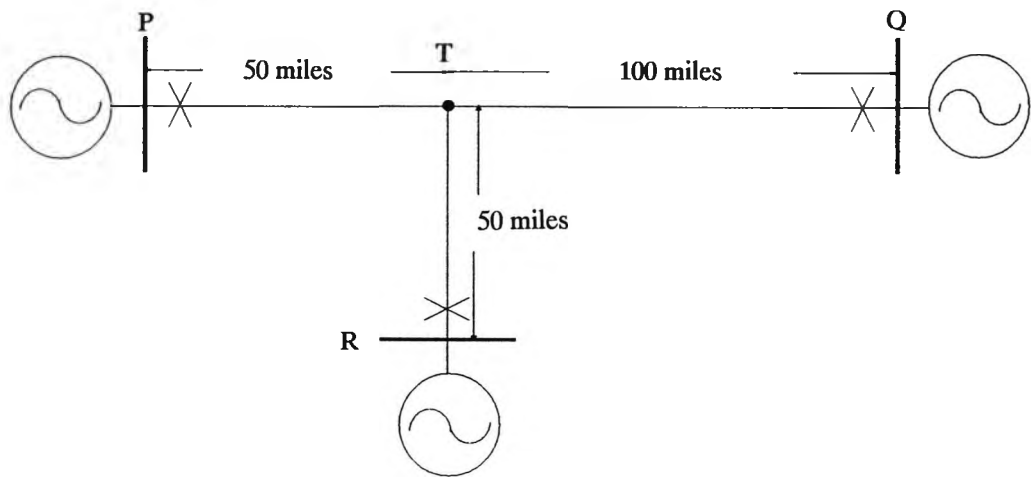
Fig. 5.1 Teed system used for relay testing.
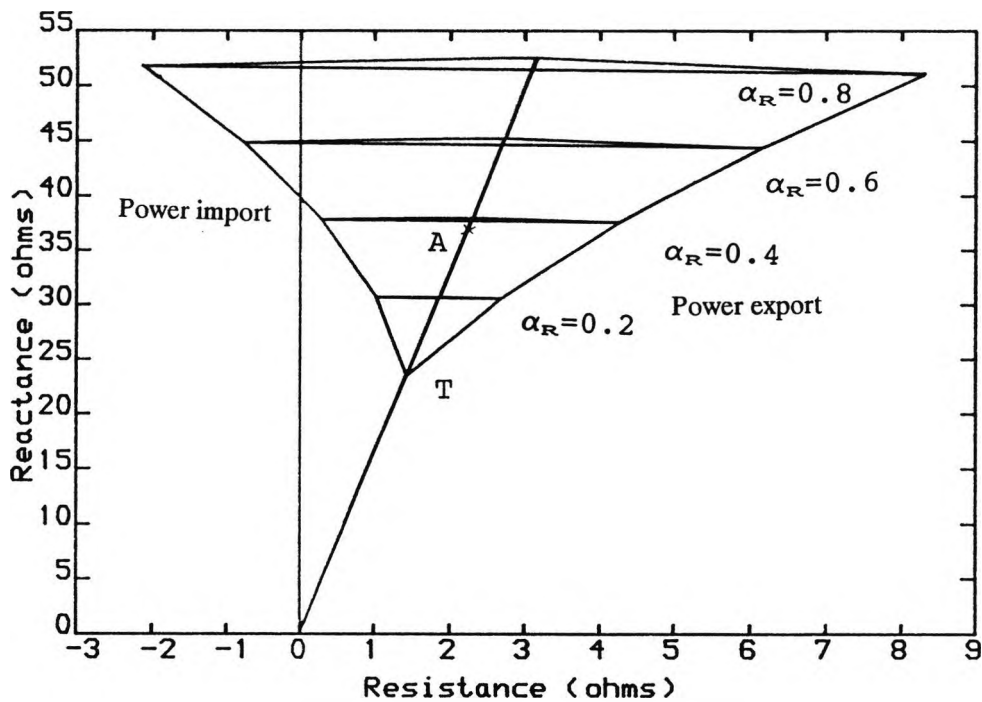
Fig.5.2 Fault areas in the impedance plane
for a fault on line P-T-R.
SCL (GVA) P=35 Q=35 R=35
Conventional measurand
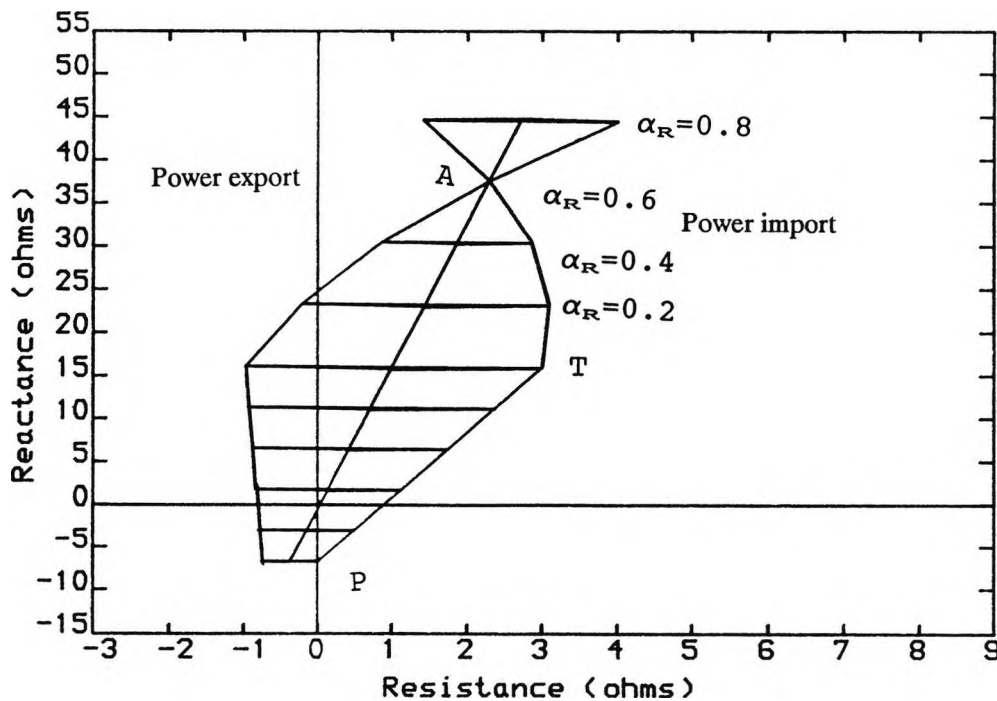
Fig.5.3 Fault areas in the impedance plane
for a fault on line P-T-R.
SCL (GVA) P=35 Q=35 R=35
ZmPR measurand
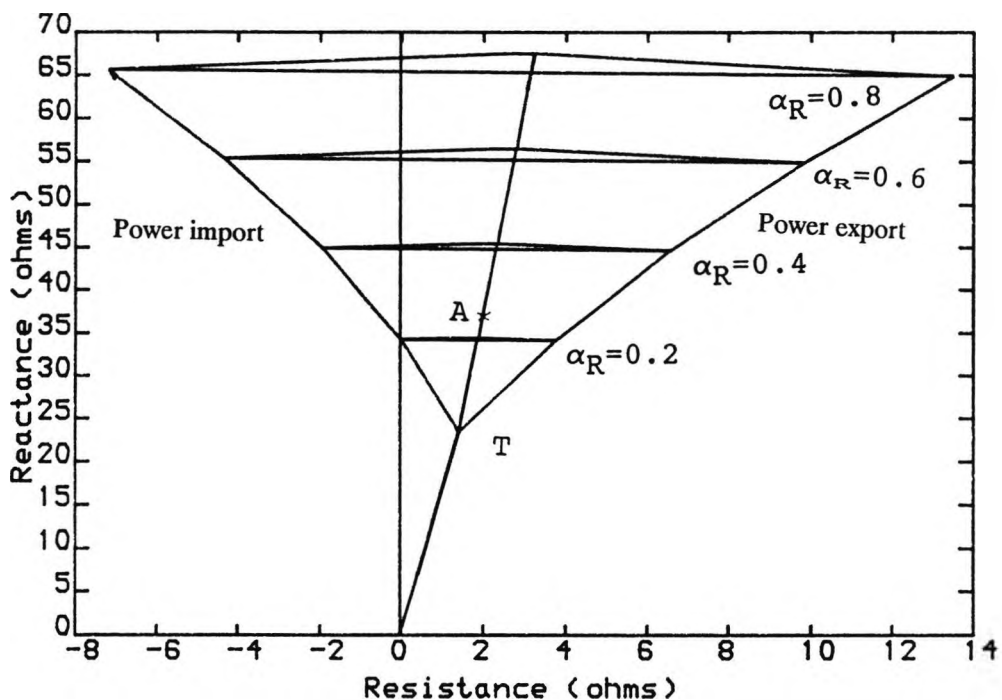
Fig.5.4 Fault areas in the impedance plane
        for a fault on line P-T-R.
SCL (GVA) P=3.5   Q=35   R=35
Conventional measurand
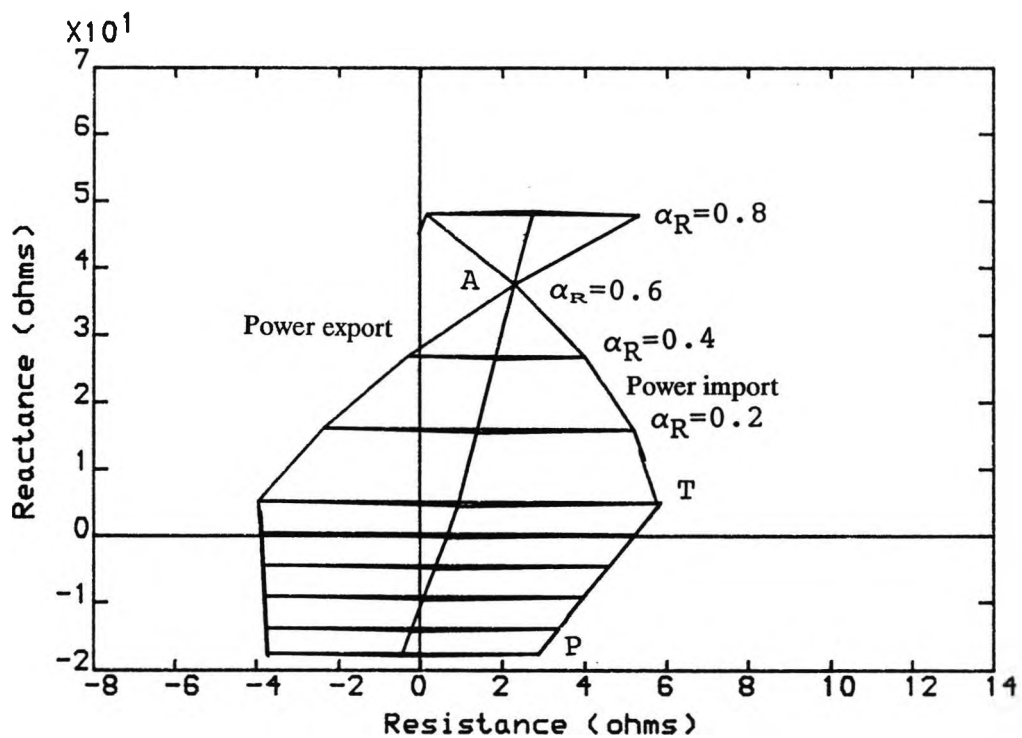
Fig.5.5 Fault areas in the impedance plane
        for a fault on line P-T-R.
SCL (GVA) P=3.5   Q=35   R=35
ZmPR measurand
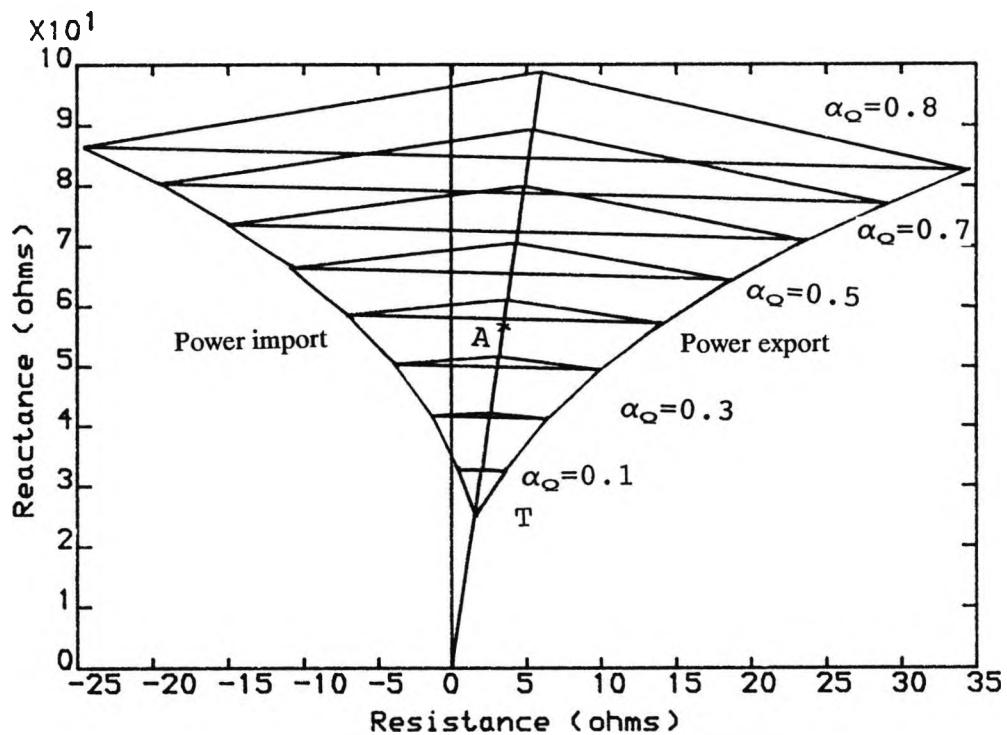
Fig.5.6 Fault areas in the impedance plane
for a fault on line P-T-Q.
SCL (GVA) P=35 Q=35 R=35
Conventional measurand
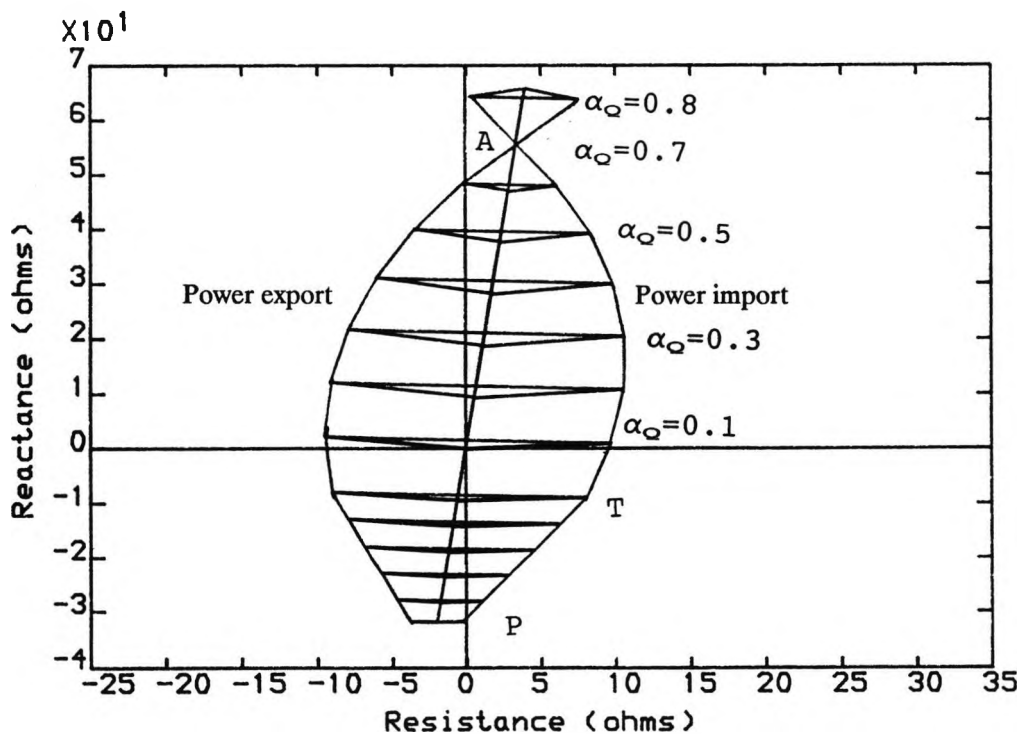
Fig.5.7 Fault areas in the impedance plane
for a fault on line P-T-Q.
SCL (GVA) P=35 Q=35 R=35
ZmPQ measurand
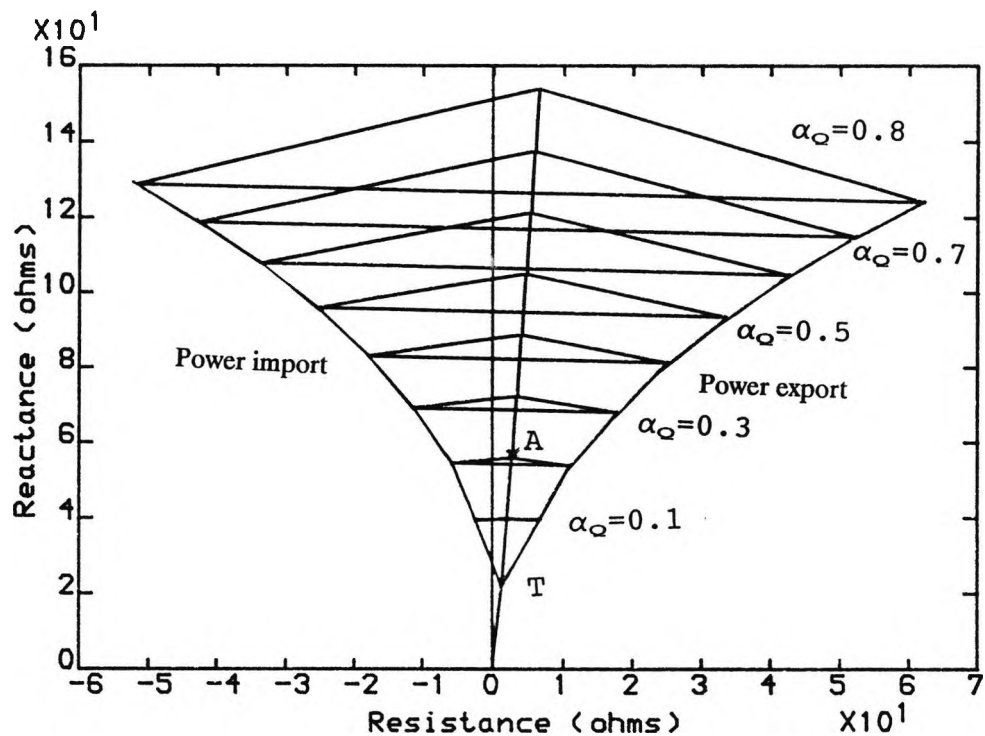
Fig.5.8 Fault areas in the impedance plane
for a fault on line P-T-Q.
SCL (GVA) P=3.5 Q=35   R=35
Conventional measurand
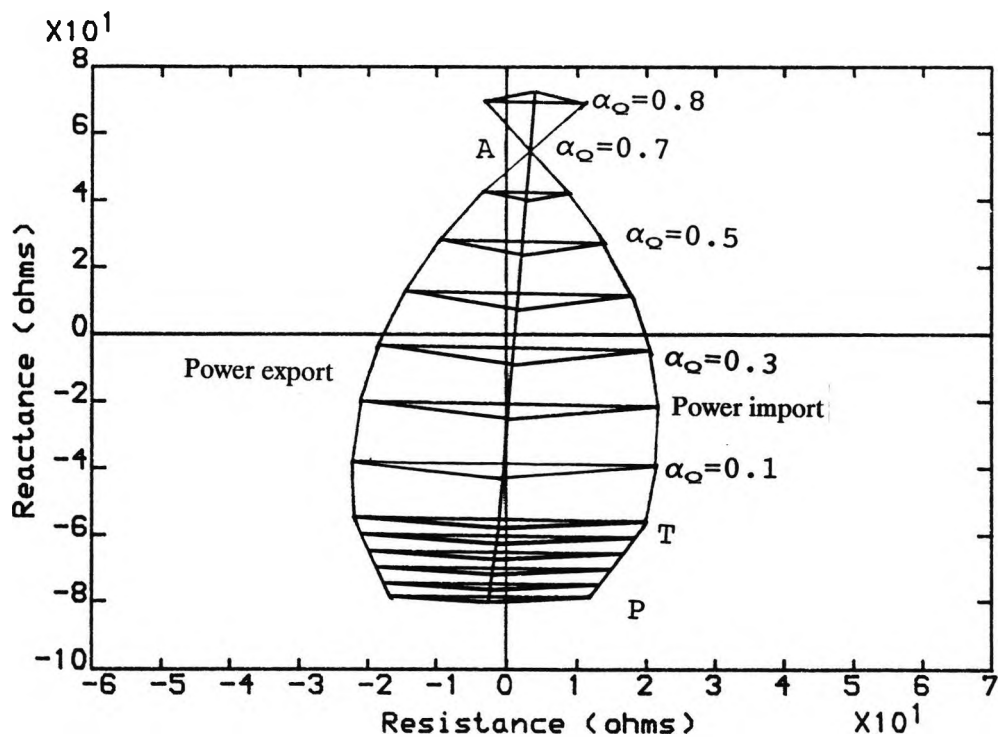
Fig.5.9 Fault areas in the impedance plane
for a fault on line P-T-Q.
SCL (GVA) P=3.5 Q=35   R=35
ZmPQ measurand
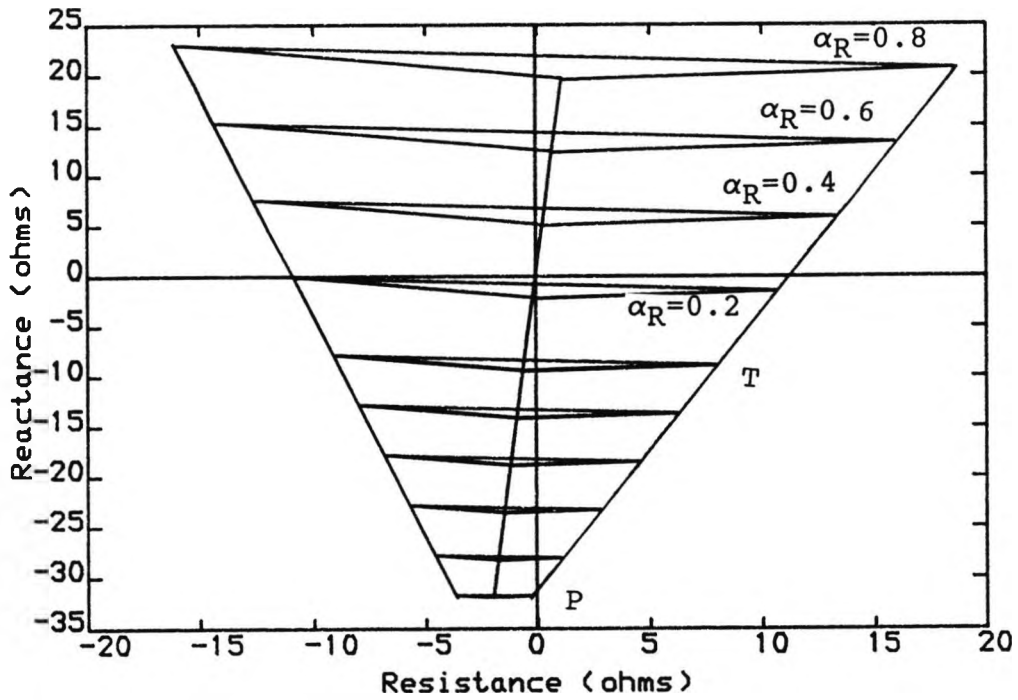
Fig.5.10 Fault areas in the impedance plane
for a fault on line P-T-R.
SCL (GVA) P=35   Q=35   R=35
ZmPQ measurand
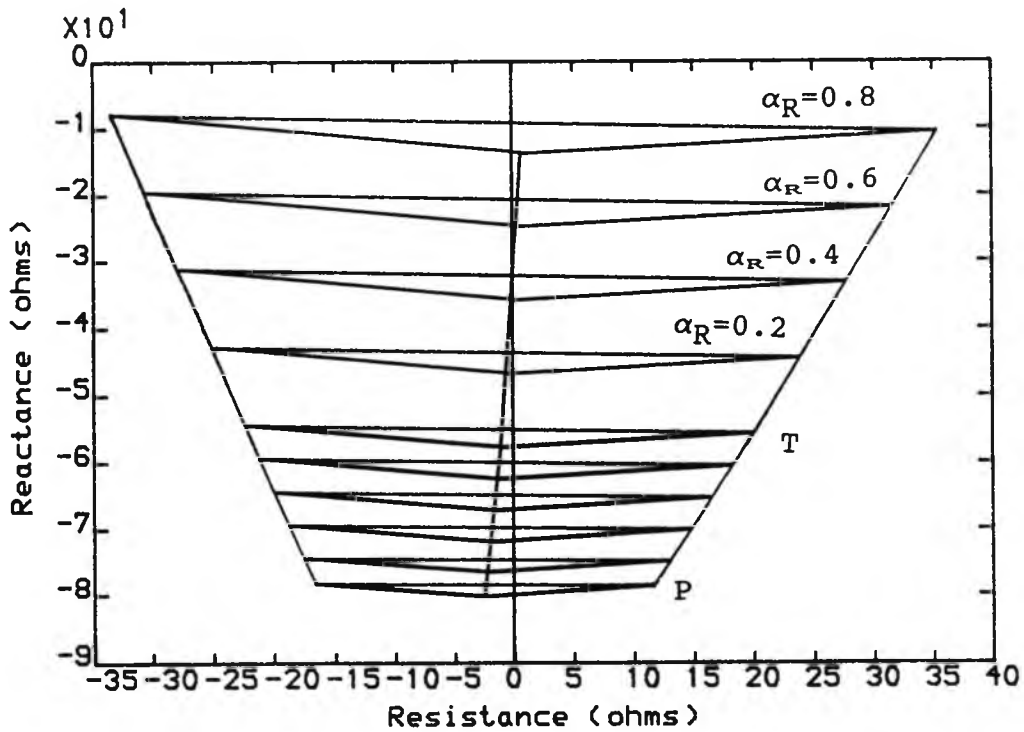
Fig.5.11 Fault areas in the impedance plane
for a fault on line P-T-R.
SCL (GVA) P=3.5   Q=35   R=35
ZmPQ measurand
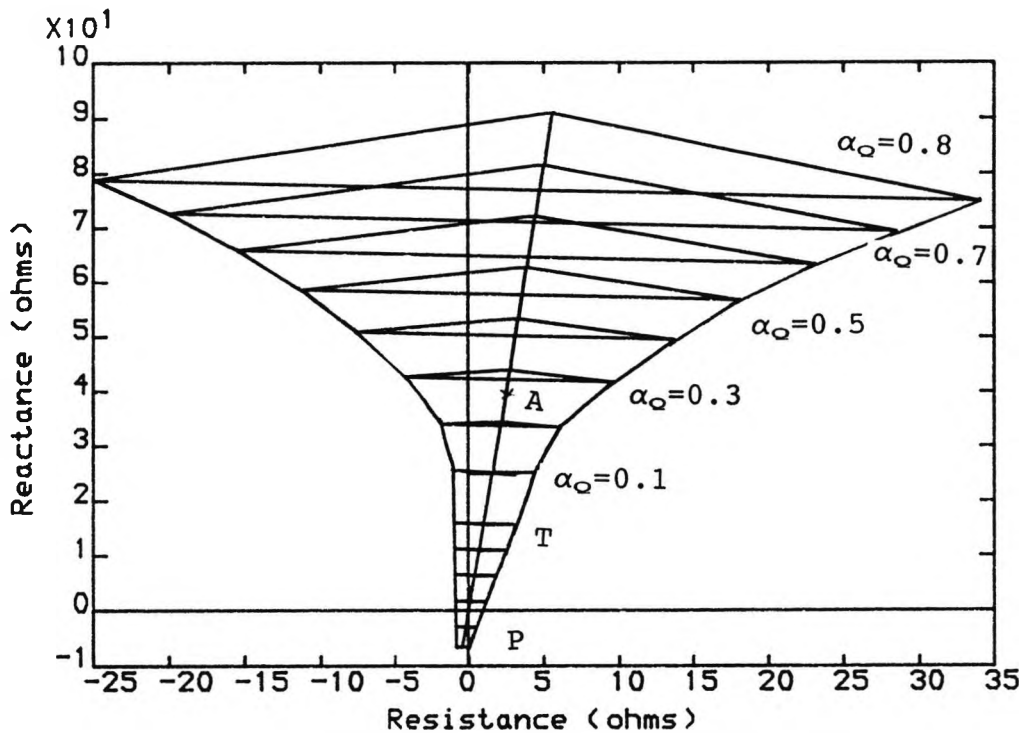
Fig.5.12 Fault areas in the impedance plane
for a fault on line P-T-Q.
SCL (GVA) P=35   Q=35   R=35
ZmPR measurand
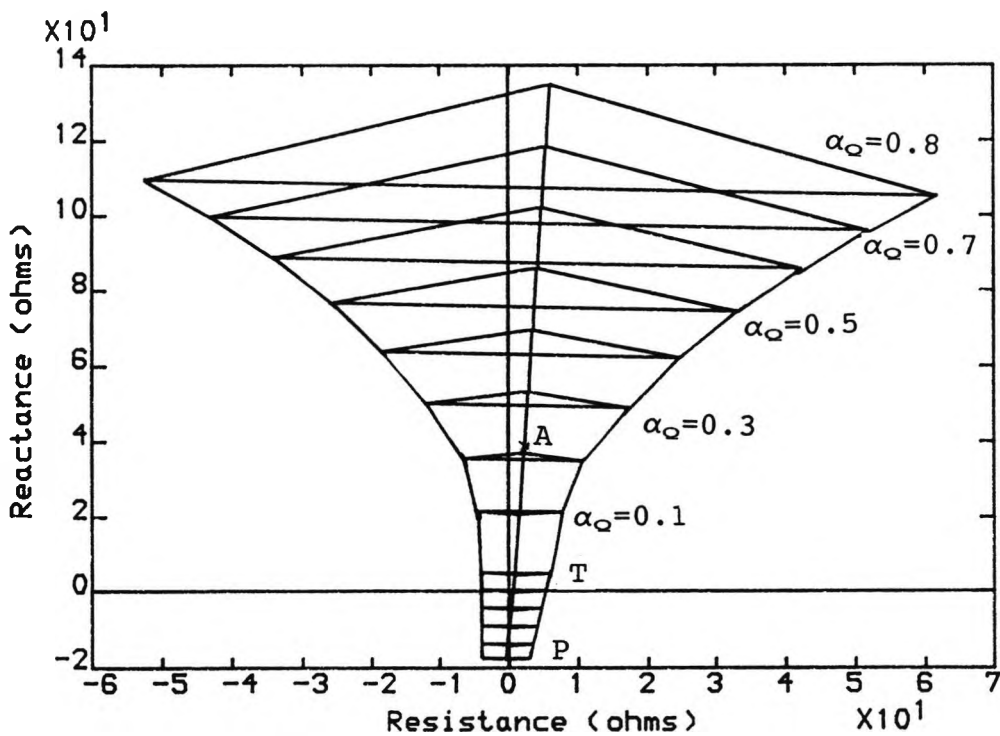
Fig.5.13 Fault areas in the impedance plane
for a fault on line P-T-Q.
SCL (GVA) P=3.5   Q=35   R=35
ZmPR measurand
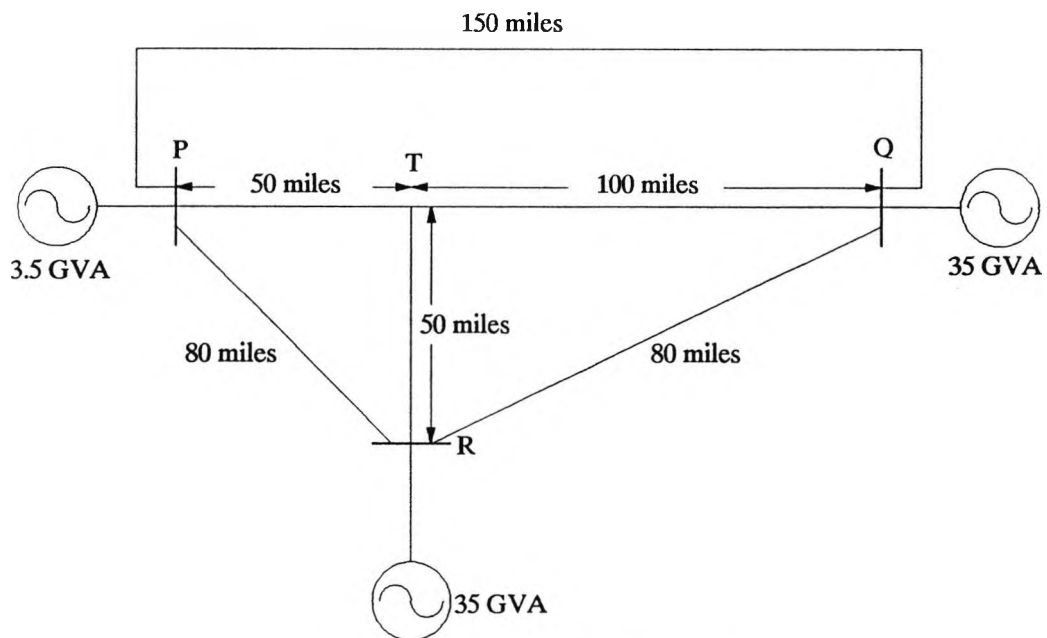
Fig. 5.14 Teed system with external ties.
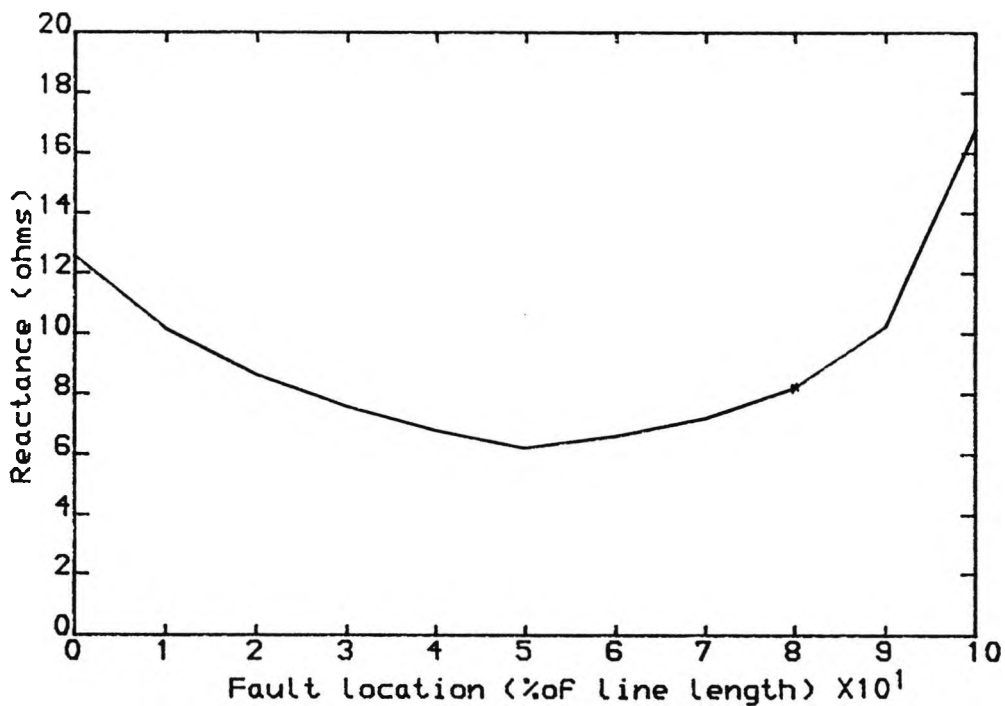
Fig.5.15
Variation of the effective source reactance
at busbar Q, with fault position.
Fault is along line P-T-R.
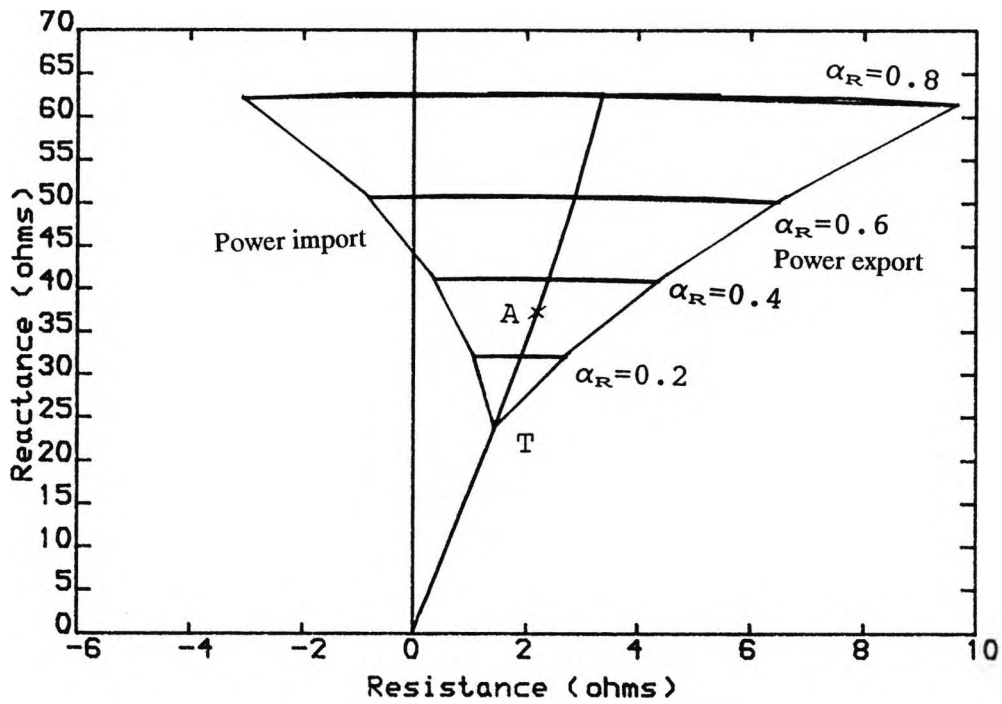
Fig.5.16 Fault areas in the impedance plane
          for a fault on line P-T-R.
SCL (GVA) P=3.5 Q=35   R=35
Conventional measurand
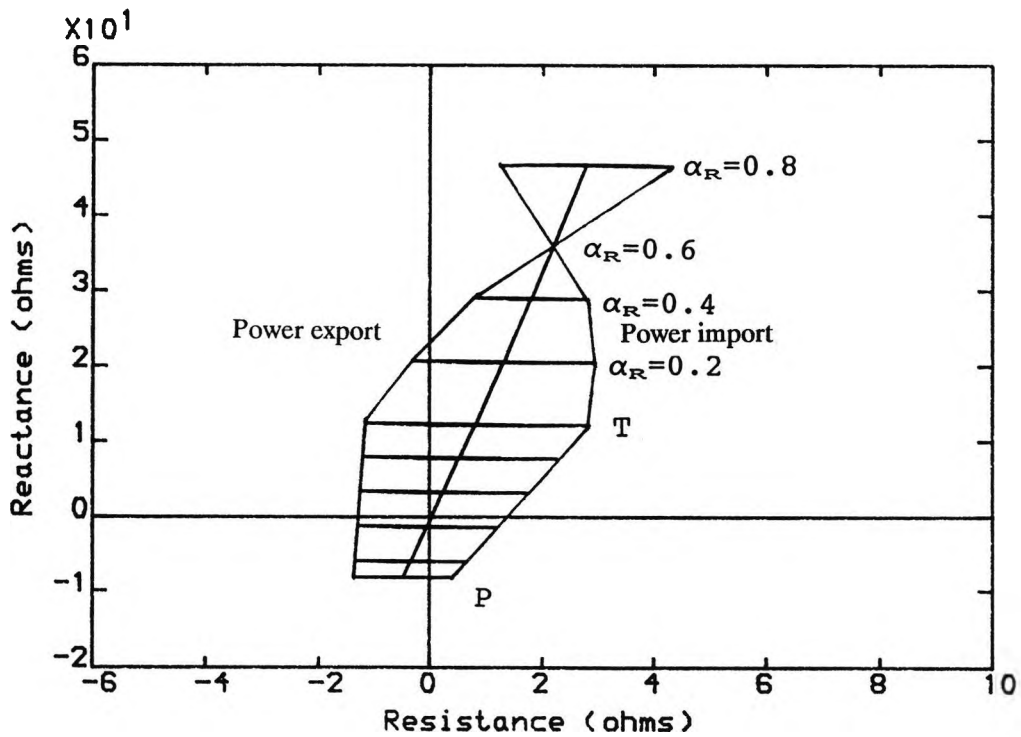

Fig.5.17 Fault areas in the impedance plane
          for a fault on line P-T-R.
SCL (GVA) P=3.5 Q=35   R=35
ZmPR measurand
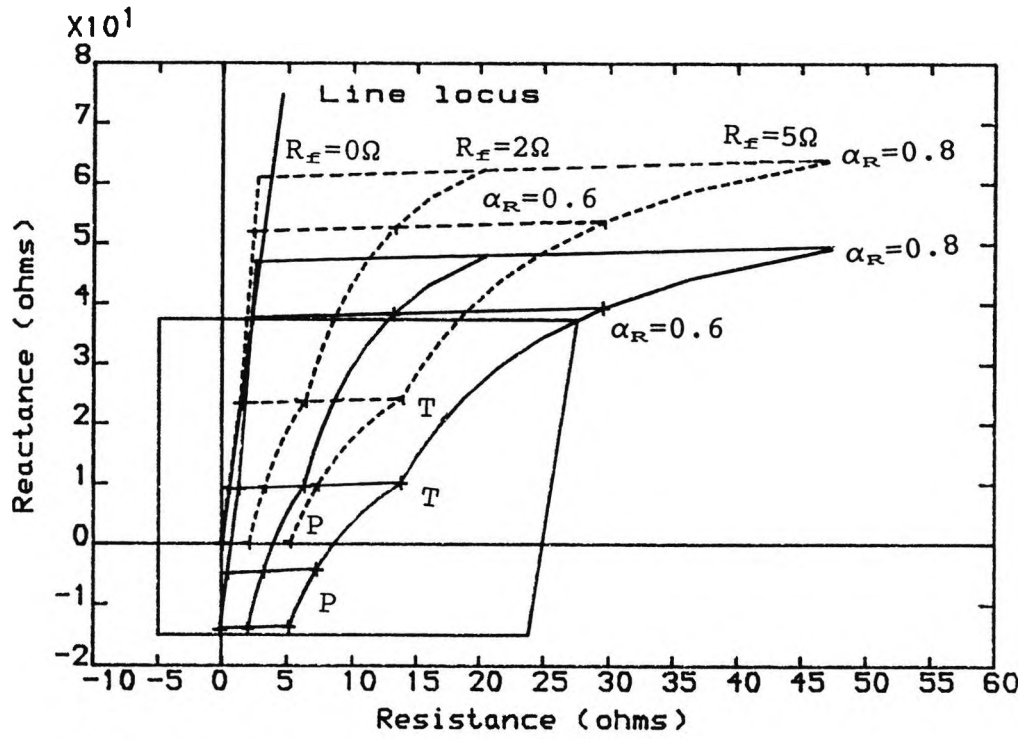
Fig.5.18

Measured impedances for single line to ground
faults along line P-T-R.
No load condition
------- Conventional relay
_____ Adaptive relay
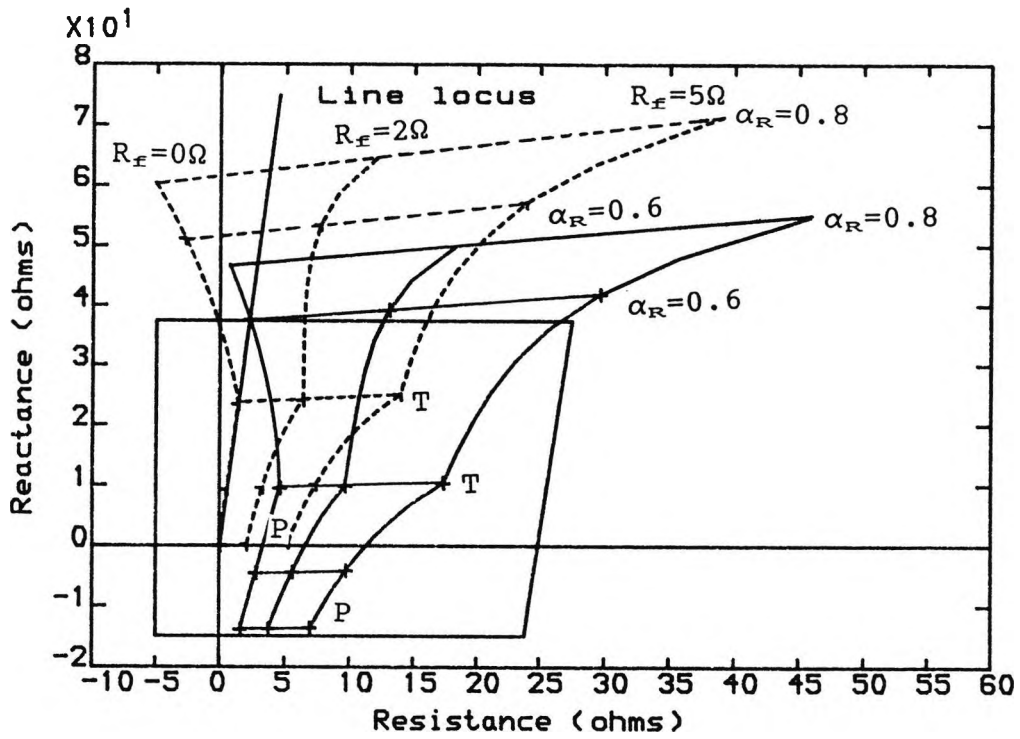
Fig.5.19

Measured impedances for single line to ground
faults along line P-T-R.
Loading angle (degrees) P=0.0 Q=15. R=0.0
------- Conventional relay
_____ Adaptive relay
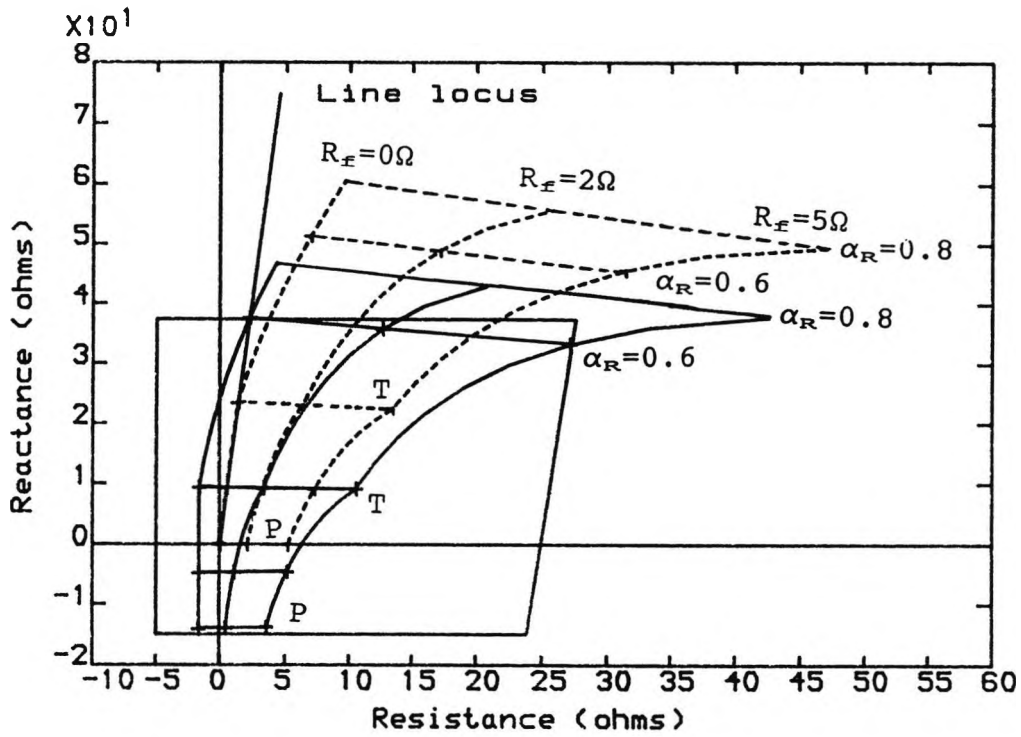
Fig.5.20

Measured impedances for single line to ground
faults along line P-T-R.
Load angle (degrees) P=15.   Q=0.0   R=0.0
------- Conventional relay
_____ Adaptive relay
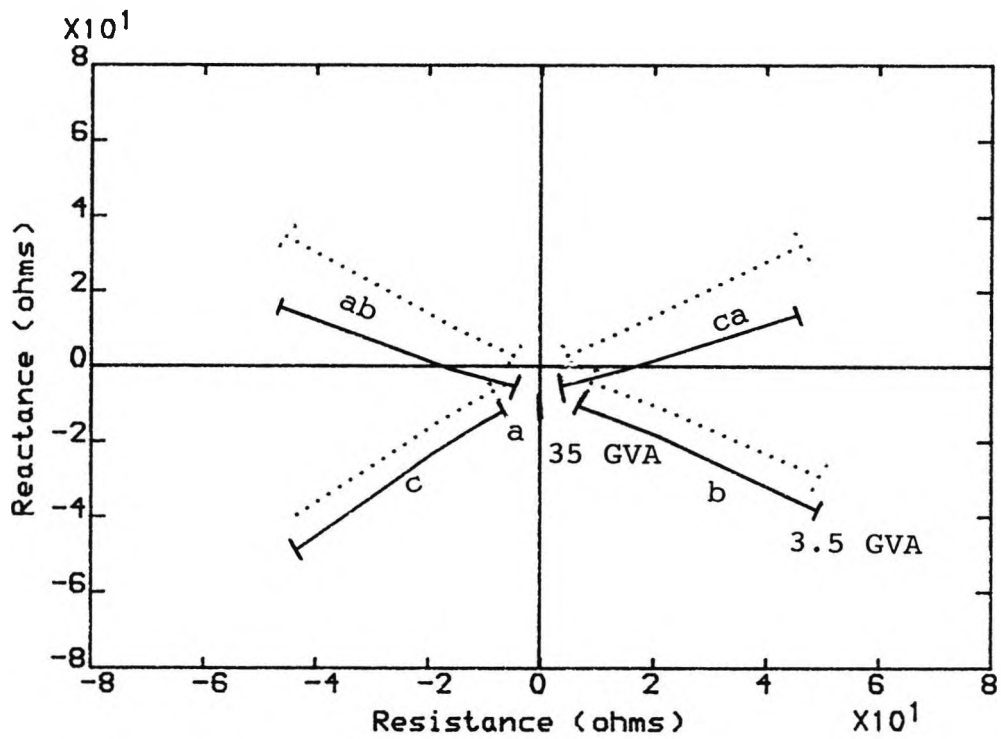
Fig.5.21

Measured impedance for 'closeup fault'
condition
For the 'a' Phase-earth fault
ab, bc, ca   Phase-phase relays
a, b, c   Phase-earth relays
For phase-earth fault, bc ⟶ ∞
_____ Adaptive relays
.... Conventional relays
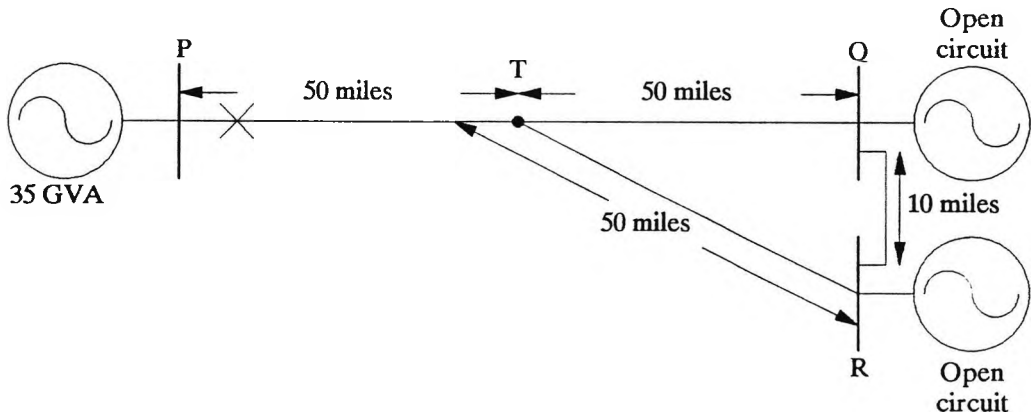
Fig. 5.22 Teed system causing outfeed for an internal fault.
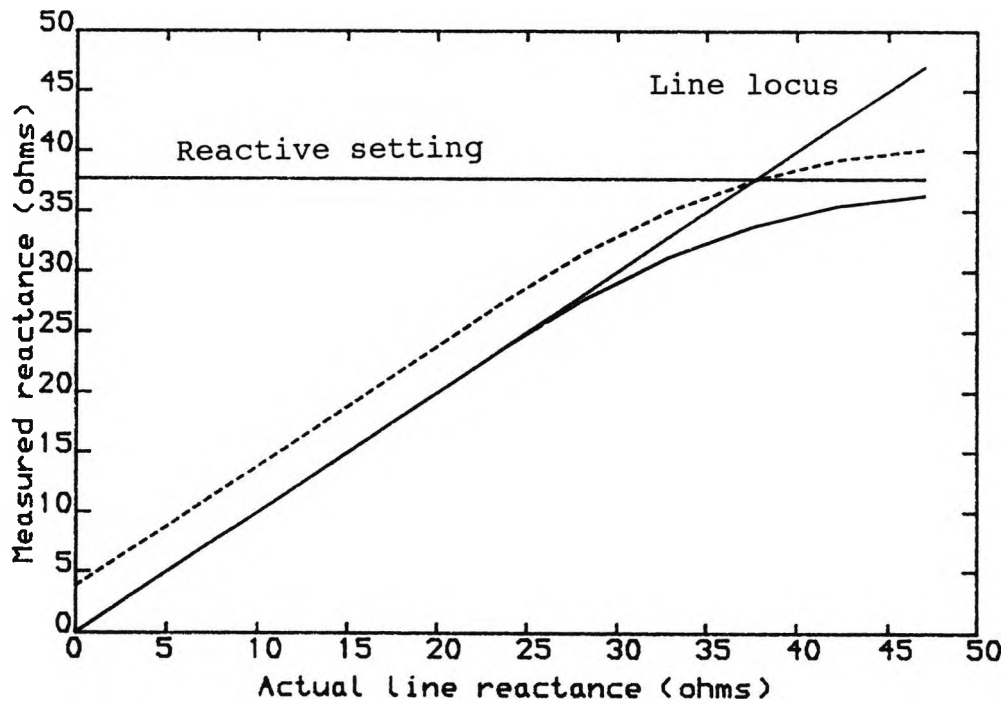
Fig.5.23   Measured reactance at end P for faults along line P-T-R

————————   Conventional measurand

------------   Adaptive measurand
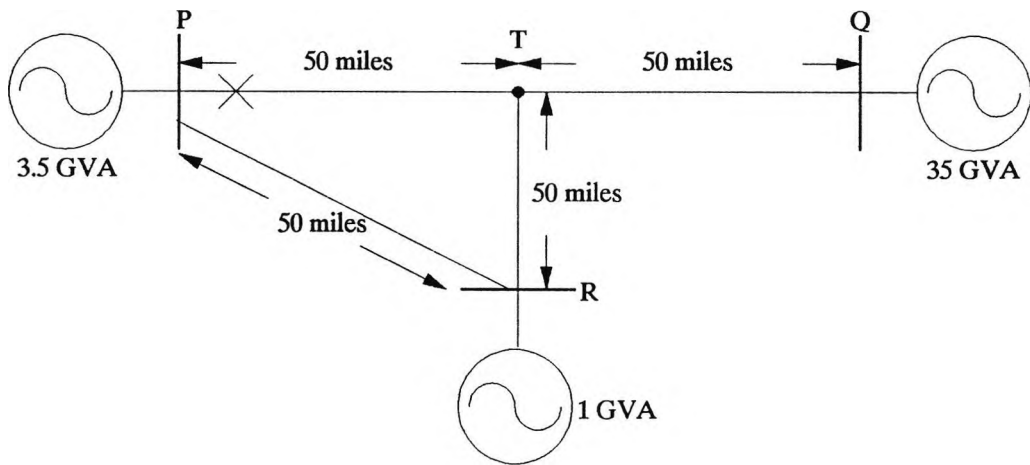
Fig. 5.24 Teed system causing outfeed at the relaying point.
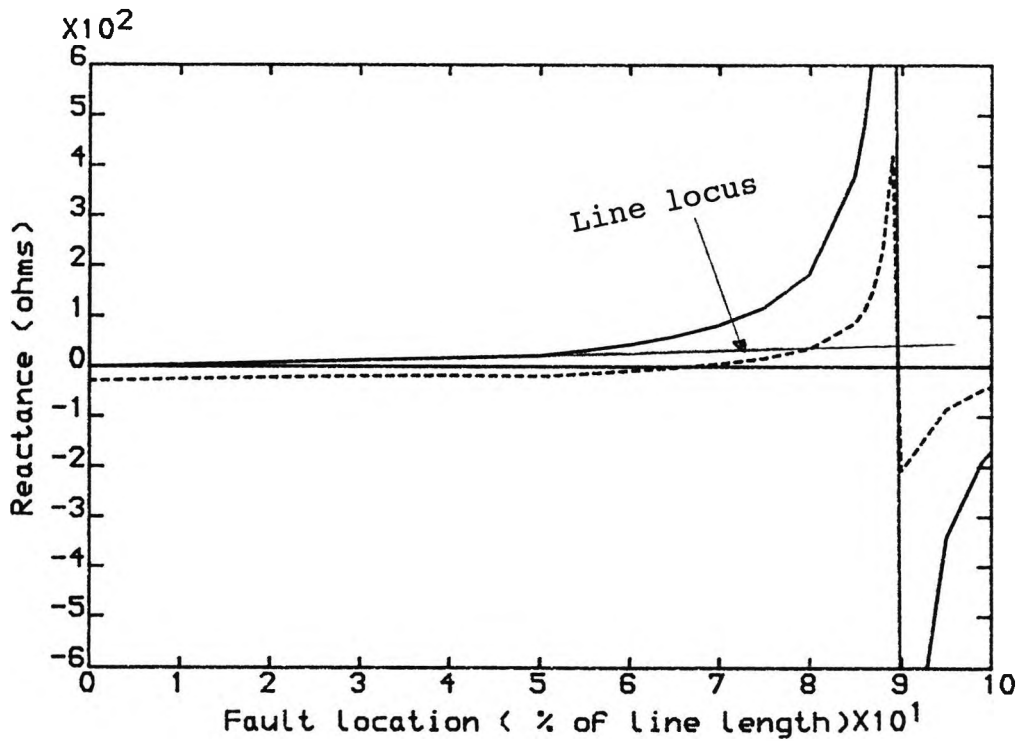
Fig.5.25 Variation of measured reactance
with fault positionm along line P-T-R.
_____ Conventional measurand
- - - - - - - -   Adaptive measurand
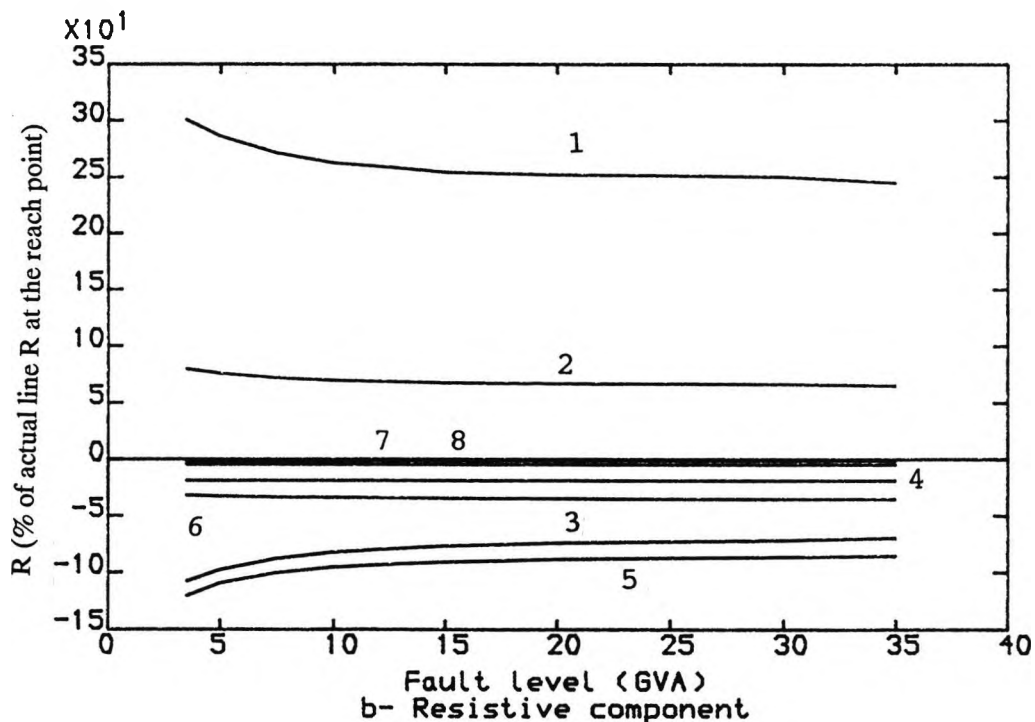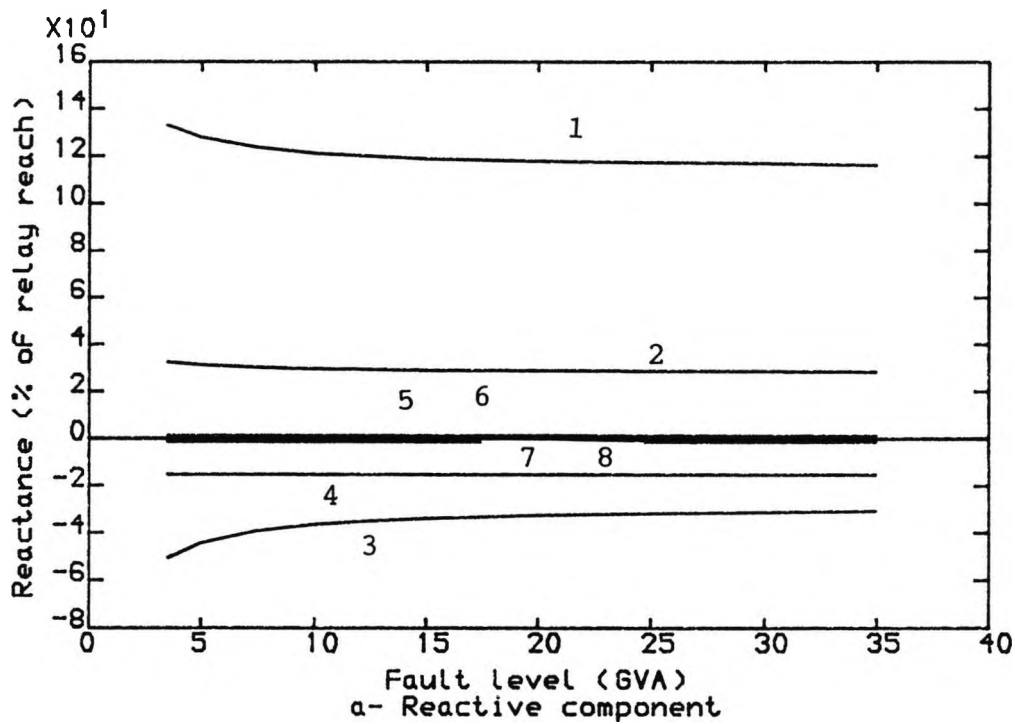
Fig.5.26 Impedance measured by various signals, vs
fault level at the relaying point.

Fault levels (GVA)   Q=35   R=35
Load angle (degrees)   P=15. Q=0.0   R=10
1 = $V_{Pa}/I_{Pa}+KI_{resP}$ (Conventional measurement)
2 = $K'_1 V_{Pa}/I_{Pa}+KI_{resP}$
3 = $K'_1 V_{PSa}/I_{Pa}+KI_{resP}$
4 = K'_6
5 = $K'_2 I_{QSa}/I_{Pa}+KI_{resP}$
6 = $K'_6 I_{PSa}/I_{Pa}+KI_{resP}$
7 = $K'_4 V_{resP}/I_{Pa}+KI_{resP}$
8 = $K'_5 I_{resP}/I_{Pa}+KI_{resP}$
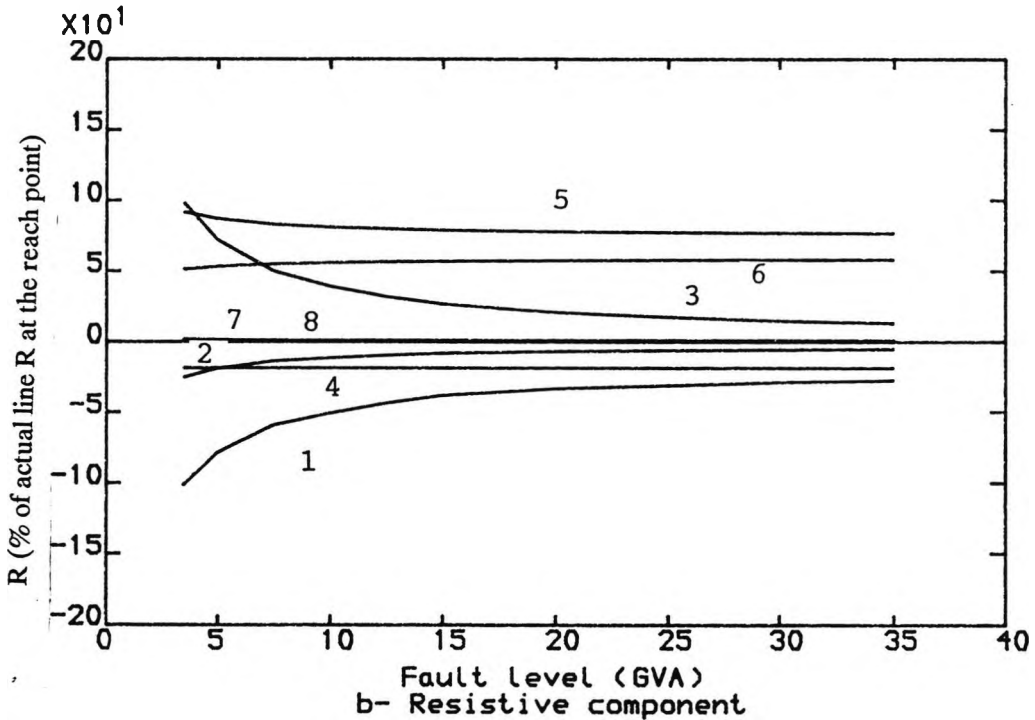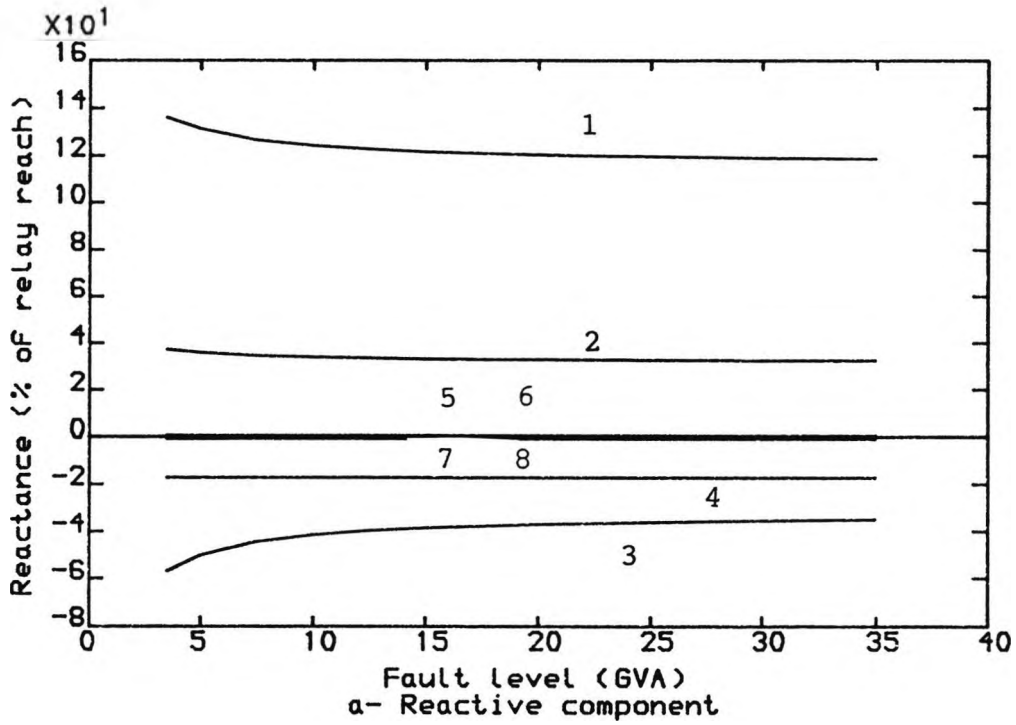
Fig.5.27 Impedance measured by various signals, vs
fault level at the relaying point.

Fault levels (GVA)   Q=35   R=35
Load angle (degrees)   P=0.0   Q=15   R=10
1 = $V_{Pa}/I_{Pa}+KI_{resP}$ (Conventional measurement)
2 = $K'_1 V_{Pa}/I_{Pa}+KI_{resP}$
3 = $K'_1 V_{PSa}/I_{Pa}+KI_{resP}$
4 = K'_6
5 = $K'_2 I_{QSa}/I_{Pa}+KI_{resP}$
6 = $K'_6 I_{PSa}/I_{Pa}+KI_{resP}$
7 = $K'_4 V_{resP}/I_{Pa}+KI_{resP}$
8 = $K'_5 I_{resP}/I_{Pa}+KI_{resP}$
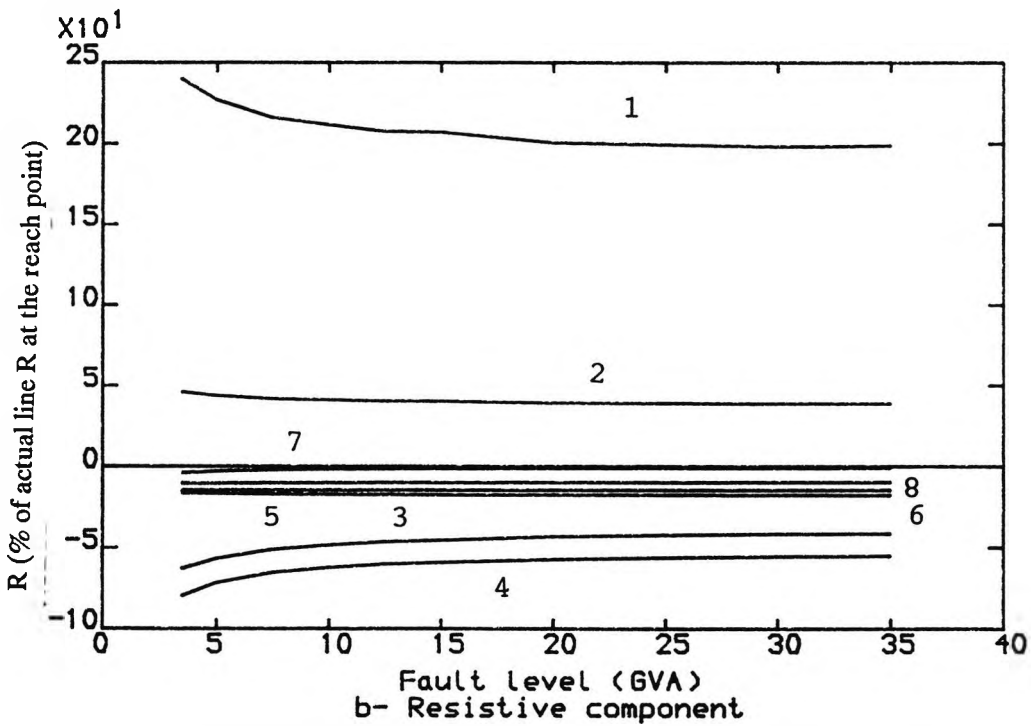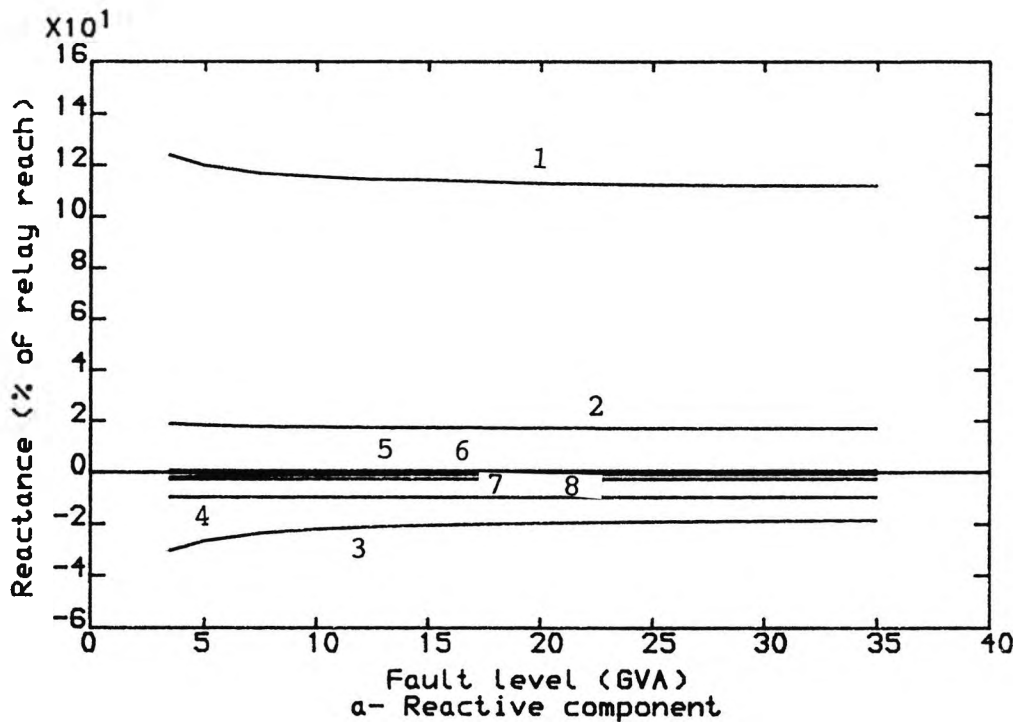
Fig.5.28 Impedance measured by various signals, vs fault level at the relaying point.

Fault levels (GVA)   Q=3.5   R=35
Load angle (degrees)   P=15.   Q=0.0   R=10
$1 = V_{Pa}/I_{Pa}+KI_{resP}$ (Conventional measurement)
$2 = K'_1 V_{Pa}/I_{Pa}+KI_{resP}$
$3 = K'_1 V_{Psa}/I_{Pa}+KI_{resP}$
$4 = K'_6$
$5 = K'_2 I_{Qsa}/I_{Pa}+KI_{resP}$
$6 = K'_6 I_{Psa}/I_{Pa}+KI_{resP}$
$7 = K'_4 V_{resP}/I_{Pa}+KI_{resP}$
$8 = K'_5 I_{resP}/I_{Pa}+KI_{resP}$

Fig.5.29 Impedance measured by various signals, vs fault level at the relaying point

Fault levels (GVA)   Q=15   R=35
Load angle (degree)   P=15   Q=0.   R=10

$1 = V_{Pa}/I_{Pa}+KI_{resP}$ (Conventional measurement)
$2 = K'_1 V_{Pa}/I_{Pa}+KI_{resP}$
$3 = K'_1 V_{PSa}/I_{Pa}+KI_{resP}$
$4 = K'_6$
$5 = K'_2 I_{QSa}/I_{Pa}+KI_{resP}$
$6 = K'_6 I_{PSa}/I_{Pa}+KI_{resP}$
$7 = K'_4 V_{resP}/I_{Pa}+KI_{resP}$
$8 = K'_5 I_{resP}/I_{Pa}+KI_{resP}$
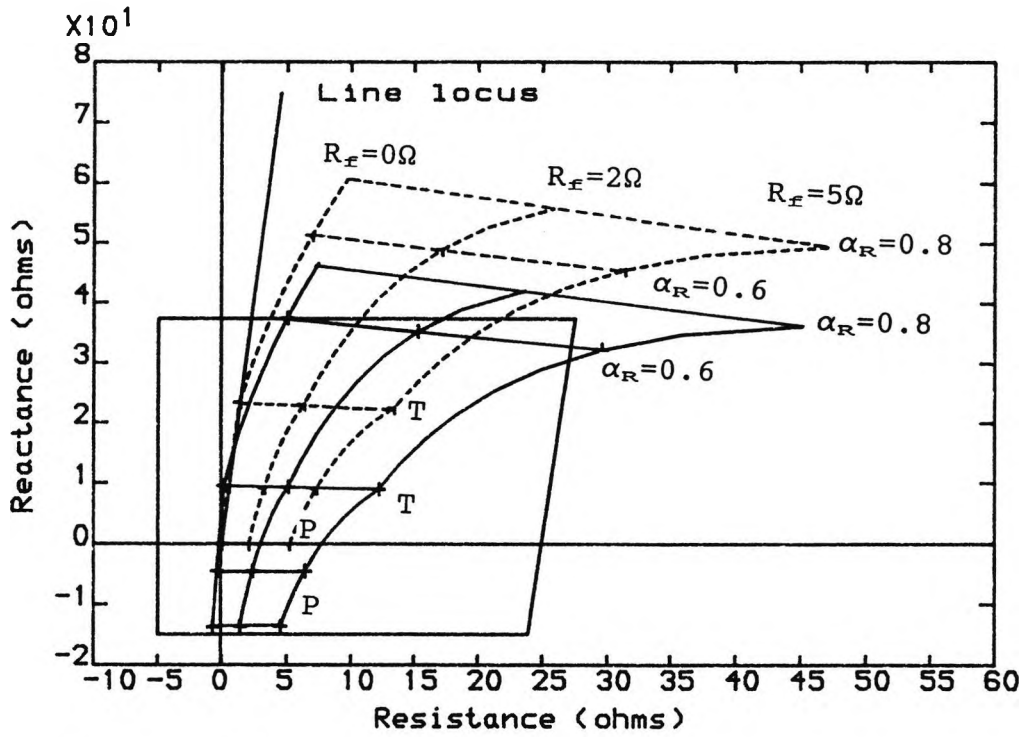
Fig.5.30

Measured impedances for single line to ground
faults along line P-T-R when using reduced relay
signals
Load angle (degrees) P=15   Q=0   R=0
------- Conventional relay
——— Adaptive relay
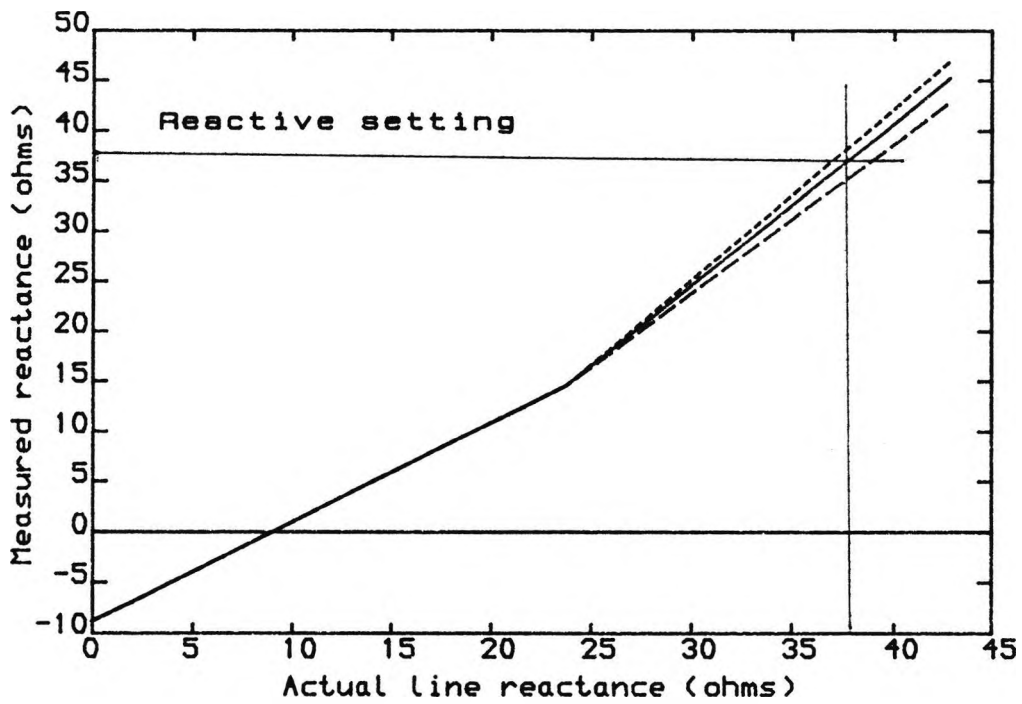
Fig.5.31

Variation of measured versus actual line
reactance for faults along line P-T-R.
_____ SCL= the value used in the relay
-------- SCL= twice the value used in the relay
— — —SCL= half the value used in the relay

CHAPTER 6

RELAY TEST

Chapter 4 has described how the impedance estimates are calculated from the voltage and current signals, and, how filtering is employed to render the impedance estimates such that they are not dominated by noise. Also described is how the counting strategy was used to give the relay more time for faults close to the boundary and a shorter time for faults well inside the characteristics.

This Chapter presents the results of applying the adaptive relay to a faulted Teed system. Particular attention is focused on the relay operating time as a function of fault position and the relay directional stability. The final section of this Chapter looks at the measurand behaviour after the relay has run out of the steady state values of the voltage and current signals.

The majority of the faults considered are of single phase to earth type; which were generated by the EMTP using a distributed parameter model of the line. Throughout the test the source is considered to have X to R and zero to positive sequence impedance ratio of 30 and 1.0 respectively. The line data, which is assumed transposed, is given in Appendix 3A.

6.1 Relay Operating Time

6.1.1 Single Phase to Earth Faults

The relay is tested for the a-phase to earth solid faults, using the system shown in Figure 6.1, for different source

100

capacities, fault inception angle, fault location and loading conditions. The fault position is expressed as a percentage of the relay reach which was set to 80% of the physical length of the line P-T-R. The fault inception angle was varied from 0° to 150° in steps of 30°.

The trip characteristics used during the test are shown in Figure 6.2. The upper limit of the reach was set at 37.6 ohms corresponding to 80% of the line P-T-R. The lower limit of the characteristics was set at -25 ohms which can be considered large enough to meet the requirements of the adaptive relay. The left hand side of the characteristics was set at -15 ohms. The right hand limits has a slope of 86° and intercepts the 'R' axis at 30 ohms (this value being close to half the maximum loading capacity of the line). The reach of the directional unit characteristics was set at 3.76 ohms which represent 10% of the forward reactive reach. It should be noted that the above limits are primary values and in the relay simulation these were scaled down according to CT and CVT ratios.

As mentioned in the previous Chapter, the reach point, on the remote sections of the Teed line, is determined for all cases by one of the two relays (Section 5.2). Therefore, for all foregoing cases only the relay which has been allocated for the remote short section is considered.

The relay measures correctly after a time of 3 cycles of power frequency (the 3 cycles is required by the relay to store the steady state values of the voltages and

currents). Based on the above requirement, the system is simulated over 10 cycles (5 prefault and 5 postfault). This results in a 2 cycles period during which the relay measures correctly when the system is in no fault state and a 3 cycles postfault period during which the relay makes the decision. The relay behaviour when the buffers, which is used to hold the values of the steady state voltages and currents, has run out of these steady state values is described in a later section.

The test results are shown in Tables 6.1 to 6.10. It can be seen that for fault inception angles of 90°, the operating time tends to be slightly higher than those for faults when the inception angle is 0°. This is mainly due to the travelling wave effects which the relay cannot eliminate totally due to the restrictions on the delay of the filtering process (the high frequency component can be reduced to the desired limit but this will take a longer time which in turn effects the operating speed of the relay). In general, faults that fall within 85% of the relay reach (along line P-T-R) is cleared in less than 10 msec. Most faults between 85% to 95% of the reach can generally be cleared in less than 12 msec, but operating times of up to 30 msec were observed in the case of a weak source at the relaying point.

Expected for faults, on Section TQ, the relay underreaches; underreach in this context means that the relay covers a distance which is shorter than that on Section TR. Faults up to 85% of relay reach can be cleared in less than 10 msec for all system operating

102

conditions. Although most faults between 85% to 92% could be cleared in less than 15 msec but some restraint is observed for faults beyond 87% of the reach in particular for the case when the short circuit level at the relaying point is minimum and that at the remote ends is maximum. All faults beyond 95% of the reach of the relay cause restraint.

Figures 6.3 and 6.4 show the operating time versus fault position for fault inception angles of 90° and 0°, for faults along line P-T-R and P-T-Q with the system loading and operating conditions as shown on the graphs. The sharp rise of the curves near the boundary is due to the fact that the measurand sees a reactance which is smaller than the actual line reactance for in-zone faults and a reactance which is larger than the actual line reactance for out-of-zone faults.

Figures 6.5 and 6.6 display the relay operating time when the fault level at the three terminals is 3.5 GVA. This situation leads to a severe distortion in the voltage and current signals. From the travelling wave theory the weaker the impedance at the point of discontinuity the higher is the reflection of the transients [42]. The relay maintains a fast operating time (less than half a cycle) which imply that the combination of signal filtering and counting strategy employed (as discussed in Chapter 4) copes well to eliminate, due to travelling wave effect, any distortion of the measured impedance.

6.1.2 Comparative Performance of Adaptive and Conventional Relays

Figures 6.7 and 6.8 display the operating time versus fault position for the conventional and adaptive relays for fault inception angles of 0 and 90 degrees respectively. It should be noted that the forward setting of both relays are identical, 80% of the physical line length of the line P-T-R (Figure. 6.1), the local fault level is 3.5 GVA and that at the far ends is 35 GVA, the loading condition is zero. It is evident that, due to the infeed effect, the conventional relay underreaches by about 20% and gives an operating time of less than 10 msec for the majority of faults that fall within its characteristics. On the other hand the adaptive relay maintain the fast operating time of the conventional relays and goes further in giving the desired reach.

For faults along the path P-T-Q the adaptive relay covers a distance which is shorter than that on Section TR. A favourable reach compared with that of the conventional is accomplished as illustrated in Figures 6.9 and 6.10, it can also be seen that both relays have similar operating time for the closeup faults.

Figures 6.11 to 6.14 show the relays performance when the local and remote fault levels are 3.5 GVA. Again, both relays have a fast operating time and the adaptive relay gives the expected reach. Comparing Figures 6.7 and 6.11 it can be noticed that the conventional relay gives a better reach when the fault level at the three terminals are identical.

6.1.3 Phase-Phase Faults

Figures 6.15 and 6.16 show the relay performance for the b-c phase fault. Figure 6.15 shows the operating time when the fault inception angle was such that the b-c voltages were equal in magnitude and sign (voltage difference between the two phases is zero which coincides with the voltage maximum at the a-phase). The travelling wave effect in this case is minimal. On the same graph the conventional relay performance is displayed, it can be seen that the relay has an operating time which is almost identical to the adaptive relay, but it underreaches due to the infeed effect.

Figure 6.16 shows the relay operating time for maximum voltage difference between the two phases; this situation leads to maximum travelling wave effect. Comparing Figures 6.15 and 6.16, it can be noticed that the effect of the travelling wave is to increase slightly the relay operating time but in both cases an operating time of less than 10 msec is maintained for most of the fault locations.

For faults along line P-T-Q the relay reach and operating time is shown in Figures 6.17 and 6.18. The relay in this case covers distance which is shorter than that on section TR but when compared with the conventional relay reach, which is shown on the graph, it can be seen that the adaptive relay gives a better reach.

6.2 Directional Reactance Behaviour

It is a common practice in distance protection to set the

relay characteristics with some incursion into the negative region of the impedance plane. This is mainly to allow the relay to clear closeup faults in particular when a fault resistance is encountered. The extension of the characteristics into the negative region, however, can result in the relay operation for reverse faults. This was overcome by employing a directional unit which actuate correctly the associated relay protection [13]. One of the requirements of the proposed adaptive scheme is to offset the relay characteristics for a considerable value into the negative region to accommodate the impedance values for the closeup faults. The same directional technique used in the conventional distance relays is found adequate to provide the directional discrimination.

In this section the relay directional stability is investigated for forward and reverse faults; as outlined in Chapter 4, the directional unit uses the undelayed samples of the current signal with the delayed voltage samples. Figure 6.19 shows the measured reactance and the directional reactance behaviour, for the phase a-earth fault immediately in front of the relay location. Clearly, the measured reactance falls in the negative region, and the directional reactance, X_M, gives an indication that the fault is in the forward position. The directional reactance setting, X_{MA}, was taken as 10% of the relay forward reach.

Figure 6.20 shows the relay measurement for a fault just behind the relaying point; the relay will see the fault as a forward fault, in this case the tripping

106

decision relies fully on the directional unit behaviour. It can be clearly seen that the directional reactance falls in the negative region i.e., outside the directional reactance setting, thus, preventing the relay operation.

In order to illustrate why the relay measures a positive impedance for a reverse fault, consider the first three terms of Equation 2.45, V_{Pa} , K'_1*V_{Pa} and K'_1*V_{PSa}. For a fault just behind the relay, the voltage signals V_{Pa} and K'_1*V_{Pa} will immediately collapse to zero while the steady state signal K'_1*V_{PSa} will be maintained for the delaying period considered in the relay simulation (3 cycles), when this signal is divided by the operating signal, $I_{Pa} + K*I_{resP}$, which in this case is in the reverse direction, an impedance which fall in the forward direction results. It should be noticed that the other terms in Equation 2.45 also have an influence on the measurand behaviour but the above argument has been used for illustration.

6.3 Relay Behaviour on a Sustained Fault

The correct operation of the relay requires that the prefault values of the voltage and current be used in conjunction with undelayed samples. In the relay simulation a buffer is used to hold the prefault samples for three cycles (see Section 4.8). However, if the fault is not cleared within this period, the buffer will run out of prefault samples and this leads to the question how will the relay behave under this condition?. Figure 6.21 shows the measured reactance for an internal fault, where

it can be clearly seen that, within the three cycles, the relay identifies the fault as an internal one but when the buffer is filled with the post values a larger reactance is encountered. It should be noted that the system simulation in this section uses a lumped parameter model of the line.

On the basis of the result shown in Fig 6.21, it is clear that the relay would not operate incorrectly or unnecessarily, but in effect it measures a higher reactance which can be very useful in providing better selectivity for external faults. It is, however, instructive to explain how the individual terms of Equation 2.45, which is reproduced below, affect the measurement during this period.

$$Z_{mPRa} = \frac{1}{I_{Pa}+KI_{resP}} \{ V_{Pa} + (K'_1 V_{Pa} - K'_1 V_{PSa}) - K'_2 I_{QSa} -$$

$$K'_3 I_{resQS} + (K'_4 V_{resP} - K'_4 V_{resPS}) -$$

$$(K'_5 I_{resP} - K'_5 I_{resPS}) +$$

$$K'_6 I_{PSa} + K'_7 I_{resPS} \} - K'_6 \qquad\qquad 6.1$$

It should be noted that the K',s which were defined in Chapter 2; when multiplied by currents have impedance dimension. However when multiplied by the voltages, it becomes dimensionless.

1- The voltage V_{Pa} divided by the phase current with the correct proportion of the residual current gives the performance of the conventional relay.

2- The signals $K'_1 * V_{Pa}$ and $K'_1 * V_{PSa}$ will cancel each other as the time passes, $K'_1 * V_{PSa}$ is the delayed version of the signal $K'_1 * V_{PS}$. Since these signals the former is

added and the later is subtracted their effect in the above equation will be nullified after the three cycles delay considered.

Similarly, if the relay cannot make a decision within the specified time (3 cycles), the signals $(K'_4*V_{resP} - K'_4*V_{resPS})$ and $(K'_5*I_{resP} - K'_5*I_{resPS})$ will cancel each other.

3- As it was suggested in Chapter 2 the prefault current from the remote end, I_{Qsa}, need to be transmitted, to the relaying point, periodically. Therefore, the probability of the fault to coincide with the instant of transmitting can be considered extremely low. Even if this is to happen it can be arranged such that if this current is above a certain limit, which could be the maximum loading current, then no signal can be received. Practically, the factor K'_2*I_{Qsa} can be ignored totally because as it was shown in Chapter 5 its effect on the measurement accuracy and in particular on the reactive component is insignificant.

4- The factors K'_3*I_{resQS} and K'_7*I_{resPS}, which are the residual steady state currents can be ignored without practically introducing any errors. It should be noticed that the common practice in distance relaying schemes, using residual or sound phase compensation methods, is to set the relay assuming a fully transposed line [36,37] which practically means that these values are zero.

5- If the buffer is filled with post values after the three cycles considered in the relay simulation, the steady state current I_{Psa} becomes the actual fault

current. In this case the term $K'_6 * I_{PSa}$ will boost the voltage signal and this results in a greater measured impedance. If the fault is external the relay will not operate in the normal state and after the 3 cycles the relay will measure a higher value which is desirable. For internal faults the relay is expected to initiate a tripping signal in less than 3 cycles but for faults near the boundary the relay may require a longer time, in this case the relay underreaches. This problem can be overcome easily by an arrangement to periodically update the steady state value of the local current, as for the case of the remote current, I_{QSa}, (see Section 2.4).

5- Hitherto, the relay behaves, in particular the reactive component, in a similar way to that of a conventional relay with the exception that the constant term, K'_6, is still subtracted at each instant from the measured impedance. Therefore, a performance that fall between two limits can be expected; the upper is that of the conventional relay and the lower is that of the adaptive relay before the buffer run out of the prefault values. The measured reactance before and after the relay runs out of the steady state values is shown in Figure. 6.22. It is clear that a performance, for the period when the buffer is filled with post fault values, is within the limits stated above the relay could underreach but no unnecessary operation occurs. An alternative arrangement can be made to disregard the term, K'_6, if no decision is made after the 3 cycles. Therefore a performance identical to that of the conventional relay

110

will be expected.

6.4 Summary

In respect of the foregoing investigation, the relay maintains a fast tripping time as in the case of the conventional digital relay. Whatever the system operating condition and regardless which is the faulted remote section of the line, a tripping time of less than half a cycles has been achieved for the faults that fall within 85% of the reach point. The relay requires a longer operating time (one power cycle or more) for faults that fall near the reach point. For closeup faults (reverse or forward) the relay maintains the proper discrimination, and in the case where the relay runs out of the steady-state values of the currents and voltages, unnecessary operation does not result.

Table 6.1 Operating time (msec) VS fault location

	End P	End Q	End R
SCL(GVA)	35.	35.	35.
Load angle(degree)	15.	0.0	10

```
        P              T                       Q
        ├──────────────┬───────────────────────┤
                       │
                       │
                    ───┴──R
```
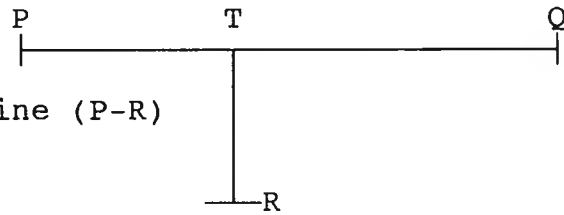
Relay setting =80% of line (P-R)

Fault Location (*)	Inception Angle (degree)					
	0	30	60	90	120	150
0.0 P	8.25	7.00	6.75	7.75	8.25	8.25
37.5 P	8.25	7.00	6.50	8.50	8.50	8.25
62.5 T	8.25	7.75	8.25	9.00	8.50	8.75
81.25 R	8.50	8.00	9.00	8.75	8.50	8.50
87.5 R	9.75	8.50	10.25	10.00	9.75	9.75
95.0 R	9.75	9.25	10.50	10.00	9.75	10.00
97.5 R	14.50	13.25	16.50	16.75	16.50	16.75
100 R	NO OP	NO OP	NO OP	NO OP	NO OP	NO OP
102.5 R	NO OP	NO OP	NO OP	NO OP	NO OP	NO OP
100 Q	NO OP	NO OP	NO OP	NO OP	NO OP	NO OP
97.5 Q	NO OP	NO OP	NO OP	NO OP	NO OP	NO OP
95 Q	NO OP	NO OP	NO OP	NO OP	NO OP	NO OP
92.5 Q	NO OP	NO OP	NO OP	NO OP	NO OP	NO OP
87.5 Q	13.00	11.75	17.00	16.75	10.50	12.25
81.25 Q	9.75	8.75	10.25	10.00	9.75	9.75

* = % of relay reach
NO OP = No operation
P = fault on leg PT
T = fault at the Tee point
R = fault on leg TR
Q = fault on leg TQ

Table 6.2 Operating time (msec) VS fault location

	End P	End Q	End R
SCL(GVA)	35.	3.5	3.5
Load angle(degree)	15.	0.0	10

```
          P              T                    Q
          |--------------+--------------------|
                         |
                         |
                       --+--R
```

Relay setting =80% of line (P-R)
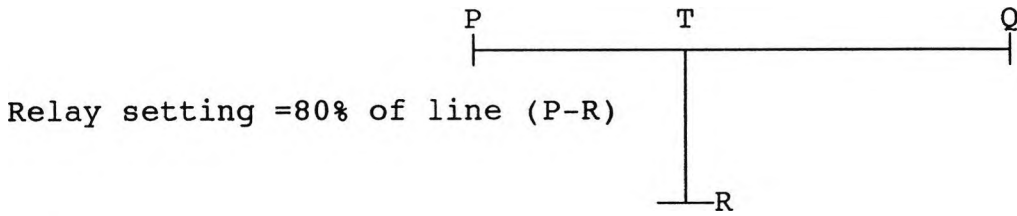
Fault Location (*)	Inception Angle (degree)					
	0	30	60	90	120	150
0.0 P	7.75	7.00	6.25	7.50	8.00	7.75
37.5 P	8.00	7.00	6.50	8.00	8.25	7.75
62.5 T	8.25	7.75	8.25	8.50	8.50	8.25
81.25 R	9.50	9.25	9.50	10.00	9.25	9.00
87.5 R	9.50	9.00	9.25	9.75	9.75	9.25
95.0 R	10.25	10.25	10.75	10.75	10.75	10.00
97.5 R	16.50	15.75	13.75	22.75	25.75	19.50
100 R	NO OP	NO OP	NO OP	NO OP	NO OP	NO OP
102.5 R	NO OP	NO OP	NO OP	NO OP	NO OP	NO OP
100 Q	NO OP	NO OP	NO OP	NO OP	NO OP	NO OP
97.5 Q	NO OP	NO OP	NO OP	NO OP	NO OP	NO OP
95 Q	NO OP	NO OP	NO OP	NO OP	NO OP	NO OP
92.5 Q	16.50	15.25	14.75	17.00	15.00	13.50
87.5 Q	9.25	9.25	9.50	10.00	9.75	9.50
81.25 Q	8.50	8.25	8.75	8.75	8.50	8.25

* = % of relay reach
NO OP = No operation
P = fault on leg PT
T = fault at the Tee point
R = fault on leg TR
Q = fault on leg TQ

Table 6.3 Operating time (msec) VS fault location

	End P	End Q	End R
SCL(GVA)	3.5	35.	35.
Load angle(degree)	0.0.	15.	10

```
        P               T                          Q
        |---------------+--------------------------|
                        |
                        |
                        |
                      --+--R
```
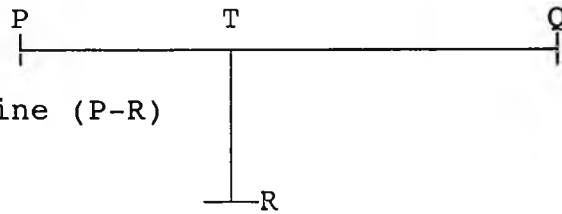
Relay setting =80% of line (P-R)

Fault Location (*)	Inception Angle (degree)					
	0	30	60	90	120	150
0.0 P	8.25	8.00	7.75	8.50	8.25	8.00
37.5 P	8.75	8.25	8.75	9.25	9.00	8.25
62.5 T	8.50	8.25	9.00	9.25	9.00	8.00
81.25 R	8.50	8.25	9.25	9.25	9.25	8.00
87.5 R	8.25	8.50	9.50	10.00	9.25	8.00
95.0 R	9.25	9.00	11.25	12.00	10.00	10.00
97.5 R	15.00	13.25	17.75	19.75	12.50	14.50
100 R	NO OP	NO OP	NO OP	NO OP	NO OP	NO OP
102.5 R	NO OP	NO OP	NO OP	NO OP	NO OP	NO OP
100 Q	NO OP	NO OP	NO OP	NO OP	NO OP	NO OP
97.5 Q	NO OP	NO OP	NO OP	NO OP	NO OP	NO OP
95 Q	NO OP	NO OP	NO OP	NO OP	NO OP	NO OP
92.5 Q	NO OP	NO OP	NO OP	NO OP	NO OP	NO OP
87.5 Q	16.00	17.25	15.00	22.00	20.50	18.50
81.25 Q	8.25	8.75	9.00	10.00	10.25	8.00

* = % of relay reach
NO OP = No operation
P = fault on leg PT
T = fault at the Tee point
R = fault on leg TR
Q = fault on leg TQ

Table **6.4** Operating time (msec) VS fault location

	End P	End Q	End R
SCL(GVA)	3.5	35.	35.
Load angle(degree)	15.	0.0	10

```
        P              T                        Q
        |──────────────┬─────────────────────── |
                       │
                       │
                     ──┴─R
```

Relay setting =80% of line (P-R)
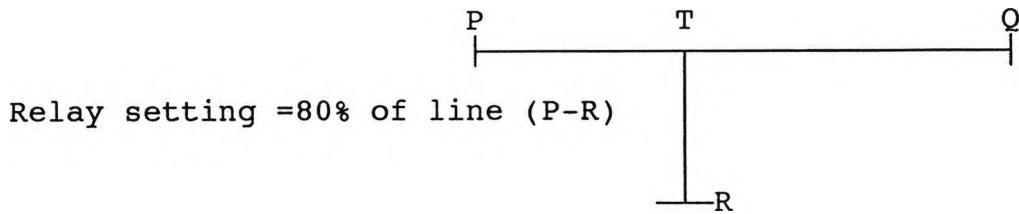
Fault Location (*)	Inception Angle (degree)					
	0	30	60	90	120	150
0.0 P	8.00	8.00	8.25	8.25	8.00	8.25
37.5 P	8.75	9.00	9.00	9.25	8.75	8.75
62.5 T	8.50	8.25	9.25	9.25	8.75	8.75
81.25 R	8.50	8.50	9.25	8.75	8.75	9.00
87.5 R	8.50	9.00	9.75	9.25	8.50	9.25
95.0 R	9.50	9.75	12.00	11.00	10.75	12.00
97.5 R	16.50	15.00	22.25	20.75	18.75	19.25
100 R	NO OP	NO OP	NO OP	NO OP	NO OP	NO OP
102.5 R	NO OP	NO OP	NO OP	NO OP	NO OP	NO OP
100 Q	NO OP	NO OP	NO OP	NO OP	NO OP	NO OP
97.5 Q	NO OP	NO OP	NO OP	NO OP	NO OP	NO OP
95 Q	NO OP	NO OP	NO OP	NO OP	NO OP	NO OP
92.5 Q	NO OP	NO OP	NO OP	NO OP	NO OP	NO OP
87.5 Q	NO OP	NO OP	NO OP	NO OP	NO OP	NO OP
81.25 Q	10.00	9.25	10.25	10.50	10.00	8.75

* = % of relay reach
NO OP = No operation
P = fault on leg PT
T = fault at the Tee point
R = fault on leg TR
Q = fault on leg TQ

Table 6.5 Operating time (msec) VS fault location

	End P	End Q	End R
SCL(GVA)	3.5	3.5	3.5
Load angle(degree)	15.	0.0	10

```
          P              T                    Q
          |--------------|--------------------|
                         |
Relay setting =80% of line (P-R)
                         |
                       --|--R
```
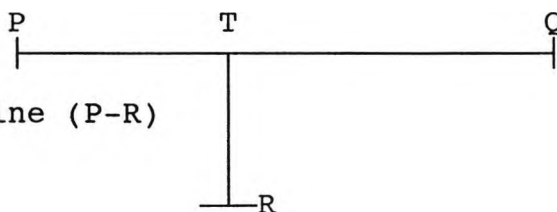
Fault Location (*)	Inception Angle (degree)					
	0	30	60	90	120	150
0.0 P	8.50	7.50	8.25	8.50	8.25	8.250
37.5 P	8.75	8.00	8.75	9.00	8.75	8.50
62.5 T	8.50	8.50	9.00	9.25	8.75	8.50
81.25 R	8.50	8.75	8.75	9.25	8.75	8.75
87.5 R	8.75	9.50	11.00	10.00	8.50	9.75
95.0 R	11.50	21.75	20.00	29.50	10.75	27.00
97.5 R	17.25	50.75	41.75	NO OP	NO OP	42.25
100 R	NO OP	NO OP	NO OP	NO OP	NO OP	NO OP
102.5 R	NO OP	NO OP	NO OP	NO OP	NO OP	NO OP
100 Q	NO OP	NO OP	NO OP	NO OP	NO OP	NO OP
97.5 Q	NO OP	NO OP	NO OP	NO OP	NO OP	NO OP
95 Q	NO OP	NO OP	NO OP	NO OP	NO OP	NO OP
92.5 Q	NO OP	NO OP	NO OP	NO OP	NO OP	NO OP
87.5 Q	15.75	13.25	11.00	12.50	9.75	13.75
81.25 Q	9.75	9.00	9.50	10.00	9.75	8.75

* = % of relay reach
NO OP = No operation
P = fault on leg PT
T = fault at the Tee point
R = fault on leg TR
Q = fault on leg TQ

Table 6.6 Operating time (msec) VS fault location

	End P	End Q	End R
SCL(GVA)	3.5	3.5	3.5
Load angle(degree)	0.0	15.	10

```
        P              T                    Q
        |──────────────┬────────────────────|
                       │
                       │
                     ──┴──R
```
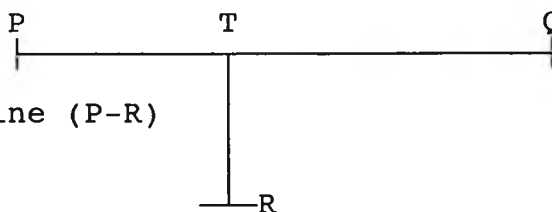
Relay setting =80% of line (P-R)

Fault Location (*)	Inception Angle (degree)					
	0	30	60	90	120	150
37.5 P	8.25	8.25	8.50	8.25	8.00	8.25
37.5 P	8.75	8.50	8.75	8.75	9.00	8.25
62.5 T	8.50	8.50	8.50	9.25	9.00	8.00
81.25 R	8.50	8.50	8.50	8.50	9.25	8.00
87.5 R	8.75	8.75	10.00	9.50	9.75	8.25
95.0 R	11.50	12.50	16.50	47.25	29.25	27.00
97.5 R	13.25	32.75	NO OP	NO OP	NO OP	27.50
100 R	35.50	NO OP	NO OP	NO OP	NO OP	NO OP
102.5 R	NO OP	NO OP	NO OP	NO OP	NO OP	NO OP
100 Q	NO OP	NO OP	NO OP	NO OP	NO OP	NO OP
97.5 Q	NO OP	NO OP	NO OP	NO OP	NO OP	NO OP
95 Q	NO OP	NO OP	NO OP	NO OP	NO OP	NO OP
92.5 Q	12.25	12.25	11.50	29.00	28.00	26.25
87.5 Q	9.50	9.25	8.75	9.50	9.75	8.50
81.25 Q	8.50	8.25	8.50	8.75	9.00	8.00

* = % of relay reach
NO OP = No operation
P = fault on leg PT
T = fault at the Tee point
R = fault on leg TR
Q = fault on leg TQ

Table 6.7 Operating time (msec) VS fault location

	End P	End Q	End R
SCL(GVA)	10.	10.	10.
Load angle(degree)	0.0	15.	10
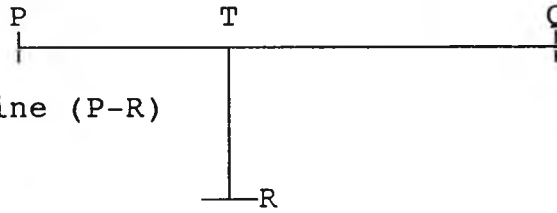
```
    P              T                    Q
    |              |                    |
    |              |                    |
                   |
                   |
                 ──┴──R
```

Relay setting =80% of line (P-R)

Fault Location (*)	Inception Angle (degree)					
	0	30	60	90	120	150
0.0 P	7.75	7.25	6.75	6.00	8.00	7.75
37.5 P	8.25	7.25	6.75	6.00	8.25	8.00
62.5 T	8.25	6.50	6.50	8.00	8.50	8.25
81.25 R	8.25	6.50	8.25	8.00	9.00	8.00
87.5 R	9.50	7.50	8.00	8.50	8.75	8.25
95.0 R	10.25	9.00	9.00	9.50	10.25	9.25
97.5 R	11.75	10.25	9.75	9.50	11.25	10.25
100 R	NO OP	12.75	11.50	10.75	31.25	NO OP
102.5 R	NO OP	NO OP	NO OP	NO OP	NO OP	NO OP
100 Q	NO OP	NO OP	NO OP	NO OP	NO OP	NO OP
97.5 Q	NO OP	NO OP	NO OP	NO OP	NO OP	NO OP
95 Q	NO OP	NO OP	NO OP	NO OP	NO OP	NO OP
92.5 Q	NO OP	NO OP	13.50	NO OP	NO OP	NO OP
87.5 Q	9.75	8.50	8.50	9.25	10.00	9.25
81.25 Q	9.25	7.50	8.25	8.50	8.75	8.00

* = % of relay reach
NO OP = No operation
P = fault on leg PT
T = fault at the Tee point
R = fault on leg TR
Q = fault on leg TQ

Table 6.8 Operating time (msec) VS fault location

	End P	End Q	End R
SCL(GVA)	25.	35.	10.
Load angle(degree)	0.0	15.	10
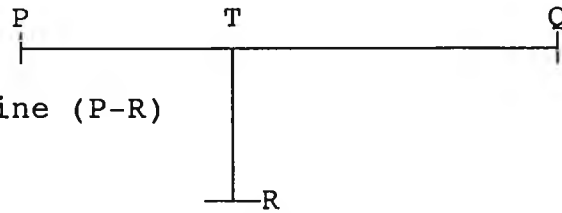
P   T   Q

Relay setting =80% of line (P-R)

R

Fault Location (*)	Inception Angle (degree)					
	0	30	60	90	120	150
0.0 P	8.00	7.00	6.25	6.00	7.50	7.75
37.5 P	8.25	7.00	6.75	6.00	8.00	7.75
62.5 T	8.00	6.50	6.50	7.50	8.25	8.00
81.25 R	8.25	6.50	7.75	8.00	8.75	8.00
87.5 R	9.50	8.25	7.75	8.25	8.75	8.00
95.0 R	10.25	8.75	8.75	9.25	10.00	9.25
97.5 R	9.75	10.25	9.25	9.00	9.75	12.00
100 R	15.50	13.50	10.25	10.50	NO OP	NO OP
102.5 R	NO OP	NO OP	NO OP	NO OP	NO OP	NO OP
100 Q	NO OP	NO OP	NO OP	NO OP	NO OP	NO OP
97.5 Q	NO OP	NO OP	NO OP	NO OP	NO OP	NO OP
95 Q	NO OP	NO OP	NO OP	NO OP	NO OP	NO OP
92.5 Q	16.25	12.50	10.00	10.75	NO OP	NO OP
87.5 Q	9.50	8.75	8.25	9.25	10.00	9.25
81.25 Q	8.75	7.50	7.75	8.25	8.75	8.00

* = % of relay reach
NO OP = No operation
P = fault on leg PT
T = fault at the Tee point
R = fault on leg TR
Q = fault on leg TQ

Table 6.9 Operating time (msec) VS fault location

	End P	End Q	End R
SCL(GVA)	20.	20.	20.
Load angle(degree)	0.0	15.	10

```
            P                 T                        Q
            ├─────────────────┼────────────────────────┤
                              │
                              │
                              │
                            ──┴─R
```

Relay setting =80% of line (P-R)
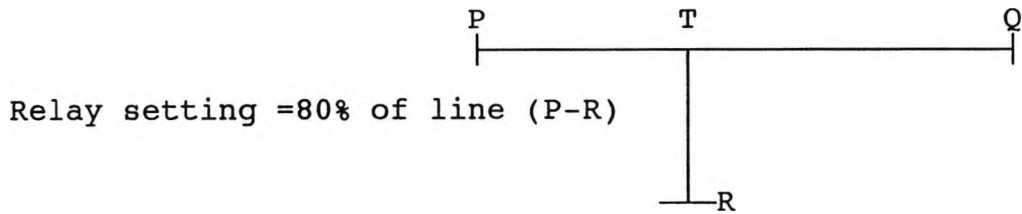
Fault Location (*)	Inception Angle (degree)					
	0	30	60	90	120	150
0.0 P	8.00	7.00	6.25	8.50	8.00	7.25
37.5 P	8.25	7.00	6.50	8.50	8.25	7.75
62.5 T	8.25	7.75	6.75	8.75	8.50	8.25
81.25 R	8.25	6.50	8.25	8.25	9.00	8.00
87.5 R	9.50	7.25	8.25	10.25	10.00	8.00
95.0 R	9.50	8.25	9.75	10.75	10.00	9.25
97.5 R	16.50	12.00	13.50	17.25	16.75	16.00
100 R	NO OP	NO OP	NO OP	NO OP	NO OP	NO OP
102.5 R	NO OP	NO OP	NO OP	NO OP	NO OP	NO OP
100 Q	NO OP	NO OP	NO OP	NO OP	NO OP	NO OP
97.5 Q	NO OP	NO OP	NO OP	NO OP	NO OP	NO OP
95 Q	NO OP	NO OP	NO OP	NO OP	NO OP	NO OP
92.5 Q	NO OP	NO OP	NO OP	NO OP	NO OP	NO OP
87.5 Q	9.50	8.00	9.25	10.25	10.00	9.25
81.25 Q	8.50	7.00	9.00	10.25	9.75	8.00

* = % of relay reach
NO OP = No operation
P = fault on leg PT
T = fault at the Tee point
R = fault on leg TR
Q = fault on leg TQ

Table 6.10 Operating time (msec) VS fault location

	End P	End Q	End R
SCL(GVA)	20.	20.	20.
Load angle(degree)	15.	0.0	10

P   T   Q

Relay setting =80% of line (P-R)

                             R
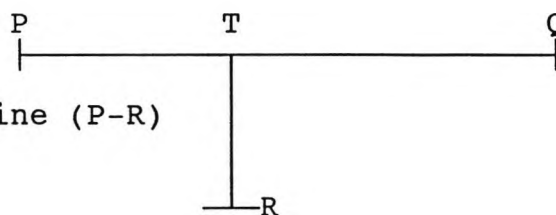
Fault Location (*)	Inception Angle (degree)					
	0	30	60	90	120	150
0.0 P	7.75	7.25	7.00	8.00	7.75	7.50
37.5 P	8.25	7.50	7.00	8.25	8.25	7.75
62.5 T	8.25	7.75	8.25	8.75	8.50	8.25
81.25 R	8.50	8.25	8.50	8.75	8.50	8.25
87.5 R	9.75	9.00	9.25	9.75	9.25	9.00
95.0 R	9.75	10.25	10.25	10.75	10.50	11.00
97.5 R	16.50	15.50	15.50	17.75	16.75	19.75
100 R	NO OP	NO OP	NO OP	NO OP	NO OP	NO OP
102.5 R	NO OP	NO OP	NO OP	NO OP	NO OP	NO OP
100 Q	NO OP	NO OP	NO OP	NO OP	NO OP	NO OP
97.5 Q	NO OP	NO OP	NO OP	NO OP	NO OP	NO OP
95 Q	NO OP	NO OP	NO OP	NO OP	NO OP	NO OP
92.5 Q	NO OP	NO OP	NO OP	NO OP	NO OP	NO OP
87.5 Q	10.00	10.75	11.25	11.25	11.25	10.00
81.25 Q	9.75	8.75	9.50	10.00	9.75	8.75

* = % of relay reach
 NO OP= No operation
P = fault on leg PT
T = fault at the Tee point
R = fault on leg TR
Q = fault on leg TQ
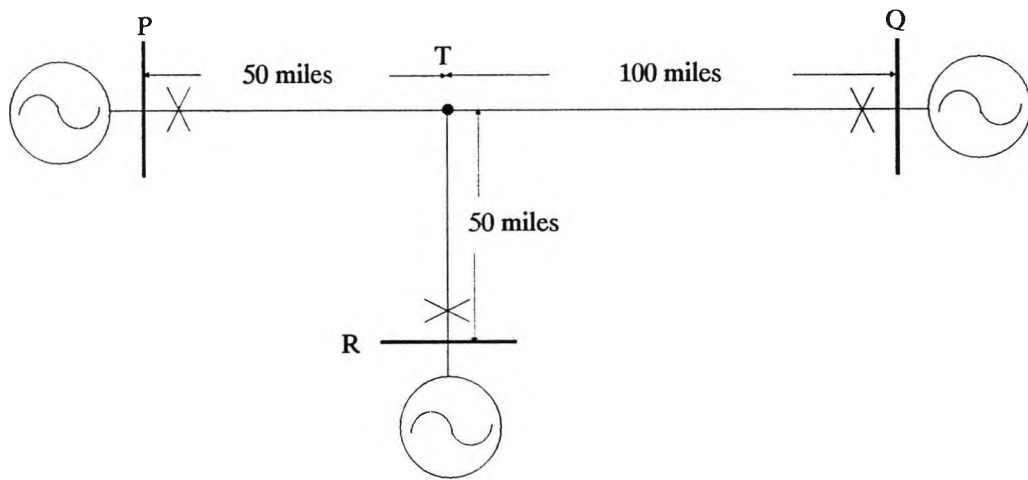
Fig. 6.1 Teed system used for relay testing.
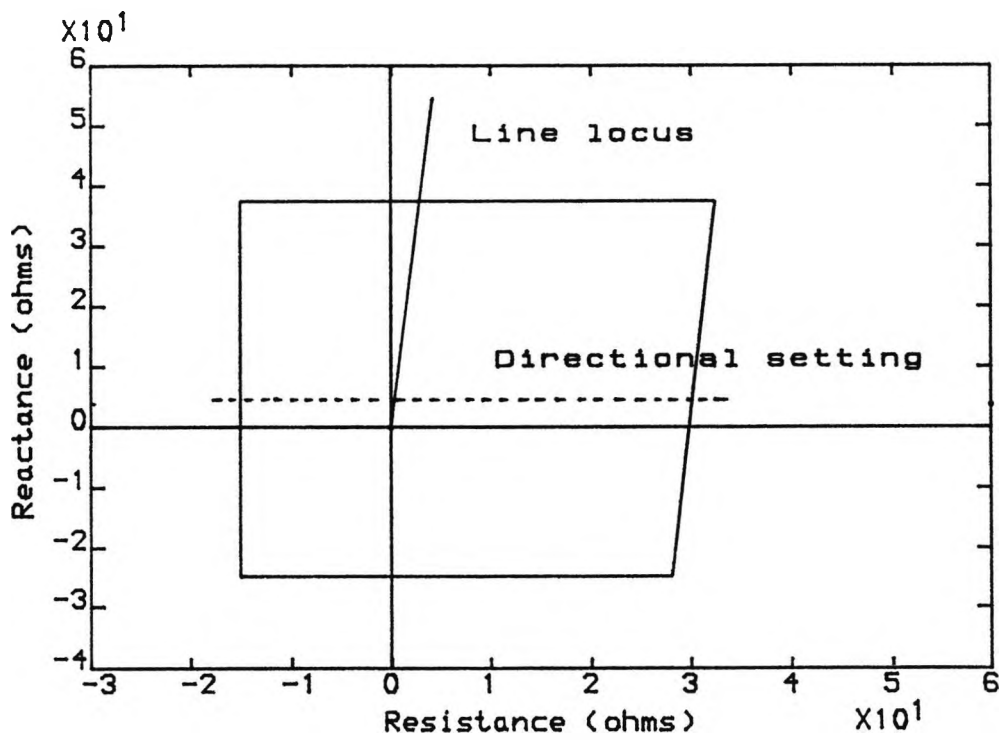
Fig.6.2 Relay tripping characteristic
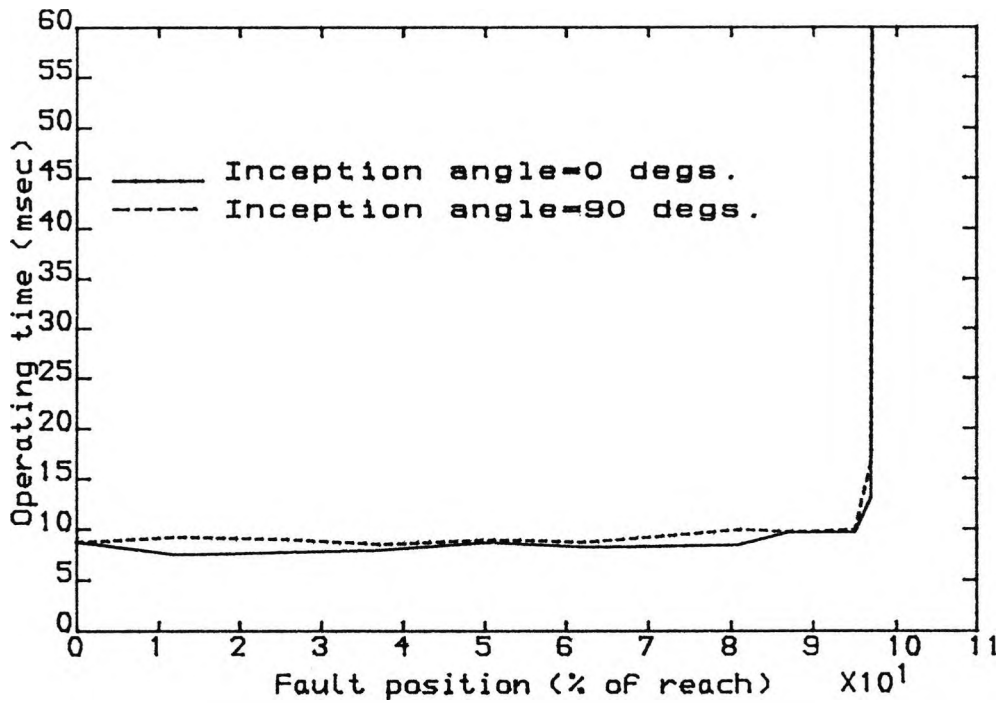
Fig.6.3 Relay operating time vs fault position
for the a-e faults along line P-T-R
SCL (GVA)   P=35   Q=35   R=35
Load angle (degs) P=15   Q=0.0   R=10
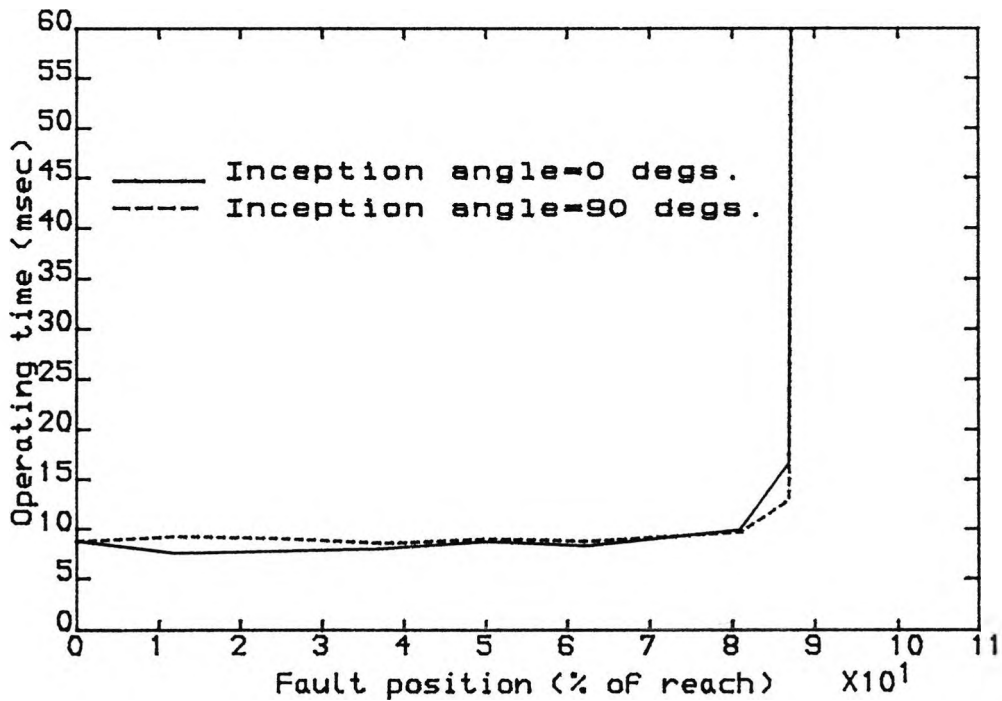
Fig.6.4 Relay operating time vs fault position
for the a-e faults along line P-T-Q
SCL (GVA)   P=35   Q=35   R=35
Load angle (degs) P=15   Q=0.0   R=10
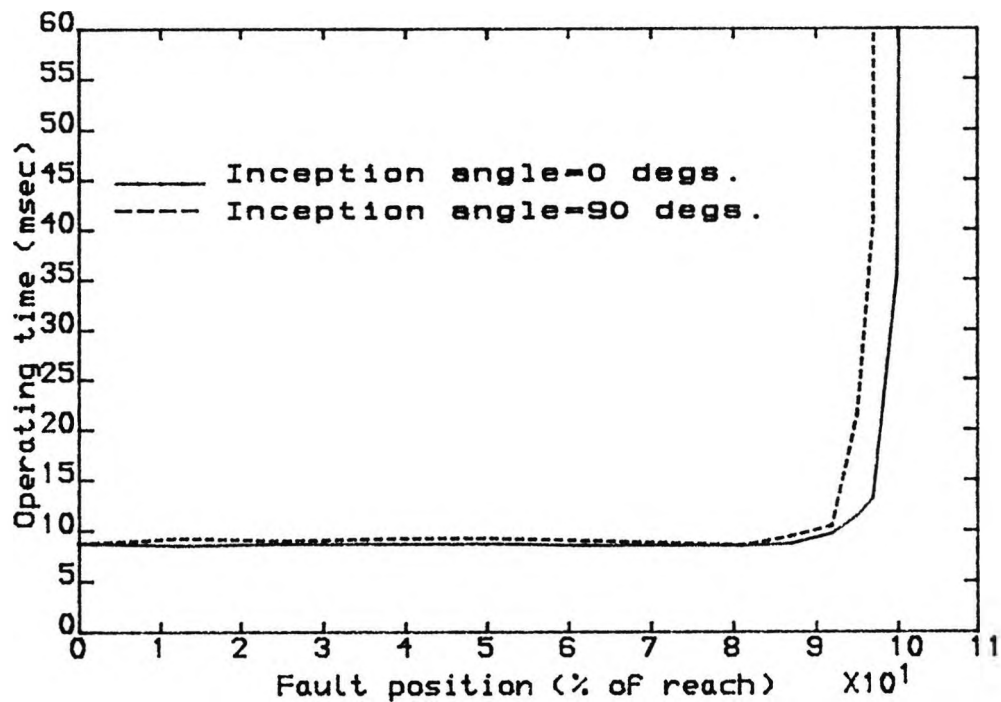
Fig.6.5 Relay operating time vs fault position
for the a-e faults along line P-T-R
SCL (GVA)   P=3.5   Q=3.5   R=3.5
Load angle (degs) P=0.0   Q=15   R=10
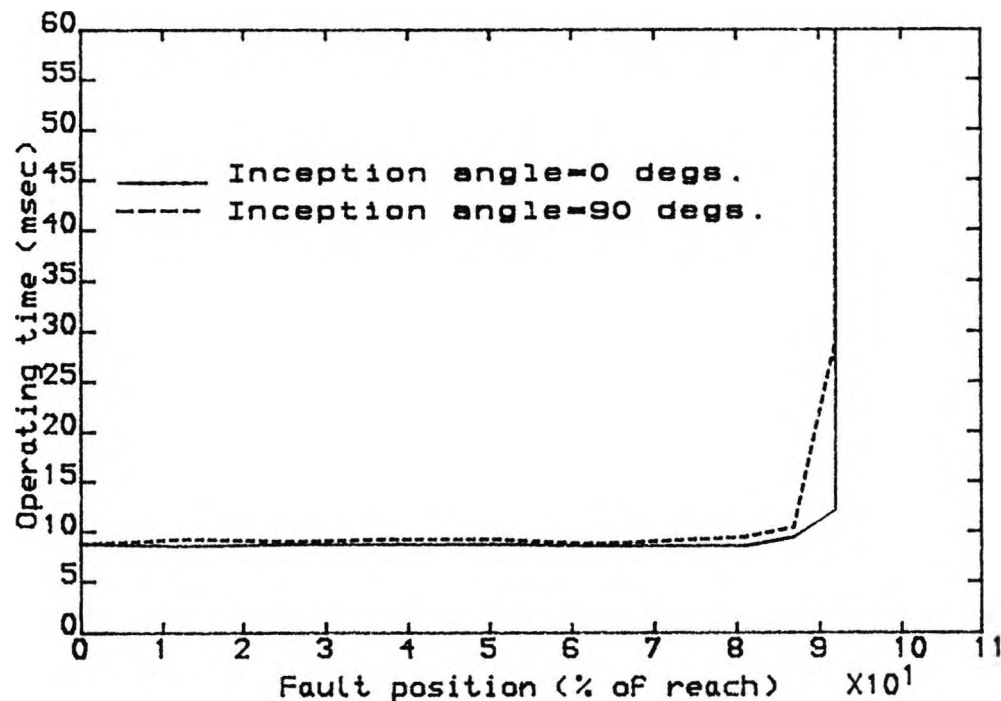
Fig.6.6 Relay operating time vs fault position
for the a-e faults along line P-T-Q
SCL (GVA)   P=3.5   Q=3.5   R=3.5
Load angle (degs) P=0.0   Q=15   R=10
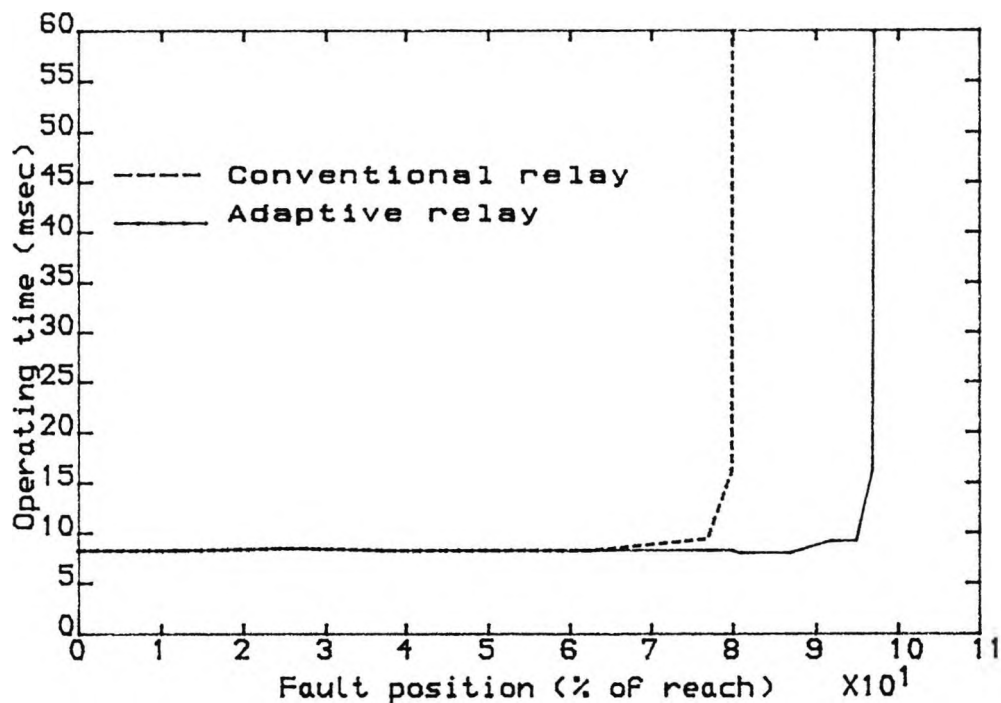
Fig.6.7 Relay operating time vs fault position
for the a-e faults along line P-T-R
Fault inception angle =0 degs.
No-load condition
SCL (GVA)   P=3.5   Q=35   R=35
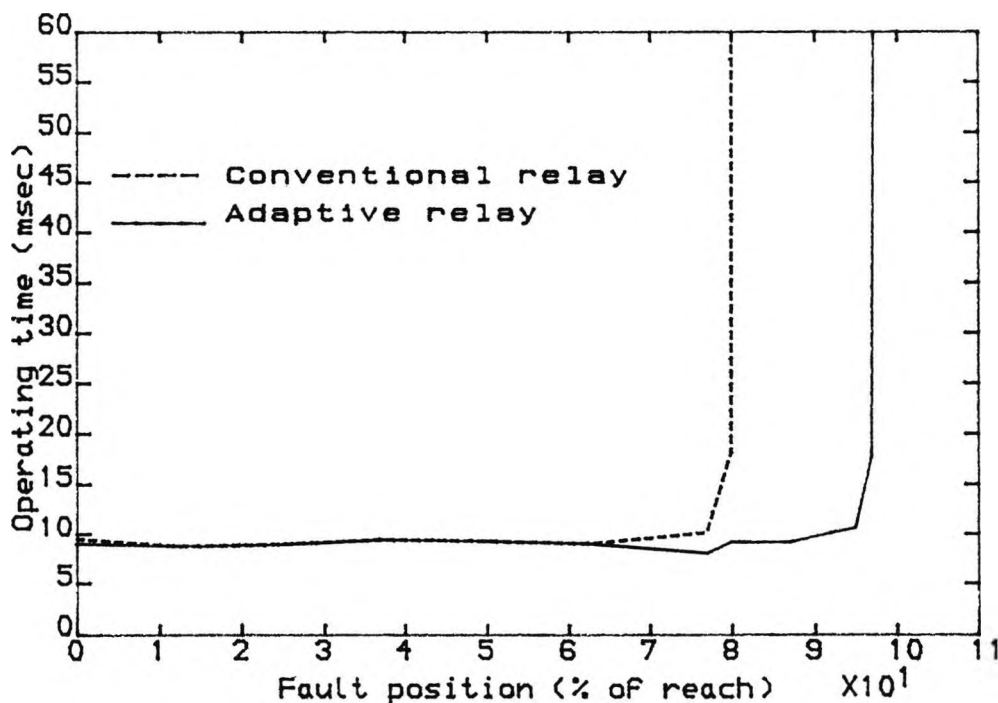
Fig.6.8 Relay operating time vs fault position
for the a-e faults along line P-T-R
Fault inception angle =90 degs.
No-load condition
SCL (GVA)   P=3.5   Q=35   R=35
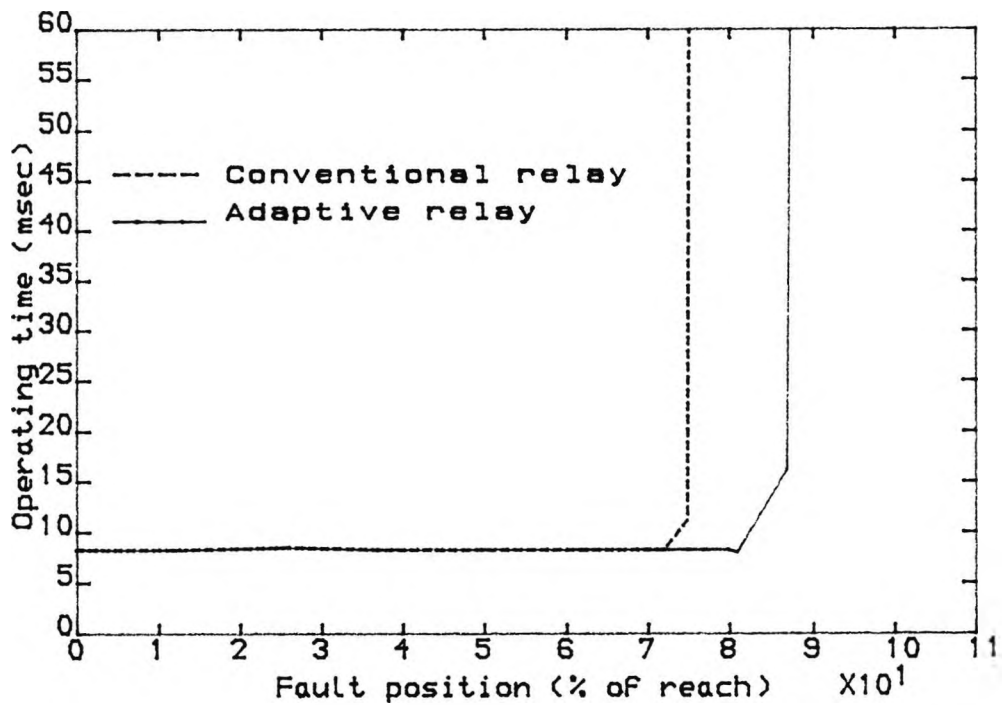
Fig.6.9 Relay operating time vs fault position
for the a-e faults along line P-T-Q
Fault inception angle =0 degs.
No-load condition
SCL (GVA)   P=3.5   Q=35   R=35
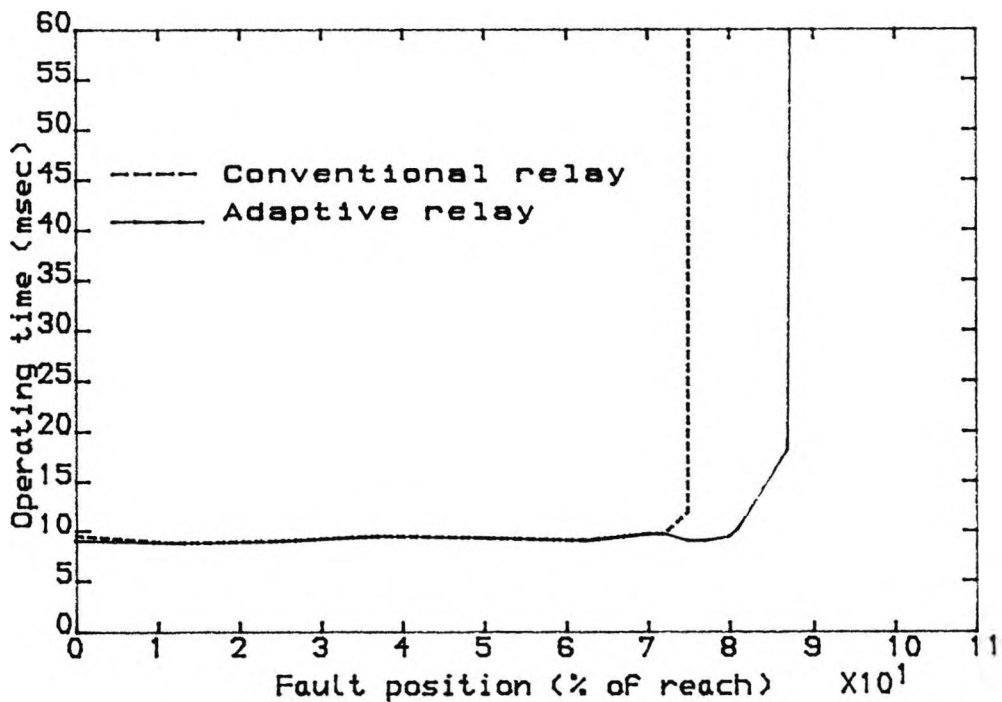
Fig.6.10 Relay operating time vs fault position
for the a-e faults along line P-T-Q
Fault inception angle =90 degs.
No-load condition
SCL (GVA)   P=3.5   Q=35   R=35
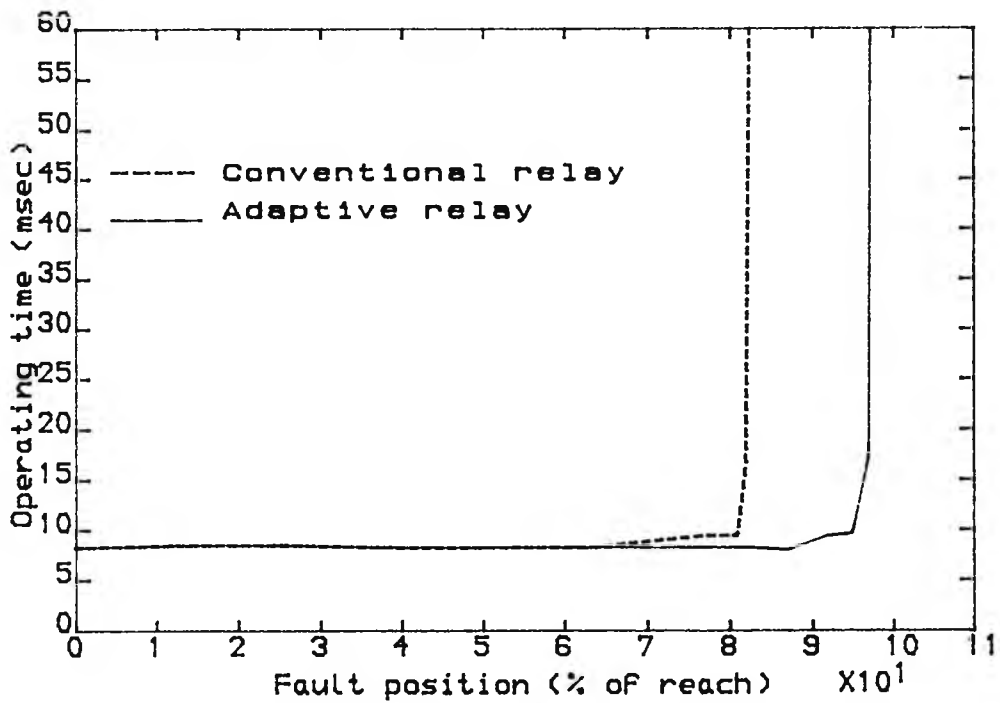
Fig.6.11 Relay operating time vs fault position
for the a-e faults along line P-T-R
Fault inception angle =0 degs.
No-load condition
SCL (GVA)   P=3.5   Q=3.5   R=3.5
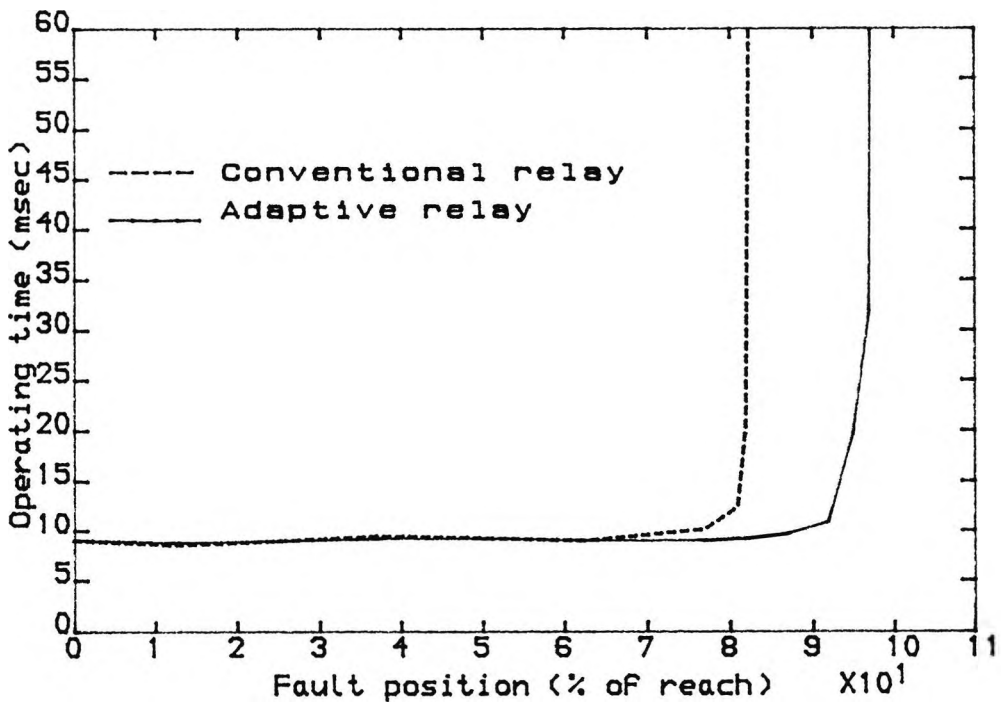
Fig.6.12 Relay operating time vs fault position
for the a-e faults along line P-T-R
Fault inception angle =90 degs.
No-load condition
SCL (GVA)   P=3.5   Q=3.5   R=3.5
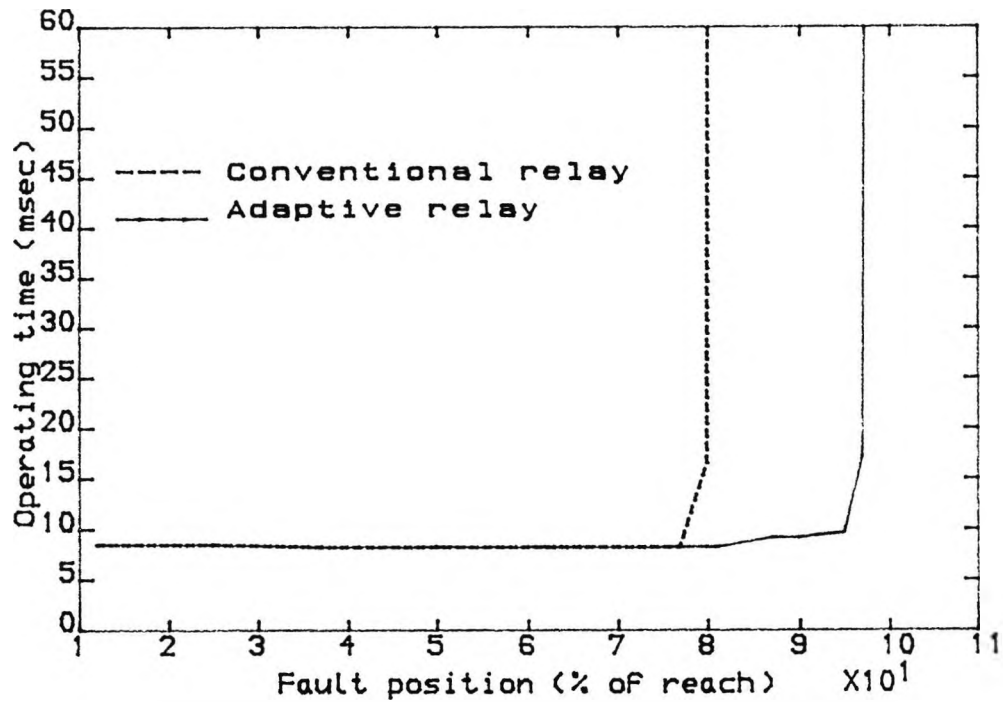
Fig.6.13 Relay operating time vs fault position
for the a-e faults along line P-T-Q
Fault inception angle =0 degs.
No-load condition
SCL (GVA)   P=3.5   Q=3.5   R=3.5
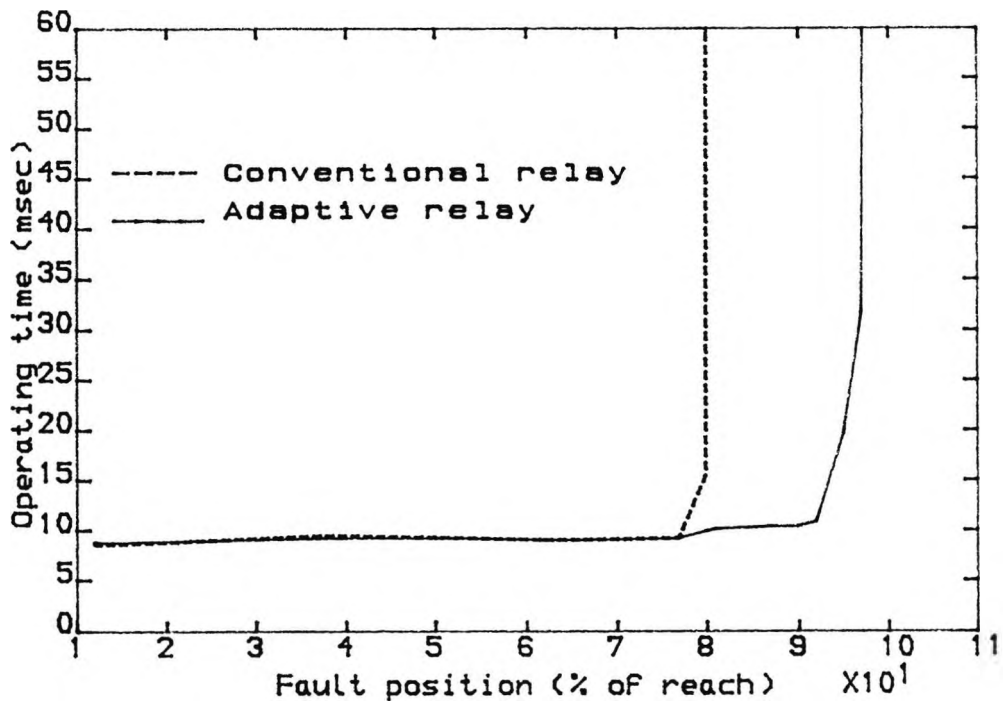
Fig.6.14 Relay operating time vs fault position
for the a-e faults along line P-T-Q
Fault inception angle =90 degs.
No-load condition
SCL (GVA)   P=3.5   Q=3.5   R=3.5
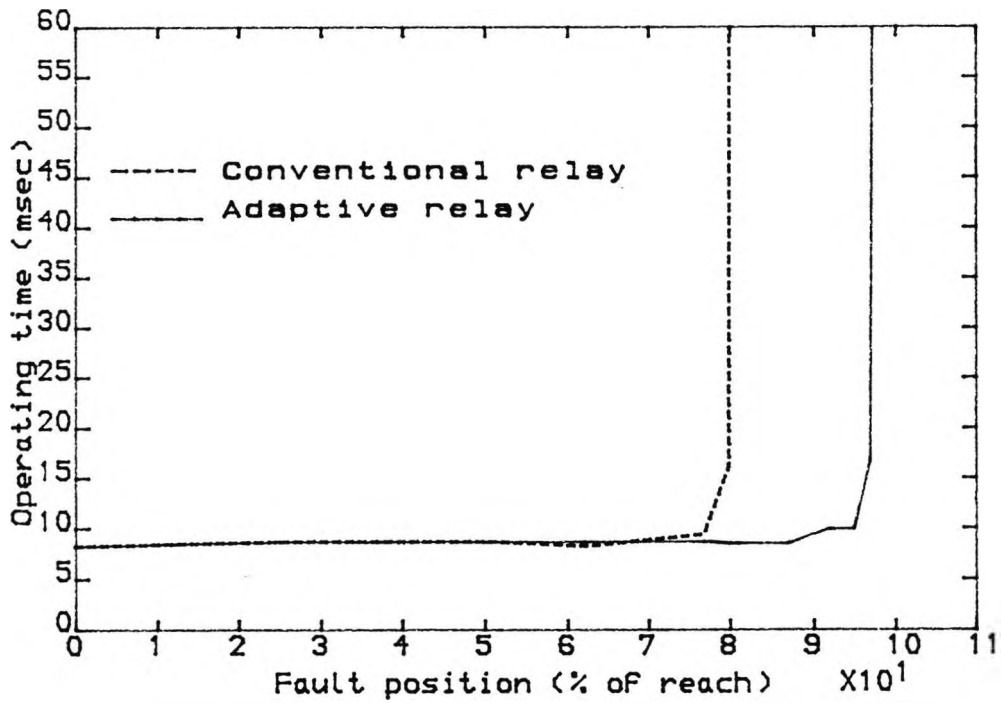
Fig.6.15 Relay operating time vs fault position
for the b-c faults along line P-T-R
Voltage minima faults
No-load condition
SCL (GVA)   P=3.5   Q=35   R=35
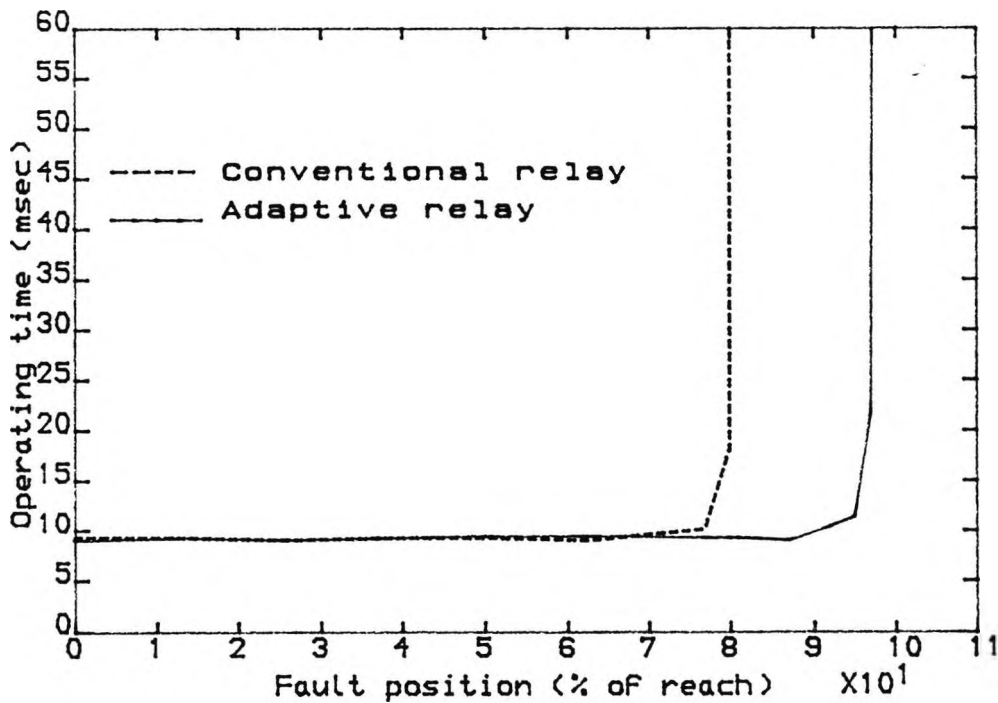
Fig.6.16 Relay operating time vs fault position
for the b-c faults along line P-T-R
Voltage maxima faults
No-load condition
SCL (GVA)   P=3.5   Q=35   R=35
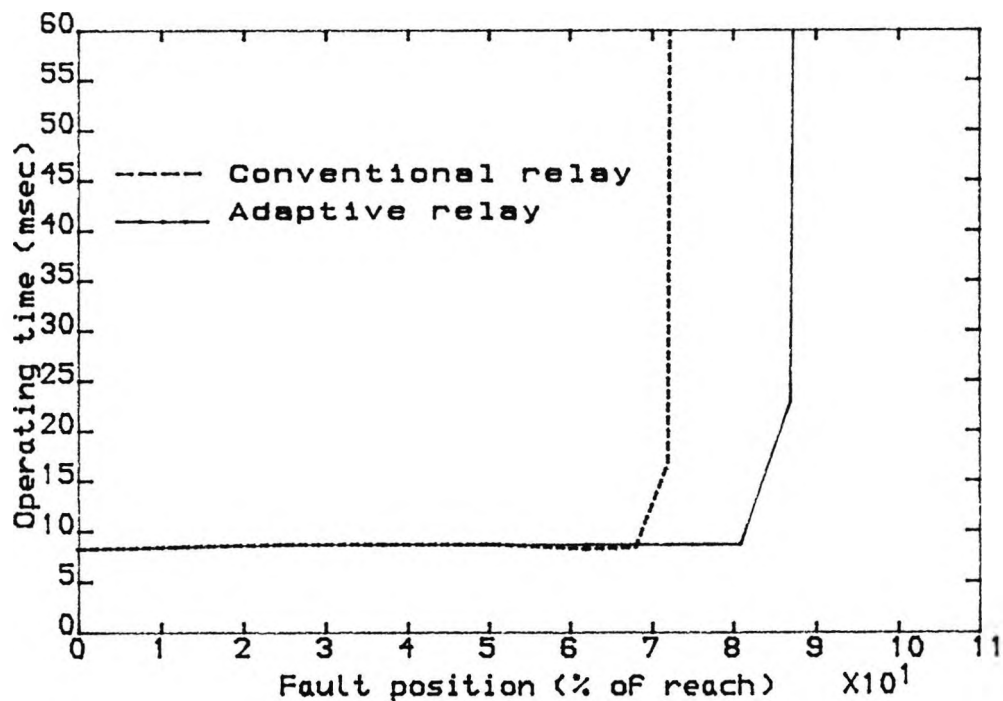
Fig.6.17 Relay operating time vs fault position
for the b-c faults along line P-T-Q
Voltage minima faults
No-load condition
SCL (GVA)   P=3.5   Q=35   R=35
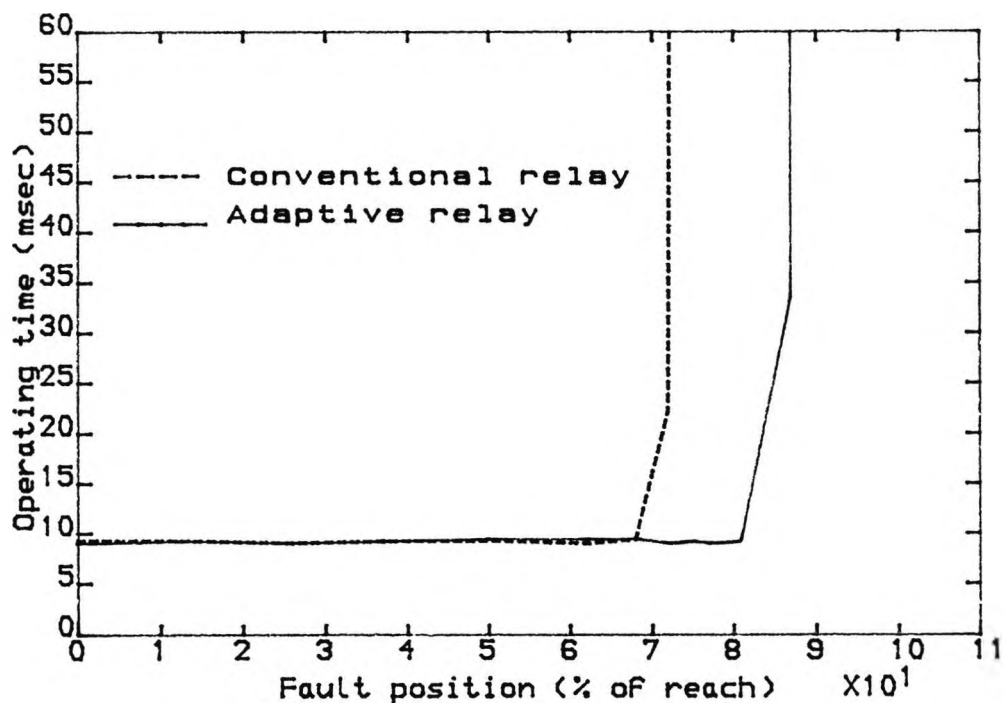
Fig.6.18 Relay operating time vs fault position
for the b-c faults along line P-T-Q
Voltage maxima faults
No-load condition
SCL (GVA)   P=3.5   Q=35   R=35
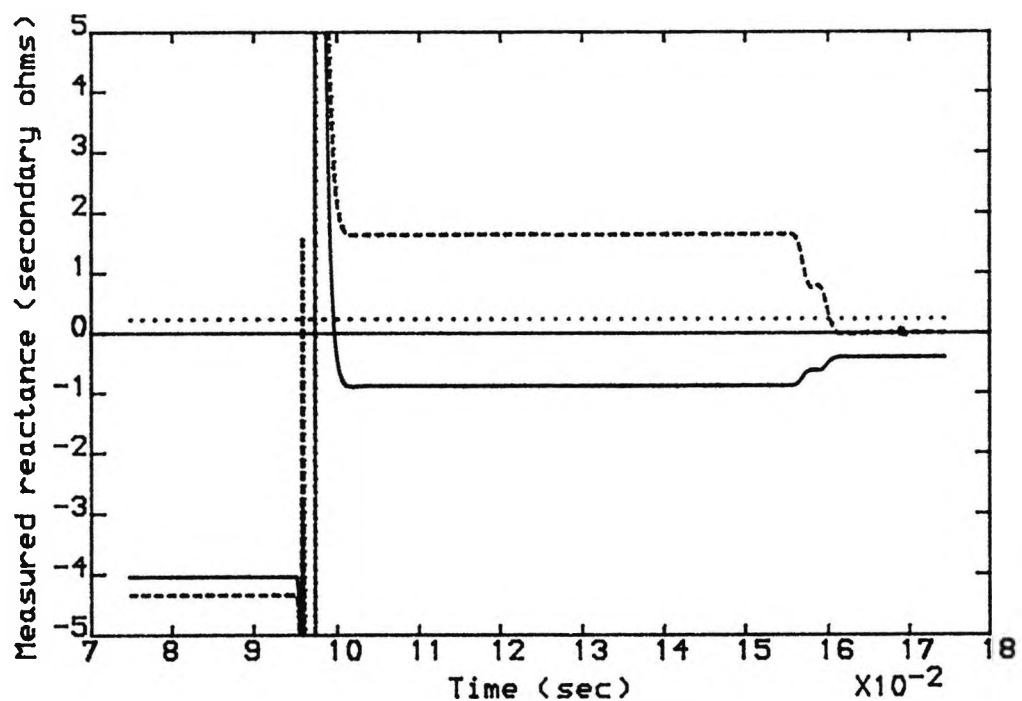
Fig.6.19 Measured reactance vs Time showing
the measured reactance and the directional
reactance for a fault in front of the relay

　　　　──────── Measured reactance
　　　　──────── Directional reactance
　　　　........ Directional reactance setting
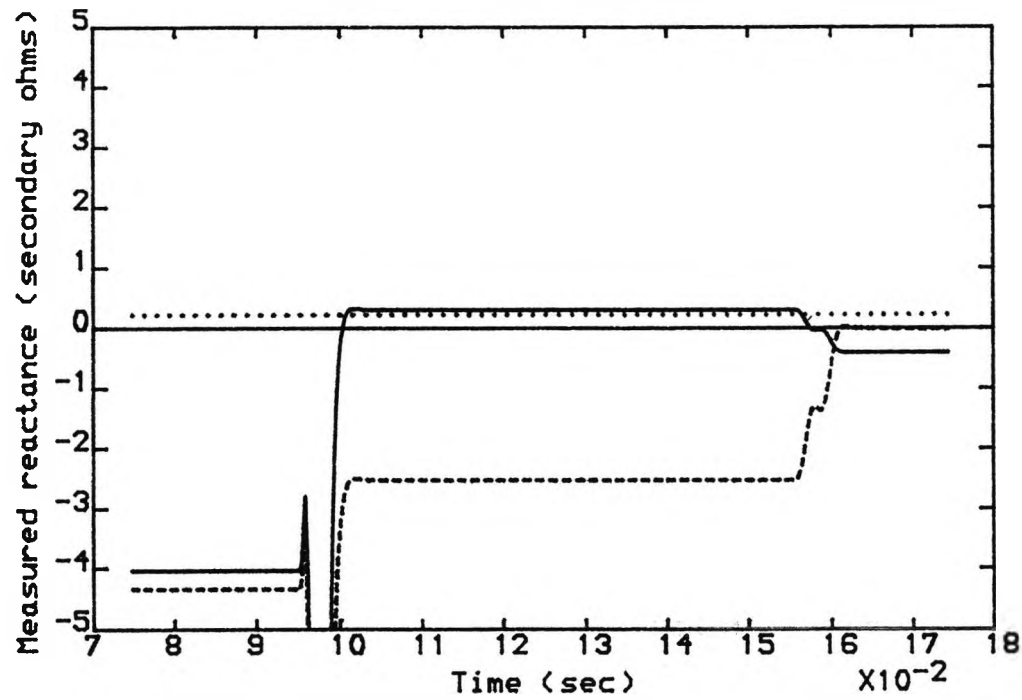
Fig.6.20 Measured reactance vs Time showing
the measured reactance and the directional
reactance for a fault behind of the relay

　　　　──────── Measured reactance
　　　　──────── Directional reactance
　　　　........ Directional reactance setting
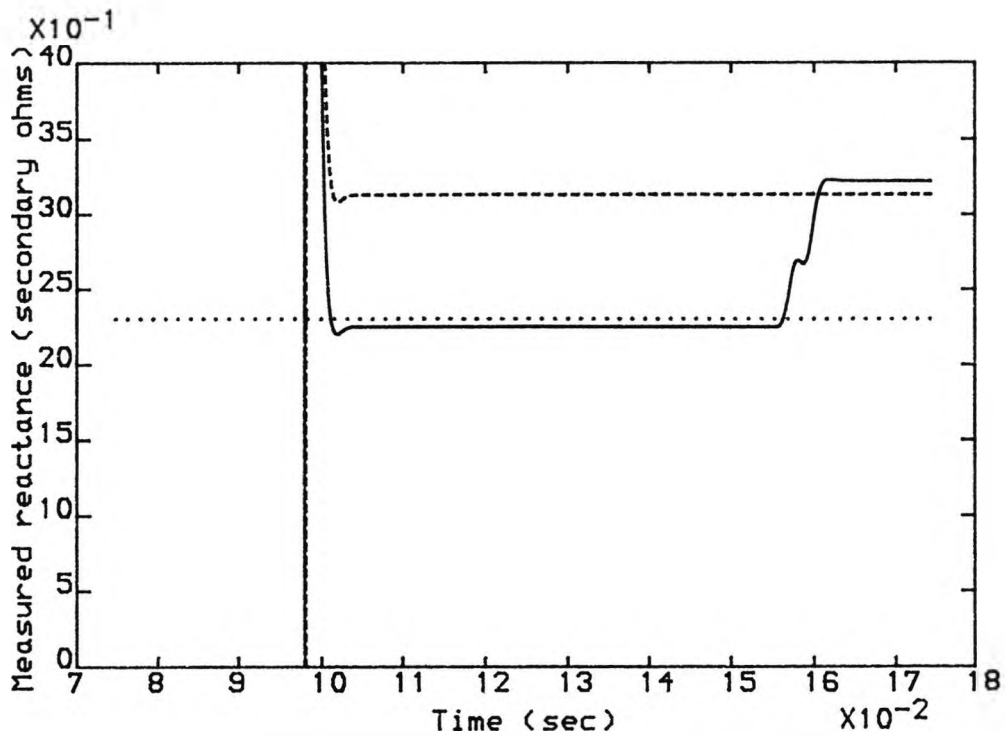
Fig.6.21 Measured reactance vs Time showing
the relay behaviour before and after the
buffer runs out of memory
        ..... Forward reactive reach
        _____ Adaptive measurand
        ----- Conventional measurand
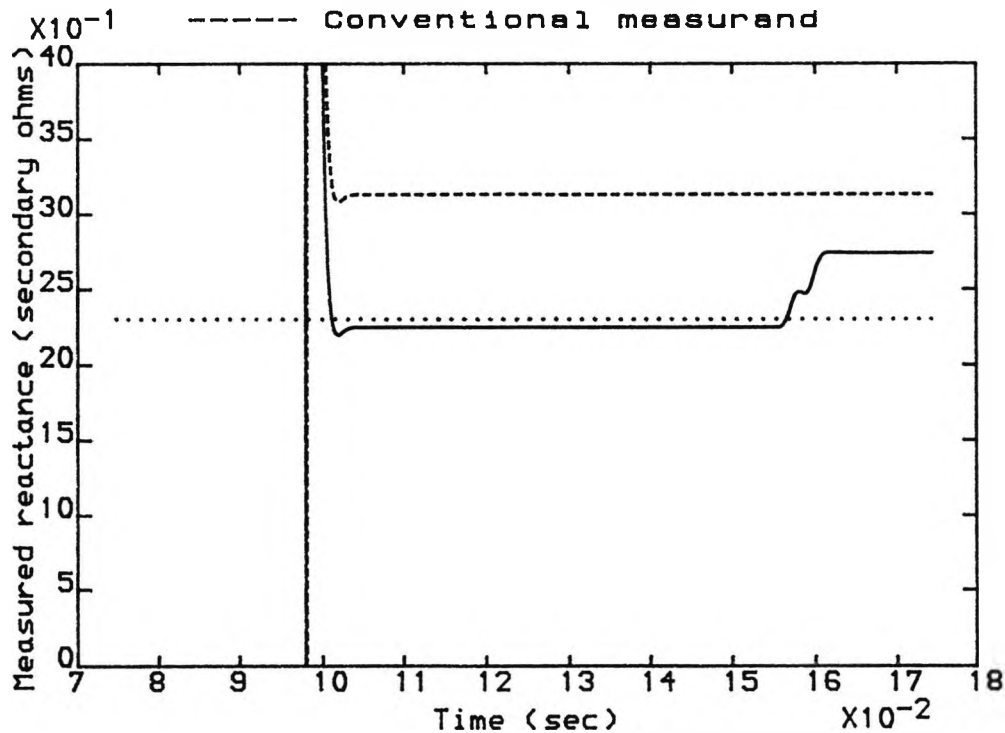
Fig.6.22 Measured reactance vs Time showing
the relay behaviour before and after the
buffer runs out of memory (after modification
        ..... Forward reactive reach
        _____ Adaptive measurand
        ----- Conventional measurand

CHAPTER 7

ALTERNATIVE METHOD FOR IMPLEMENTING THE ADAPTIVE SCHEME

The discussions and results presented so far are based on adjusting the measured impedance to give the exact line value at the reach point and the proper discrimination between internal and external faults. This Chapter introduces an alternative way to implement the adaptive scheme. Basically the same requirements and derivations as discussed in Chapter 2 are valid. The difference is in the implementation within the computer relay, i.e., instead of manipulating the signals to change the measured impedance these can be used to adjust the relay setting so that it can correspond to the apparent impedance at the reach point. It is not the intention in this chapter to repeat fully the analysis, instead, only some key points and results will be presented to show the difference between the two methods.

7.1 Basic Mathematical Equations

Some equations will be recalled from Chapter 2 to illustrate how the scheme can be implemented.

The measured impedance for a fault along line P-T-R is

$$Z_{mP} = \frac{V_P}{I_P} = Z_P + \alpha_R Z_R + \alpha_R Z_R k_R \qquad 7.1$$

The relay conventional setting is:

$$S_R = Z_P + \alpha_{RS} Z_R \qquad 7.2$$

If the relay is to measure correctly its setting should be adjusted in a way such that the measured impedance and the

112

setting are equal at the reach point, in mathematical terms this can be expressed as:

$$Z_P + \alpha_R Z_R + \alpha_R Z_R k_R = Z_P + \alpha_{RS} Z_R + \alpha_{RS} Z_R k_R \qquad 7.3$$

In the above equation if α_R is equal to α_{RS} the two sides will be identical this implies that the fault is at the reach point, if $\alpha_R > \alpha_{RS}$ the fault will looks as external and if $\alpha_R < \alpha_{RS}$ the fault can be identified as internal.

For the system shown in Figure 7.1, the variation of the measured impedance with fault position is shown in Figure 7.2 if this is to be compared with the fixed setting then the relay will underreach. The apparent impedance at the reach point being equal to 2.08 pu and the setting is 1.6 pu. By increasing the setting by the factor $\alpha_{RS} Z_R k_R$ the apparent impedance and the setting are equal at the reach and the relay gives the correct discrimination.

The equations and illustration discussed above are for a single phase system the same argument is also applicable for the phase-earth and phase to phase faults of a three phase system.

7.2 Practical Implementation Consideration

For practical implementation Equation 2.31 can be written as

$$Z_{mPR} = \frac{V_P}{I_P} + \frac{k'_1 V_P - k'_1 V_{PS} + k'_2 I_{PS} - k'_3 I_{QS}}{I_P} - k'_2 \qquad 7.4$$

Simply, the second and third terms of the above equation should be used to adjust the relay setting i.e., subtracted from the fixed setting of the conventional

113

relay.

Then the modified setting becomes:

$$S_{mR}=Z_P + \alpha_{RS}Z_R - \frac{k'_1V_P-k'_1V_{PS}+k'_2I_{PS}-k'_3I_{QS}}{I_P} + k'_2 \qquad 7.5$$

The relay can be implemented by feeding the above signals and constants to an impedance measurement processor and comparing each value of the sampled impedance with the samples of the impedance derived from the local voltage and current. Figure 7.3 shows the basic relay arrangement.

Comparing Figures 7.3 and 2.11 it is clear that to implement the new option the relay requires two separate algorithms to convert the current and voltage samples into a measured resistance and reactance.

Similarly the same process is applicable for the three phase system and the analysis will not be repeated in this chapter.

7.3 Relay Test

The relay was implemented in software, following the same procedures as in Chapter 4, which includes the signal conditioning, filtering, impedance calculation algorithm, directionality, transient suppresion and trip decisions.

The relay was tested using the three phase system described in the previous chapter (Figure 6.1). Figure 7.4 shows the measured reactance and the adaptive setting for the a-phase to earth fault just inside the reach point where it can be clearly seen that the relay sees the fault as an internal one. Also on the same graph

114

the conventional fixed reactive setting is shown. Figure 7.5 displays the measurements for a fault just beyond the reach point. It is obvious that the relay gives an indication that the fault is external. The fault is not considered at the exact reach point because for this case the setting and the measured reactance coincide and can not be distinguished if displayed on the same graph.

The above discussions are related to the 3 cycle power frequency period during which the relay should operate correctly. An illustration of the relay behaviour in the interval when the relay runs out of the prefault values of the voltage and current is shown in Figure 7.6, the fault considered is external and in the vicinity of the reach point, it can be seen that the during the period when the steady state values are still available, the fault is identified as out of zone. Later on the margin between the setting and the measured reactance becomes greater which is advantageous and desirable. For an internal fault, the relay behaviour is shown in Figure 7.7, the relay sees the fault within its reach for three cycles after that it underreaches; the measured reactance being higher than the setting. Note that the relay still gives a better coverage than the conventional relay.

Figure 7.8 and 7.9 show the earth fault operating times, as a function of the fault position. The fault position is expressed as a percentage of the relay reach which was set to 80% of the line P-T-R. It can be clearly

seen that, regardless of the fault inception angle, the relay operating time is less than 10 msec for the majority of faults that fall within it reach.

The conventional relay operating time is shown on the same graph where it is obvious that the relay underreaches and the operating time is identical to that of the adaptive relay for faults that fall within its characteristics.

For faults along the line P-T-Q, the relay reach and operating time is shown in Figures 7.10 and 7.11 for fault inception angle of 0° and 90°. The relay in this case covered a distance which is shorter than on Section TR but it gives a better reach compared with the conventional relay.

By comparing the results shown in Figures 7.8 to 7.11 with results of Chapter 6 (Figures 6.7-6.10) (the system and the operating conditions being identical in both cases), it is evident that both options for implementing the schemes can give identical results.

7.4 Relay Behaviour for Closeup Faults

This section examines the behaviour of the relay when subjected to closeup faults in the forward and reverse directions. Both faults are of the a-phase to earth type occurring at a zero distance from the relay location. The measured impedance in both cases converges to zero after the fault. The measurands of interest in this case are the relay setting and the directional reactance. For the forward fault, Figure 7.12, it can be seen that the

116

reactive setting maintains a value which is higher than the fixed setting so the tripping decision is not affected, also the directional reactance remains above the directional limit. Figure 7.13 shows the reactances for the reverse fault, the setting in this case takes a smaller value than the fixed setting but this is not of any concern as the relay is not required to operate. In fact, it is advantageous if the relay characteristics is reduced for reverse faults. The directional reactance is negative which prevent the relay operation.

7.5 Summary

This Chapter has outlined a new method for implementing the adaptive scheme. The basic idea of this method is the adjustment of the relay setting so that it can correspond to the apparent impedance at the reach point. The relay characteristics need not be extended into the negative region as required by the previous scheme. It should be noted, however, that two separate impedance calculation algorithms are required to convert the current and voltage samples into a measured resistance and reactance.

The results confirmed that the relay maintains a fast operating time; less than half a cycle for the majority of the faults that can fall within it reach. Also it has been demonstrated that the relay gives a favourite reach compared with the conventional relay.
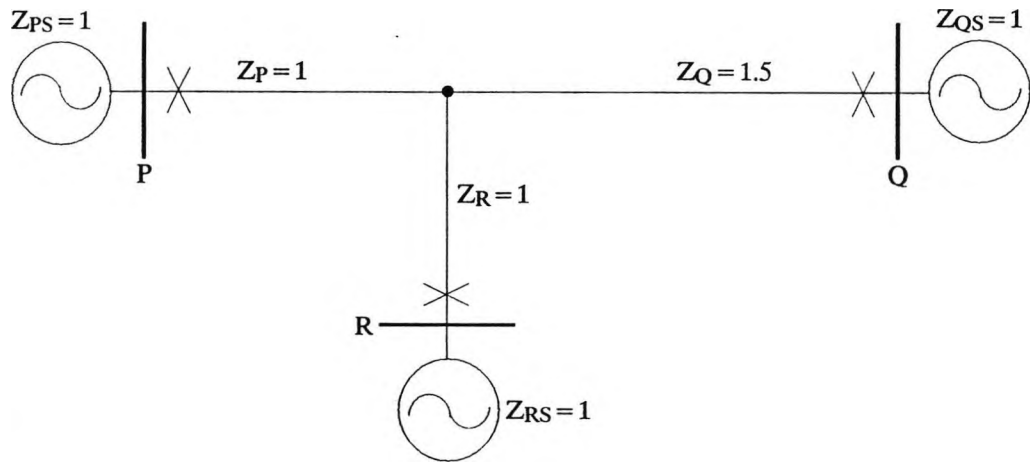
Fig. 7.1 3-Terminal line configuration with p.u. impedances
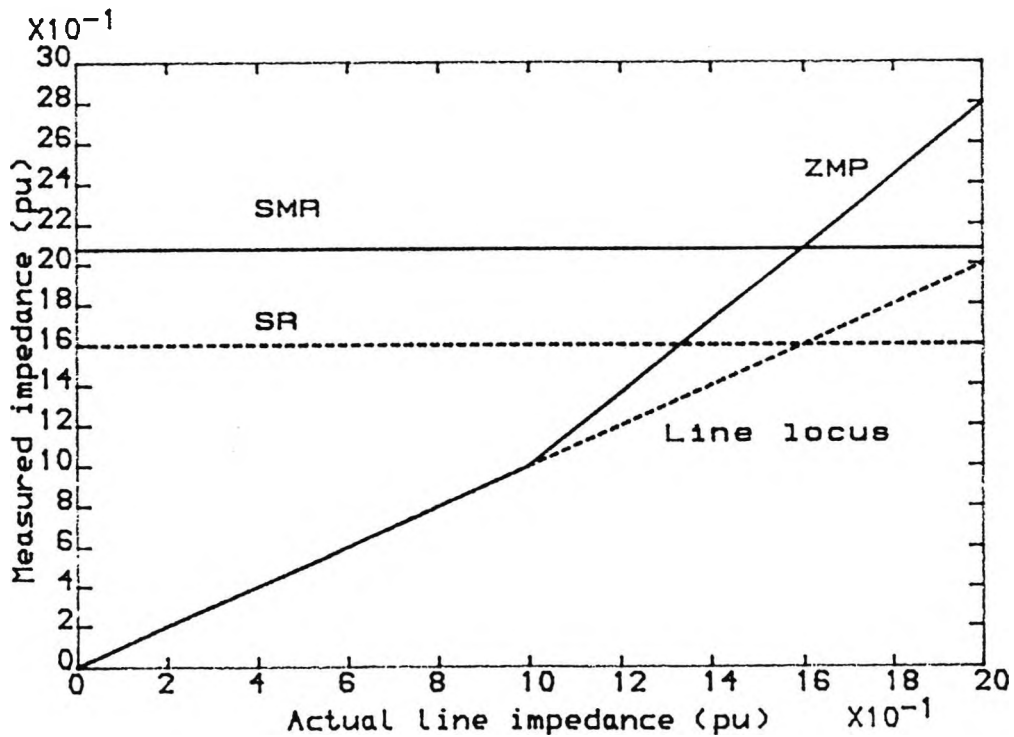
Fig.7.2 Relay measurement at end P for
faults along line P-T-R
------ Conventional setting
_____ Adaptive setting
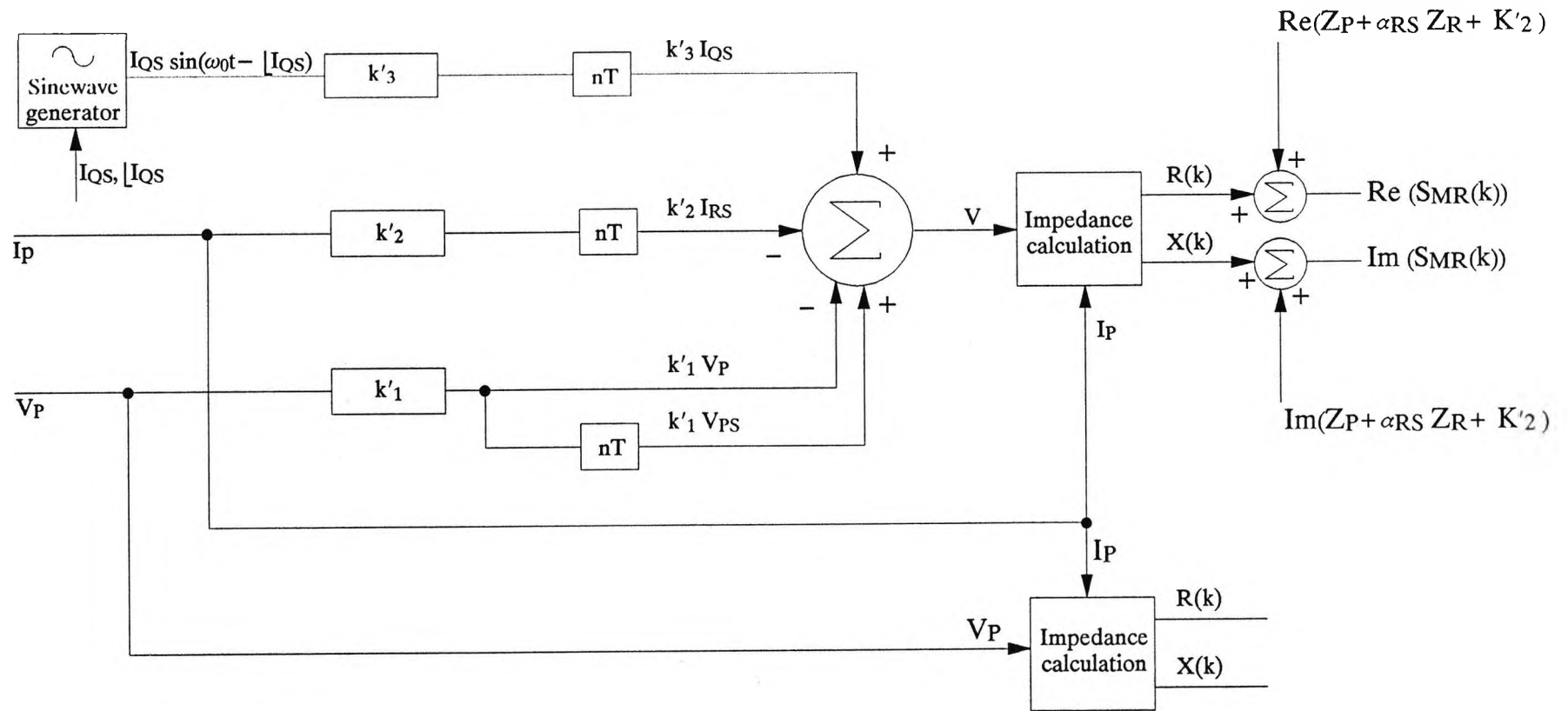
Fig. 7.3 Basic arrangment of the adaptive distance relay
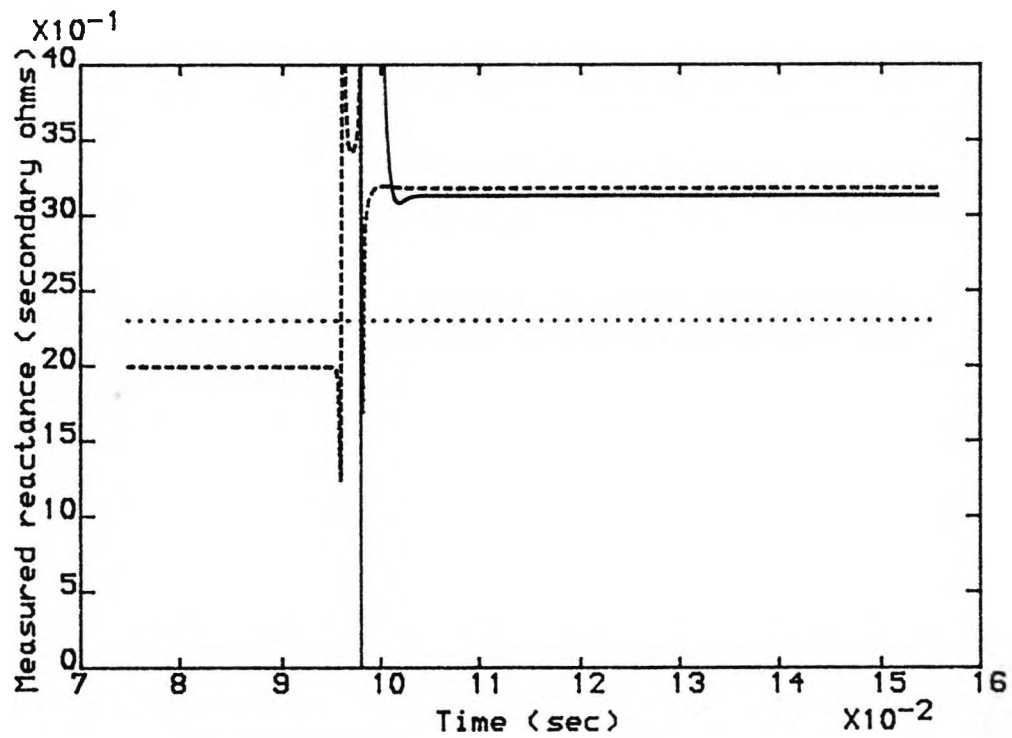
Fig.7.4 Measured reactance vs Time showing
the measured reactance and the reactive
setting for a fault inside the relay reach

———————— Measured reactance
———————— Adaptive reactive setting
. . . . Conventional setting
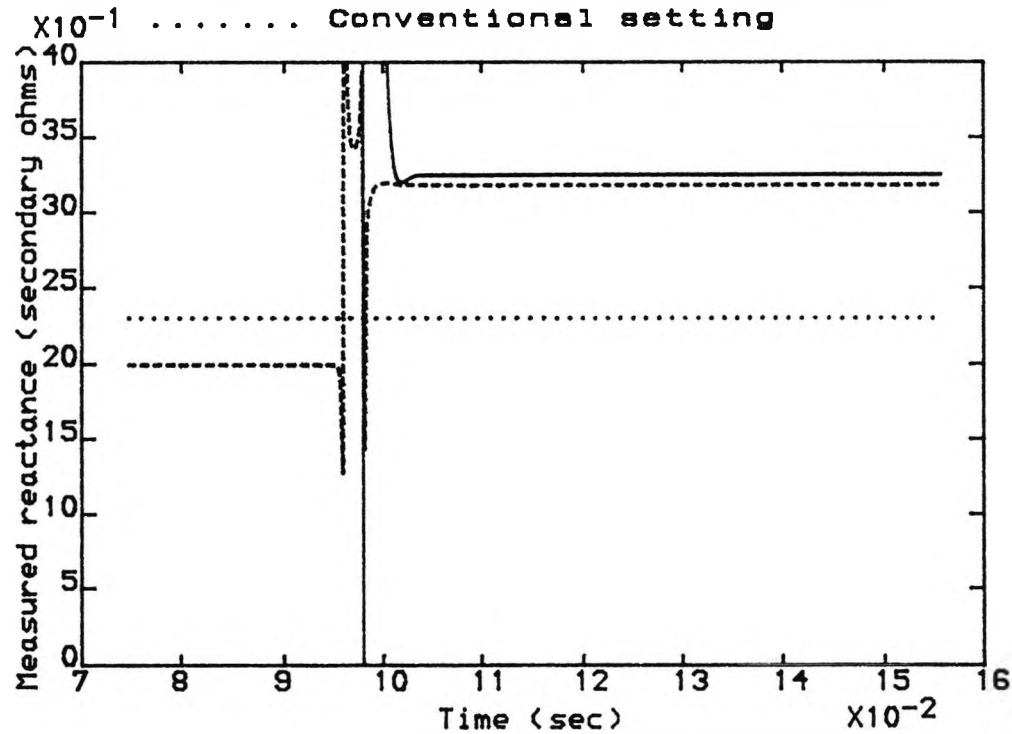
Fig.7.5 Measured reactance vs Time showing
the measured reactance and the reactive
setting for a fault outside the relay reach

———————— Measured reactance
———————— Adaptive reactive setting
. . . . Conventional setting
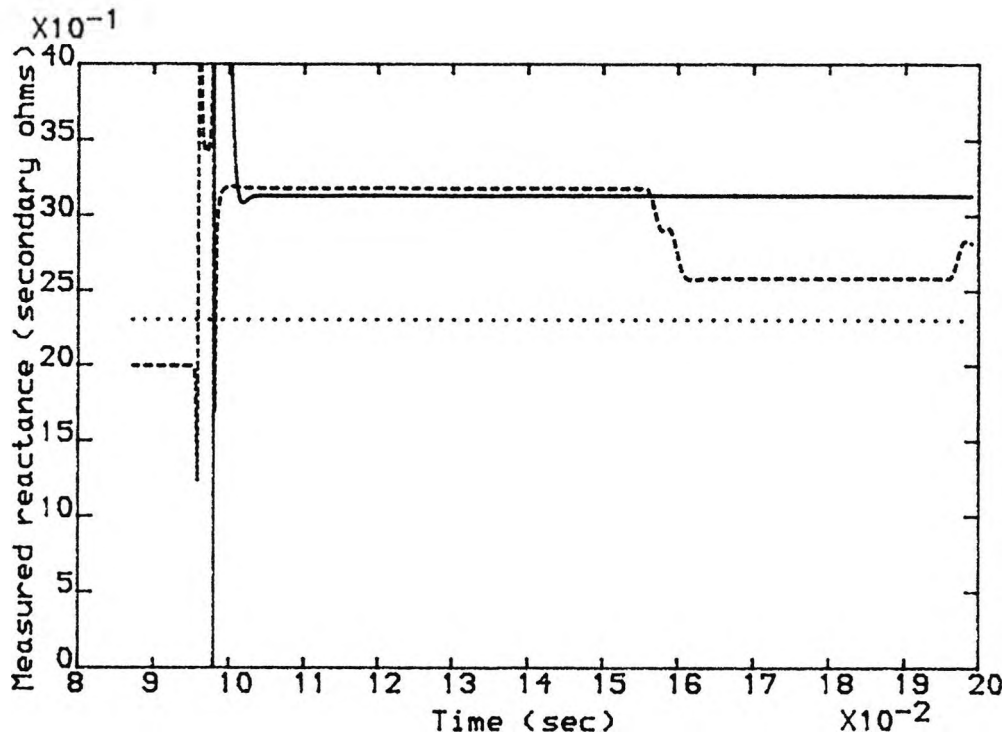
Fig.7.6 Relay behaviour showing the measured
reactance and the reactive setting during
different periods for an internal fault
────────── Measured reactance
────── Adaptive reactive setting
.... Conventional setting
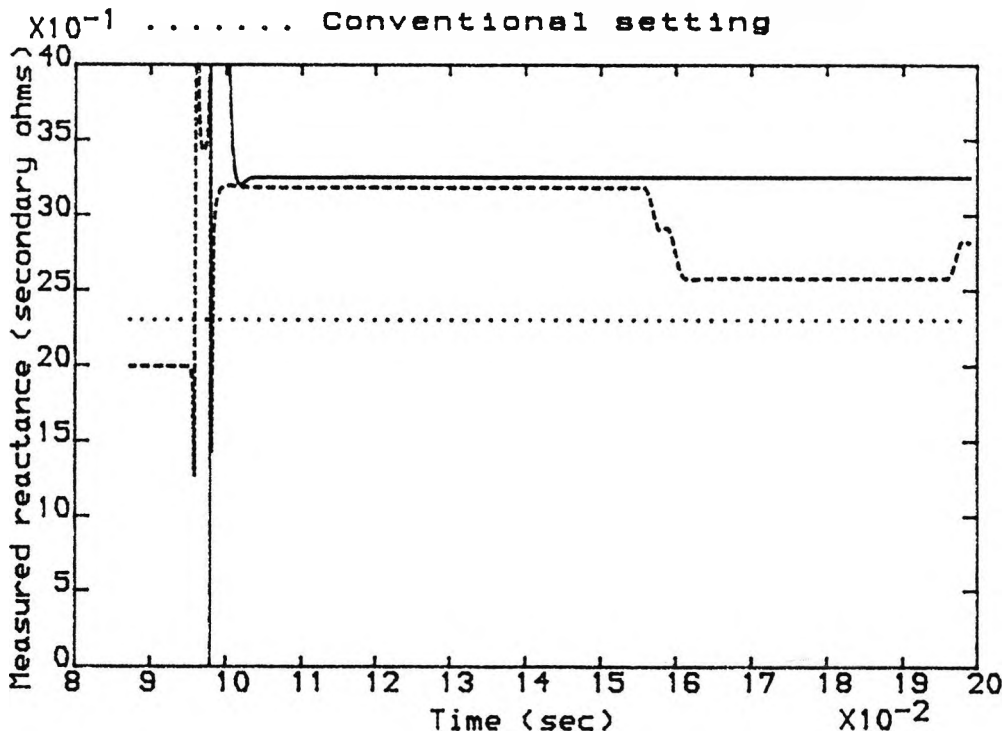
Fig.7.7 Relay behaviour showing the measured
reactance and the reactive setting during
different periods for an external fault
────────── Measured reactance
────── Adaptive reactive setting
.... Conventional setting
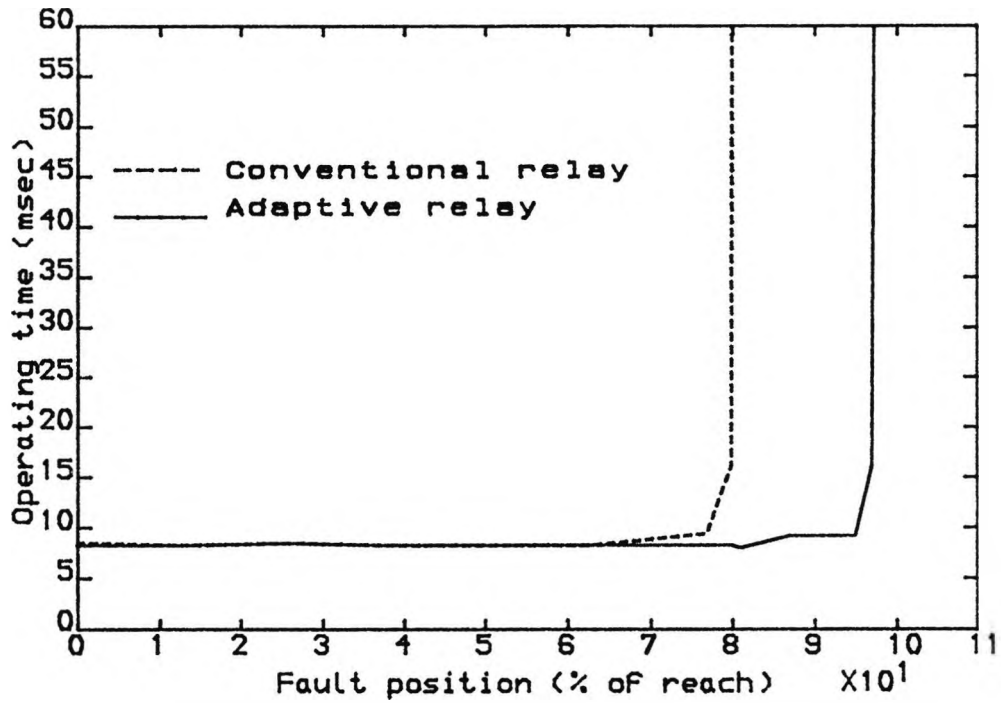
Fig.7.8 Relay operating time vs fault position
for the a-e faults along line P-T-R
Fault inception angle =0 degs.
No-load condition
SCL (GVA)   P=3.5   Q=35   R=35
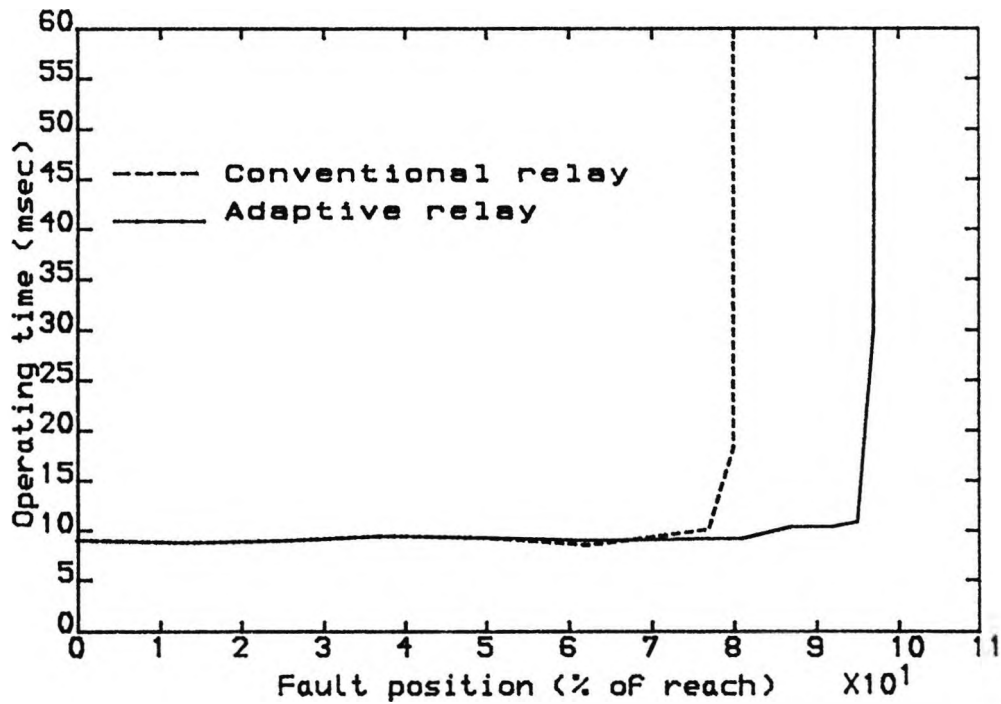
Fig.7.9 Relay operating time vs fault position
for the a-e faults along line P-T-R
Fault inception angle =90 degs.
No-load condition
SCL (GVA)   P=3.5   Q=35   R=35
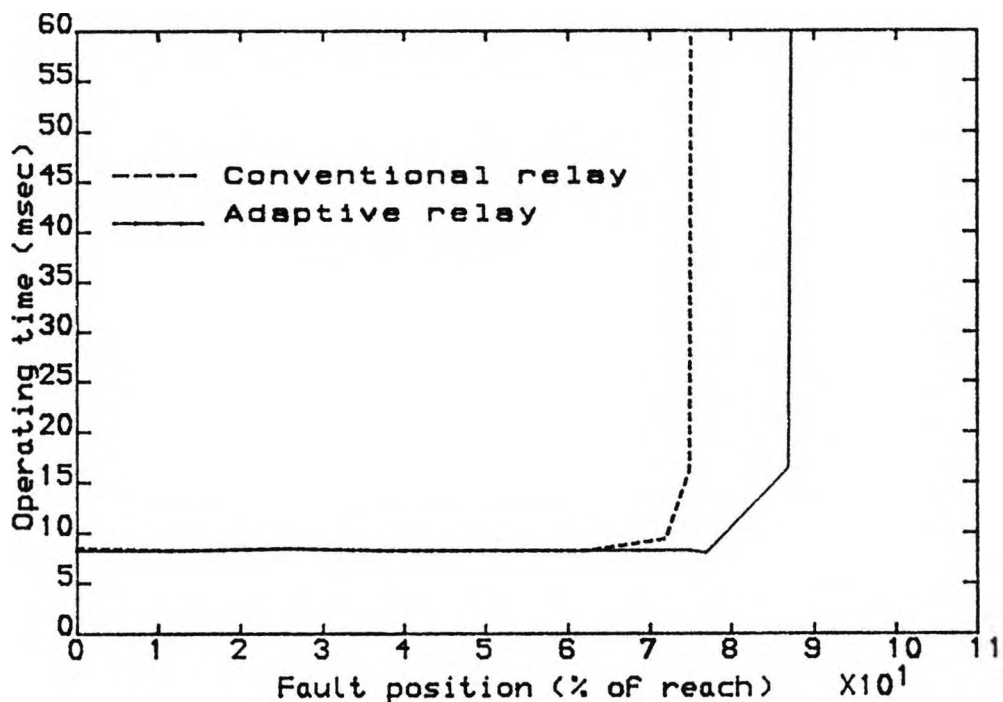
Fig.7.10 Relay operating time vs fault position
for the a-e faults along line P-T-Q
Fault inception angle =0 degs.
No-load condition
SCL (GVA)   P=3.5   Q=35   R=35
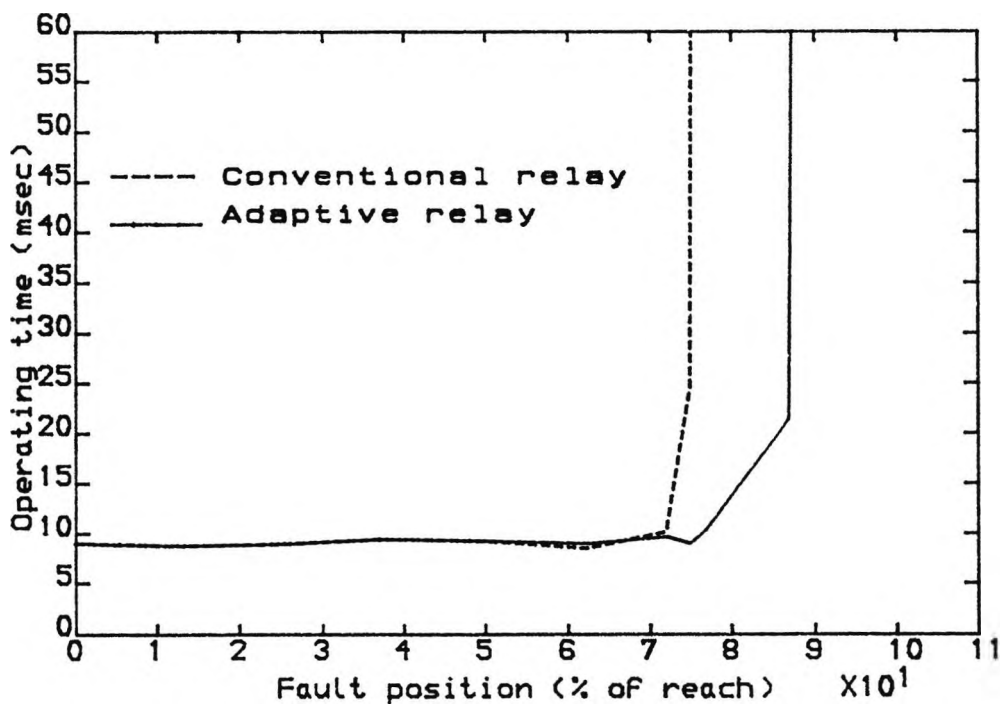
Fig.7.11 Relay operating time vs fault position
for the a-e faults along line P-T-Q
Fault inception angle =90 degs.
No-load condition
SCL (GVA)   P=3.5   Q=35   R=35
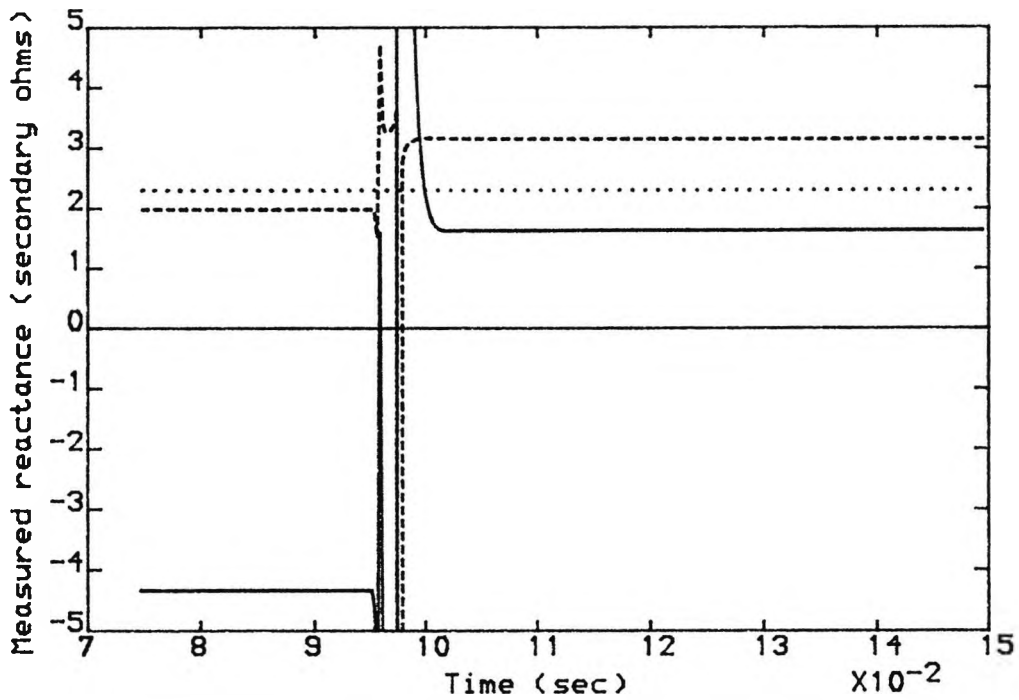
Fig.7.12 Measured reactance vs Time showing
the directional reactance and the reactive
setting for a fault in front of the relay
_____ Directional reactance
------ Adaptive reactive setting
..... Conventional setting
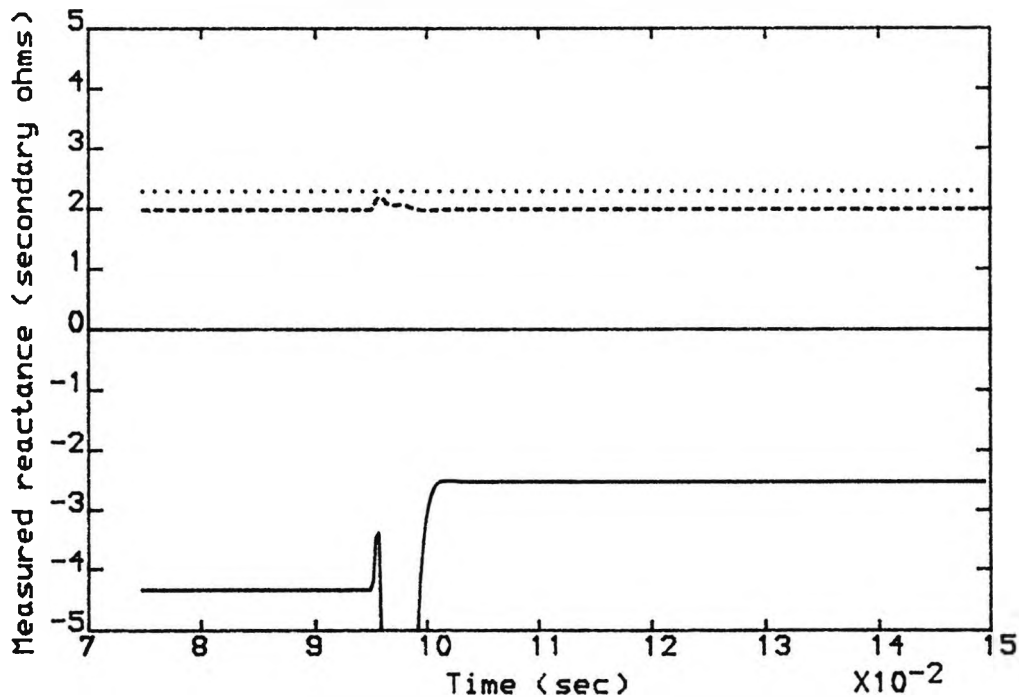
Fig.7.13 Measured reactance vs Time showing
the directional reactance and the reactive
setting for a fault behind of the relay
_____ Directional reactance
------ Adaptive reactive setting
..... Conventional setting

CHAPTER 8

CONCLUSIONS AND SUGGESTIONS FOR FUTURE WORK

8.1 General Conclusions

The work presented in this thesis has introduced and described the requirements, design and performance of a new adaptive digital scheme suitable for Teed feeder applications. Based on an impedance measuring technique, it has been shown that the scheme restores the desired reach on one of the remote sections of the line. A better coverage, compared with conventional relays, on the other remote section has been achieved.

The infeed/outfeed current from the remote terminal has been related to the source and line impedances and also to the steady-state values of the current and voltage. The advantage of this approach is that real time signalling from the remote ends is not required. The most important parameter required from the remote ends is an approximate value for the sequence source impedance in order to account for phase and ground faults. It has been suggested that these impedances can be determined at the control centre and transmitted as update values to the relays at each end. Prefault currents at each end of the line should be available as measured. The amount of data need not be transmitted in real-time since it only needs to be made available at the relay in time for the next disturbance. Thus, the speed and accuracy of the distance relay functions during a fault are not affected.

118

Since, for a Teed system, there are two line sections beyond the Tee junction seen from any terminal, two different relays have been used. Each relay measures correctly on its allocated path. However, it has been found difficult to identify locally the remote faulted leg and, because no real-time signalling has been considered from the remote terminals to assist in identifying the faulted leg, therefore, the relay which is allocated for the remote short leg will in general determine the reach on either leg.

The method used to compensate for the fault current from the remote end assumes that the fault is always at the relay zone-1 forward reach; hence it implies that the measurement is accurate only if the fault occurs at that point. For faults at other locations, the relay indication does not correspond to the actual line value; it is immaterial whether the indication is proportional to the distance from the relay to the fault point, provided the indication given does not exceed the limits provided by faults at the reach point. Due to the non-linear relation between the fault position and the measured reactance, it has been shown that the relay measures a reactance which is smaller than the actual line reactance for internal faults and larger than the actual line value for external faults. The resistive component is accurate at the reach point only; for faults at other locations, it can be smaller or larger than the actual line values. This depends on the direction of the load current prior to

the fault. These resistances are small and can easily be contained within the relay characteristics as these are extended to contain a finite fault resistance.

The relay utilises the remote source impedance and is prone to errors if the set value is different from the actual one. The new relay has been proved to be highly insensitive to large variations in this source of error. The tests showed that for a ± 100% change in the values of this impedance, the effect on the relay accuracy is about ± 3% of the reach value.

Distance protection based on impedance measurement uses information contained in the power frequency components of the voltage and current signals. In the relay simulation, the instantaneous values of the voltage and current signals were stepped down to levels compatible with the digital processing (±10 V). The signals were filtered by analogue filter with a cut-off frequency of 800 Hz to prevent aliasing error in the sampling process. The filtered signals were then converted to digital values using a 14 bit A/D converter. In order to account for phase to ground and phase to phase faults, the voltage and current signals required by the scheme were formed digitally. A sampling rate of 80 per power system cycle was considered. A digital band-pass filter with 14 points in its impulse response was employed to attenuate the dc exponentials and the frequencies above 500 Hz. In order to convert the voltage and current samples into measured resistance and reactance values, the time spaced solution

technique has been used to solve a first order differential line equation. The simulation of the relay has closely emulated the operation of a 16 bit microprocessor and particular attention has been paid to the fact that digital division in such a device is a time consuming process and has therefore been minimised.

According to the shape of the fault areas and in common with some commercially available equipment, the relay has a quadrilateral characteristic. The occurrence of a single impedance value falling within the characteristic was shown not to be a reliable situation to initiate a tripping signal and a counting strategy was therefore employed[35] and implemented which had the effect of giving the relay more time for faults in the vicinity of the reach point. In order to prevent the relay operating during the transition period from the prefault to postfault condition and to overcome any overreach that can result from the variation of fault inception angle, a technique of adapting the counter increment to reflect the certainty of the impedance measurement was implemented. Also, to smooth any high frequency on the measured resistance and reactance which cannot be reduced to the desired level, due to restriction on the group delay of the prefilter, an adaptive filtering arrangement was employed. This filter, which is a low-pass filter, attenuates any frequency component but the dc, is applied shortly after the fault has been detected. The adaptive filter has been carefully designed so that its use does

not incur any operating time penalty.

A directional element was incorporated in the relay in order to ensure that it maintains correct discrimination for forward and reverse faults. The directional element utilises the postfault current and prefault voltage. Examples were shown of the relay operation for closeup faults and it was seen that the relay behaved correctly.

Results for a 400 kV line application showed that the adaptive relay, in line with the conventional digital distance relay, maintains a fast operating time (less than 1/2 power frequency cycle) for the majority of the faults that fall within its characteristics; independent of fault inception angle. However, for faults near the boundary, the operating time tends to be higher and appears to be dependent upon the fault inception angle.

The relay restrained for all fault tests behind the measuring point. This is important because the adaptive relay sees a positive impedance and hence falls inside the relay characteristic. It has also been shown that when the relay runs out of the steady-state prefault values no adverse relay behaviour occurs.

An alternative method for implementing the scheme has been introduced in Chapter 7. The signals and parameters involved has been arranged to adjust the relay setting such that it can correspond to the apparent impedance at the reach point and gives the proper discrimination. This approach has the advantage that the reactive reach need

not be extended into the negative region as required by the previous scheme but on the other hand it requires two algorithms to convert the voltage and current signals into measured resistance and reactance. An application study for a 400kV system showed, again, that the relay has a fast operating time and maintains the correct directionality.

8.2 Suggestions for Future Work

Based on the work presented, further work can usefully be carried out in the following areas.

1- The simulation tests were carried out for different operating conditions on a transposed line. Further tests can be performed on an untransposed line to evaluate the magnitude of errors that will be involved.

2- The scheme was tested for a 400 kV line. It is known that high voltage systems are characterised by high X/R ratios and for this reason the fault area presents no problem with respect to resistive setting. However, on lower voltage systems, where the X/R ratio is relatively small, the fault area can cover a large region and this could affect the loadabilty of the line. Investigation of the scheme performance on low voltage systems, at typically 132 kV, is therefore recommended.

3- The optimum performance of the scheme can be achieved if the remote faulted leg is identified locally. Finding a method to do this is required. Also,

evaluation of the scheme behaviour as part of a composite relaying system using the direct intertripping or blocking schemes could be undertaken.

4- Investigation of the adaptive scheme behaviour when used in a double circuit applications. Since the relay requires the effective source impedance for the critical fault position, the mutual coupling between the two circuits will be included in the source impedance value. It will be instructive to investigate the relay behaviour with or without the residual current from the other circuit.

APPENDIX 2A

Identification of signals and parameters involved in determining the apparent impedance.

For the single phase Teed system of Fig. 2.1, the measured impedance for a fault on leg Q, using the local voltage and current signals, at the relaying point, P, is given by:

$$Z_{mP} = \frac{V_P}{I_P} = \frac{I_P Z_P + \alpha_Q Z_Q (I_P + I_R)}{I_P} \qquad 2A.1$$

$$Z_{mP} = Z_P + \alpha_Q Z_Q + \alpha_Q Z_Q \left(\frac{I_R}{I_P} \right) \qquad 2A.2$$

where I_R can be written

$$I_R = I_{RS} + I_{RT} \qquad 2A.3$$

I_{RS} is the pre-fault current and voltage at R.

I_{RT} is the superimposed current and voltage at R.

$$Z_{mP} = Z_P + \alpha_Q Z_Q + \alpha_Q Z_Q \left(\frac{I_{RS}}{I_P} + \frac{I_{RT}}{I_P} \right) \qquad 2A.4$$

The superimposed current at end R can be related to that at end P as:

$$V_{TT} = V_{RT} - Z_R I_{RT} \qquad 2A.5$$

$$V_{TT} = V_{PT} - Z_P I_{PT} \qquad 2A.6$$

where

V_{TT} =superimposed voltage at the tee point.

From 2A.5 and 2A.6

$$I_{RT} = \frac{V_{RT} - V_{PT} + Z_P I_{PT}}{Z_R} \qquad 2A.7$$

V_{RT} can be expressed as

$$V_{RT} = -I_{RT} Z_{R\bullet} \qquad 2A.8$$

125

$$I_{RT} = \frac{Z_P I_{PT} - V_{PT} - I_{RT} Z_{RS}}{Z_R} \qquad 2A.9$$

$$I_{RT} = \frac{Z_P I_{PT} - V_{PT}}{Z_R + Z_{RS}} \qquad 2A.10$$

From 2A.4 and 2A.10

$$Z_{mP} = Z_P + \alpha_Q Z_Q + \alpha_Q Z_Q \left[\frac{I_{RS}}{I_P} + \frac{Z_P I_{PT} - V_{PT}}{(Z_R + Z_{RS}) I_P} \right] \qquad 2A.11$$

Some idea of the behaviour of Eqn. 2A.11 can be gained from making the assumption of zero prefault load in which case

$$I_P = I_{PT}$$

$$I_{RS} = 0$$

then

$$Z_{mP} = Z_P + \alpha_Q Z_Q + \alpha_Q Z_Q \left(\frac{Z_P + Z_{PS}}{Z_R + Z_{RS}} \right) \qquad 2A.12$$

Similarly the measured impedance at end P for a fault on leg R is given generally by Eqn. 2A.13, and for the special case of zero prefault load in Eqn. 2A.14

$$Z_{mP} = Z_P + \alpha_R Z_R + \alpha_R Z_R \left[\frac{I_{QS}}{I_P} + \frac{Z_P I_{PT} - V_{PT}}{(Z_Q + Z_{QS}) I_P} \right] \qquad 2A.13$$

$$Z_{mP} = Z_P + \alpha_R Z_R + \alpha_R Z_R \left(\frac{Z_P + Z_{PS}}{Z_Q + Z_{QS}} \right) \qquad 2A.14$$

Eqn. 2A.11 can be written in the form of Eqn. 2A.15

$$Z_{mP} = \frac{V_P}{I_P} = Z_P + \alpha_Q Z_Q + \alpha_Q Z_Q K_Q \qquad 2A.15$$

where

$$K_Q = \frac{I_{RS}}{I_P} + \frac{Z_P I_{PT} - V_{PT}}{(Z_R + Z_{RS}) I_P} \qquad 2A.16$$

$$K_Q = \frac{Z_P + Z_{PS}}{Z_R + Z_{RS}} \qquad \text{for zero prefault load}$$

Eqn. 2A.13 can be written in the form of Eqn. 2A.17

$$Z_{mP} = \frac{V_P}{I_P} = Z_P + \alpha_R Z_R + \alpha_R Z_R K_R \qquad \qquad 2A.17$$

$$K_R = \frac{I_{QS}}{I_P} + \frac{Z_P I_{PT} - V_{PT}}{(Z_Q + Z_{QS}) I_P} \qquad \qquad 2A.18$$

$$K_R = \frac{Z_P + Z_{PS}}{Z_Q + Z_{QS}} \qquad \text{for zero prefault load}$$

APPENDIX 2B

Arrangement of the performance equation for practical implementation for faults along line P-T-R.

Considering Eqn. 2.12, where the measurand is of the form:

$$Z_{mPR} = Z_{mP} - \alpha_{RS}Z_R K_R \qquad \text{2B.1}$$

$$Z_{mPR} = \frac{V_P}{I_P} - \alpha_{RS}Z_R K_R \qquad \text{2B.2}$$

where

$$K_R = \frac{I_{QS}}{I_P} + \frac{Z_P I_{PT} - V_{PT}}{(Z_Q + Z_{QS})I_P} \qquad \text{2B.3}$$

we can write

$$V_{PT} = V_P - V_{PS} \qquad \text{2B.4}$$

$$I_{PT} = I_P - I_{PS} \qquad \text{2B.5}$$

I_{PS}, V_{PS} are the pre-fault current and voltage at P

I_{PT}, V_{PT} are the superimposed current and voltage at P

substituting for I_{PT}, V_{PT} in Eqn. 2B.2 gives:

$$Z_{mPR} = \frac{V_P - \alpha_{RS}Z_R I_{RS} - \alpha_{RS}Z_R\{[Z_P(I_P - I_{PS}) - (V_P - V_{PS})]/(Z_Q + Z_{QS})\}}{I_P}$$

$$\text{2B.6}$$

$$Z_{mPR} = \left\{ \frac{V_P\left(1 + \dfrac{\alpha_{RS}Z_R}{Z_Q + Z_{QS}}\right) - \alpha_{RS}Z_R\left[I_{RS} - \dfrac{I_{PS}\,Z_P}{Z_Q + Z_{QS}} + \dfrac{V_{PS}}{Z_Q + Z_{QS}}\right]}{I_P} \right.$$

$$\left. - \frac{\alpha_{RS}\,Z_R\,Z_P}{Z_Q + Z_{QS}} \right\} \qquad \text{2B.7}$$

$$Z_{mPR} = \frac{V_P + k'_1 V_P - k'_1 V_{PS} + k'_2 I_{PS} - k'_3 I_{RS}}{I_P} - \frac{\alpha_{RS}\,Z_R\,Z_P}{Z_Q + Z_{QS}} \qquad \text{2B.8}$$

where

$$|k'_1| = \left| \frac{\alpha_{RS} \; Z_R}{Z_Q + Z_{QS}} \right|$$

$$\underline{/k'}_1 = \underline{/\frac{Z_R}{Z_Q + Z_{QS}}}$$

$$|k'_2| = \left| \frac{\alpha_{RS} \; Z_R \; Z_P}{Z_Q + Z_{QS}} \right|$$

$$\underline{/k'}_2 = \underline{/\frac{Z_R \; Z_P}{Z_Q + Z_{QS}}}$$

$$|k'_3| = \left| \alpha_{RS} \; Z_R \right|$$

$$\underline{/k'}_3 = \underline{/Z_R}$$

APPENDIX 2C

Derivation   of   modified   measured   impedances   for
single-phase earth faults

The impedance measured at the relaying point P, using
the normal residually compensating signals, for the a-
earth fault element on leg Q in Fig. 2.1 would be given by

$$Z_{mPa} = \frac{V_{Pa}}{I_{Pa} + KI_{resP}} \qquad \text{2C.1}$$

where

K is the residual compensation factor

I_{resP} is the residual current at end P

$$K = \frac{1}{3} \left(\frac{Z_{L0}}{Z_{L1}} - 1 \right) \qquad \text{2C.2}$$

but for this fault

$$V_{Pa} = (I_{Pa} + KI_{resP}) Z_{P1} +$$
$$\alpha_Q Z_{Q1} (I_{Pa} + I_{Ra} + KI_{resP} + KI_{resR}) \qquad \text{2C.3}$$

the impedance presented to the relay is

$$Z_{mPa} = Z_{P1} + \alpha_Q Z_{Q1} + \alpha_Q Z_{Q1} \left(\frac{I_{Ra} + KI_{resR}}{I_{Pa} + KI_{resP}} \right) \qquad \text{2C.4}$$

where the suffix 1 devotes positive-phase-sequence value,
I_{resR} is the residual current fed from end R.

The modified measurands that correspond to Eqns. 2.11
and 2.12 are thus

$$Z_{mPQa} = Z_{mPa} - \alpha_{QS} Z_{Q1} K_{Qa} = Z_{P1} + \alpha_{QS} Z_{Q1} \qquad \text{2C.5}$$

$$Z_{mPRa} = Z_{mPa} - \alpha_{RS} Z_{R1} K_{Ra} = Z_{P1} + \alpha_{RS} Z_{R1} \qquad \text{2C.6}$$

where

$$K_{Qa} = \frac{I_{Ra} + KI_{resR}}{I_{Pa} + KI_{resP}} \qquad \text{2C.7}$$

130

in the above equation the currents can be expressed in terms of prefault and superimposed values i.e.

$$I_{Ra} = I_{RSa} + I_{RTa} \qquad \text{2C.8}$$

$$I_{resR} = I_{resRS} + I_{resRT} \qquad \text{2C.9}$$

therefore

$$K_{Qa} = \frac{I_{RSa} + KI_{resRS}}{I_{Pa} + KI_{resP}} + \frac{I_{RTa} + KI_{resRT}}{I_{Pa} + KI_{resP}} \qquad \text{2C.10}$$

for the faults on leg R

$$K_{Ra} = \frac{I_{Qa} + KI_{resQ}}{I_{Pa} + KI_{resP}} \qquad \text{2C.11}$$

$$K_{Ra} = \frac{I_{QSa} + KI_{resQS}}{I_{Pa} + KI_{resP}} + \frac{I_{QTa} + KI_{resQT}}{I_{Pa} + KI_{resP}} \qquad \text{2C.12}$$

We will recall the modified measurand Z_{mPQa} given in Eqn. 2C.5. Now with reference to Eqn. 2C.10, the superimposed currents I_{RTa} and I_{resRT} could be related to those at end P. This is done using the following analysis

$$V_{TTa} = V_{RTa} - Z_{R1} (I_{RTa} + KI_{resRT}) \qquad \text{2C.13}$$

$$V_{TTa} = V_{PTa} - Z_{P1} (I_{PTa} + KI_{resPT}) \qquad \text{2C.14}$$

where V_{TTa}, V_{RTa}, V_{PTa} are the superimposed voltage on a-phase at the Tee, R, P points respectively.

By equating Eqns. 2C.13 and 2C.14 then

$$I_{RTa} + KI_{resRT} = \frac{V_{RTa} - V_{PTa} + (I_{PTa} + KI_{resPT})Z_{P1}}{Z_{R1}} \qquad \text{2C.15}$$

but

$$V_{RTa} = - Z_{RS1} (I_{RTa} + K_{RS}I_{resRT}) \qquad \text{2C.16}$$

where

K_{RS} is the source residual compensation factor at end R

$$K_{RS} = \frac{1}{3} (\frac{Z_{RS0}}{Z_{RS1}} - 1) \qquad \text{2C.17}$$

131

Z_{RS1}= positive-sequence source impedance at end R

Z_{RSO}= zero-sequence source impedance at end R

by substituting 2C.16 into 2C.15 then

$$I_{RTa} + KI_{resRT} =$$
$$- \frac{Z_{RS1}(I_{RTa}+K_{RS}I_{resRT})-V_{PTa}+(I_{PTa}+KI_{resPT})Z_{P1}}{Z_{R1}} \qquad 2C.18$$

Similarly Eqns. 2C.19 and 2C.20 are the currents for the b and c phases

$$I_{RTb} + KI_{resRT}=$$
$$- \frac{Z_{RS1}(I_{RTb}+K_{RS}I_{resRT})-V_{PTb}+(I_{PTb}+KI_{resPT})Z_{P1}}{Z_{R1}} \qquad 2C.19$$

$$I_{RTc} + KI_{resRT}=$$
$$- \frac{Z_{RS1}(I_{RTc}+K_{RS}I_{resRT})-V_{PTc}+(I_{PTc}+KI_{resPT})Z_{P1}}{Z_{R1}} \qquad 2C.20$$

by adding 2C.18, 2C.19, 2C.20 and putting $I_{RTa} + I_{RTb} + I_{RTc} = I_{resRT}$ then

$$(1+3K) Z_{R1}I_{resRT} = - (1+3K_{RS}) Z_{RS1}I_{resRT} -$$
$$V_{resPT} + (1 + 3K) Z_{P1}I_{resPT} \qquad 2C.21$$

from which

$$I_{resRT} = - \frac{V_{resPT} - (1 + 3K) Z_{P1}I_{resPT}}{(1 + 3K)Z_{R1} + (1 + 3K_{RS}) Z_{RS1}} \qquad 2C.22$$

from Eqn. 2C.18

$$I_{RTa} = - \frac{Z_{RS1}(I_{RTa}+K_{RS}I_{resRT})-V_{PTa}+(I_{PTa}+KI_{resPT})Z_{P1}}{Z_{R1}} - KI_{resRT}$$
$$2C.23$$

rearranging

$$(Z_{R1}+Z_{RS1})I_{RTa}=$$
$$-(K_{RS}Z_{RS1}+KZ_{R1})I_{resRT}-V_{PTa}+(I_{PTa}+KI_{resPT})Z_{P1} \qquad 2C.24$$

solving for I_{RTa} gives

$$I_{RTa} = - \frac{1}{Z_{R1}+Z_{RS1}} *$$

$$[(K_{RS}Z_{RS1}+KZ_{R1})I_{resRT}+V_{PTa}-(I_{PTa}+KI_{resPT})Z_{P1}] \qquad 2C.25$$

Eqns. 2C.22 and 2C.25 may be arranged to give

$$I_{RTa}+KI_{resRT} = - \frac{1}{Z_{R1}+ Z_{RS1}} *$$

$$[(K_{RS}Z_{RS1}+KZ_{R1}-KZ_{R1}-KZ_{RS1})I_{resRT} +$$

$$V_{PTa}-(I_{PTa}+KI_{resPT})Z_{P1}] \qquad 2C.26$$

$$I_{RTa}+KI_{resRT}= - \frac{1}{Z_{R1}+ Z_{RS1}} *$$

$$[(K_{RS}-K)Z_{RS1}I_{resRT}+V_{PTa}-(I_{PTa}+KI_{resPT})Z_{P1}] \qquad 2C.27$$

$$I_{RTa}+KI_{resRT}= - \frac{1}{Z_{R1}+ Z_{RS1}} *$$

$$[\frac{(K-K_{RS})Z_{RS1}((1+3K)Z_{P1}I_{resPT}- V_{resPT})}{((1+3K)Z_{R1}+(1+3K_{RS})Z_{RS1})} -$$

$$V_{PTa}+(I_{PTa}+KI_{resPT})Z_{P1}] \qquad 2C.28$$

From Eqns. 2C.10 and 2C.28

$$K_{Qa}= \frac{I_{RSa}+KI_{resRS}}{I_{Pa}+KI_{resP}} + \frac{1}{(Z_{R1}+Z_{RS1})(I_{Pa}+KI_{resP})} *$$

$$[\frac{(K-K_{RS})Z_{RS1} ((1+3K)Z_{P1}I_{resPT}- V_{resPT})}{((1+3K)Z_{R1}+(1+3K_{RS})Z_{RS1})} -$$

$$V_{PTa}+(I_{PTa}+KI_{resPT})Z_{P1}] \qquad 2C.29$$

In Eqn. 2C.29 if a 3-phase fault were involved, then this should reduce to the form of Eqn. 2.10. Where in this case

$$I_{resPT} , V_{resPT}=0$$

$$V_{PTa} = V_{PT} \text{ and } I_{PTa} = I_{PT}$$

$$I_{RSa} = I_{RS}$$

$$I_{Pa} + KI_{resP} = I_{Pa} = I_P$$

133

Similarly, for faults on leg R we can have

$$K_{Ra} = \frac{I_{QSa} + KI_{resQS}}{I_{Pa} + KI_{resP}} + \frac{1}{(Z_{Q1} + Z_{QS1})(I_{Pa} + KI_{resP})} *$$

$$[\frac{(K-K_{QS})Z_{QS1} ((1+3K)Z_{P1}I_{resPT} - V_{resPT})}{((1+3K)Z_{R1} + (1+3K_{QS})Z_{QS1})} -$$

$$V_{PTa} + (I_{PTa} + KI_{resPT})Z_{P1}] \quad 2C.30$$

Similar measurands for b and c phases could be formed

$$Z_{mPQb} = Z_{mPb} - K_{Qb}\alpha_{QS}Z_{Q1} \quad\quad\quad 2C.31$$

this should be compared with $Z_{P1} + \alpha_{QS}Z_{Q1}$

where

$$Z_{mPb} = \frac{V_{Pb}}{(I_{Pb} + KI_{resP})} \quad\quad\quad 2C.32$$

and K_{Qb} is obtained by replacing the a-phase quantities in Eqn. 2C.29 by those for the b-phase

$$K_{Qb} = \frac{I_{RSb} + KI_{resRS}}{I_{Pb} + KI_{resP}} + \frac{1}{(Z_{R1} + Z_{RS1})(I_{Pb} + KI_{resP})} *$$

$$[\frac{(K-K_{RS})Z_{RS1}((1+3K)Z_{P1}I_{resPT} - V_{resPT})}{((1+3K)Z_{R1} + (1+3K_{RS})Z_{RS1})} -$$

$$V_{PTb} + (I_{PTb} + KI_{resPT})Z_{P1}] \quad 2C.33$$

Similarly

$$K_{Rb} = \frac{I_{QSb} + KI_{resQS}}{I_{Pb} + KI_{resP}} + \frac{1}{(Z_{Q1} + Z_{QS1})(I_{Pa} + KI_{resP})} *$$

$$[\frac{(K-K_{QS})Z_{QS1} ((1+3K)Z_{P1}I_{resPT} - V_{resPT})}{((1+3K)Z_{R1} + (1+3K_{QS})Z_{QS1})} -$$

$$V_{PTb} + (I_{PTb} + KI_{resPT})Z_{P1}] \quad 2C.34$$

And for phase c

$$Z_{mPQc} = Z_{mPc} - K_{Qc}\alpha_{QS}Z_{Q1} \quad\quad\quad 2C.35$$

is compared with $Z_{P1} + \alpha_{QS}Z_{Q1}$

where

$$Z_{mPc} = \frac{V_{Pc}}{(\ I_{Pc} + KI_{resP}\ )} \qquad\qquad 2C.36$$

and K_{Qc} is obtained by replacing a-phase quantities in Eqn. 2C.28 by those for the c-phase.

Similar procedure could be adopted for faults along leg R.

APPENDIX 2D

Derivation of modified measured impedance for Phase-phase faults

This case is relatively simple in that the basic Eqns. 2.4, 2.7, 2.11, 2.12 apply with the relative difference voltage and current measurands

Thus for the b-c element we employ the modified measurands.

$$Z_{mPQbc} = Z_{mPbc} - \alpha_{QS} Z_{Q1} K_{Qbc} \qquad \text{2D.1}$$

this should be compared with $Z_{P1} + \alpha_{QS} Z_{Q1}$

and

$$Z_{mPRbc} = Z_{mPbc} - \alpha_{RS} Z_{R1} K_{Rbc} \qquad \text{2D.2}$$

is compared with $Z_{P1} + \alpha_{RS} Z_{R1}$

Where

$$Z_{mPbc} = \frac{V_{bc}}{I_{Pb} - I_{Pc}} \qquad \text{2D.3}$$

$$= \frac{V_{bc}}{I_{Pbc}} \qquad \text{2D.4}$$

$$K_{Qbc} = \frac{I_{RSbc}}{I_{Pbc}} + \frac{Z_{P1} I_{PTbc} - V_{PTbc}}{(Z_{R1} + Z_{RS1}) I_{Pbc}} \qquad \text{2D.5}$$

$$K_{Rbc} = \frac{I_{QSbc}}{I_{Pbc}} + \frac{Z_{P1} I_{PTbc} - V_{PTbc}}{(Z_{Q1} + Z_{QS1}) I_{Pbc}} \qquad \text{2D.6}$$

Where
$I_{RSbc} = I_{RSb} - I_{RSc}$ the difference of b and c phase steady state current at end R.

Similarly, differencing is applied when other phases are employed

$$Z_{mPQab} = Z_{mPab} - \alpha_{QS} Z_{Q1} K_{Qab} \qquad \text{2D.7}$$

is compared with $Z_{P1} + \alpha_{QS} Z_{Q1}$

and

$$Z_{mPRab} = Z_{mPab} - \alpha_{RS} Z_{R1} K_{Rab} \qquad\qquad 2D.8$$

is compared with $Z_{P1} + \alpha_{RS} Z_{R1}$

For the c-a phases

$$Z_{mPQca} = Z_{mPca} - \alpha_{QS} Z_{Q1} K_{Qca} \qquad\qquad 2D.9$$

is compared with $Z_{P1} + \alpha_{QS} Z_{Q1}$

and

$$Z_{mPRca} = Z_{mPca} - \alpha_{RS} Z_{R1} K_{Rca} \qquad\qquad 2D.10$$

is compared with $Z_{P1} + \alpha_{RS} Z_{R1}$

APPENDIX 3A:Line data

The line configuration used in the simulation is shown in Figure 1. The following power frequency (50 Hz) parameters are then applicable:

Self impedance $\quad Z_{LS}$= 0.0742 + j0.730 $\quad \Omega$/mile

Mutual impedance $\quad Z_{LM}$= 0.0454 + j0.259 $\quad \Omega$/mile

Self admittance $\quad Y_{LS}$= j5.232$\cdot$10^{-6} $\qquad \Omega^{-1}$/mile

Mutual admittance Y_{LM}= j2.568$\cdot$10^{-7} $\qquad \Omega^{-1}$/mile

The positive and zero phase sequence impedances and admittances of the line are:

Z_{L1}= 0.0288 + j0.4708 $\qquad \Omega$/mile

Z_{L0}= 0.165 + j1.25 $\qquad \Omega$/mile

Y_{L1}= j0.5488$\cdot$10^{-5} $\qquad \Omega^{-1}$/mile

Y_{L0}= j0.471$\cdot$10^{-5} $\qquad \Omega^{-1}$/mile
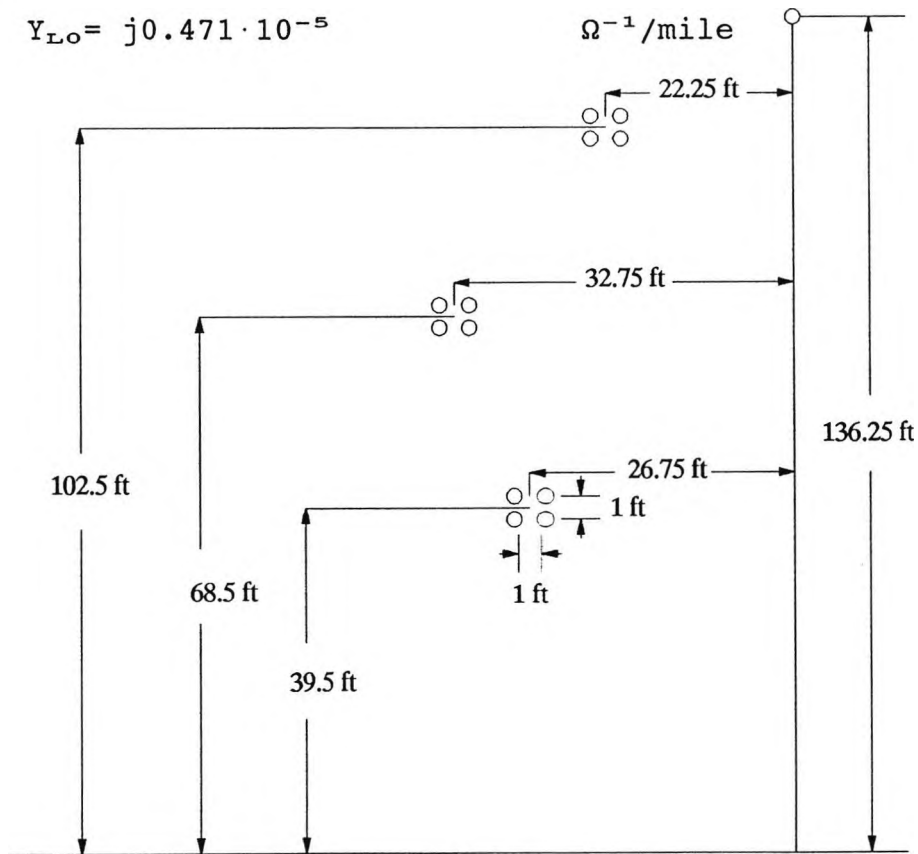
Fig. 1 Configuration for 400 kV line used

APPENDIX 4A

Derivation of the recursive equation of the analogue filter

The transfer function of the second order butterworth filter is given by:

$$G(s) = \frac{w^2_n}{s^2 + 2.d.w_n \ s + w^2_n} \qquad\qquad 4A.1$$

d is the damping factor

$$d = 1/\sqrt{2}$$

Assuming the time domain function

$$u(t) = \frac{di(t)}{dt} \qquad\qquad 4A.2$$

The s domain function of Eqn. 4A.2 is

$$u(s) = s \ i(s) \qquad\qquad 4A.3$$

This can be expressed in discrete form as

$$u(n) = \frac{i(n) - i(n-1)}{T} \qquad\qquad 4A.4$$

where T is the time between two samples

The transformation of Eqn. 4A.4 into z domain is

$$u(z) = \frac{1 - z^{-1}}{T} \ i(z) \qquad\qquad 4A.5$$

Comparing Eqns. 4A.3 and 4A.5, we have

$$s = \frac{1 - z^{-1}}{T} \qquad\qquad 4A.6$$

substituting for s in 4A.1 gives

$$G(z) = \frac{w^2_n}{\dfrac{(1 - z^{-2})^2}{T^2} + 2.d.w_n \dfrac{1 - z^{-1}}{T} + w^2_n} \qquad\qquad 4A.7$$

139

$$\frac{X_o(z)}{X_{in}(z)} = \frac{A_o}{B_o - B_1 z^{-1} + z^{-2}} \qquad \text{4A.8}$$

where

$$A_o = T^{-2} w_n^{-2}$$

$$B_o = 1 + 2.d.T.w^{-2} + T^{-2} w_n^{-2}$$

$$B_1 = 2 + 2.d.T.w_n$$

in discrete time domain, Eqn. 4A.8, after taking the inverse z transform, can be written as

$$X_o(z) = \frac{A_o X_{in}(n) - B_1 X_o(n-1) - X_o(n-2)}{B_o} \qquad \text{4A.9}$$

APPENDIX 4B

Derivation of the recursive equation of the filtering function K_1.

$$K_1 = \frac{\alpha_{Qs} \ Z_{Q1}}{Z_{R1} + Z_{RS1}} \qquad 4B.1$$

in s domain

$$K_1(s) = \frac{\alpha_{Qs} \ (\ R_{Q1} + s \ L_{Q1} \ )}{(\ R_{R1} + s \ L_{R1} \ ) + (\ R_{RS1} + s \ L_{RS1} \ )}$$

$$K_1(s) = \frac{\alpha_{Qs} \ (\ R_{Q1} + s \ L_{Q1} \ )}{(\ R_{R1} + R_{RS1} \ ) + s \ (\ L_{R1} + L_{RS1} \ )}$$

$$K_1(s) = \frac{\alpha_{Qs} \ (\ A_0 + A_1 \ s \ )}{(\ B_0 + B_1 \ s \ )} \qquad 4B.2$$

where

$$A_0 = R_{Q1}$$
$$A_1 = L_{Q1}$$
$$B_0 = R_{R1} + R_{RS1}$$
$$B_1 = L_{R1} + L_{RS1}$$

in z domain

$$\text{Let } s = \frac{1 - z^{-1}}{T} \qquad 4B.3$$

where T is the time between two samples

$$\frac{X_o(z)}{X_{in}(z)} = \frac{\alpha_{Qs} \ [\ A_0 + A_1 \ (1-z^{-1}/T \ )]}{B_0 + B_1 \ (1-z^{-1}/T \ )}$$

$$\frac{X_o(z)}{X_{in}(z)} = \frac{\alpha_{Qs} \ (\ T \ A_0 + A_1 - A_1 \ z^{-1} \ )}{T \ B_0 + B_1 - B_1 \ z^{-1}}$$

$$\frac{X_o(z)}{X_{in}(z)} = \frac{\alpha_{Qs} \ (\ C_0 - C_1 \ z^{-1} \ )}{D_0 - D_1 \ z^{-1}} \qquad 4B.4$$

where

$$C_0 = T \ A_0 + A_1$$

$$C_1 = A_1$$

$$D_o = T \, B_o + B_1$$

$$D_1 = B_1$$

in discrete time domain, Eqn. 4B.4, after taking the inverse z transform, can be written as

$$X_o(n) = \frac{\alpha_{os} \, [\, C_o \, X_{in}(n) - C_1 \, X_{in}(n-1) + D_1 \, X_o(n-1)]}{D_o}$$

4B.5

APPENDIX 4C

Derivation of the recursive equation of the filtering function K_2.

$$K_2 = \alpha_{Qs} Z_{Q1} \qquad\qquad 4C.1$$

in s domain

$$K_2(s) = \alpha_{Qs} (R_{Q1} + s L_{Q1}) \qquad\qquad 4C.2$$

in z domain

Let $s = \dfrac{1 - z^{-1}}{T}$

$$\frac{X_o(z)}{X_{in}(z)} = \alpha_{Qs} [R_{Q1} + L_{Q1} (1 - z^{-1}/T)]$$

$$\frac{X_o(z)*T}{X_{in}(z)} = \alpha_{Qs} (T R_{Q1} + L_{Q1} - L_{Q1} z^{-1})$$

$$\frac{X_o(z)*T}{X_{in}(z)} = \alpha_{Qs} (A_o - A_1 z^{-1}) \qquad\qquad 4C.3$$

where

$$A_o = T R_{Q1} + L_{Q1}$$

$$A_1 = L_{Q1}$$

in time domain

$$X_o(n) = \frac{\alpha_{Qs} [A_o X_{in}(n) - A_1 X_{in}(n-1)]}{T} \qquad\qquad 4C.4$$

APPENDIX 4D

Derivation of the recursive equation of the filtering function K_3.

In the foregoing analysis the legs of the Teed circuit are assumed homogeneous i.e;

$$\frac{Z_{PO}}{Z_{P1}} = \frac{Z_{RO}}{Z_{R1}} = \frac{Z_{QO}}{Z_{Q1}} \qquad \qquad 4D.1$$

$$K_3 = \alpha_{QS} \, Z_{Q1} \, K$$

$$K_3 = \alpha_{QS} \, Z_{Q1} \, (\, 1/3 \, (\, Z_{QO}/Z_{Q1} \, -1 \,)$$

$$K_3 = 1/3 \, \alpha_{QS} \, Z_{Q1} \, (\, Z_{QO} - Z_{Q1}/ \, Z_{Q1} \,)$$

$$K_3 = 1/3 \, \alpha_{QS} \, (\, Z_{QO} - Z_{Q1} \,) \qquad \qquad 4D.2$$

in s domain

$$K_3(s) = 1/3 \, \alpha_{QS} \, (\, R_{QO} - R_{Q1} \,) + s \, (\, L_{QO} - L_{Q1} \,)$$

$$K_3(s) = 1/3 \, \alpha_{QS} \, (\, A_0 + A_1 \, s \,) \qquad \qquad 4D.3$$

where

$$A_0 = R_{QO} - R_{Q1}$$

$$A_1 = L_{QO} - L_{Q1}$$

in z domain

$$\text{Let } s = \frac{1 - z^{-1}}{T}$$

$$\frac{X_o(z)}{X_{in}(z)} = 1/3 \, \alpha_{QS} \, [\, A_0 + A_1 \, (1 - z^{-1}/T \,)]$$

$$\frac{X_o(z)*T}{X_{in}(z)} = 1/3 \, \alpha_{QS} \, (\, T \, A_0 + A_1 - A_1 \, z^{-1} \,)$$

$$\frac{X_o(z)*T}{X_{in}(z)} = 1/3 \, \alpha_{QS} \, (\, C_0 - C_1 \, z^{-1} \,) \qquad \qquad 4D.4$$

where

$$C_0 = T \, A_0 + A_1$$

$$C_1 = A_1$$

144

in time domain

$$X_o(n) = \frac{1/3\ \alpha_{Qs}\ [\ C_o\ X_{in}(n)\ -\ C_1\ X_{in}(n-1)]}{T} \qquad 4D.5$$

APPENDIX 4E

Derivation of the recursive equation of the filtering function K_4.

$$K_4 = \frac{\alpha_{QS}\, Z_{Q1}\, Z_{RS1}(K-K_{RS})}{(Z_{R1}+Z_{RS1})\{\,(1+3K)Z_{R1}+(1+3K_{RS})Z_{RS1})\,\}} \qquad 4E.1$$

this can be reduced to the form;

$$K_4 = \frac{1/3\,\alpha_{QS}\,(\,Z_{RS1}\,Z_{QO}\,-\,Z_{Q1}\,Z_{RSO}\,)}{(\,Z_{R1}\,+\,Z_{SR1}\,)(\,Z_{RO}\,+\,Z_{RSO}\,)} \qquad 4E.2$$

in s domain

$$K_4(s) = \frac{1/3\,\alpha_{QS}(R_{RS1}+sL_{RS1})(R_{QO}+sL_{QO})-(R_{Q1}+sL_{Q1})(R_{RSO}+sL_{RSO})}{(R_{R1}+sL_{R1}+R_{RS1}+sL_{RS1})(R_{RO}+sL_{RO}+R_{RSO}+sL_{RSO})}$$

this can be written in the form

$$K_4(s) = \frac{1/3\,\alpha_{QS}\,(\,A_0\,+\,A_1\,s\,+\,A_2\,s^2\,)}{B_0\,+\,B_1\,s\,+\,B_2\,s^2} \qquad 4E.3$$

where

$$A_0 = R_{RS1}\,R_{QO}\,-\,R_{Q1}\,R_{RSO}$$

$$A_1 = R_{RS1}\,L_{QO}\,+\,R_{QO}\,L_{RS1}\,-\,R_{Q1}\,L_{RS1}\,-\,R_{RSO}\,L_{Q1}$$

$$A_2 = L_{RS1}\,L_{QO}\,-\,L_{Q1}\,L_{RSO}$$

$$B_0 = R_{RS1}\,R_{RO}\,+\,R_{RS1}\,R_{RSO}\,+\,R_{R1}\,R_{RO}\,+\,R_{R1}\,R_{RSO}$$

$$B_1 = (\,R_{RS1}\,L_{RO}\,+\,R_{RO}\,L_{RS1}\,+\,R_{RS1}\,L_{RSO}\,+\,R_{RSO}L_{RS1}\,+\,R_{R1}\,L_{RO}\,+\,R_{RO}\,L_{R1}\,+\,R_{R1}\,L_{RSO}\,+\,R_{RSO}L_{R1}\,)$$

$$B_2 = L_{RS1}\,L_{RO}\,+\,L_{RS1}\,L_{RSO}\,+\,L_{R1}\,L_{RO}\,+\,L_{R1}\,L_{RSO}$$

in z domain

$$\frac{X_o(z)}{X_{in}(z)} = \frac{1/3\,\alpha_{QS}\,[\,A_0\,+\,A_1\,(1-z^{-1}/T\,)\,+\,A_2\,(1-z^{-1}/T\,)^2\,]}{B_0\,+\,B_1\,(1-z^{-1}/T)\,+\,B_2\,(1-z^{-1}/T\,)^2}$$

$$\frac{X_o(z)}{X_{in}(z)} = \frac{1/3\,\alpha_{QS}\,[T^2A_0\,+TA_1(1-z^{-1}\,)\,+\,A_2\,(1-z^{-1}\,)^2\,]}{T^2\,B_0\,+T\,B_1\,(1-z^{-1})\,+\,B_2\,(1-z^{-1}\,)^2}$$

$$\frac{X_o(z)}{X_{in}(z)} = \frac{1/3\,\alpha_{QS}\,[T^2A_0+TA_1+A_2\,)-(TA_1\,+2\,A_2)z^{-1}\,+\,A_2\,z^{-2}]}{T^2B_0+TB_1+B_2)-(TB_1+2B_2)z^{-1}+A_2z^{-2}}$$

146

$$\frac{X_o(z)}{X_{in}(z)} = \frac{1/3\ \alpha_{Qs}\ (\ C_o\ -\ C_1\ z^{-1}\ +\ C_2\ z^{-2}\ )}{(\quad D_o\ -\ D_1\ z^{-1}\ +\ D_2\ z^{-2}\ )} \qquad \text{4E.4}$$

where

$$C_o = T^2\ A_o\ +\ T\ A_1\ +\ A_2$$

$$C_1 = T\ A_1\ +\ 2\ A_2$$

$$C_2 = A_2$$

$$D_o = T^2\ B_o\ +\ T\ B_1\ +\ B_2$$

$$D_1 = T\ B_1\ +\ 2\ B_2$$

$$D_2 = B_2$$

in time domain

$$X_o(n) = \frac{1/3\alpha_{Qs}\{(C_oX_{in}(n)-C_1X_{in}(n-1)+C_2X_{in}(n-2)\}\ +\ D_1X_o(n-1)-D_2X_o(n-2)}{D_o}$$

$$\text{4E.5}$$

APPENDIX 4F

Derivation of the recursive equation of the filtering function K_5.

$$K_5 = \frac{\alpha_{QS} \, Z_{P1} \, Z_{Q1} \, Z_{RS1}(K-K_{RS})(1+3\,K)}{(Z_{R1}+Z_{RS1})\{\,(1+3K)Z_{R1}+(1+3K_{RS})Z_{RS1})\,\}} \qquad 4F.1$$

this could be reduced to the form;

$$K_5 = \frac{1/3 \, \alpha_{QS} \, (\, Z_{RS1} \, Z_{Q0} \, Z_{P0} - Z_{Q1} \, Z_{RS0} \, Z_{P1}\,)}{(\, Z_{R1} + Z_{RS1}\,)(\, Z_{R0} + Z_{RS0}\,)} \qquad 4F.2$$

in s domain

$$K_5(s) = \frac{1/3\alpha_{QS}[(R_{RS1}+sL_{RS1})(R_{Q0}+sL_{Q0})(R_{P0}+sL_{P0}) - (R_{Q1}+sL_{Q1})(R_{RS0}+sL_{RS0})(R_{P1}+sL_{P1})]}{(R_{R1}+sL_{R1}+R_{RS1}+sL_{RS1})(R_{R0}+sL_{R0}+R_{RS0}+sL_{RS0})}$$

this can be written as

$$K_5(s) = \frac{1/3 \, \alpha_{QS} \, (\, A_0 + A_1 \, s + A_2 \, s^2 + A_3 \, s^3\,)}{B_0 + B_1 \, s + B_2 \, s^2} \qquad 4F.3$$

where

$A_0 = R_{RS1} \, R_{Q0} \, R_{P0} - R_{RS0} \, R_{Q1} \, R_{P0}$

$A_1 = (\, L_{Q0} \, R_{RS1} \, R_{P0} - L_{Q1} \, R_{RS0} \, R_{P0} + L_{RS1} \, R_{Q0} \, R_{P0} - L_{RS0} \, R_{Q1} \, R_{P0} + L_{P0} \, R_{RS1} \, R_{Q0} - L_{P0} \, R_{RS0} \, R_{Q1}\,)$

$A_2 = (\, L_{P0} \, L_{Q0} \, R_{RS1} - L_{Q1} \, L_{P0} \, R_{RS0} + L_{RS1} \, L_{P0} \, R_{Q0} - L_{RS0} \, L_{P0} \, R_{Q1} + L_{RS1} \, L_{Q0} \, R_{P0} - L_{RS0} \, L_{Q1} \, R_{P0}\,)$

$A_3 = L_{RS1} \, L_{Q0} \, L_{P0} - L_{RS0} \, L_{Q1} \, L_{P0}$

$B_0 = R_{RS1} \, R_{R0} + R_{RS1} \, R_{RS0} + R_{R1} \, R_{R0} + R_{R1} \, R_{RS0}$

$B_1 = (\, R_{RS1} \, L_{R0} + R_{R0} \, L_{RS1} + R_{RS1} \, L_{RS0} + R_{RS0}L_{RS1} + R_{R1} \, L_{R0} + R_{R0} \, L_{R1} + R_{R1} \, L_{RS0} + R_{RS0} \, L_{R1}\,)$

$B_2 = L_{RS1} \, L_{R0} + L_{RS1} \, L_{RS0} + L_{R1} \, L_{R0} + L_{R1} \, L_{RS0}$

in z domain

$$\frac{X_0(z)}{X_{in}(z)} = \frac{1/3\alpha_{QS}[A_0+A_1(1-z^{-1}/T)+A_2(1-z^{-1}/T)^2+A_3(1-z^{-1}/T)^3]}{B_0 + B_1 \, (1-z^{-1}/T) + B_2 \, (1-z^{-1}/T\,)^2}$$

$$\frac{X_0(z)}{X_{in}(z)} = \frac{1/3\alpha_{QS}[(T^3A_0+T^2A_1+TA_2+A_3) - (T^2A_1+2TA_2-3A_3)z^{-1}+(TA_2+3A_3)z^{-2}-A_3)z^{-3}\,]}{T[T^2 \, B_0 + T \, B_1 \, (1-z^{-1}) + B_2 \, (1-z^{-1}\,)^2\,]}$$

148

$$\frac{X_o(z)}{X_{in}(z)} = \frac{1/3\ \alpha_{QS}\ (\ C_0\ -\ C_1\ z^{-1}\ +\ C_2\ z^{-2}\ +\ C_3\ z^{-3}\ )}{(\ \ D_0\ -\ D_1\ z^{-1}\ +\ D_2\ z^{-2}\ )}$$

4F.4

where

$$C_0 = T^3 A_0 + T^2 A_1 + T\ A_2 + A_3$$

$$C_1 = T^2 A_1 + 2\ T\ A_2\ -\ 3\ A_3$$

$$C_2 = T\ A_2 + 3\ A_3$$

$$C_3 = A_3$$

$$D_0 = T^3\ B_0 + T^2\ B_1 + T\ B_2$$

$$D_1 = T^2\ B_1 + 2\ T\ B_2$$

$$D_2 = T\ B_2$$

in time domain

$$X_o(n) = \frac{1/3\ \alpha_{QS}\{(C_0 X_{in}(n) - C_1\ X_{in}(n-1) + C_2\ X_{in}(n-2)\ -\ C_3\ X_{in}(n-3)\} + D_1\ X_o(n-1) - D_2\ X_o(n-2)}{D_0}$$

4F.5

149

APPENDIX 4G

Derivation of the recursive equation of the filtering function K_6.

$$K_6 = \frac{\alpha_{QS} \ Z_{Q1} \ Z_{P1}}{Z_{R1} + Z_{RS1}} \qquad\qquad 4G.1$$

in s domain

$$K_6(s) = \frac{\alpha_{QS} \ (\ R_{Q1} + s \ L_{Q1}\ )(\ R_{P1} + s \ L_{P1}\ )}{(\ R_{R1} + s \ L_{R1}\ ) + (\ R_{RS1} + s \ L_{RS1}\ )}$$

$$K_6(s) = \frac{\alpha_{QS}[\ (R_{Q1}R_{P1}) + s(R_{Q1}L_{P1} + R_{P1}L_{Q1}) + s^2(L_{Q1}L_{P1})\ ]}{(\ R_{R1} + R_{RS1}\ ) + s \ (\ L_{R1} + L_{RS1}\ )}$$

$$K_6(s) = \frac{\alpha_{QS} \ (\ A_0 + \ A_1 \ s + A_2 \ s^2 \ )}{(\ B_0 + \ B_1 \ s \ )} \qquad\qquad 4G.2$$

where

$$A_0 = R_{Q1} \ R_{P1}$$

$$A_1 = R_{Q1} \ L_{P1} + R_{P1} \ L_{Q1}$$

$$A_2 = L_{Q1} \ L_{P1}$$

$$B_0 = R_{R1} + R_{RS1}$$

$$B_1 = L_{R1} + L_{RS1}$$

in z domain

Let $s = \dfrac{1 - z^{-1}}{T}$

$$\frac{X_o(z)}{X_{in}(z)} = \frac{\alpha_{QS} \ [\ A_0 + A_1 \ (1-z^{-1}/T\ ) + A_2 \ (1-z^{-1}/T\ )^2\ ]}{B_0 + B_1 \ (1-z^{-1}/T\ )}$$

$$\frac{X_o(z)}{X_{in}(z)} = \frac{\alpha_{QS}[\ T^2A_0 + TA_1 + A_2\ ) - (TA1 + 2A_2)z^{-1} + A_2 z^{-2}\ ]}{T^2 \ B_0 + T \ B_1 - T \ B_1 \ z^{-1}}$$

$$\frac{X_o(z)}{X_{in}(z)} = \frac{\alpha_{QS} \ (\ C_0 - C_1 \ z^{-1} + C_2 \ z^{-2}\ )}{D_0 - D_1 \ z^{-1}} \qquad\qquad 4G.3$$

where

$$C_0 = T^2 \ A_0 + T \ A_1 + A_2$$

$$C_1 = T\ A_1 + 2\ A_2$$

$$C_2 = A_2$$

$$D_0 = T^2\ B_0 + T\ B_1$$

$$D_1 = T\ B_1$$

in time domain

$$X_0(n) = \frac{\alpha_{os}[C_0 X_{in}(n) - C_1 X_{in}(n-1) + C_2 X_{in}(n-2) + D_1 X_0(n-1)]}{D_0}$$

4G.4

APPENDIX 4H

Derivation of the recursive equation of the filtering function K_7.

$$K_7 = \frac{\alpha_{QS} \, Z_{Q1} \, Z_{P1} \, K}{Z_{R1} + Z_{RS1}}$$

$$K_7 = \frac{1/3 \, \alpha_{QS}(\, Z_{Q1} \, Z_{PO} - Z_{Q1} \, Z_{P1})}{Z_{R1} + Z_{RS1}} \qquad 4H.1$$

in s domain

$$K_7(s) = \frac{1/3\alpha_{QS}[(R_{Q1}+sL_{Q1})(R_{PO}+sL_{PO})-(R_{Q1}+sL_{Q1})(R_{P1}+sL_{P1})]}{(R_{R1} + s \, L_{R1}) + (R_{RS1} + s \, L_{RS1})}$$

$$K_7(s) = \frac{1/3 \, \alpha_{QS} (A_0 + A_1 \, s + A_2 \, s^2)}{(B_0 + B_1 \, s)} \qquad 4H.2$$

where

$$A_0 = R_{Q1} \, R_{PO} - R_{Q1} \, R_{P1}$$

$$A_1 = R_{Q1} \, L_{PO} + R_{PO} \, L_{Q1} - R_{Q1} \, L_{P1} - R_{P1} \, L_{Q1}$$

$$A_2 = L_{Q1} \, L_{PO} - L_{Q1} \, L_{P1}$$

$$B_0 = R_{R1} + R_{RS1}$$

$$B_1 = L_{R1} + L_{RS1}$$

in z domain

Let $s = \dfrac{1 - z^{-1}}{T}$

$$\frac{X_0(z)}{X_{in}(z)} = \frac{1/3\alpha_{QS}[(A_0 + A_1(1-z^{-1}/T) + A_2(1-z^{-1}/T)^2]}{B_0 + B_1 (1-z^{-1}/T)}$$

$$\frac{X_0(z)}{X_{in}(z)} = \frac{1/3 \, \alpha_{QS}[(T^2 A_0 + T A_1 + A_2) - (T A_1 + 2 A_2) z^{-1} + A_2 z^{-2}]}{T^2 B_0 + T B_1 - T B_1 z^{-1}}$$

$$\frac{X_0(z)}{X_{in}(z)} = \frac{\alpha_{QS} (C_0 - C_1 z^{-1} + C_2 z^{-2})}{D_0 - D_1 z^{-1}} \qquad 4H.3$$

where

$$C_0 = T^2 \, A_0 + T \, A_1 + A_2$$

152

$$C_1 = T\ A_1 + 2\ A_2$$

$$C_2 = A_2$$

$$D_o = T^2\ B_o + T\ B_1$$

$$D_1 = T\ B_1$$

in time domain

$$X_o(n) = \frac{1/3\alpha_{Qs}[(C_oX_{in}(n)-C_1\ X_{in}(n-1)+C_2X_{in}(n-2)]+D_1X_o(n-1)}{D_o}$$

4H.4

APPENDIX 4I

Derivation of the recursive equation of the filtering function K.

$$K = 1/3 \ (\ Z_{PO} - Z_{P1}/Z_{P1} \ )$$
<div align="right">4I.1</div>

in s domain

$$K(s) = \frac{1/3 \ [(\ R_{PO} - R_{P1} \ ) + s \ (\ L_{PO} - L_{P1} \ )]}{(\ R_{P1} - s \ L_{P1} \ )}$$

$$K(s) = \frac{1/3 \ (\ A_o - s \ A_1 \ )}{(\ B_o - s \ B_1 \ )}$$
<div align="right">4I.2</div>

where
$$A_o = R_{PO} - R_{P1}$$
$$A_1 = L_{PO} - L_{P1}$$
$$B_o = R_{P1}$$
$$B_1 = L_{P1}$$

in z domain

Let $s = \dfrac{1 - z^{-1}}{T}$

$$\frac{X_o(z)}{X_{in}(z)} = \frac{1/3 \ [\ A_o + A_1 \ (1-z^{-1}/T \ )]}{B_o + B_1 \ (1-z^{-1}/T \ )}$$

$$\frac{X_o(z)}{X_{in}(z)} = \frac{1/3 \ [T \ A_o + A_1 \ (1-z^{-1} \ )]}{T \ B_o + B_1 \ (1-z^{-1} \ )}$$

$$\frac{X_o(z)}{X_{in}(z)} = \frac{1/3 \ [\ T \ A_o + A_1 - A_1 \ z^{-1})]}{T \ B_o + B_1 - B_1 \ z^{-1}}$$

$$\frac{X_o(z)}{X_{in}(z)} = \frac{1/3 \ (\ C_o - C_1 \ z^{-1})}{D_o - D_1 \ z^{-1}}$$
<div align="right">4I.3</div>

where
$$C_o = T \ A_o + A_1$$
$$C_1 = A_1$$
$$D_o = T \ B_o + B_1$$
$$D_1 = B_1$$

in time domain

$$X_o(n) = \frac{1/3 \ [\ C_o \ X_{in}(n) - C_1 \ X_{in}(n-1)] + D_1 \ X_o(n-1)}{D_o}$$
<div align="right">4I.4</div>

154

APPENDIX 4J

Separation of the real and imaginary parts of the constant K_6 .

$$K_6 = \frac{\alpha_{QS}\ Z_{Q1}\ Z_{P1}}{Z_{R1} + Z_{RS1}} \qquad\qquad 4J.1$$

the above equation can be written as

$$K_6 = \frac{\alpha_{QS}\ (\ R_{Q1} + jX_{Q1}\ )(\ R_{P1} + jX_{P1}\ )}{(\ R_{R1} + jX_{R1}\ ) + (\ R_{RS1} + jX_{RS1}\ )}$$

$$K_6 = \frac{\alpha_{QS}[(R_{Q1}R_{P1} - X_{Q1}X_{P1}) + j(R_{Q1}X_{P1} + R_{P1}X_{Q1})]}{(\ R_{R1} + R_{RS1}\ ) + j\ (\ X_{R1} + X_{RS1}\ )}$$

$$K_6 = \frac{\alpha_{QS}\ (\ A_0 + jA_1\ )}{(\ B_0 + jB_1\ )} \qquad\qquad 4J.2$$

where
$$
\begin{aligned}
A_0 &= R_{Q1}R_{P1} - X_{Q1}X_{P1}\\
A_1 &= R_{Q1}X_{P1} + R_{P1}X_{Q1}\\
B_0 &= R_{R1} + R_{RS1}\\
B_1 &= X_{R1} + X_{RS1}
\end{aligned}
$$

$$K_6 = \frac{\alpha_{QS}\ (\ A_0\ B_0 + A_1\ B_1 + j(A_1\ B_0 - A_0\ B_1\ )}{(\ B_0{}^2 + B_1{}^2\ )} \qquad\qquad 4J.3$$

$$Real(\ K_6) = \frac{\alpha_{QS}\ (\ A_0\ B_0 + A_1\ B_1\ )}{(\ B_0{}^2 + B_1{}^2\ )} \qquad\qquad 4J.4$$

$$Img(\ K_6\ ) = \frac{\alpha_{QS}\ (\ A_1\ B_0 - A_0\ B_1\ )}{(\ B_0{}^2 + B_1{}^2\ )} \qquad\qquad 4J.5$$

155

REFERENCES

1. Esztergalyos, J. and Einarsson, E., "Ultra High Speed Protection of Three-Terminal Lines", CIGER 34-06, Session 1-9 Sept. 1982.

2. Intrabartola, J.M, et al., "Protection Aspects of Multi-Terminal Lines", IEEE Trans. PAS, Vol. PAS- 94, May 1975, pp. 544-547.

3. Humpage, W.D. and Lewis, D.W., "Distance Protection of Teed Circuits", Proc. IEE, Vol. 114, No. 10, October 1967, pp. 1483-1498.

4. Rushton, J., "Pilot-Wire Differential-Protection Characteristics for Multiended Circuits", Proc. IEE, Vol. 112, No. 11, November 1965, pp. 2095-2102.

5. Chamia, R.E. and Liberman, S., "Ultra-high speed relay for EHV/UHV transmission lines - development, design and application", IEEE Trans. PAS, Vol. PAS-97, 1978, pp. 2104-2116.

6. Tripp, D., "The design & application of a new directional comparison line protection scheme to series compensated systems", Ph.D. Thesis, University Of Bath, 1986.

7. Aggarwal, R.K. and Johns, A.T., "The development of a new high speed 3-terminal line protection scheme", IEEE/PES Summer Meeting, July 12-19, 1985. Paper No. 85 SM 320-7.

8. Rockefeller, G.D., Wagner, C.L., Linders, J.R., Hicks, K.L. and Rizy, D.T., "Adaptive transmission relaying concepts for improved performance" IEEE/PES Summer Meeting, July 12-17, 1987. Paper No. 87 SM 632-3.

9. Horowitz, S.H., Phadke, A.G. and Thorp, J.S., "Adaptive Transmission System Relaying ", IEEE/PES Summer Meeting, July 12-17, 1987. Paper No. 87 SM 625-3.

10. McInnes, B.E. and Morrison, I.F., "Real time calculation of resistance and reactance for transmission line protection by digital computer", Institute of Eng. (Australia), March 1971, pp. 16-24.

11. Phadke, A.G., Hlibka, T. and Ibrahim, M., "A digital computer system for EHV substations: Analysis and field test", IEEE Trans. on PAS, Vol. PAS-95, No. 1, Jan/Feb. 1976, pp. 291-301.

12. Mann, B.J. and Morrison, I.F., "Digital calculation of impedance of transmission line protection", IEEE Trans. on PAS, Vol. PAS-90, No. 1, Jan/Feb 1971, pp. 270-279.

13. Johns, A.T. and Martin, M.A., "New Ultra-High-Speed distance protection using Finite-Transform techniques", IEE Proc., Vol. 130, Pt. C, No. 3, May 1983, pp. 127-138.

14. Moore, P.J. and Johns, A.T., "Impedance measurement techniques for digital EHV line protection", Universities Power Eng. Conf., September 1988.

15. Warrington, A.R., "Protective Relays - Their theory and practice", Vol. 1, 3rd edition, Chapman and Hall Ltd., 1977.

16. Phadke, A.G. and Thorp, J.S., "Computer relaying for power systems", John Wiley & Sons Inc., 1989.

17. Johns, A.T. and Aggarwal, R.K., "Digital simulation of faulted E.H.V transmission lines with particular reference to Very-High-Speed protection", IEE Proc., Vol. 123, No. 4, April 1976.

18. Aggarwal, R.K., Johns, A.T. and Kalam, A., "Computer modelling of series compensated E.H.V transmission systems", IEE Proc. Vol. 131, Pt.C, No. 5, September 1984.

19. Electro-magnetic Transient Program (EMTP), Handbook.

20. Stagg, G.W. and El-Abiad, A.H., "Computer methods in power system analysis", McGraw-Hill Book Company, New York, 1968.

21. Elgerd, O., " Electric energy system theory", McGraw-Hill Book Company, New York, 1971.

22. IEEE Tutorial Course, "Digital Simulation of Electrical Transient Phenomena", No 81EH0173-5-PWR, 1981.

23. Dommel, H.W., "Digital computer solution of electromagnetic transients in single and multiphase networks", IEEE Trans. on PAS, Vol. PAS-88, No. 4, April 1969, pp. 390-399.

24. IEEE Power System Relaying Committee Report, "EHV Protection Problems", IEEE Trans. on PAS, PAS-100, No. 5, pp. 2399-2406, May 1981.

25. Stalewski, A. and Weller, G.C., "Novel capacitor-divider voltage sensor for high voltage transmission systems", IEE Proc. Vol. 126, No. 11, November 1979.

26. Sweetana, A., "Transient response characteristics of potential devices", IEEE Trans on PAS, Vol. PAS-89, pp.1649-1658, Nov. 1970.

27. Moore, P.J. and Johns, A.T., "The performance of new Ultra-High-Speed distance protection", 24th Universities Power Eng. Conf., Sunderland, April 1986.

28. IEEE Tutorial Course, "Microprocessor relays and protection systems", No. 88EH0269-1-PWR, 1988.

29. Ghassemi, F., "Adaptive digital distance protection for series compensated transmission lines", Ph.D Thesis, City University, 1989.

30. Swift, G.W., "The spectra of fault-induced transients", IEEE Trans. on PAS, Vol. PAS-98, No. 3, 940- 947.

31. Ranjbar, A.M. and Cory, B.j., "Filters for digital protection of long transmission lines", IEEE Trans. PAS, Vol. PAS- 94, May 1975, pp. 544-547.

32. IEEE Tutorial Course on Computer Relaying. PB 33390, 79EH0145-7-PWR, 1979.

33. Newbould, A. and Hindle, P., "Series compensated lines: Application of distance protection", 14th Annual western protection relay conference, Washington State University, Spokane, Washington, 20-22 Oct. 1987.

34. Martin, M.A. and Johns, A.T., "New approach to digital distance protection using time graded impedance characteristic", paper A 5.5.11, Proc. 16th UPEC 1981.

35. Moore, P.J., "Adaptive digital distance protection", Ph.D Thesis, City University, 1989.

36. Adamson, C. and Türeli, A., "Errors of sound-phase-compensation and residual compensation systems in earth-fault distance relaying", IEE Proc. Vol. 112, No. 7, July 1965, pp. 1369-1382.

37. Davison, E.B. and Wright, A., "Some factors affecting the accuracy of distance-type protective equipment under earth-fault conditions", IEE Proc. Vol. 110, No. 9, Sep. 1963, pp. 1678-1688.

38. Rushton, J. and Humpage, W.D., "Power-system studies for the determination of distance-protection performance", IEE Proc. Vol.119, No. 6, June 1972, pp. 677-688.

39. Warrington, A.R. Van C., "Graphical method for estimating the performance of distance relays during faults and power swings", AIEE Trans. Vol. 64, 1945, pp. 372-384.

40. Johns, A.T., "New discriminative distance-protective relays for selective-pole autoreclosure applications", IEE Proc. Vol. 126, No. 2, Feb. 1979, pp. 159-161.

41. Warrington, A.R., "Protective Relays - Their theory and practice", Vol. 2, 3rd edition, Chapman and Hall Ltd., 1977.

42. Bickford, J.P., "Electrical power transmission", M.Sc. course studying notes, UMIST, UK, 1985.

PUPLISED WORK

The following paper was presented to the Universities Power Engineering Conference at Queen's University of Belfast, 19-12 September 1989.

ADAPTIVE DISTANCE RELAYING SCHEME FOR THE PROTECTION OF TEED CIRCUITS

A.T. Johns and M.K. Teliani

Electrical Power and Energy System Research Centre
City University, London , U.K.

ABSTRACT

This paper investigates the possibility of using adaptive distance relaying techniques for the protection of transmission lines of the Teed type. The relay can adapt its setting according to the system operating conditions by means of an interface between the digital relay and a control centre where information about system operating conditions is provided.

The new method incorporates the source impedance and the load current from the remote ends into the local relay which in turn makes it possible to maintain the relay zone-1 reach for one remote end. A sample system which is used to study the behaviour of the new scheme is included.

INTRODUCTION

The problems of protecting three terminal lines are well known [1,2]. These stem from the current contribution from the remote leg, and the difference in relay response when the contribution is, or is not present. The current contribution can be either into the protected line section (in-feed) or out of the protected section (out-feed), depending on system parameters involved. Distance relays when applied to transmission lines of the Teed type can measure correctly up to the Tee point, but from on there, their reach is affected by the magnitude and direction of the current from the far end. Since the zone-1 must never overreach the remote shortest leg, under all system operating conditions, the relay is set without in-feed [3], i.e., assuming a two terminal configuration. Thus, with in-feed, the relay reach is reduced.

In this paper the requirements of an adaptive distance relaying scheme, where the zone-1 reach can be restored, is outlined. The scheme relies on transmitting and updating periodically the system operating conditions at the remote ends by means of slow speed non-continuous communication links. The in-feed current can be determined from remote source and line impedances together with the remote load current. These impedances are used in the relay to modify the measured impedance. The performance equation is derived and the correctness of its response is checked. In addition, a suggestion for its application in a digital computer based distance relay is included.

SINGLE PHASE CIRCUIT

The underlying principle of the new technique is best illustrated by reference to Fig. 1, which represents a single phase Teed circuit subject to a solid fault at leg Q. The measured impedance, using the local current and voltage signals, for a relay at end P, is given by:

$$Z_{mP} = \frac{V_P}{I_P} = \frac{I_P Z_P + \alpha_Q Z_Q (I_P + I_R)}{I_P} \quad 1$$

This can be written (see Appendix A) as:

$$Z_{mP} = Z_P + \alpha_Q Z_Q + \alpha_Q Z_Q [\frac{I_{RS}}{I_P} + \frac{Z_P I_{PT} - V_{PT}}{(Z_R + Z_{RS}) I_P}] \quad 2$$

where

Z_P = total impedance of leg P-T
Z_Q = total impedance of leg Q-T
Z_R = total impedance of leg R-T
$\alpha_Q Z_Q$ = proportional impedance to fault for T-F
I_R is the contribution of fault current from end R
I_{RS} is the load current at end R
I_{RT}, V_{RT} are the superimposed current and voltage at R.
I_{PT}, V_{PT} are the superimposed current and voltage at P.
The remote source impedance, Z_{RS}, is determined from

$$Z_{RS} = -\frac{V_{RT}}{I_{RT}} \quad 3$$

Assuming zero prefault loading
$I_P = I_{PT}$
$I_{RS} = 0$

$$Z_{mP} = Z_P + \alpha_Q Z_Q + \alpha_Q Z_Q (\frac{Z_P + Z_{PS}}{Z_R + Z_{RS}}) \quad 4$$

Similarly the measured impedance at end P for a fault on leg R is given generally by equation 5, and for the special case of zero prefault load in equation 6

$$Z_{mP} = Z_P + \alpha_R Z_R + \alpha_R Z_R [\frac{I_{QS}}{I_P} + \frac{Z_P I_{PT} - V_{PT}}{(Z_Q + Z_{QS}) I_P}] \quad 5$$

$$Z_{mP} = Z_P + \alpha_R Z_R + \alpha_R Z_R (\frac{Z_P + Z_{PS}}{Z_Q + Z_{QS}}) \quad 6$$

Similar measurands could be obtained for the relays at the other ends.

The basic principle employed would involve transmitting the values I_{RS}, I_{QS}, Z_{RS}, Z_{QS} to end P.

Z_{RS}, Z_{QS} are the effective source impedances looking into the busbar remote from the point of measurement for the critical fault position i.e., at zone-1 reach. In other words, for a fault at zone-1 reach on leg R, Z_{QS} should be determined and for faults at zone-1 reach on leg Q, Z_{RS} should be determined. It should be noted that the effective source impedance of the system considered in Fig. 1 is constant for all fault locations, but if there are ties between the three generating stations, other than the Teed circuit , the effective source impedance varies with fault position. These impedances could be obtained, as suggested by Rockefeller et al [4] i.e. by using a central computer system to update an impedance model each time the system changes. These could be updated periodically so as to correspond to the system configuration.

Similarly I_{RS}, I_{QS} are steady-state prefault values; their values change only slowly and periodically. Updating via a slow speed channel is what is required.

In essence, the relay would adapt its setting so as to be set optimally irrespective of any prospective fault condition. The advantages of this adaptive approach are:

1- A slow speed non-continuous single value communication channel is all that is required. This contrasts sharply with the requirements for differential schemes where integrity is determined largely by the security and dependability of the channel itself.

2- Speed of tripping can be retained without having to employ wideband (expensive) signalling equipment.
The scheme would thus retain the desirable features of non-unit measurement (distance protection) principles and, in the event of no periodic update, the setting could revert to values producing a performance that is no worse than that of conventional distance protection commonly applied to teed feeders.

INFEED COMPENSATION CONSIDERATION

Considering Eqn. 2 which is the measured impedance at end P ,for a fault on leg Q, written in the form of Eqn. 7

$$Z_{mP} = \frac{V_P}{I_P} = Z_P + \alpha_Q Z_Q + \alpha_Q Z_Q K_Q \quad 7$$

where

$$K_Q = \frac{I_{RS}}{I_P} + \frac{Z_P I_{PT} - V_{PT}}{(Z_R + Z_{RS}) I_P} \quad 8$$

If the measured impedance Z_{mP} is as in a conventional distance relay, compared with a fixed zone-1 boundary, for example on the basis of $0.8(Z_P + Z_Q)$ i.e., corresponding to $\alpha_Q = \alpha_{QS} = 0.8-0.2$ (Z_P/Z_Q) that extends into leg Q then the relay will in general underreach by virtue of the measured impedance being greater than the actual impedance to the fault ($Z_P + \alpha_Q Z_Q$) by the an amount $\alpha_Q Z_Q K_Q$.

By using an alternative measurand to Eqns. 2 and 5 written in the form of Eqn. 9 and 10, it is possible to compensate for the infeed from the remote ends R and Q. In this way the modified measurand corresponds exactly to the actual line impedance at the critical fault position.

$$Z_{mPQ} = Z_{mP} - \alpha_{QS}Z_Q K_Q = Z_P + \alpha_{QS}Z_Q \qquad 9$$
$$Z_{mPR} = Z_{mP} - \alpha_{RS}Z_R K_R = Z_P + \alpha_{RS}Z_R \qquad 10$$

The scheme in effect comprises two distance relays each set for one remote leg. The two relays will measure simultaneously and the following questions then arise.
a) In what way would the measurand Z_{mPQ} behave for a fault on leg R, and vice versa, how would Z_{mPR} behave for a fault on leg Q.?
b) In what way would they behave for a fault on leg P.?
Considering the system of Fig.1, and assigning the following scalar values for the source and line impedances; $Z_P = Z_R = 1.0$ pu, $Z_Q = 1.5$ pu, $Z_{PS} = Z_{RS} = 0.1$ pu and $Z_{QS} = 0.15$ pu. This system is used to illustrate the variation of the apparent impedance with fault position for a conventional relay together with the measurnads of the new scheme. For tripping logic it is decided to adopt the criteria that, in case of a fault both relays should operate. It can be clearly seen from Fig. 2a that the zone-1 reach is restored on one remote end which in this case is the short one (leg R). Fig. 2b shows the measurands for faults along line P-T-Q, in this case zone-1 is not restored but an improvement in coverage over conventional schemes is achieved.

PRACTICAL IMPLEMENTATION

Considering Eqn. 9, where the measurand is of the form:
$$Z_{mPQ} = Z_{mP} - \alpha_{QS}Z_Q K_Q$$
$$Z_{mPQ} = \frac{V_P}{I_P} - \alpha_{QS}Z_Q K_Q \qquad 11$$

This can be arranged to the form(see Appendix B):
$$Z_{mPQ} = \frac{V_P + X_1 V_P - K_1 V_{PS} + K_2 I_{PS} - K_3 I_{RS}}{I_P} - \frac{\alpha_{QS} Z_Q Z_P}{Z_R + Z_{RS}} \qquad 12$$

The following comments can be made on the above factors.
a) The angle of K_1 is in general negative but is small and tends to zero, because $/Z_Q$ tends to $/Z_R + Z_{RS}$.
b) The component $|K_2|/K_2 I_{PS}$ can be derived by passing I_P through a delay circuit adjusted to a value $nT - /K_2/W_o$ where nT is an integer number of multiples of the nominal power frequency period T; $/K_2$ is positive and hence the negative sign places I_P in the correct position. A value of n=5 would ensure that, following a fault, the steady state component of I_P is maintained long enough until the tripping is initiated.
c) The component $|K_1|/K_1 V_{PS}$ is similarly derived by delaying V_P by an amount $nT - /K_1/W_o$.
d) The component $|K_3|/K_3 I_{RS}$ would need to be derived from a circuit generating a sine wave of magnitude $K_3|I_{RS}|$ and adjusted to be in phase with $/I_{RS}$. This could be done by periodically transmitting a signal from end R to identify say the negative to positive zero crossing of I_{RS} together with a signal describing its peak value or magnitude. This could be achieved by means of a suitable array within a digital processor, which provides updating of the magnitude and phase of the generated sine wave in accordance with variations in I_{RS} and $/I_{RS}$ observed at the remote end. Since $/K_3$ is positive it would be necessary to delay the output of the sine wave generator as described above by an amount $nT - /K_3/W_o$.
e) If a voltage signal comprising the 4 components derived as indicated in (a) through (d) above is fed to an impedance measurement processor together with the locally derived signal I_P then each value of the sampled impedance thereby derived can be used in conjunction with the real and imaginary components of the constant values $\alpha_{QS} Z_Q Z_P / Z_R + Z_{RS}$ as indicated in Fig. 3
Similar arrangement can be made for the impedance Z_{mPR} by using the related parameters (Appendix C).

SAMPLE SYSTEM
A 400 kV three-phase system shown in Fig. 4a is used to illustrate the behaviour of the measurands, Z_{mPQ} and Z_{mPR}, for different fault locations. The system is assumed to be symmetrical and a three-phase fault is considered. The measurands in this case are applicable to each phase. The source capacity at the three ends is taken to be 35 GVA, the line length and the impedance per mile are as depicted.

Fig. 4b shows on an R-X diagram the behaviour of the measurands for a fault along line P-T-R; the line loading conditions are as indicated on the graph and it can be clearly seen that Z_{mPR} gives the exact line impedance at the reach point only. For internal faults, the measurand can fall on the left or right of the line locus this depends on the direction of flow of load current. Notice that, in case of an internal fault, if the impedance falls within the relay characteristic it is immaterial if it corresponds to the exact line impedance or not. In the case of a close-up fault the adaptive measurands measure a negative impedance its value being determined by the relative strength of the sources, the reach beyond the tee point and the direction of power flow prior to a fault. The quadrilateral characteristics used in digital relays applied for plain feeders are basically suitable for the adaptive scheme with the exception that, their reach should be extended into the negative region to cover close-up faults. The Z_{mPQ} measurand, can operate for external faults on leg R but this will not produce false tripping as both relays are required to operate.
For faults on line P-T-Q, the Z_{mPQ} measurand gives the proper discrimination between internal and external faults but the reach is governed by the Z_{mPR} measurand as shown in Figure 4c.

CONCLUSIONS
In this paper a novel concept, which could extend the potential of digital relays, has been introduced. This suggests coordination between a digital computer based distance relay and a central computer system, where information about the system operating conditions can be obtained. The primary investigation showed that the proposed adaptive scheme gives improved coverage over conventional distance relays and this leads to a solution which is close to ideal.

REFERENCES
1. Intrabartola, J.M. et al "Protection aspects of multi-terminal lines", IEEE report no. 79 TH0056-2-PWR.11-18, 1979.
2. Esztergalyos, J. and Einarsson, E. "Ultra high speed protection of three terminal lines" CIGRE 34-06, Session 1-9 Sept 1982.
3. Humpage, W.D., and Lewis, D.W., "Distance protection of teed circuits",PROC. IEE, 1967, 114,(10),pp. 1483-1498. Vol.
4. Rockefeller, G.D. et al "Adaptive transmission relaying concepts for improved performance" IEEE/PES Summer Meeting, July 12-17, 1987. Paper No.87 SM 632-3.

APPENDIX A
Identification of signals and parameters involved in determining the apparent impedance.
For the single phase Teed system of Fig. 1, the measured impedance, using the local voltage and current signals, at the relaying point, P, is given by:

$$Z_{mP} = \frac{V_P}{I_P} = \frac{I_P Z_P + \alpha_Q Z_Q (I_P + I_R)}{I_P} \qquad A-1$$

$$Z_{mP} = Z_P + \alpha_Q Z_Q + \alpha_Q Z_Q (\frac{I_R}{I_P}) \qquad A-2$$

Where I_R can be writen
$$I_R = I_{RS} + I_{RT} \qquad A-3$$

$$Z_{mP} = Z_P + \alpha_Q Z_Q + \alpha_Q Z_Q (\frac{I_{RS}}{I_P} + \frac{I_{RT}}{I_P}) \qquad A-4$$

The superimposed current at end R can be related to that at end P as:
$$V_{TT} = V_{RT} - Z_R I_{RT} \qquad A-5$$
$$V_{TT} = V_{PT} - Z_P I_{PT} \qquad A-6$$
where
V_{TT} =superimposed voltage at the tee point.
From A-5 and A-6

If the measured impedance Z_{mP} is as in a conventional distance relay, compared with a fixed zone-1 boundary, for example on the basis of $0.8(Z_P + Z_Q)$ i.e., corresponding to $\alpha_Q = \alpha_{QS} = 0.8-0.2$ (Z_P/Z_Q) that extends into leg Q then the relay will in general underreach by virtue of the measured impedance being greater than the actual impedance to the fault ($Z_P + \alpha_Q Z_Q$) by the an amount $\alpha_Q Z_Q K_Q$.

By using an alternative measurand to Eqns. 2 and 5 written in the form of Eqn. 9 and 10, it is possible to compensate for the infeed from the remote ends R and Q. In this way the modified measurand corresponds exactly to the actual line impedance at the critical fault position.

$$Z_{mPQ} = Z_{mP} - \alpha_{QS}Z_Q K_Q = Z_P + \alpha_{QS}Z_Q \qquad 9$$
$$Z_{mPR} = Z_{mP} - \alpha_{RS}Z_R K_R = Z_P + \alpha_{RS}Z_R \qquad 10$$

The scheme in effect comprises two distance relays each set for one remote leg. The two relays will measure simultaneously and the following questions then arise.

a) In what way would the measurand Z_{mPQ} behave for a fault on leg R, and vice versa, how would Z_{mPR} behave for a fault on leg Q.?

b) In what way would they behave for a fault on leg P.?

Considering the system of Fig.1, and assigning the following scalar values for the source and line impedances; $Z_P = Z_R = 1.0$ pu, $Z_Q = 1.5$ pu, $Z_{PS} = Z_{RS} = 0.1$ pu and $Z_{QS} = 0.15$ pu. This system is used to illustrate the variation of the apparent impedance with fault position for a conventional relay together with the measurnads of the new scheme. For tripping logic it is decided to adopt the criteria that, in case of a fault both relays should operate. It can be clearly seen from Fig. 2a that the zone-1 reach is restored on one remote end which in this case is the short one (leg R). Fig. 2b shows the measurands for faults along line P-T-Q, in this case zone-1 is not restored but an improvement in coverage over conventional schemes is achieved.

PRACTICAL IMPLEMENTATION

Considering Eqn. 9, where the measurand is of the form:

$$Z_{mPQ} = Z_{mP} - \alpha_{QS}Z_Q K_Q$$

$$Z_{mPQ} = \frac{V_P}{I_P} - \alpha_{QS}Z_Q K_Q \qquad 11$$

This can be arranged to the form(see Appendix B):

$$Z_{mPQ} = \frac{V_P + K_1 V_P - K_1 V_{PS} + K_2 I_{PS} - K_3 I_{RS}}{I_P} - \frac{\alpha_{QS} Z_Q Z_P}{Z_R + Z_{RS}} \qquad 12$$

The following comments can be made on the above factors.

a) The angle of K_1 is in general negative but is small and tends to zero, because $/Z_Q$ tends to $/Z_R + Z_{RS}$.

b) The component $|K_2|/K_2 I_{PS}$ can be derived by passing I_P through a delay circuit adjusted to a value $nT - /K_2/W_0$ where nT is an integer number of multiples of the nominal power frequency period T; $/K_2$ is positive and hence the negative sign places I_P in the correct position. A value of $n=5$ would ensure that, following a fault, the steady state component of I_P is maintained long enough until the tripping is initiated.

c) The component $|K_1|/K_1 V_{PS}$ is similarly derived by delaying V_P by an amount $nT - /K_1/W_0$.

d) The component $|K_3|/K_3 I_{RS}$ would need to be derived from a circuit generating a sine wave of magnitude $K_3|I_{RS}|$ and adjusted to be in phase with $/I_{RS}$. This could be done by periodically transmitting a signal from end R to identify say the negative to positive zero crossing of I_{RS} together with a signal describing its peak value or magnitude. This could be achieved by means of a suitable array within a digital processor, which provides updating of the magnitude and phase of the generated sine wave in accordance with variations in I_{RS} and $/I_{RS}$ observed at the remote end. Since $/K_3$ is positive it would be necessary to delay the output of the sine wave generator as described above by an amount $nT - /K_3/W_0$.

e) If a voltage signal comprising the 4 components derived as indicated in (a) through (d) above is fed to an impedance measurement processor together with the locally derived signal I_P then each value of the sampled impedance thereby derived can be used in conjunction with the real and imaginary components of the constant values $\alpha_{QS} Z_Q Z_P/ Z_R + Z_{RS}$ as indicated in Fig. 3.

Similar arrangement can be made for the impedance Z_{mPR} by using the related parameters (Appendix C).

A 400 kV three-phase system shown in Fig. 4a is used to illustrate the behaviour of the measurands, Z_{mPQ} and Z_{mPR}, for different fault locations. The system is assumed to be symmetrical and a three-phase fault is considered. The measurands in this case are applicable to each phase. The source capacity at the three ends is taken to be 35 GVA, the line length and the impedance per mile are as depicted.

Fig. 4b shows on an R-X diagram the behaviour of the measurands for a fault along line P-T-R; the line loading conditions are as indicated on the graph and it can be clearly seen that Z_{mPR} gives the exact line impedance at the reach point only. For internal faults, the measurand can fall on the left or right of the line locus this depends on the direction of flow of load current. Notice that, in case of an internal fault, if the impedance falls within the relay characteristic it is immaterial if it corresponds to the exact line impedance or not. In the case of a close-up fault the adaptive measurands measure a negative impedance its value being determined by the relative strength of the sources, the reach beyond the tee point and the direction of power flow prior to a fault. The quadrilateral characteristics used in digital relays applied for plain feeders are basically suitable for the adaptive scheme with the exception that, their reach should be extended into the negative region to cover close-up faults. The Z_{mPQ} measurand, can operate for external faults on leg R but this will not produce false tripping as both relays are required to operate.

For faults on line P-T-Q, the Z_{mPQ} measurand gives the proper discrimination between internal and external faults but the reach is governed by the Z_{mPR} measurand as shown in Figure 4c.

CONCLUSIONS

In this paper a novel concept, which could extend the potential of digital relays, has been introduced. This suggests coordination between a digital computer based distance relay and a central computer system, where information about the system operating conditions can be obtained. The primary investigation showed that the proposed adaptive scheme gives improved coverage over conventional distance relays and this leads to a solution which is close to ideal.

REFERENCES
1. Intrabartola, J.M. et al "Protection aspects of multi-terminal lines", IEEE report no. 79 TH0056-2-PWR.11-18, 1979.
2. Esztergalyos, J. and Einarsson, E. "Ultra high speed protection of three terminal lines" CIGRE 34-06, Session 1-9 Sept 1982.
3. Humpage, W.D., and Lewis, D.W., "Distance protection of teed circuits",PROC. IEE, 1967, 114,(10),pp. 1483-1498. Vol.
4. Rockefeller, G.D. et al "Adaptive transmission relaying concepts for improved performance" IEEE/PES Summer Meeting, July 12-17, 1987. Paper No.87 SM 632-3.

APPENDIX A

Identification of signals and parameters involved in determining the apparent impedance.

For the single phase Teed system of Fig. 1, the measured impedance, using the local voltage and current signals, at the relaying point, P, is given by:

$$Z_{mP} = \frac{V_P}{I_P} = \frac{I_P Z_P + \alpha_Q Z_Q (I_P + I_R)}{I_P} \qquad A-1$$

$$Z_{mP} = Z_P + \alpha_Q Z_Q + \alpha_Q Z_Q (\frac{I_R}{I_P}) \qquad A-2$$

Where I_R can be written

$$I_R = I_{RS} + I_{RT} \qquad A-3$$

$$Z_{mP} = Z_P + \alpha_Q Z_Q + \alpha_Q Z_Q (\frac{I_{RS}}{I_P} + \frac{I_{PT}}{I_P}) \qquad A-4$$

The superimposed current at end R can be related to that at end P as:

$$V_{TT} = V_{RT} - Z_R I_{RT} \qquad A-5$$
$$V_{TT} = V_{PT} - Z_P I_{PT} \qquad A-6$$

where

V_{TT} =superimposed voltage at the tee point.

From A-5 and A-6

ADAPTIVE DISTANCE RELAYING SCHEME FOR THE PROTECTION OF TEED CIRCUITS

A.T. Johns and M.K. Teliani

Electrical Power and Energy System Research Centre
City University, London , U.K.

ABSTRACT
This paper investigates the possibility of using adaptive distance relaying techniques for the protection of transmission lines of the Teed type. The relay can adapt its setting according to the system operating conditions by means of an interface between the digital relay and a control centre where information about system operating conditions is provided.

The new method incorporates the source impedance and the load current from the remote ends into the local relay which in turn makes it possible to maintain the relay zone-1 reach for one remote end. A sample system which is used to study the behaviour of the new scheme is included.

INTRODUCTION
The problems of protecting three terminal lines are well known [1,2]. These stem from the current contribution from the remote leg, and the difference in relay response when the contribution is, or is not present. The current contribution can be either into the protected line section (in-feed) or out of the protected section (out-feed), depending on system parameters involved. Distance relays when applied to transmission lines of the Teed type can measure correctly up to the Tee point, but from on there, their reach is affected by the magnitude and direction of the current from the far end. Since the zone-1 must never overreach the remote shortest leg, under all system operating conditions, the relay is set without in-feed [3], i.e., assuming a two terminal configuration. Thus, with in-feed, the relay reach is reduced.

In this paper the requirements of an adaptive distance relaying scheme, where the zone-1 reach can be restored, is outlined. The scheme relies on transmitting and updating periodically the system operating conditions at the remote ends by means of slow speed non-continuous communication links. The in-feed current can be determined from remote source and line impedances together with the remote load current. These impedances are used in the relay to modify the measured impedance. The performance equation is derived and the correctness of its response is checked. In addition, a suggestion for its application in a digital computer based distance relay is included.

SINGLE PHASE CIRCUIT
The underlying principle of the new technique is best illustrated by reference to Fig. 1, which represents a single phase Teed circuit subject to a solid fault at leg Q. The measured impedance, using the local current and voltage signals, for a relay at end P, is given by:

$$Z_{mP} = \frac{V_P}{I_P} = \frac{I_P Z_P + a_Q Z_Q (I_P + I_R)}{I_P} \qquad 1$$

This can be written (see Appendix A) as:

$$Z_{mP} = Z_P + a_Q Z_Q + a_Q Z_Q [\frac{I_{RS}}{I_P} + \frac{Z_P I_{PT} - V_{PT}}{(Z_R + Z_{RS}) I_P}] \qquad 2$$

where

Z_P = total impedance of leg P-T
Z_Q = total impedance of leg Q-T
Z_R = total impedance of leg R-T
$a_Q Z_Q$ = proportional impedance to fault for T-F
I_R is the contribution of fault current from end R
I_{RS} is the load current at end R
I_{RT}, V_{RT} are the superimposed current and voltage at R.
I_{PT}, V_{PT} are the superimposed current and voltage at P.
The remote source impedance, Z_{RS}, is determined from

$$Z_{RS} = - \frac{V_{RT}}{I_{RT}} \qquad 3$$

Assuming zero prefault loading
$I_P = I_{PT}$
$I_{RS} = 0$

$$Z_{mP} = Z_P + a_Q Z_Q + a_Q Z_Q (\frac{Z_P + Z_{PS}}{Z_R + Z_{RS}}) \qquad 4$$

Similarly the measured impedance at end P for a fault on leg R is given generally by equation 5, and for the special case of zero prefault load in equation 6

$$Z_{mP} = Z_P + a_R Z_R + a_R Z_R [\frac{I_{QS}}{I_P} + \frac{Z_P I_{PT} - V_{PT}}{(Z_Q + Z_{QS}) I_P}] \qquad 5$$

$$Z_{mP} = Z_P + a_R Z_R + a_R Z_R (\frac{Z_P + Z_{PS}}{Z_Q + Z_{QS}}) \qquad 6$$

Similar measurands could be obtained for the relays at the other ends.
The basic principle employed would involve transmitting the values I_{RS}, I_{QS}, Z_{RS}, Z_{QS} to end P.
Z_{RS}, Z_{QS} are the effective source impedances looking into the busbar remote from the point of measurement for the critical fault position i.e., at zone-1 reach. In other words, for a fault at zone-1 reach on leg R, Z_{QS} should be determined and for faults at zone-1 reach on leg Q, Z_{RS} should be determined. It should be noted that the effective source impedance of the system considered in Fig. 1 is constant for all fault locations, but if there are ties between the three generating stations, other than the Teed circuit , the effective source impedance varies with fault position. These impedances could be obtained, as suggested by Rockefeller et al [4] i.e. by using a central computer system to update an impedance model each time the system changes. These could be updated periodically so as to correspond to the system configuration.
Similarly I_{RS}, I_{QS} are steady-state prefault values; their values change only slowly and periodically. Updating via a slow speed channel is what is required.
In essence, the relay would adapt its setting so as to be set optimally irrespective of any prospective fault condition. The advantages of this adaptive approach are:

1- A slow speed non-continuous single value communication channel is all that is required. This contrasts sharply with the requirements for differential schemes where integrity is determined largely by the security and dependability of the channel itself.

2- Speed of tripping can be retained without having to employ wideband (expensive) signalling equipment.
The scheme would thus retain the desirable features of non-unit measurement (distance protection) principles and, in the event of no periodic update, the setting could revert to values producing a performance that is no worse than that of conventional distance protection commonly applied to teed feeders.

INFEED COMPENSATION CONSIDERATION
Considering Eqn. 2 which is the measured impedance at end P ,for a fault on leg Q, written in the form of Eqn. 7

$$Z_{mP} = \frac{V_P}{I_P} = Z_P + a_Q Z_Q + a_Q Z_Q K_Q \qquad 7$$

where

$$K_Q = \frac{I_{RS}}{I_P} + \frac{Z_P I_{PT} - V_{PT}}{(Z_R + Z_{RS}) I_P} \qquad 8$$

$$I_{RT} = \frac{V_{RT} - V_{PT} + Z_P \, I_{PT}}{Z_R} \qquad A-7$$

V_{RT} can be expressed as

$$V_{RT} = -I_{RT} \, Z_{RS} \qquad A-8$$

$$I_{RT} = \frac{Z_P \, I_{PT} - V_{PT} - I_{RT} \, Z_{RS}}{Z_R} \qquad A-9$$

$$I_{RT} = \frac{Z_P I_{PT} - V_{PT}}{Z_R + Z_{RS}} \qquad A-10$$

From A-4 and A-10

$$Z_{mP} = Z_P + a_Q Z_Q + a_Q Z_Q \left\{ \frac{I_{RS}}{I_P} + \frac{Z_P I_{PT} - V_{PT}}{(Z_R + Z_{RS}) I_P} \right\} \quad A-11$$

Some idea of the behaviour of Eqn. A-11 can be gained from making the assumption of zero prefault load in which case

$$I_P = I_{PT}$$
$$I_{RS} = 0$$

then

$$Z_{mP} = Z_P + a_Q Z_Q + a_Q Z_Q \left(\frac{Z_P + Z_{PS}}{Z_R + Z_{RS}} \right) \qquad A-12$$

Similarly the measured impedance at end P for a fault on leg R is given generally by Eqn. A-13, and for the special case of zero prefault load in Eqn. A-14

$$Z_{mP} = Z_P + a_R Z_R + a_R Z_R \left\{ \frac{I_{QS}}{I_P} + \frac{Z_P I_{PT} - V_{PT}}{(Z_Q + Z_{QS}) I_P} \right\} \quad A-13$$

$$Z_{mP} = Z_P + a_R Z_R + a_R Z_R \left(\frac{Z_P + Z_{PS}}{Z_Q + Z_{QS}} \right) \qquad A-14$$

Eqn. A-11 can be written in the form of Eqn. A-15

$$Z_{mP} = \frac{V_P}{I_P} = Z_P + a_Q Z_Q + a_Q Z_Q K_Q \qquad A-15$$

where

$$K_Q = \frac{I_{RS}}{I_P} + \frac{Z_P I_{PT} - V_{PT}}{(Z_R + Z_{RS}) I_P} \qquad A-16$$

$$K_Q = \frac{Z_P + Z_{PS}}{Z_R + Z_{RS}} \qquad \text{for zero prefault load}$$

Eqn. A-13 can be written in the form of Eqn. A-17

$$Z_{mP} = \frac{V_P}{I_P} = Z_P + a_R Z_R + a_R Z_R K_R \qquad A-17$$

$$K_R = \frac{I_{QS}}{I_P} + \frac{Z_P I_{PT} - V_{PT}}{(Z_Q + Z_{QS}) I_P} \qquad A-18$$

$$K_R = \frac{Z_P + Z_{PS}}{Z_Q + Z_{QS}} \qquad \text{for zero prefault load}$$

APPENDIX B
Arrangement of the performance equation for practical implementation for faults along line P-T-Q.
Considering Eqn. 9, where the measurand is of the form:

$$Z_{mPQ} = Z_{mP} - a_{QS} Z_Q K_Q \qquad B-1$$

$$Z_{mPQ} = \frac{V_P}{I_P} - a_{QS} Z_Q K_Q \qquad B-2$$

where

$$K_Q = \frac{I_{RS}}{I_P} + \frac{Z_P I_{PT} - V_{PT}}{(Z_R + Z_{RS}) I_P} \qquad B-3$$

we can write

$$V_{PT} = V_P - V_{PS} \qquad B-4$$
$$I_{PT} = I_P - I_{PS} \qquad B-5$$

I_{PS}, V_{PS} are the pre-fault current and voltage at P.

I_{PT}, V_{PT} are the superimposed current and voltage at P.

$$Z_{mPQ} = \frac{V_P - a_{QS} Z_Q I_{RS} - a_{QS} Z_Q \{ [Z_P (I_P - I_{PS}) - (V_P - V_{PS})] / (Z_R - Z_{RS}) \}}{I_P}$$

$$B-6$$

$$Z_{mPQ} = \left\{ \frac{V_P \left(1 + \dfrac{a_{QS} Z_Q}{Z_R + Z_{RS}} \right) - a_{QS} Z_Q \left[I_{RS} - \dfrac{I_{PS} Z_P}{Z_R + Z_{RS}} + \dfrac{V_{PS}}{Z_R + Z_{RS}} \right]}{I_P} \right.$$

$$\left. - \frac{a_{QS} Z_Q Z_P}{Z_R + Z_{RS}} \right\} \qquad B-7$$

$$Z_{mPQ} = \frac{V_P + K_1 V_P - K_1 V_{PS} + K_2 I_{PS} - K_3 I_{RS}}{I_P} - \frac{a_{QS} Z_Q Z_P}{Z_R + Z_{RS}} \quad B-8$$

where

$$|K_1| = \left| \frac{a_{QS} Z_Q}{Z_R + Z_{RS}} \right| \qquad \underline{/K_1} = \underline{/ \frac{Z_Q}{Z_R + Z_{RS}}}$$

$$|K_2| = \left| \frac{a_{QS} Z_Q Z_P}{Z_R + Z_{RS}} \right| \qquad \underline{/K_2} = \underline{/ \frac{Z_Q Z_P}{Z_R + Z_{RS}}}$$

$$|K_3| = |a_{QS} Z_Q| \qquad \underline{/K_3} = \underline{/ Z_Q}$$

APPENDIX C
Arrangement of the performance equation for practical implementation for faults along line P-T-R.
Considering Eqn. 10, where the measurand is of the form:

$$Z_{mPR} = Z_{mP} - a_{RS} Z_R K_R \qquad C-1$$

$$Z_{mPR} = \frac{V_P}{I_P} - a_{RS} Z_R K_R \qquad C-2$$

where

$$K_R = \frac{I_{QS}}{I_P} + \frac{Z_P I_{PT} - V_{PT}}{(Z_Q + Z_{QS}) I_P} \qquad C-3$$

$$Z_{mPR} = \frac{V_P - a_{RS} Z_R I_{RS} - a_{RS} Z_R \{ [Z_P (I_P - I_{PS}) - (V_P - V_{PS})] / (Z_Q + Z_{QS}) \}}{I_P}$$

$$C-4$$

$$Z_{mPR} = \left\{ \frac{V_P \left(1 + \dfrac{a_{RS} Z_R}{Z_Q + Z_{QS}} \right) - a_{RS} Z_R \left[I_{RS} - \dfrac{I_{PS} Z_P}{Z_Q + Z_{QS}} + \dfrac{V_{PS}}{Z_Q + Z_{QS}} \right]}{I_P} \right.$$

$$\left. - \frac{a_{RS} Z_R Z_P}{Z_Q + Z_{QS}} \right\} \qquad C-5$$

$$Z_{mPR} = \frac{V_P + K'_1 V_P - K'_1 V_{PS} + K'_2 I_{PS} - K'_3 I_{RS}}{I_P} - \frac{a_{RS} Z_R Z_P}{Z_Q + Z_{QS}} \quad C-6$$

where

$$|K'_1| = \left| \frac{a_{RS} Z_R}{Z_Q + Z_{QS}} \right| \qquad \underline{/K'_1} = \underline{/ \frac{Z_R}{Z_Q + Z_{QS}}}$$

$$|K'_2| = \left| \frac{a_{RS} Z_R Z_P}{Z_Q + Z_{QS}} \right| \qquad \underline{/K'_2} = \underline{/ \frac{Z_R Z_P}{Z_Q + Z_{QS}}}$$

$$|K'_3| = |a_{RS} Z_R| \qquad \underline{/K'_3} = \underline{/ Z_R}$$



Fig. 1 Typical three terminal line with current contribution for a fault on leg Q.

$$I_{RT} = \frac{V_{RT} - V_{PT} + Z_P I_{PT}}{Z_R} \qquad \text{A-7}$$

V_{RT} can be expressed as

$$V_{RT} = -I_{RT} Z_{RS} \qquad \text{A-8}$$

$$I_{RT} = \frac{Z_P I_{PT} - V_{PT} - I_{RT} Z_{RS}}{Z_R} \qquad \text{A-9}$$

$$I_{RT} = \frac{Z_P I_{PT} - V_{PT}}{Z_R + Z_{RS}} \qquad \text{A-10}$$

From A-4 and A-10

$$Z_{mP} = Z_P + \alpha_Q Z_Q + \alpha_Q Z_Q \{ \frac{I_{RS}}{I_P} + \frac{Z_P I_{PT} - V_{PT}}{(Z_R + Z_{RS})I_P} \} \qquad \text{A-11}$$

Some idea of the behaviour of Eqn. A-11 can be gained from making the assumption of zero prefault load in which case

$$I_P = I_{PT}$$
$$I_{RS} = 0$$

then

$$Z_{mP} = Z_P + \alpha_Q Z_Q + \alpha_Q Z_Q (\frac{Z_P + Z_{PS}}{Z_R + Z_{RS}}) \qquad \text{A-12}$$

Similarly the measured impedance at end P for a fault on leg R is given generally by Eqn. A-13, and for the special case of zero prefault load in Eqn. A-14

$$Z_{mP} = Z_P + \alpha_R Z_R + \alpha_R Z_R \{ \frac{I_{QS}}{I_P} + \frac{Z_P I_{PT} - V_{PT}}{(Z_Q + Z_{QS})I_P} \} \qquad \text{A-13}$$

$$Z_{mP} = Z_P + \alpha_R Z_R + \alpha_R Z_R (\frac{Z_P + Z_{PS}}{Z_Q + Z_{QS}}) \qquad \text{A-14}$$

Eqn. A-11 can be written in the form of Eqn. A-15

$$Z_{mP} = \frac{V_P}{I_P} = Z_P + \alpha_Q Z_Q + \alpha_Q Z_Q K_Q \qquad \text{A-15}$$

where

$$K_Q = \frac{I_{RS}}{I_P} + \frac{Z_P I_{PT} - V_{PT}}{(Z_R + Z_{RS})I_P} \qquad \text{A-16}$$

$$K_Q = \frac{Z_P + Z_{PS}}{Z_R + Z_{RS}} \quad \text{for zero prefault load}$$

Eqn. A-13 can be written in the form of Eqn. A-17

$$Z_{mP} = \frac{V_P}{I_P} = Z_P + \alpha_R Z_R + \alpha_R Z_R K_R \qquad \text{A-17}$$

$$K_R = \frac{I_{QS}}{I_P} + \frac{Z_P I_{PT} - V_{PT}}{(Z_Q + Z_{QS})I_P} \qquad \text{A-18}$$

$$K_R = \frac{Z_P + Z_{PS}}{Z_Q + Z_{QS}} \quad \text{for zero prefault load}$$

APPENDIX B

Arrangement of the performance equation for practical implementation for faults along line P-T-Q.
Considering Eqn. 9, where the measurand is of the form:

$$Z_{mPQ} = Z_{mP} - \alpha_{QS} Z_Q K_Q \qquad \text{B-1}$$

$$Z_{mPQ} = \frac{V_P}{I_P} - \alpha_{QS} Z_Q K_Q \qquad \text{B-2}$$

where

$$K_Q = \frac{I_{RS}}{I_P} + \frac{Z_P I_{PT} - V_{PT}}{(Z_R + Z_{RS})I_P} \qquad \text{B-3}$$

we can write

$$V_{PT} = V_P - V_{PS} \qquad \text{B-4}$$
$$I_{PT} = I_P - I_{PS} \qquad \text{B-5}$$

I_{PS}, V_{PS} are the pre-fault current and voltage at P.

I_{PT}, V_{PT} are the superimposed current and voltage at P.

$$Z_{mPQ} = \frac{V_P - \alpha_{QS} Z_Q I_{RS} - \alpha_{QS} Z_Q \{ [Z_P(I_P - I_{PS}) - (V_P - V_{PS})]/(Z_R - Z_{RS}) \}}{I_P} \qquad \text{B-6}$$

$$Z_{mPQ} = \{ \frac{V_P(1 + \frac{\alpha_{QS} Z_Q}{Z_R + Z_{RS}}) - \alpha_{QS} Z_Q [I_{RS} - \frac{I_{PS} Z_P}{Z_R + Z_{RS}} - \frac{V_{PS}}{Z_R + Z_{RS}}]}{I_P}$$
$$- \frac{\alpha_{QS} Z_Q Z_P}{Z_R + Z_{RS}} \} \qquad \text{B-7}$$

$$Z_{mPQ} = \frac{V_P + K_1 V_P - K_1 V_{PS} + K_2 I_{PS} - K_3 I_{RS}}{I_P} - \frac{\alpha_{QS} Z_Q Z_P}{Z_R + Z_{RS}} \qquad \text{B-8}$$

where

$$|K_1| = |\frac{\alpha_{QS} Z_C}{Z_R + Z_{RS}}| \qquad \qquad /K_1 = /\frac{Z_Q}{Z_R + Z_{RS}}$$

$$|K_2| = |\frac{\alpha_{QS} Z_Q Z_P}{Z_R + Z_{RS}}| \qquad \qquad /K_2 = /\frac{Z_Q Z_P}{Z_R + Z_{RS}}$$

$$|K_3| = |\alpha_{QS} Z_Q| \qquad \qquad /K_3 = /Z_C$$

APPENDIX C

Arrangement of the performance equation for practical implementation for faults along line P-T-R.
Considering Eqn. 10, where the measurand is of the form:

$$Z_{mPR} = Z_{mP} - \alpha_{RS} Z_R K_R \qquad \text{C-1}$$

$$Z_{mPR} = \frac{V_P}{I_P} - \alpha_{RS} Z_R K_R \qquad \text{C-2}$$

where

$$K_R = \frac{I_{QS}}{I_P} + \frac{Z_P I_{PT} - V_{PT}}{(Z_Q + Z_{QS})I_P} \qquad \text{C-3}$$

$$Z_{mPQ} = \frac{V_P - \alpha_{RS} Z_R I_{RS} - \alpha_{RS} Z_R \{ [Z_P(I_P - I_{PS}) - (V_P - V_{PS})]/(Z_Q + Z_{QS}) \}}{I_P} \qquad \text{C-4}$$

$$Z_{mPR} = \{ \frac{V_P(1 + \frac{\alpha_{RS} Z_R}{Z_Q + Z_{QS}}) - \alpha_{RS} Z_R [I_{RS} - \frac{I_{PS} Z_P}{Z_Q + Z_{QS}} + \frac{V_{PS}}{Z_Q + Z_{QS}}]}{I_P}$$
$$- \frac{\alpha_{RS} Z_R Z_P}{Z_Q + Z_{QS}} \} \qquad \text{C-5}$$

$$Z_{mPR} = \frac{V_P + K'_1 V_P - K'_1 V_{PS} + K'_2 I_{PS} - K'_3 I_{RS}}{I_P} - \frac{\alpha_{RS} Z_R Z_P}{Z_Q + Z_{CS}} \qquad \text{C-6}$$

where

$$|K'_1| = |\frac{\alpha_{RS} Z_R}{Z_Q + Z_{QS}}| \qquad \qquad /K'_1 = /\frac{Z_R}{Z_Q + Z_{QS}}$$

$$|K'_2| = |\frac{\alpha_{RS} Z_R Z_P}{Z_Q + Z_{QS}}| \qquad \qquad /K'_2 = /\frac{Z_R Z_P}{Z_Q + Z_{QS}}$$

$$|K'_3| = |\alpha_{RS} Z_R| \qquad \qquad /K'_3 = /Z_R$$

Fig. 1 Typical three terminal line with current contribution for a fault on leg Q.

Fig. 2a Variation of the apparent impedance VS actual line impedance for faults along line P-T-R.

Fig. 2b Variation of the apparent impedance VS actual line impedance for faults along line P-T-Q.
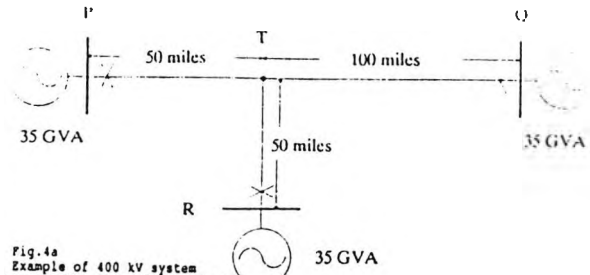

Fig.4a
Example of 400 kV system
$Z_1= 0.0288+j0.4708$ ohms/mile
Load angle: P=15° R=10° Q=0°
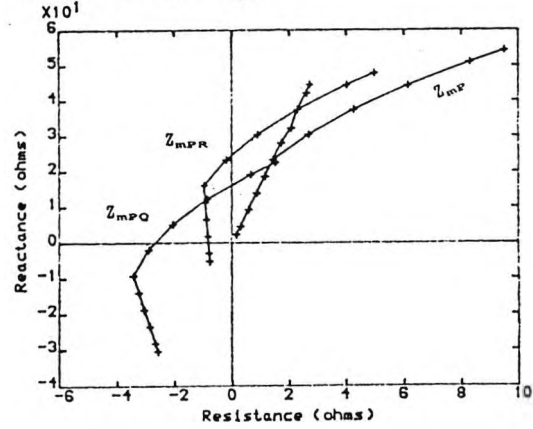
Fig. 4b Variation of measured impedances VS fault position for faults on line P-T-R.
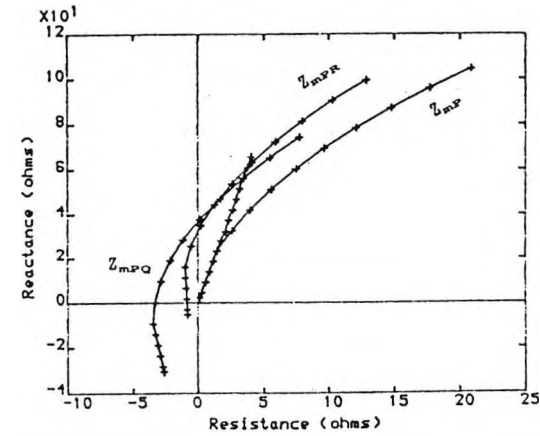
Fig. 4c Variation of measured impedances VS fault position for faults on line P-T-Q.
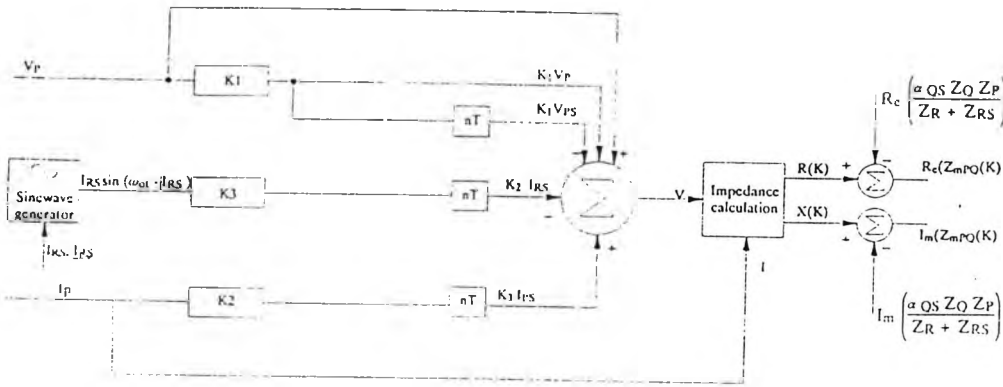
Fig. 3 Basic arrangement of the adaptive distance relay

Fig. 2a Variation of the apparent impedance VS actual line impedance for faults along line P-T-R.

Fig. 2b Variation of the apparent impedance VS actual line impedance for faults along line P-T-Q.

Fig.4a
Example of 400 kV system
$Z_1 = 0.0288 + j0.4708$ ohms/mile
Load angle: P=15°   R=10°   Q=0°

Fig. 4b Variation of measured impedances VS fault position for faults on line P-T-R.


Fig. 4c Variation of measured impedances VS fault position for faults on line P-T-Q.

Fig. 3 Basic arrangement of the adaptive distance relay